Behavioural and Neuroimaging Investigations of the Relationship between Visual Attention, Affordance and Action

Frances Anne Maratos

Doctor of Philosophy

Aston University

June 2005

Aston University

Behavioural and neuroimaging investigations of the relationship between visual attention, affordance and action

F.A. Maratos

Postgraduate degree: Doctorate of Philosophy

Year of submission: 2005

Primate studies provide evidence to suggest that the efficiency with which we are able to grasp objects is attributable to a repertoire of motor signals derived directly from vision. This is in general agreement with the belief that affordance is critical for the automatic generation of motor codes through visual perception. However, evidence also exists suggesting that attentional biases underlie visual routes to action. In this thesis the relationship between visual attention, affordance and action was investigated using a combination of neuroimaging and behavioural studies. Neuronal activity and movement construction were assessed when individuals passively viewed or produced action towards stimuli varying in their affordance and/or attentional attributes. The main findings were: (i) the passive perception of both object and abstract visual patterns was associated with decreased alpha and/or beta activity in sensori-motor cortex, occipito-temporal cortex and cerebellum. These are brain regions associated with the planning and production of visually guided action; (ii) for object patterns, decreased alpha and beta activity was also observed in regions of superior parietal and premotor cortex. These regions contain neurons argued to be essential for matching hand kinematics with manipulable objects; and (iii) in both control participants and a deafferented individual, studies of planned and unplanned pointing manoeuvres revealed that the attentional bias of a stimulus was critical for fast, efficient action production whereas the affordance bias was critical in determining end-point accuracy. Taken together, these findings demonstrate that affordance is not a necessary prerequisite for the potentiation of motor codes. Rather, affordance enables the construction of motor responses that reflect object functionality and/or manipulability. They further demonstrate that visual attention is associated with the potentiation of motor codes. Indeed, directed visual attention would appear critical for speeded responses. These findings provide new insights into the roles of directed visual attention and affordance upon action.

Key Words: *Dorsal Stream, Magnetoencephalography, Visuomotor Processing Movement Construction, Motor Codes*

Declaration

I Frances Anne Maratos hereby certify that no part of this thesis, in any form, has been submitted for any other higher degree or qualification at any university or college. To the best of my knowledge, none of the experiments reported here have been previously carried out by any other investigator. All experimental work was undertaken at Aston University. I was supported by a postgraduate research scholarship from the Neuroscience Research Institute, Aston University. Some of this thesis has been published (Maratos, Anderson and Barnes, 2002; Maratos, Anderson and Barnes, 2003; Maratos & Anderson, 2004; Maratos, Anderson, Hillebrand, Singh & Barnes, 2004).

Acknowledgements

List of Contents

Chapter 1: The Dorsal 'action' Stream

Chapter 2: *Methods A* - Magnetoencephalography

Chapter 3: Passive Perception and Sensori-motor Activation

Chapter 4: Visual Attention, Affordance and Movement Construction

Chapter 5: *Methods B* - General Behavioural Methods

Chapter 6: The Influence of Visual Attention and Affordance on Planned Movements

Chapter 7: The Influence of Visual Attention and Affordance on the On-line Control of Movements

Chapter 8: The Influence of Visual Attention and Affordance on Movement Efficiency in a Deafferented Individual

List of Figures

Chapter 4: Visual Attention, Affordance and Movement Construction

Chapter 5: *Methods B* - General Behavioural Methods

Chapter 6: The Influence of Visual Attention and Affordance on Planned Movements

Chapter 7: The Influence of Visual Attention and Affordance on the On-line Control of Movements

Chapter 8: The Influence of Visual Attention and Affordance on Movement Efficiency in a Deafferented Individual

List of Tables

List of Equations

Chapter 2: *Methods A* - Magnetoencephalography

Chapter 1

The Dorsal 'action' Stream

1.1 Introduction

A range of experimental studies in *homo sapiens* and primates have demonstrated that the various properties of a visual percept are processed in different brain regions under different time constraints. Yet, perceptual experience appears to be both unified and coherent - the perceived positions of objects, surfaces, colour and motion are smoothly integrated and tied to a single whole. This unified perception of our surroundings allows for the visual control of action with an ease that is taken for granted.

In this introductory chapter an exploration of research investigating the processing of visual information, with respect to action, is presented. Primarily, evidence for a two visual stream 'perception/action' hypothesis is reviewed [Section 1.2], including evidence for a direct visual route to action [Section 1.3]. In providing an analysis of the specific visual events that precede motor responses, an understanding of connectivity and communication between brain areas is needed. A critique of current theories and suitable neuroimaging techniques in the investigation of connectivity between distinct brain regions is therefore provided [Section 1.4]. The main aims of the thesis are then outlined [Section 1.5].

1.2 Perception and Action

1.2.1: Primary processing of visual information

Visual information is relayed to the brain from the retina (via the optic nerve) by two distinct pathways, the *retino-geniculate* pathway and the *retino-collicular* pathway. These pathways differ with respect to where they terminate in the subcortex, and whilst the retino-geniculate pathway projects to the primary visual area [V1], the retino-collicular pathway innervates subcortical structures (Gazzaniga, Ivry & Mangun, 1998). The retino-collicular pathway constitutes approximately 10% of axonal neurons from the optic nerve and is viewed as the more primitive system. It is thought to be involved in the unconscious processing of vision, such as 'blindsight' (see for example Weinskrantz, 1986; Holliday, Anderson & Harding, 1997). Conversely, the retino-geniculate pathway is postulated to regulate the conscious decoding of the visual world. This pathway constitutes the majority of axonal neurons (i.e. 90%) from the optic nerve.

The retino-geniculate pathway relays visual signals to a sub-division of the cerebral hemispheres, the lateral geniculate nucleus [LGN]. This nucleus is a complex six-layered structure, which consists of four upper parvocellular [P] layers containing cells with small bodies, and two lower magnocelulllar [M] layers containing cells with large cell bodies (Fitzgerald & Folan-Curran, 2002). Zeki (1993) states that the P pathway has characteristics that make it suitable for relaying colour and form information, whereas the M pathway has characteristics that make it suitable for detecting dynamic form and motion. The destination of M & P neurons is the medial portion of the occipital cortex (i.e. area 17 or V1).

Once information from the retino-geniculate pathway reaches primary visual cortex, a mass of cortical neurons project to a variety of extrastriate visual areas [see Figure 1.1]. These areas, which include V2-V5, the posterior part of the inferior cortex [TEO], the inferior temporal cortex [IT], the lateral occipital cortex [LOC] and the fusiform gyrus, have been linked to a variety of visual processing tasks. For example, whereas areas V2, V3, V4, V5, TEO and the fusiform gyrus are known to be involved in the perception of simple stimulus qualities such as colour, texture, motion and orientation (e.g.; Dubner & Zeki, 1971; Zeki, 1973; Zeki, 1993; Ahlfors *et al.*, 1999), regions of the LOC, IT & the fusiform gyrus are thought to process more complex stimuli such as
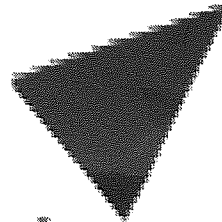
Figure 1.1: A two-dimensional map of cerebral cortex in the right hemisphere of the macaque monkey. The 32 visual areas presented occupy an estimated 54% of the cerebral neocortex (copied from Van Essen *et al.*, 1990). Connectivity between these many areas is to date still disputed.

objects and faces (Perett, Mistlin & Chitty, 1987; Gulyas, Ottoson & Roland, 1993, Malach *et al.*, 1995; Grill-Spector, Kourtzi & Kanwisher, 2001). However, exactly how information flows from the primary visual cortex to extrastriate visual areas remains unclear. Theories of hierarchical processing (e.g. Hubel & Wiesel, 1962; Felleman & Van Essen, 1990), parallel processing (e.g. Livingstone & Hubel, 1987; Mishkin, Mortimer, Ungerleider & Macko, 1983; Schiller, 1993) and more recently distributed feedforward and feedback models (e.g. Bullier & Nowak, 1995; Lee, 2003) have all been proposed. Indeed, in understanding how visual information (i.e. perception) is translated in to motor codes (i.e. action), an eclectic approach with components of many of these theories has been put forward.

1.2.2: Functional specialisation in extrastriate visual cortex: a two stream hypothesis

Schnieder (1969) was the first to propose the existence of separate visual streams for object identification and spatial localisation. In conducting work upon rodents he demonstrated that cortical lesions of visual areas 17/18 impaired an animal's performance on visual discrimination tasks, whereas collicular lesions impaired their performance on spatial orientation tasks. Two decades later, inferred largely from primate lesion studies (e.g. Pohl, 1973), Ungerleider and Mishkin (1982) noted a functional distinction between two major parts of the primate visual system: a *ventral* pathway (specialised for object perception and recognition) and a *dorsal* pathway (specialised for spatial perception and analyses of spatial configuration between different scene entities). Ungerleider & Mishkin (1982; Mishkin, Lewis & Ungerleider, 1983) observed that whilst primates with parietal lobe lesions could not compute spatial relations among items, primates with temporal lobe lesions could not compute object-based discriminations among items. This lead them to speculate that the ventral stream projected through V1, V2, V3, V4 and TEO to IT and the dorsal stream through V1, V2, V3, MT [middle temporal area] and MST [medial superior temporal area] to the posterior parietal cortex [Figure 1.2].

Aston University

Content has been removed due to copyright restrictions
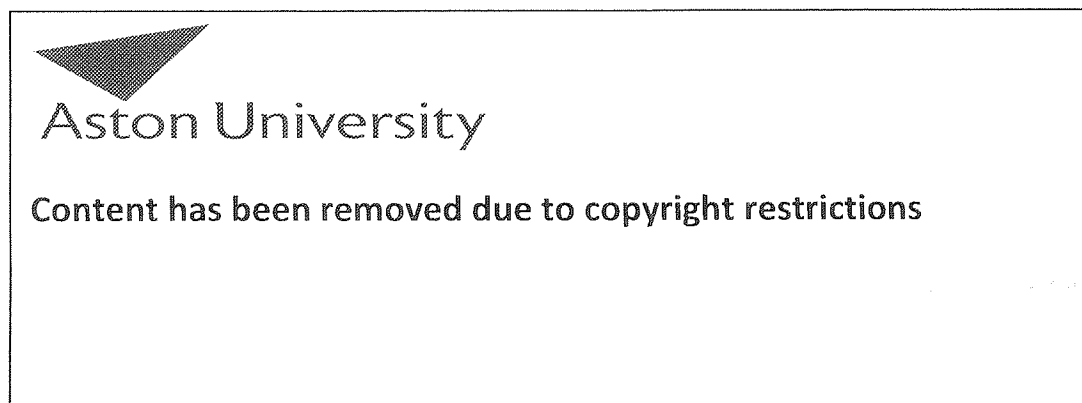
Figure 1.2: Schematic diagram of the dorsal & ventral stream projections as hypothesised by Ungerleider & Mishkin (1982).

Consistent with this model, single cell recordings from ventral stream areas V4, TEO and IT have shown response selectivity for stimulus attributes important for object vision, such as shape, colour and texture (e.g. Desimone & Ungerleider, 1989). Conversely, neurons of MT and further stations of the dorsal stream have demonstrated response selectivity for stimulus attributes important for spatial location, such as speed and direction of stimulus motion (e.g. Goebel, Khorram-Sefat, Muckli, Hacker, & Singer, 1998). Livingstone and Hubel (1988) have further revealed that in primates the *M* pathway (suitable for processing colour and motion) traverses V1, V2, V5 and the parietal cortex, whereas the *P* pathway (suitable for processing colour and form) traverses V1, V4 and inferior temporal cortex. Accordingly, they suggest that the functional architecture of these streams lends support to the 'what/where' dichotomy (see also Zeki, 1993). In relation to *homo sapiens*, functional brain imaging studies (e.g. Haxby *et al.*, 1994; Ungerleider & Haxby, 1994) have further demonstrated that the 'what/where' dichotomy pertains to processing in man, with object-identity and spatial location tasks activating regions of inferior and medial temporal cortex and parietal cortex, respectively.

Maunsell, Nealy & Depriest (1990) presented evidence of crosstalk between the two streams and suggested that the separation of *M* and *P* information in the cortex was not as distinct as initially thought (see also Nealy & Maunsell, 1994; DeYoe & Van Essen, 1988; Anderson & Yamagashi, 2000). The discovery that both the dorsal and ventral streams received input from the *M* and *P* pathways cast doubt on the 'what/where' dichotomy and led to an elegant re-working of the two-stream hypothesis by Goodale & Milner (1992; Milner & Goodale, 1995). They diverged from the traditional dichotomy of 'what/where' by focusing on the outcome requirements of the task (i.e. the goal of the observer) rather than the input distinctions (i.e. object location vs. object recognition). The model Milner & Goodale presented was of a division between visual perception (what) and visuomotor processing (how). Whilst up-holding the idea of a ventral perception stream, Milner & Goodale asserted that the dorsal stream, rather than being simply concerned with where an object is, transforms information about the location, orientation and size of an object for action-tasks such as pointing or grasping.

1.2.3: Current opinions of the dorsal stream

Drawing upon neurophysiological and neuropsychological research in both human and non-human primate studies, Goodale & Milner (1992; Milner & Goodale, 1995) noted key disparities regarding the Ungerleider & Mishkin (1982) model. In patients with optic ataxia, for example, they noted discrepancies between symptomatic diagnosis and actual behaviour.

Optic ataxia is a disorder indicative of posterior parietal lobe damage and affects accurate reaching towards a visual object, but not the identification of that object (e.g. Ferro, 1984; Perenin & Vighetto, 1988). On closer inspection, however, observation of optic ataxic patients (e.g. Jakobson, Archibald, Carey, Goodale 1991; Jeannorod, Decety & Michael, 1994) has revealed that these individuals do not only have difficulty reaching towards an object (apprehension) but also difficulty with the prehensile grip they would use to acquire an object. Goodale & Milner (1992, Milner & Goodale, 1995) conclude, therefore, that a disorder of spatial vision fails to capture the range of visuomotor impairments these patients suffer from. Consistent with this idea, a dissociation between perception and visuomotor control has recently been studied in a patient [I.W.] with left parietal lobe damage (Castiello, Paine & Wales, 2002). When required to reach and grasp stationary or rotating objects, I.W. grasps objects to the left side, despite showing no signs of sensory dysfunction. From this result it is evident that information available at a perceptual sensory level can be unavailable at a (visuo) motor level.

In a second case, Goodale & Milner (1992; Milner & Goodale, 1995; Goodale & Haffenden, 1998; Milner, 1998) report work on a patient [DF] with 'visual form agnosia' (Milner *et al.*, 1991). Visual form agnosia is typified by deficits in the ability to recognise/perceive objects, and is symptomatic of damage to the ventral stream. DF, as expected, has a profound inability to recognise the size, shape and orientation of objects, but in agreement with the theorem of Goodale & Milner, shows accurate guidance of hand and finger movements directed at the very same object. Such studies provide evidence that visual projection to the human parietal cortex provides action-relevant information about the structural characteristics and orientations of objects.

In reference to neurophysiological studies of primates (e.g. Taira, Mine, Georgopoulos, Mutara & Sakata, 1990) Milner & Goodale (1995) noted that special visuomotor properties of posterior parietal neurons are absent in ventral stream neurons. Certain parietal cells, for instance, are sensitive to the visual qualities of an object that determine the posture of the hand and fingers during a grasping movement. Moreover, a number of studies (e.g. Sakata, Taira, Kusunoki, Murata & Tanaka, 1997; Kalaska, Scott, Cisek & Sergio, 1997; Gold & Mazurek, 2002) have now revealed clusters of parietal neurons to play a crucial role in depth perception and visually guided hand movement. For example, Sakata *et al.* (1997) have demonstrated that certain posterior parietal cortex neurons represent 3-D shape information, or 'orientation-of-object' information, for manipulation. Additionally, it has been observed that these parietal neurons have reciprocal connections with primate ventral premotor area F5 (Sakata *et al.*, 1998; Quintana & Fuster, 1999). This area is speculated to contain 'canonical' neurons responsive to the visual perception of an object (Rizolatti, Fogassi & Gallese, 2000). Sakata and colleagues (1997, 1998) have therefore argued that parietal neurons play an essential role in the visual guidance of hand actions, matching hand orientation and shaping with 3-D objects for manipulation.

More recently, Rizzolatti, Fogassi & Gallese (2002) have demonstrated that reciprocal parietal-premotor connections pertain to *Homo sapiens* and the possible human homologue of area F5 in ventral premotor cortex. Furthermore, several researchers (e.g. Glickstein & May 1982; Wise, Boussaoud, Johnson & Caminiti, 1997; Glickstein, 2000) have presented evidence demonstrating that the first step in a pathway linking perception to action is by way of the dorsal stream extrastriate visual areas; with the parietal cortex strategically positioned to serve a mediating role in the visual guidance and integration of grasping and other skilled actions. In sum, the dorsal stream would appear to be appropriately equipped to serve the immediate function of guiding our actions from moment to moment.

In consideration of these dorsal stream properties, Milner and Goodale (1992, Goodale & Milner, 1995) proposed that in this visual stream information is coded in a view-specific, quick, and ephemeral form. The contents of which are probably not accessible to conscious monitoring or cognitive elaborations. Such assumptions have been supported by a plethora of modern research. For example, several studies on

neurologically normal individuals have demonstrated that the dorsal stream is susceptible to time-delays (e.g. Creem & Profit, 1998; Rossetti; 1998; Yamagashi, Anderson & Ashida, 2001; Bradshaw & Watt, 2002), and in the case of DF, grip scaling of different sized blocks falls to chance if a delay of two or more seconds is imposed (Milner, 1998). Additionally, the dorsal stream has been found to be impervious to visual illusions (e.g. Agliotti, Goodale & DeSouza, 1995; Haffenden & Goodale, 1998; Holmes, 1998; Bridgeman, 2002), a finding one would expect if this system codes information outside of cognitive awareness.

The idea of clear-cut dissociable streams is, however, not without its critics. A number of recent studies have, for instance, revealed bi-directional interactions between ventral and dorsal stream extrastriate areas (e.g. Vanni, Revonsuo & Hari, 1997; Faillenot, Decety, Jeannerod, 1999; Braddick, O'Brien, Wattam-Bell, Atkinson & Turner, 2000), and that perception and action are both influenced by illusory stimuli (Pavani, Boscagli, Benvenuti, Rabuffetti & Farne, 1999). Such findings have lead to questions concerning the view of distinct and functionally independent dorsal-ventral pathways. Kerzel, Hommel & Bekkering (2001), for example, speculate that perception and action are fed by a common, cognitively penetratable spatial representation, not dissociable pathways. Relatedly, several authors argue that many apparent dissociations between the streams in normal adults could be experimental artefacts, dependent on a variety of confounds. These include the frame of reference (e.g. object- or observer-related) incorporated into the study design (Bruno, 2001) and the occlusion of illusory display parts by the hand used to make responses affecting the viability of the stimuli (Carey, 2001). Moreover, Franz (2001) observes that research regarding whether grasping resists illusion is inconclusive, with a number of studies failing to reach significance. He therefore suggests that if the action vs. perception hypothesis is to be reconciled, visual illusions must be assumed to be generated relatively early on in the visual system before the two systems separate. Most controversially, Glover (2004) suggests a 'planning and control model' of action provides an account of data superior to a model based on a distinction between perception and action [A hypothesis returned to in Chapter 4]. The ventral-dorsal stream dichotomy is therefore not without its critics, and concerns relate not only to the extent the streams operate in isolation (see Deco & Lee, 2002 or Vecera, 2000, for interesting reconciliations of this issue), but also as to whether the division of perception/action pathways is valid or indeed adequate, in explaining all data presented.

1.3 Visual Routes to Action

In the following section a range of evidence is presented to assess whether the perception of object stimuli can result in the automatic potentiation of motor responses and, relatedly, the direct activation of motor areas by visual stimuli.

1.3.1 Patient studies

A common finding of patients with frontal lobe damage is the automatic elicitation of motor responses such as reaching and grasping when a known object is presented in their field of view (see for example Forde & Humphreys, 1998; Humphreys, Forde & Francis, 2000). Often the behaviour is an automated unconscious response or 'utilization' behaviour (Lhermite, 1983). Occasionally, however, such as in the case of 'anarchic hand syndrome', the automated response is conscious (Riddoch, Edwards, Humphreys, West & Heafield, 1998). From the study of individuals suffering with these behaviours, it is evident that visual familiarity with objects can activate motor responses. However, as the processes controlling these involuntary motor behaviours involves frontal lobe regions, the inference that vision automatically potentiates motor responses cannot be verified. In these individuals the perception-action alliance is mediated through higher-level functioning (see for example Cooper & Shallice, 2000), and as such, the resulting behaviour is reflective of both dorsal stream and frontal lobe processes.

A disorder common to patients with right parietal lobe damage (i.e. dorsal stream damage) is neglect, whereby patients fail to attend, report or represent information which appears in their contralesional hemispace (see Walker, 1995 for a comprehensive review). Neglect can compromise not only an individual's perception of objects and space, but also visuomotor control. Several authors have shown, for example, that hemispatial neglect can impair the ability to plan and initiate visually guided leftward limb movements (e.g. Mattingly & Driver, 1997; Behrmann & Meegan, 1998; Marotta, McKeeff & Behrmann, 2003). For instance, Marotta *et al.* (2003) demonstrated that neglect patients, in comparison to controls, showed more variance in the positioning of their grasp when grasping irregularly shaped objects, with a decreased preference to clasp the left-side (see also the research of Castiello *et al.*, (2002), Section **1.2.3**).

Additionally, Grea *et al.* (2002) revealed that damage to the posterior parietal cortex [PPC] disrupts on-line adjustment during aiming movements. The patient they studied could easily grasp stationary objects seen in foveal view, but could not amend ongoing movements in response to object perturbations of location at movement onset. Failure to amend an ongoing movement has also been demonstrated in normal participants when subjected to virtual lesions of the PPC using Transcranial Magnetic Stimulation (see Desmurget *et al.*, 1999). Such studies provide direct evidence that visual perception affects action production, and that the parietal region is critical in translating visuospatial signals into direct on-line motor commands.

In sum, from frontal and parietal lobe lesion data it is apparent that both the functional properties of objects and visual attention can influence action production.

1.3.2 Behavioural research

At a relatively abstract level, robust evidence exists demonstrating that the time needed for a participant to make a speeded response to a particular stimulus is dependent not only upon the characteristics of the stimulus and response, but also on the irrelevant relationship between the two (e.g. Simon, 1969; Bauer & Miller, 1982; Wascher, Schatz, Kuder & Verleger, 2001). Coined 'stimulus-response compatibility' [SRC], investigations of SRC effects can be divided into three streams of research; spatial compatibility, symbolic compatibility and the 'Simon effect' (Simon, Sly & Vilapakkan, 1981). These facets of SRC differ in regard to the irrelevant characteristics that influence reaction time responses [See Table **1.1**]. Of key importance, the use of SRC paradigms has revealed that:

a) When a stimulus and a response choice share some common mapping, reaction time decreases.

b) When no common mapping is shared, reaction time increases.

c) In consequence, an overlap of codes generated by a target stimulus and its associated response can 'prime' the motor system (see Kornblum, Hasbroucq & Osman, 1990).

Table 1.1: *The three facets of stimulus-response compatibility effects as defined by Simon, Sly & Vilapakkan, 1981*
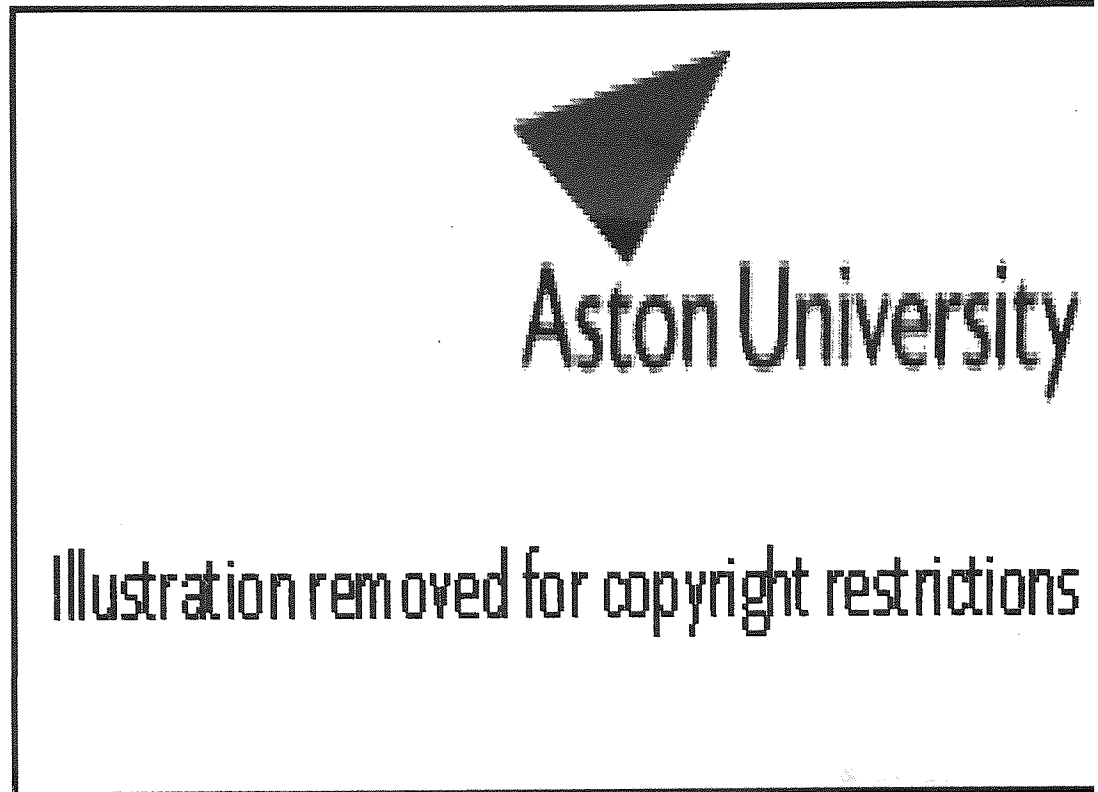
SRC paradigms have therefore been particularly useful in demonstrating the role of preparatory motor codes in relation to visual perception. Michaels (1988; Michaels & Carello, 1981), for example, proposed that SRC effects are not just constrained to position (e.g. spatial compatibility) but can apply to a variety of task situations describable by Gibson's (1979) theory of ecological affordance.

Central to the Gibsonian perspective is that the core function of vision is to provide information about the possibilities for action, and that a repertoire of potential movements, termed *affordances*, can be directly derived from vision. Gibson (1979) based his theory of affordance on three main tenets. The first tenet identifies that an observer's environment comprises affordances; these affordances are invariant and not bestowed upon an object (or entity) by the needs of the observer. The second tenet relates to perception and concerns the information available to perceptual systems to specify affordances. The third tenant also related to perception, concerns the actual

needs of an observer, i.e. whether an affordance is perceived. Subsequently, whilst the prime affordance of an object does not change as the needs of an observer change, an object can 'afford' many different actions. For example, although a saucepan is designed for cooking, if the situation necessitated, it could also be used as a footstool to reach an object out of normal limits. In adopting a Gibsonian approach, a situation is 'compatible' if the information inherent to an object or array matches with the needs of the observer and the physical programming of a to-be-executed action.

To date, several authors have used stimulus-response compatibility paradigms to explore the notion of Gibsonian affordance in relation to objects encountered in everyday behaviour (e.g. Craighero *et al.*, 1996, 1998; Tucker & Ellis, 1998, 2001, 2004; Rumiati & Humphreys, 1998; Gentilucci, 2002; Hommel, 2002; Ellis & Tucker, 2000). For example, Tucker & Ellis (1998, 2001; Ellis & Tucker, 2000) posit that action-relevant objects automatically elicit components of the actions they afford, and that intentions to act are based on a repertoire of already existing motor representations. They suggest, for instance, that upon viewing a cup, the action relevant information related to its use will be automatically activated regardless of intentions to act. In this respect they diverged away from the third tenet of the Gibsonian ecological perspective by postulating that *'in contrast to the notion of affordances being dispositional properties of objects and events, our notion has them as dispositional properties of a viewers nervous system'* (Ellis & Tucker, 2000, pg 466). Therefore, Ellis & Tucker propose that regardless of the observer's intention (or needs), perceived objects automatically potentiate the actions most regularly associated with them.

In support of this idea, Tucker & Ellis (1998) have demonstrated that the task irrelevant left-right orientation of common graspable objects (e.g. teapot, frying pan) influenced performance in reaction time tasks. In this study, participants were instructed to make a speeded button-press response with the left or right hand, dependent upon whether an object was upright or inverted. It was observed that the side of space the object's irrelevant graspable handle appeared in significantly affected participants' responses. In a second study, Tucker & Ellis (2001) demonstrated that grip type was significantly affected by the task-irrelevant factor of object size. In this investigation, participants' had to make a speeded power grip (full hand response) or precision grip (finger and thumb opposition response), dependent upon whether an object was natural or man-

made. Object size, although immaterial to the task, significantly affected response compatibility. If, for instance, a power grip was the correct response for man-made objects, reaction time was facilitated by large objects (e.g. hammer, saucepan) but impeded by small objects (e.g. thimble, needle). In consequence, Tucker & Ellis concluded that the visual representation of an object includes the partial activation of associated motor patterns related to the object, i.e. its 'affordances'. Therefore, they suggest, viewing 'usable' objects will directly activate associated motor codes. Additionally, particular object features/components may even specify an action directly relevant to the usual (cognitively related) action afforded by the object, i.e. its 'micro-affordance' (Ellis & Tucker, 2000).

Tucker & Ellis (2004) have recently demonstrated that the route through which such micro-affordance effects are generated can depend upon stored knowledge of the object and its associated actions (a conjecture shared by Hommel, 2002). Gentilucci (2002), however, disputes the idea of 'micro-affordances'. Consistent with the original theorem of Gibson, he suggests that upon viewing an object, motor codes for all concurrent affordances are represented (rather than only those that are task relevant). In support of this hypothesis, Phillips and Ward (2002) have demonstrated that the same prime affordance can produce facilitative effects for the ipsilateral hand, the contralateral hand (when positioned to correspond with the affordance location) and the ipsilateral foot. They suggest that a single affordance can potentiate a range of responses and that these responses do not necessarily reflect the motor commands best suited for manipulation of the object.

In sum, the evidence suggests that fast (appropriate) actions critically depend upon immediate on-line visual information. Namely, on-line information concerned with the relation between extrinsic object properties (e.g. orientation) and consequentially produced actions. A finding further substantiated by Craighero and colleagues (1996, 1998, 1999), Rumiati & Humphreys (1998) and Humphreys (2001). Craighero and co-workers (1996, 1998, 1999) have demonstrated that the visual presentation of a graspable task-irrelevant object/stimulus decreased the time to initiate a grasping movement to a real object, provided the intrinsic properties of the drawing/stimulus were congruent with those of the visual stimuli to-be-grasped. Craighero et al. revealed therefore, that the perception of a graspable object can automatically activate object

affordances. Relatedly, Humphreys (2001) has further postulated that the link between perceived object properties and actions might, on occasion, be based on the stored representation of a particular object. In contrast to the suggestion of Tucker & Ellis (2004), Humphreys proposed that the purpose of such stored knowledge is to allow specific categories of action to be cued directly by the visual properties of an object never encountered before. Hence, this stored 'action' knowledge is immediately available upon the viewing of a novel object to provide a direct route to action (see also Rumiati & Humphreys, 1998).

In addition to affordance, attentional processes have also been implicated in the generation of motor codes. There is, for example, convincing evidence that attention directed to the location of a visual stimulus results in the automatic generation of some motor response codes (e.g. Rizzolatti, Riggio, Dascola & Umilita, 1994; Sheliga, Craighero, Riggio & Rizzolatti, 1997). A similar argument has been advanced to explain the recruitment of oculo-motor systems during orienting and search (e.g. Goldberg & Segraves, 1987; Corbetta & Shulman, 1998). That is, shifts of attention to visual locations (or objects) recruit brain regions involved in eye movement programming and execution.

The medium(s) through which visual attention operates are proposed to be location-based, object-based, scene-based and/or a combination of the above [see Figure 1.3]. In traditional theories of location-based attention (e.g. James, 1890; Posner, 1980), visual attention is likened to a 'spot-light' with events occurring within the area of focus processed to a greater degree than those outside this area. Experimental manipulations of attentional selectivity within a visual scene, however, have demonstrated that visual attention to a specific location can be narrowed or widened depending upon task constraints (e.g. Eriksen & Lavie, 1987; Lavie, 1995). This has lead to the analogy of a variable zoom-lens (Erikson & Murphy, 1987), rather than a simple spot-light.

Additional research further demonstrated that visual attention has access to both object- (e.g. Duncan, 1984; Gibso & Egeth, 1994; Leslie, Xu, Tremoulet & Scholl, 1998) and scene-based representations (e.g. Bisiach & Luzatti, 1978; Abrams & Dobkin, 1994). In relation to the former, Berhmann & Tipper (1994) revealed that in several patients with visual neglect, rotation of a 2-D barbell stimulus resulted in a reversal of neglect. That

Figure 1.3: The possible mediums of visual attention. The shading signifies the focus of attention. **A** represents location-based attention, where the left side of space is the focus. **B** depicts object-based attention, where the focus of attention is the left side of the object. **C** represents both object- and location-based attention. **D** demonstrates scene-based attention, where the scene to the right is attended. *[Adapted from Tipper & Weaver (1998).]*

is, as the object rotated, participants failed to observe the left part of the barbell even when it had moved into the right-side of space. Such studies have not only prompted research into object-based visuomotor control in both individuals with neglect [see Section 1.3.1] and unselected individuals (see Linnell, Humphreys, McIntyre, Laitinen & Wing, 2005), but also the exploration of object (a)symmetries in visual routes to action (Anderson, Yamagashi & Karavia, 2002).

Employing a standard SRC paradigm, Anderson *et al.* (2002) presented participants with a number of 2-D object and non-object stimuli displayed in either a clockwise or anti-clockwise orientation. The task of the participants was to make speeded left- or right-handed responses, dependant on the orientation of the stimuli. The stimuli differed with respect to symmetry about the vertical axis [see Figure **1.4a**]. Whilst this attentional bias was irrelevant to the mapping response, it significantly affected reaction time. Object stimuli with an intrinsic attentional bias (e.g. an analogue clock displaying the time 3.15) and asymmetric non-object stimuli both elicited stimulus-response compatibility effects, even though neither stimulus-type afforded any actions. Additionally, in regard to the asymmetric scissors stimulus, it was found that the critical factor related to reaction time differences was the location of the objects conspicuous feature **and not** the behaviourally relevant action afforded. This conspicuous feature (i.e. the handle or scissor tip) was furthermore dependent on participant idiosyncrasies [see Figure **1.4b**]. Therefore, Anderson *et al.* (2002) concluded that it is attentional modulation (rather than affordance bias) within an object that leads to motor response advantages for one hand over the other.
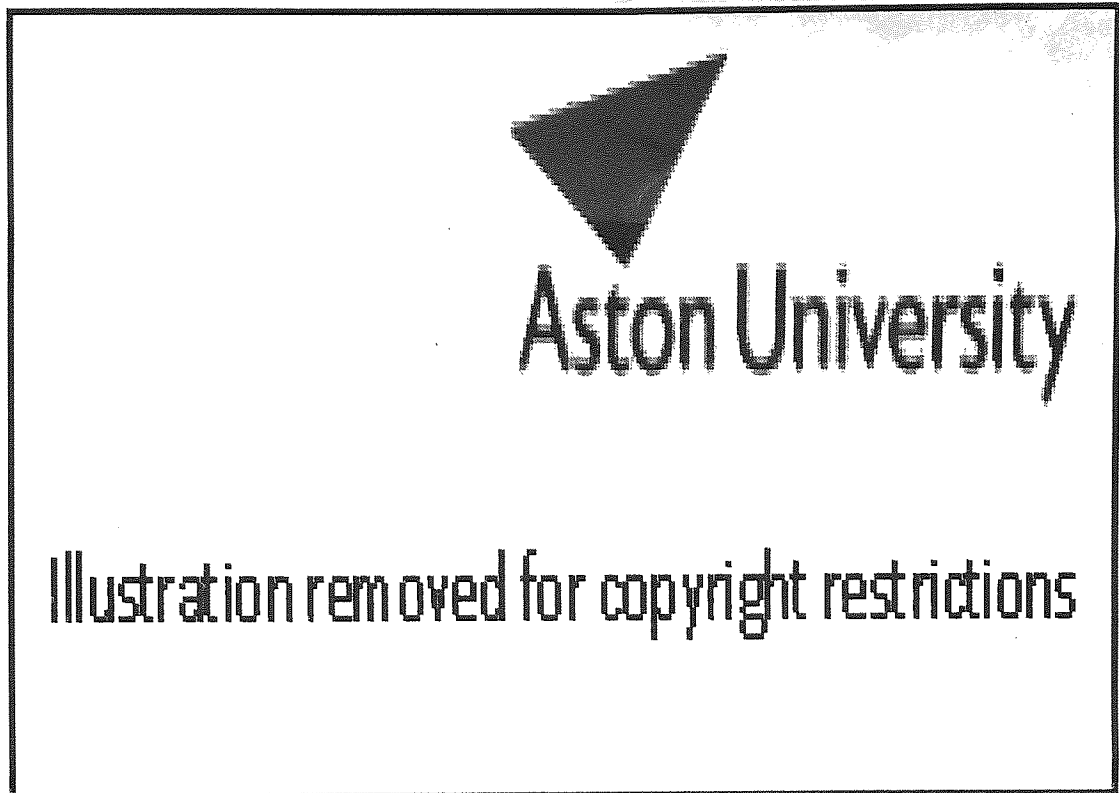
Figure 1.4: (A) Examples of Stimuli used by Anderson, Yamagashi & Karavia (2002) study. The stimuli, presented here in a clock-wise orientation of 18^0 differed with respect to attentional bias and affordance properties. **(B)** Selected findings from the study of Anderson *et al* (2002) demonstrating that the conspicuous feature of a stimulus, and not an object's primary affordance, influenced reaction times. The left-hand panel displays results from participants who reported the handle of the scissor stimulus to be the conspicuous feature, whereas the right-hand panel displays results from participants who reported the point of the scissors to be the salient feature.

To summarise, behavioural studies lend support to the notion of a 'visual route to action'. Accumulated evidence suggests that attentional biases and/or object affordances may potentiate motor responses. However, the unique contributory roles of these factors remains unknown.

1.3.3 Neuroimaging investigations

A number of neuroimaging studies have revealed that sensori-motor areas are activated in response to the preparation and planning of action (e.g. Bastiaansen, Brunia & Bocker, 1999; Endo, Kizuka, Masuda, Takeda, 1999; Guieu, Bourriez, Derambure, Defebvre & Cassim, 1999; Szurhaj *et al.*, 2003), the observation of action (e.g. Hari *et al.*, 1998; Hari, Levanen & Raij, 2000; Avaikinen, Forss & Hari, 2002), the prediction of action (Schubotz & von Cramme; 2002) and motor imagery (e.g. Pfurtscheller &

31

Neuper, 1997; Leocani, Magnani & Comi, 1999; Neuper & Pfurtscheller, 1999; Chaminade, Meltzoff & Decety, 2002; Stippich, Ochmann, Sartor, 2002). However, few studies have considered the role of passive perception and of those that have the focus has been on visual object affordances.

Using functional Magnetic Resonance Imaging [fMRI], Chao & Martin (2000) observed that pictures of tools elicited greater activation in both left ventral premotor and left posterior parietal cortex [PPC] than pictures of other object categories such as houses, faces and animals. In agreement with the research of Rizolatti and colleagues (2000; 2002: presented in Section **1.2.3**), Chao & Martin proposed that in left ventral premotor cortex there are specific neurons that respond to the visual presentation of graspable objects (canonical neurons). They further speculate that this area (i.e. Ba6) might be the human homologue of primate area F5 and suggest that within right-handed individuals, regions of left PPC and premotor cortex are important in forming the dorsal stream network. A network that could link information about the visual features and attributes of objects characterized as distinct tools, with appropriate hand and finger movements necessary for using them.

More recently, Grezes & Decety (2002) used Positron Emission Topography [PET] to examine whether the perception of objects automatically affords actions that can be made towards them. In a boxcar-type design, colour photographs of real graspable objects were presented to participants who had to a) judge the object's orientation, b) imagine grasping and using the object and c) silently name the object. In a fourth baseline condition, non-object stimuli consisting of scrambled versions of the real photographs were visually presented every three seconds. Grezes & Decety noted that, irrespective of task undertaken, the perception of object stimuli (in comparison to baseline measures) was associated with regional cerebral blood flow [rCBF] increases in a common set of cortical regions. The cortical regions encompassed the occipito-temporal junction, the inferior parietal lobule, the SMA-proper (i.e. Ba6), the pars triangularis in the inferior frontal gyrus, and the dorsal and ventral precentral gyrus. Summarising their findings, Grezes & Decety observed that the parietal and premotor activity was again comparable to that of canonical neurons in primates. They proposed that the network of cortical areas activated during the perception of graspable objects is consistent with the hypothesised anatomical route of the dorsal 'action' stream. Grezes

& Decety therefore concluded that their research provides strong neurophysiological evidence for the concept of object affordance.

Evidence of sensori-motor activation related to the passive perception of graspable objects in man has since been revealed using event-related fMRI by Handy, Grafton, Shroff, Ketay & Gazanniga (2003) and Grezes, Armony, Rowe & Passingham (2003). In both studies, graspable objects were shown to activate regions of premotor, prefrontal and superior parietal cortices, areas consistent with the location of canonical neurons in primates.

In summary, neuroimaging data provides direct evidence for a visual route to action. Or namely, that the perception of known object stimuli, with associated action affordances, automatically results in the elicitation of neural activity in motor areas. However, the role of attentional modulation in producing such sensori-motor activation has not been investigated.

1.3.4: Section synopsis

Lesion, behavioural and imaging data all provide evidence for the potentiation of action through visual perception. Additionally, imaging and lesion data reveal that the brain regions postulated to be involved in transforming visual information into motor codes are those located within the hypothesised dorsal 'action' stream. However, ambiguities arise with respect to the attributes of a stimulus that potentiate motor codes, with opinion divided as to whether the affordance attributes or the attentional attributes of a stimulus are the critical prerequisite for the generation of such codes. Moreover, whilst the neural correlates of perceptual affordances have been directly studies, the role of attentional modulation in eliciting such neural activation (in reference to sensorimotor activation) has not. To address these issues, the neural correlates of visual attention, and the relative contributions of directed visual attention and affordance upon action production need to be examined.

1.4: The Role of Oscillatory Activity in Perception and Action

It is clear from physiological and neuroimaging studies that the transformation of visual information into motor commands necessarily involves a diverse number of cortical regions. However, the processes underlying coherent and coordinated networks of activity between different brain regions are not well understood. Classical theories of the brain as a passive (i.e. stimulus-driven) modular device are being challenged and replaced with theories of the brain as a system that 'actively seeks' sensory stimuli through chaotic oscillatory processes (e.g. Freeman, 2000). These recent theories stem from advances in brain-imaging techniques and emphasise the role of neuronal oscillatory activity.

1.4.1 Generation of neuronal oscillations

Caton (1875) discovered that the mammalian brain generated rhythmic oscillatory activity. Until Berger (1930), however, the idea that such activity might correlate with brain processes and behavioural states was not considered. Berger noted a rhythmic activity in the region of 8 to 12 Hz over occipital scalp areas (i.e. the alpha rhythm), which was blocked upon sensory stimulation or purposeful visual activity.

To date, many such natural brain rhythms have been observed [See Table **1.2**]. These rhythms reflect differences in the synchronous firing of cortical neurons and are functionally distinguishable from each other on the basis of scalp distributions, reactivity to experimental manipulations and resonant frequency. The frequency at which neurons resonate, for example, is dependant upon the number of synchronously firing neurons in a network; with oscillations at low frequencies comprising more neurons than oscillations at high frequencies (Singer, 1993). Additionally, with increasing numbers of coherently activated interconnecting neurons, the amplitude of the oscillations increases (Pfurtscheller & Lopes da Silva, 1999). In accordance with these findings, Nunez (1995) notes that the rhythmic activity of the brain can be sub-divided into three categories: that which occurs at the global, regional or local level. Global rhythms are oscillations in specific low range frequency bands, which can be recorded all over the scalp (e.g. the 8-12 Hz alpha rhythm). Regional rhythms are restricted to a cortical boundary and tend to oscillate in mid frequency ranges (e.g. the

Table 1.2: *Rhythms of the brain, regions of maximum prominence and functional implications*

Nomenclature	Frequency/Region	Functional Implications & References
Delta	~0.5-3 Hz Variable	Fatigue, nREM sleep, 'Internal' attention. E.g. Lai & Craig, 2001; Nobili *et al.*, 2001; Harmony *et al.*, 1996.
Theta	~4-7 Hz Frontal & Temporal	Cognitive function (e.g. mood, memory, reasoning, fatigue, REM sleep). E.g. Muzur, 2004; Kaplan *et al.*, 2000; Comi, 1997
Alpha	~8-13 Hz Occipital and Parietal	Visual attention, Auditory memory, Visual imagery (e.g. Fingelkurts *et al.*, 2003; Cremades, 2002; Salenius *et al.*, 1995)
Beta	~14-25 Hz Precentral and Frontal	Motor control (e.g. motor attention, movement, imagery), Attention. E.g. Pfurtscheller *et al.*, 2003; Clark *et al.*, 2001
Gamma	>25 Hz Occipital and Frontal	Object representation, Cognitive processes (e.g. attention). E.g. Sokolov *et al.*, 2004, Summerfield *et al.*, 2002; Haig *et al.*, 2000
Mu	~8-16 Hz Pre and post-central	Motor processes (e.g. action observation, voluntary movement). E.g. Muthukumaraswamy *et al.*, 2004; Pfurtscheller *et al.*, 2000
Tau	~10 Hz Temporal	Auditory processes (e.g. anticipatory attention, sound processing). E.g. Bastiaansen *et al.*, 2001; Lehtelä *et al.*, 1997

10-20 Hz mu rhythms). Local rhythms represent specific neuronal activity recorded from spatial patterns of intra-cortical connectivity (e.g. the 40Hz gamma rhythm).

The actual pace-making mechanisms that control the synchronous rhythmic activity of neuronal populations are not well understood. Mountcastle (1998) suggests that the various rhythms could be generated in dorsal-thalamic circuits and imposed upon cortical neurons in spatial patterns set by the relevant thalamocortical projections. Consistent with this theory, Mountcastle observed that when the cortex was disconnected from subcortical structures, oscillatory activity in all but the lowest frequencies disappeared. Additionally, Steriade, Gloor, Llinas, Lopes da Silva & Mesulam (1990) recognised that neurons in the thalamus have specialised electrophysiological attributes that endow them with oscillatory properties, a finding substantiated by a number of studies (e.g. Steriade, Domich & Oakson, 1986; Lopes da Silva, 1991). However, Mountcastle (1998) also suggests that many cortical oscillations may depend on non-rhythmic afferent inputs (see also Silva, Amitai &

Connors, 1991). Thus, the exact contributory role of thalamo-cortical circuits and cortico-cortical circuits in regulating oscillatory activity remains unclear. Nonetheless, it is known that even the briefest of externally or internally related phenomena can influence the synchronous oscillatory activity of neuronal populations. This activity is manifested as an evoked response and/or an induced response.

Evoked activity represents change in a series of local transient post-synaptic responses triggered by a specific stimulus. Induced activity, however, represents not only modification of this activity, but also modification of the inter-neuronal thalamo-cortical and/or cortico-cortical networks that are proposed to control ongoing rhythmic frequency components (see also Pfurtscheller & Lopes da Silva, 1999). This induced activity predominates as either an event-related synchronization [ERS] or an event-related desynchronization [ERD], and is often poorly time-locked and non-phase-locked to the stimulus. ERD is manifest as a short-lasting, localised amplitude decrease in activity whereas ERS is manifest as a short-lasting, localised increase in activity (see Pfurtscheller et al, 2001).

Induced activity is produced by partial synchronisation of neuronal-scale field potentials across areas of cortex of centimetre-squared scale, rather than local finite synchronised event related potentials (Makeig, Debener, Onton & Delorme, 2004). Indeed, Elul (1972) estimated that only 10% of a population of neurons in a given region need to be synchronised to produce an (induced) activity amplitude 10-fold that of 90% non-synchronised neurons. No longer dismissed as noise, the function of such ERD/ERS oscillatory activity is discussed both below and in Chapter 2 [Section 2.3].

1.4.2 Function of induced neuronal oscillations

Stemming from theories of connectionism in the mid 1980's (e.g. Rumelhart & McClelland, 1986), induced activity is proposed to reflect the 'top-down' control of behaviour. The idea is that synchrony, as a consequence of response saliencies, can select and group subsets of neuronal responses for further processing or inhibition.

In models of oscillatory activity (e.g. Freeman, 1994; Freeman, 2000; Engel, Fries & Singer, 2001; Varela, Lachaux, Rodriquez & Martinere, 2001), this neuronal synchrony is thought to be crucial for a variety of processes including sensori-motor integration

(e.g. Pfurtscheller, Pichler-Zalaudek, Neuper, 1999; Bastiaansen, Bocker, Brunia, Munck & Spekreijse, 2001), object representation (e.g. Bertrand & Tallon-Baudry, 2001; Grossberg, 2001), response selection (e.g. von Stein, Chiang & Konig, 2000) memory processes (e.g. Krause, Lang, Laine, Kuusisto, Porn, 1996; Jensen, Gelfand, Kounios & Lisman, 2002) and visual attention (e.g. Foxe, Simpson & Ahlfors, 1998; Kanwisher & Wojciulik, 2000; Driver & Frith, 2000). In such models, the sensitivity of neuronal populations to sensory inputs is modulated by ERD/ERS activity. In the following subsections the manifestations and functional implications of such induced oscillatory activity are discussed with specific reference to processing in visual and motor areas.

1.4.2.1: Induced activity in low frequencies

Alpha blocking occurs when an individual uses their sense of vision (i.e. opens their eyes) and is the dissipation of 8-12 Hz oscillatory activity manifested as an event-related desynchronisation. Upon eye closure or relaxation of the individual, the rhythmic activity re-appears and can be enhanced (an ERS) by the transfer of attention from the visual modality to a different modality. In consequence, the alpha rhythm has been proposed to relate to processes of visual attention (e.g. Niebur, Hsaio & Johnson, 2002; Yamagashi *et al.*, 2003). Comparatively, the mu rhythm of the sensori-motor cortices is dissipated and replaced with an ERD when an individual makes a voluntary movement (e.g. Taniguchi *et al.*, 2000). However, on movement termination the ERD is replaced with an ERS (e.g. Pfurtscheller & Lopes da Silva, 1999b; Taniguichi *et al.*, 2000). Thus the mu rhythm has been proposed to relate to processes of motor attention.

Recently, Pfurtscheller and colleagues (1999a; 1999b; 2001) have further observed that voluntary hand movement results in mu rhythm ERD of the (motor cortex) hand area and mu rhythm ERS of the foot area; and vice-versa for foot movement. This phenomenon of simultaneously occurring ERD and ERS has been interpreted as a focal ERD and surround ERS (Pfurtscheller & Neuper, 1997; Brunia, 2001), supporting the idea that rhythmic activity occurs when a cortical area is 'idling' or 'has nothing to do' (Adrians & Mathews, 1934; Pfurtscheller, 2001). Early support for this idea came from observations of mu ERS as a consequence of visual attention (e.g. Breschet & Lescable, 1965; Koshino & Niedermeyer, 1975) and alpha ERS as a consequence of voluntary movement (Pfurtscheller & Neuper, 1992). Synchronization in low frequency bands

may therefore be important in introducing powerful inhibitory effects when an individual is conducting a task and, as such, prevent irrelevant information entering the 'active' neural networks (Klimesch, 1996).

In sum, event-related synchronisation and desynchronisation of lower-band frequency rhythms is recognised to occur in a number of brain regions when an individual is engaged in a number of tasks. In addition to processes of visual and motor attention (see also Ray & Cole, 1985a; 1985b; Foxe *et al.*, 1998), such tasks include the expectation, anticipation and imagination of movement (see Chapter **3**), and the engagement of working memory (Dujardin, Bourriez & Guieu, 1994; Klimesh, Schimke & Schwaiger, 1994; Krause, Lang, Laine, Kuusisto & Porn, 1996; Sterman, Kaiser & Veigel, 1996; Jenson, Gelfand, Kounios & Lisman, 2002). In a small number of these studies an augmentation (i.e. an ERS) of lower-band frequency ranges was recorded when the cortex was in an activated state.

1.4.2.2: Induced activity in higher frequencies
Enhancement of a 40Hz rhythm (i.e. Gamma ERS) over visual cortices has been postulated to represent the cortex in an active state and is specifically thought to relate to the resolution of the 'binding problem' (e.g. Treisman, 1996). This relates to how we experience objects as complete entities, when the many processes by which they are represented differ with respect to both the spatial and temporal properties of the brain regions they encompass. Yet, whilst in 1919 DeLage postulated that rhythmic synchronization of neuronal discharges could provide a link between and within areas involved in a given network, the idea that oscillatory synchronisation plays a key role in feedforward visual feature binding has only recently been explored (see, for example, Bringuier, Fregnac, Baranyi, Debanne & Shulz, 1997; Singer, 1999; Gross *et al.*, 2001). Furthermore, until the work of Tallon-Baudry and colleagues (1996; 1997; 1999; Bertrand & Tallon-Baudry, 2000), the functional role of gamma in relation to internally driven object processing had not been examined.

Tallon-Baudry *et al.* (1996) reasoned that, if synchronised oscillatory activity played a role in linking together different neural regions involved in 'same object processing', then whenever a coherent percept is being built, the resonant activity should be enhanced. They presented participants with coherent triangular stimuli (illusory and

real) and an 'incoherent' control [Figure 1.4a]. All stimuli consisted of similar component parts, yet only perception of the real and illusory triangles involved binding between the different image components to build a coherent representation. Consistent with their coherent percept hypothesis, only the real and illusory triangles elicited significant gamma ERS in visual and parietal regions. In a second experiment, Tallon-Baudry *et al.* (1997) demonstrated that the activation of an 'internal object representation' also enhanced gamma activity. In using a modified version of the Dalmatian dog picture [Figure 1.5b], Tallon-Baudry *et al.* demonstrated a highly significant occipital/parietal gamma ERS in trained subjects when actively searching for the animal, compared with a negligible ERS change in naïve participants who perceived the image as a collection of meaningless black and white dots.

Aston University

Content has been removed due to copyright restrictions
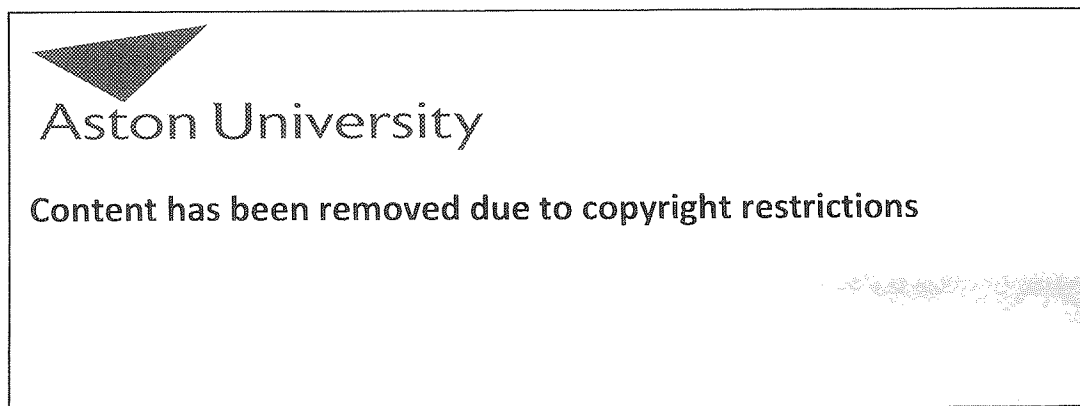
Figure 1.5: (a) Experimental stimuli used in the Tallon-Baudry *et al* 1996 experiment included an illusory triangle (top) real triangle (middle) and 'no triangle' stimulus (bottom) (b) The Dalmatian dog picture, an adaptation of which was used in Tallon-Baudry *et al* 1997 experiment.

In summarising their investigations, Tallon-Baudry *et al.* (2001) conclude that the establishment of a coherent and unified percept is achieved through oscillatory activity in varied and distributed neural networks. This finding is supported by research of Rodriguez *et al.* (1999) who also revealed increased occipital/parietal gamma ERS if a percept (in this case ambiguous faces) was perceived. However, Rodriguez *et al.* further demonstrated that if a button press response was required on the perception of a face stimulus, then a period of gamma desynchronisation in occipital and parietal

regions marked the transition between the moment of perception and the motor response.

To recapitulate, from the electrophysiological data presented, the idea that neuronal oscillations provide the underlying basis for a range of (human) behaviours is well established. Indeed, such studies demonstrate that processes of visual attention, motor attention and perceiving a coherent percept all involve oscillatory synchrony.

In understanding how visual information is transformed into motor codes, because visual routes to action are proposed to involve a distributed network of cortical areas, it is possible that the neural basis of these processes (e.g. affordance/visual attention) encompasses change in oscillatory behaviour too. However, to investigate this theory a method of imaging oscillatory neural activity is needed.

1.4.3 Imaging oscillatory activity

The methodological advances that have allowed for the direct study of the neural correlates of human behaviour take two forms, those that measure *hemodynamic* changes such as PET and fMRI, and those that measure *electromagnetic* changes such as ElectroEncephaloGraphy [EEG] and MagnetoEncephaloGraphy [MEG]. Measures of hemodynamic change rely on the assumption that local metabolic changes of blood flow and venous oxygenation reflect increased neuronal function. These methods have proven the more popular imaging techniques and are briefly reviewed below. For a detailed explanation of fMRI and PET refer to Orrison, Lewine, Sanders & Hartshorne (1995).

PET provides a measure of regional cerebral blood flow [rCBF] and involves the injection of small radioactive traces (usually O^{15} molecules) into the bloodstream. These molecules, because of local metabolic changes during neural activity, are found in greatest concentrations near the sources of such activity (Baillet, Mosher & Leahy, 2001). Upon decaying, the radioactively labelled traces emit positrons. Each positron rapidly loses energy and within a short distance (<5mm) annihilates with a negatively charged electron. This event produces two high-energy gamma rays that travel from the site of annihilation opposing each other at an angle of 180^{0}. The 'back-to-back' rays escape the brain and are detected almost simultaneously at (opposing) photocell sensors

surrounding the individuals head (Banich, 1997; Anderson, 2002). Adopting source reconstruction techniques, the location of each ray is used to define a line of response along which the annihilation(s) occurred allowing the photon's site of emanation to be determined [see Figure **1.5**]. Images of blood flow in the brain can then be created. PET has many limitations, these include:

1) It involves exposing the participant to ionising radiation.

2) The half-life of the radioactive atoms is necessarily brief, preventing a full investigation of activity within cortical regions.

3) It has poor temporal resolution (as O^{15} molecules have a half-life of about two minutes).

4) It also has poor spatial resolution with one cubic centimetre the best it can yield (Savoy, 2001).

5) It assumes that there is a close relationship between local neuronal activity and local blood flow.

Aston University

Content has been removed due to copyright restrictions
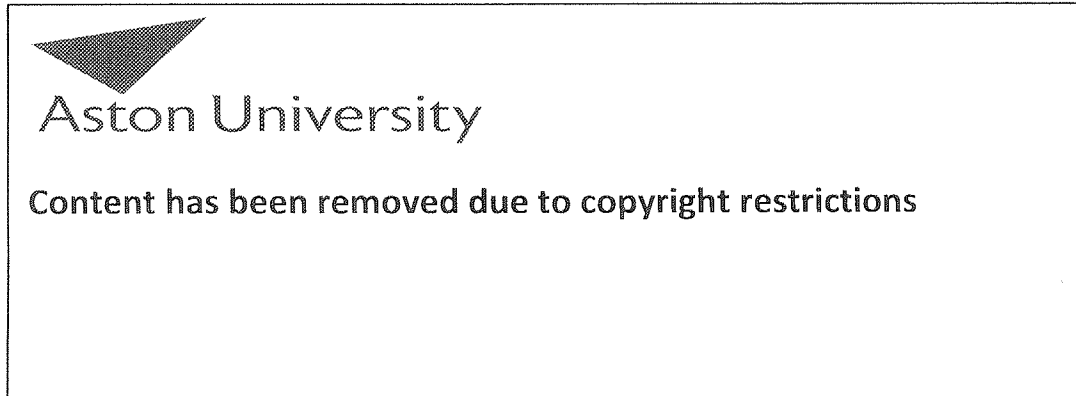
Figure 1.6: Back-to-back gamma rays produced when a positron annihilates with an electron are detected at opposing photocell receptors. Using source reconstruction techniques the location of each ray is used to determine a line of response along which the annihilation occurred. [*Adapted from Anderson, 2002*]

MRI provides a method for establishing detailed brain anatomy through the exploitation of the magnetic properties of atoms. In the normal environment, atoms such as hydrogen spin randomly. However, when such atoms are placed within a static magnetic field most tend to align with the direction of the magnetic field. In MRI, a

static magnetic field is first created. A radio-frequency [RF] pulse (tuned to the resonant frequency of the atom under investigation) is then applied. This RF pulse results in an increase in the proportion of atoms aligned **against** the direction of the main field. For brain-imaging purposes the resonant frequency is usually set to that specific for hydrogen atoms, as hydrogen atoms both provide a strong magnetic signal and are found in abundance in brain tissue (Sanders, 1995; Anderson, 2002). When the RF pulse is terminated the hydrogen atoms rebound towards the orientation of the static magnetic field. This synchronised rebound enables the detection of RF signals emitted from the rebounding atoms, the intensity of which indicates the concentration of the atom type within the brain (Banich, 1997; Gazzaniga, 1998; Savoy, 2001). To locate the signal, the application of a gradient field is necessary. This field has the effect of varying the frequency of the returning signals along the direction of the gradient and, in consequence, allows for different signal locations to be established (Anderson, 2002). Of importance, in MRI, the returning RF signals (i.e. spin frequencies) are affected by the number of protons that constitute a specific atom type. It is this feature of the MRI signal that is especially important for fMRI.

fMRI is based upon the fact that an increase in blood flow triggered by neural activity is not matched by an equal increase in oxygen utilisation (Fox & Raichle, 1986). During neural activity, the levels of oxygen delivered to an active brain region exceed those required for the activity. This results in a large increase of oxyhaemoglobin and a small increase of deoxyhaemoglobin in such regions (Savoy, 2001). These changes affect the magnetic properties of blood (or specifically the oxygen molecules) flowing near the regions of neural activity, which can be assessed through the manipulation of the static, pulsed and gradient magnetic fields an individual is placed in. In fMRI the technique is termed 'blood oxygen level dependent' [BOLD] imaging. In comparison to PET, fMRI has the advantage of excellent spatial resolution (e.g. 0.1 cubic cm of the BOLD signal). Nevertheless, it does have several disadvantages including:

1) Poor temporal resolution (i.e. in the order of several seconds).
2) Individuals with ferromagnetic surgical implants (e.g. pace-makers/joint-clips) cannot undergo fMRI.
3) As with PET, it assumes a close relationship between local blood flow and neural activity.

Another limitation of both PET and fMRI is that measures of haemodynamic change cannot distinguish between evoked and/or induced oscillatory activity (see Yamagishi *et al.*, 2003). In consequence, neither method can establish the type of neuronal activity displayed. To investigate whether activity is induced or evoked, neuroimaging methods based upon electromagnetic responses must be utilised. These methods, including EEG and MEG, measure electrical activity in neuronal cell assemblies rather than the blood flow and/or oxygen levels associated with such changes. Therefore, both EEG and MEG allow for the differentiation of neural activity patterns (i.e. whether such activity is evoked or induced) and have millisecond resolution.

In electromagnetic techniques, neural activity is recorded through either the measurement of scalp electrical potentials (EEG) or the measurement of associated magnetic fields (MEG). In EEG, voltage change is recorded using scalp-based electrodes referenced to an electrode positioned on another body-part (e.g. the ear, nose or chin). The voltage change recorded reflects the electrical currents of synchronously firing neurons. This method of recording neuronal activity, reviewed in detail elsewhere (see Niedermeyer, 1993), has several limitations including:

1) The spatial patterns of electrical currents recorded at the scalp are distorted as brain tissue and skull vary in conductivity and thickness (Rose & Ducla-Soares, 1990). Subsequently, the spatial localisation of the signal is limited to approximately one cubic centimetre (Orrison *et al.*, 1995).

2) The resolution of signals at deep sources is poor.

3) The placement of scalp electrodes on an individual is time consuming.

Associated with every electrical current is a magnetic field. Magnetic fields, detected using MEG, are minimally affected by scalp, skull or cerebral tissue etc. (Williamson & Kaufman, 1981). In consequence, the spatial resolution of magnetic fields arising from neuronal currents can be accurately determined to within a region of 2-5mm (Hämäläinen, Hari Ilmoniemi, Knuutila & Lounasmaa, 1993). Thus MEG offers a spatial resolution superior to that of EEG. Additionally, although MEG has been criticised with respect to the resolution of signals at deep sources (see Tallon-Baudry, Bertrand & Pernier, 1999), Hari, Joutsiniemi & Sarvas (1988) and Lutkenhoner (1996) have demonstrated that deep sources can be localised with limited spatial accuracy loss.

In consequence, MEG was used for all imaging investigations in this thesis, and is reviewed in detail in Chapter 2.

1.5 Thesis Aims

There is now considerable evidence for the existence of at least two visual pathways in the primate visual system; a *ventral* visual stream specialised for object perception and recognition, and a *dorsal* visual stream specialised for visuomotor processing (i.e. action). In this thesis, the action pathway will be investigated using both neuroimaging (i.e. MEG) and behavioural (i.e. movement construction) paradigms. The specific aims include:

1) The assessment of sensori-motor activation by the passive visual perception of a wide variety of object and abstract stimuli varying in their associations with a grasping action.

2) The analysis of the spatio-temporal pattern of activity during the passive perception of object and abstract stimuli.

3) The investigation of visual attention and affordance upon movement construction (i.e. how these perceptual attributes influence the construction of reaching/pointing manoeuvres). A wide range of visual stimuli will again be used to ascertain whether the influence of affordance upon action is distinct from that of directed visual attention.

4) The exploration of visual attention and affordance upon reaching/pointing manoeuvres in a deafferented individual. Devoid of proprioceptive abilities, deafferented individuals must consciously monitor their every movement through visual feedback. In consequence, the effects of affordant and attentional stimulus attributes upon movement construction may be different in deafferented individuals compared with neurologically normal controls.

The thesis is divided into two parts. In the first part, neuroimaging studies are used to investigate the passive perception of visual stimuli (aims 1 and 2). In the second part, behavioural studies are used to investigate action construction (aims 3 and 4). The behavioural studies encompass both the construction of planned and unplanned movements, the basis of which are discussed in Chapter 4.

CHAPTER 2

METHODS A: MAGNETOENCEPHALOGRAPHY

2.1 Introduction

Magnetoencephalography [MEG] is a non-invasive functional neuroimaging technique that provides a method for localising sources of neuronal current. Within the cerebral cortex there are in excess of 10^{10} neurons connected by a vast network of at least 10^4 synapses (Wikswo, 1989). When an area of cortex is active, current flow between a number of neurons is established through the influx of ions across cell membranes. A consequence of such current flow is the production of a magnetic field perpendicular to the current's transposition (Papanicolaou, 1995). Therefore, as a direct result of neuronal excitement, extracranial magnetic fields are produced (Hämäläinen, Hari Ilmoniemi, Knuutila & Lounasmaa, 1993). Using magnetoencephalography, these extracranial magnetic fields can be detected and activation of specific brain regions inferred.

The following chapter details the neurophysiological basis of MEG, source reconstruction techniques and Synthetic Aperture Magnetometry [SAM]. This is followed by an overview of the specific methods adopted in this thesis.

2.2: Neural Basis and Implementation of MEG

2.2.1 Neuron physiology

A neuron consists of a cell body (soma), dendrites and an axon. It is connected to other neurons through synapses on its dendrites, cell body and *boutons* (which contain neurotransmitters). In its resting state, a neuron has a negative potential of around −70 mV. On excitation, however, the cell becomes either depolarized or hyperpolarized. This excitation is caused by the release of neurotransmitters in a secondary connected cell, which transcend across the synaptic cleft (gap) to bind with receptor sites on the neuron's dendrites at synaptic sites (Carlson, 2004). The diffusion of neurotransmitters across the synaptic cleft changes the permeability of the cell's membrane, causing an increase in the absorption rate of the post-synaptic membrane to sodium, potassium or chloride ions. The increase of ion up-take is dependent upon post-synaptic receptors, i.e. what type of ionic channel they activate. An influx of sodium ions results in a net current flow into the cell. This leads to an excitatory postsynaptic potential [EPSP] and cell depolarization. An influx of potassium or chloride ions results in a net current flow out of the cell, an inhibitory post-synaptic potential [IPSP], and cell hyperpolarization (Kolb, 1995; Hämäläinen *et al.*, 1993). Thus, whereas EPSP's increase the probability of a neuron's firing rate, IPSP's decrease the probability of neural firing. It is, however, only in the case of EPSP's that an axon potential can be elicited and a second current propagated down an axon to a neuron's boutons. The latter event occurs when excitatory postsynaptic potentials reach a pre-defined threshold causing a rapid reversal of a membrane's potential. Although both excitatory and inhibitory synaptic inputs lead to *dentritic* currents, only excitatory currents cause the propagation of an action potential along a neuron's axon.

In the following sections [*2.2.1.1*, *2.2.1.2* & *2.2.1.3*], a consideration of the relative contributions of the different current types to the production of measurable extracranial magnetic fields are reviewed.

2.2.1.1: Axial currents

An action potential is characterized by a leading edge depolarization resulting in an accumulation of positive charge, and a trailing edge repolarization resulting in a

negative charge. This wave of activation causes three volume currents: *intracellular*, *transmembrane* and *extracellular* [Figure **2.1**]. Intracellular and transmembrane volume currents are due to the repellent nature of positively charged sodium ions within the neuron and produce currents leading away from the region of synapse, and outward of the cell, respectively. Extracellular volume currents are due to the repellent nature of positively charged sodium ions within extracellular space and produce currents leading back to the site of depolarisation (Pizella & Romani, 1990; Lewine & Orrison, 1995).
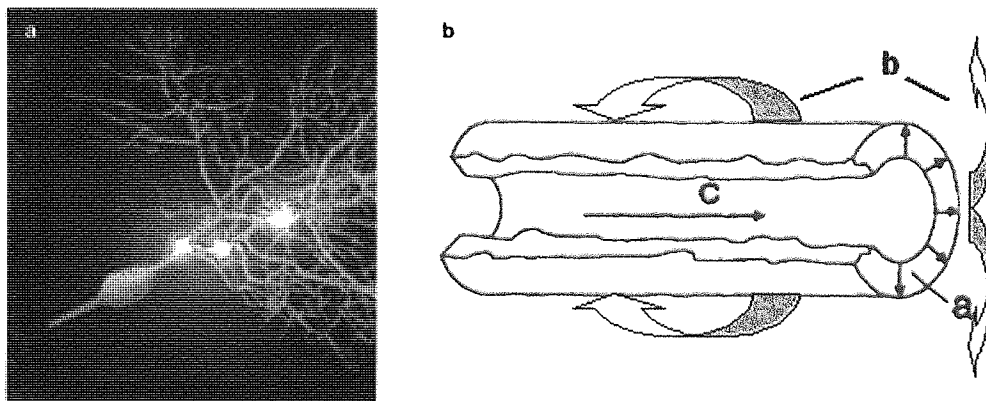
Figure 2.1: (a) A neuron in a state of depolarization can lead to the elicitation of an action potential. (b) Associated with the transmission of an action potential are three types of currents: *a* transmembrane, *b* extracellular and *c* intracellular.

Each of these currents generates a magnetic field, although their net outputs are thought to contribute little to the measurable extracranial magnetic field. Transmembrane currents, because of their radial symmetry around the axonal trunk, produce self-cancelling magnetic fields (Papanicolau, 1995). Extracellular volume currents, because of their widespread backflow toward the site of depolarization, leave a relatively low current density along the external surface of the membrane (Okada, 1982). Finally, intracellular volume currents have opposing dipolar magnetic fields associated with the outflow and return flow of sodium ions [see Figure **2.2**]. Hence, the quadrupolar nature of the magnetic field results in rapid signal attenuation over distance ($1/distance^3$). Therefore, many hundreds of thousands of synchronous axonal impulses would need to be generated for the signal to surpass the skull. This, coupled with the fast propagation of action potentials (1 to 100 meters per second), renders the necessary synchronous activation of so many axons highly unrealistic and temporal summation of the associated EPSP's unlikely (Lewine & Orrison, 1995).

Figure 2.2: Opposing dipolar magnetic fields associated with intracellular axonial currents. The currents associated with the leading edge and repolarization front can be modelled as current dipoles orientated in opposite directions; away from the cell body and toward the soma, respectively. The resultant field pattern is therefore quadropolar and signal attenuation over distance great. [*Adapted from Lewine & Orrison, 1995*]

2.2.1.2: Dendritic currents

With the exception of temporal resolution, dendritic currents associated with post-synaptic potentials are similar to those associated with action potentials. In consequence, magnetic fields produced by transmembrane and extracellular currents are unlikely to contribute to the measurable extracranial signal (Hämäläinen *et al.*, 1993; Lewine & Orrison, 1995; Papanicolau, 1995; Vrba & Robinson, 2001). However, the flow of ions across a synaptic cleft is a steady phenomenon which can last for hundreds of milliseconds (Pizella & Romani, 1990; Baillet, Mosher & Leahy, 2001). The synchronous activity of many thousands of neurons is therefore a feasible event. Okada (1982) states that excitatory inputs are the most probable cause of extracranial magnetic fields as current density is greater for EPSP's than for IPSP's. Additionally, excitatory intracellular dendritic currents can be modelled as a single dipole, with a uni-directional current flow from dendrite to soma. Thus, the magnitude of associated magnetic fields decreases at a lesser rate ($1/\text{distance}^2$) and is therefore considerably greater than that produced by the axonal intracellular action potential currents (Okada, 1982; Lewine & Orrison, 1995).

2.2.1.3: Dendritic field patterns

The morphology of the dendrites is critical in establishing whether a neuron contributes to the measurable signal. Neurons with circular field symmetry, such as stellate cells, fail to produce an external magnetic signal because the closed field pattern of the dentritic currents are self-cancelling [Figure **2.3a**]. Pyramidal cells, in contrast, have a highly asymmetric dentritic field pattern and as such have an open field structure that produces a net output of current [Figure **2.3b**]. Pyramidal neurons are therefore generally accepted to be the dominant contributors to the measurable extracranial neuromagnetic signals, especially as they constitute 70% of all neocortical neurons

Aston University

Content has been removed for copyright reasons
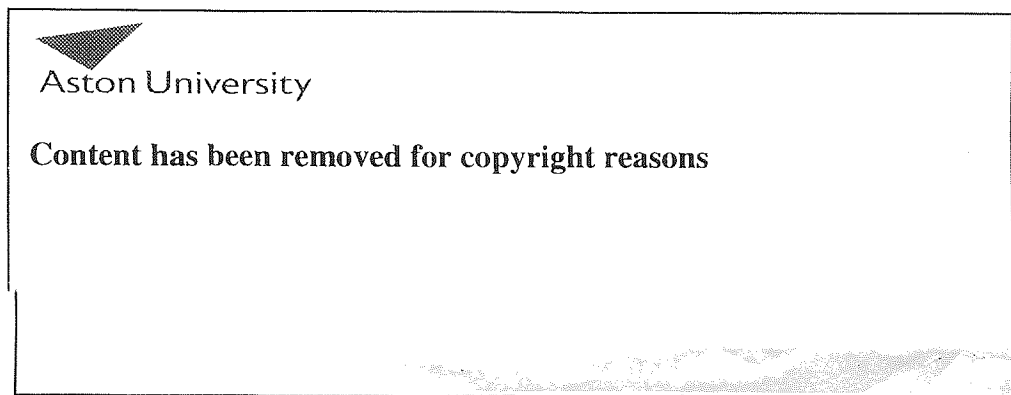
Figure 2.3: The dendritic pattern of a stellate cell is roughly symmetrical, hence the field pattern of the current is self-cancelling (**a**). The dendritic pattern of a pyramidal cell, in contrast, is highly asymmetric (**b**). *[from Lewis & Orrison, 1995]*

A second consideration is the orientation of the pyramidal cell. The apical dendrites of pyramidal neurons tend to be perpendicular to the cortical surface, rendering current flow approximately perpendicular to the cortex (Hämäläinen *et al.*, 1993). However, as the cortex is convoluted with numerous sulci and gyri, the flow of current can be anything from tangential or radial. Further discussion of the relevance of these current types to the measurable extracranial magnetic field is discussed in Section *2.3.2.2.*

2.2.3 Signal detection

The magnetic field generated from the dendritic current flow within a single pyramidal neuron is too small to be detected externally [Vrba, 2002]. Using MEG, it is necessary to have 10^4 to 10^5 neurons simultaneously activated for a field to be detectable

(Wikswo, 1989). However, this does not pose a problem given that there are approximately 10^5 to 10^6 cells in a cortical area of 10mm^2 (Vrba & Robinson, 2001) and that activation of large numbers of cells is often spatially confined. Even so, the magnetic field produced by this number of activated neurons is extremely small [see Figure 2.4]. To detect such small signals, highly sensitive Superconducting QUantum Interference Devices [SQUIDS] are needed

Aston University

Content has been removed for copyright reasons
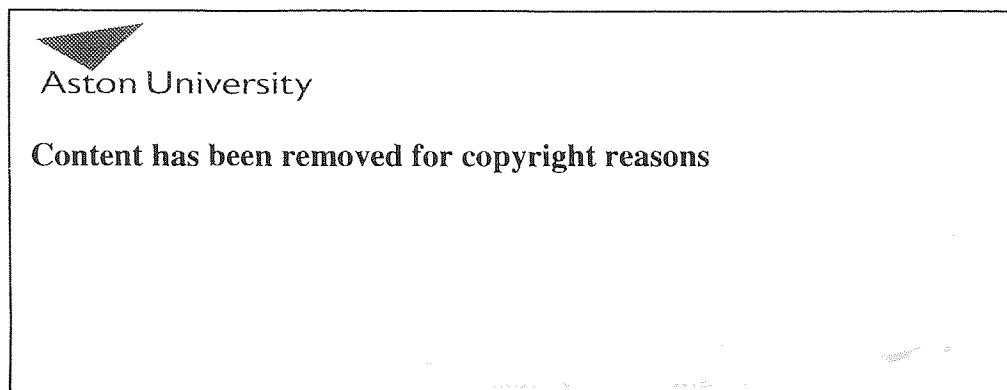
Figure 2.4: Magnetic field produced by human brain, logarithmic scale. [*Adapted from Vrba, 2002*]

A SQUID consists of a ring of superconducting material, interrupted by weak Josephson junctions (Josephson, 1962), and is connected to circuitry for detecting changes in flux penetrating the loop [section 2.2.6]. In principle, when a resistive region interrupts a loop of superconducting wire it behaves the same as a continuous loop of metal. That is, current flow within the loop decays rapidly. If however the ring is interrupted by thin sections of nonsuperconducting materials (e.g. two weak Josephson junctions), currents less than this 'weak link' (i.e. the critical Josephson value [I_c]) can penetrate the resistive barrier with no voltage drop. Changes in the magnetic field alter the magnitude of current flow in the ring. If the current level within the ring is already at the critical value, a small change in the impinging magnetic field causes the total current flow to exceed the critical value, and a measurable voltage drop across the Josephson Junctions occurs. Flux changes are hence detected by monitoring the voltage across the junctions, allowing the SQUID electronics to detect small time-varying neuromagnetic field changes associated with neural activity (Fagaly, 1990; Hamalainen *et al.*, 1993).

2.2.4 Signal preservation, noise reduction and amplification

Ambient magnetic noise in the environment, such as the noise from power lines, moving vehicles, electronic equipment and elevators, can be eliminated or minimised by conducting all recordings in a magnetically shielded room. Most magnetically shielded rooms are comprised of one or more layers of mu metal typically mounted on aluminium plates (Lewine & Orrison, 1995). As magnetic flux prefers to take the path of highest permeability (Fagaly, 1990), shielding a room with mu metal and aluminium results in an eddy-current flow routed around the walls and away from the internally located sensor system. Furthermore, as the eddy currents in the aluminium layers produce magnetic fields that oppose the external world noise, the signals cancel out.

The CTF system at Aston is encompassed in a shielded room designed by Vacuumschmeltze GMBH and contains one layer of mu metal mounted on one layer of aluminium. Nonetheless, weak distant sources can still pervade the shielding. Fortunately these noise sources are mostly eliminated using a gradiometer design.

Gradiometers exploit the fact that the strength of the magnetic field generated by a dipolar magnetic source decreases with the square of distance from the source. Whereby distance sources produce a magnetic field that is almost spatially uniform, nearby sources produce magnetic fields with comparatively large spatial gradients. In its simplest configuration, a gradiometer consists of two magnometers arranged in series and wound in opposition [Figure **2.5a**]. When a time-varying magnetic signal passes through the gradiometer, oppositely directed currents within the lower pick-up coil and upper bucking coil are induced. If the signal is from a distant source, the currents induced in each loop will be almost identical, but of opposing directions, resulting in no net signal. If the signal is from a near source, the gradient of the signal will be steep and a significant mismatch of current in the two coils induced; consequently a net signal will be produced (Papanicolaou, 1995; Vrba & Robinson, 2001). This arrangement gives noise reduction for distant sources and is known as a first-order axial gradiometer. The CTF system at Aston consists of 151 first order axial gradiometers, with 2cm diameter coils, and a baseline distance between the pick-up coil and upper bucking coil of 5cm. An additional feature of the system is the presence of 30 reference channels. Data from these channels can be combined with data from the sensor channels to simulate second- and third-order gradiometers. A second-order gradiometer is

insensitive to magnetic noise that does not have a uniform gradient over space. This provides better rejection of far-field noise but does reduce the sensitivity of the system to deep sources (Papanicolaou, 1995). Synthetic third-order gradiometers attenuate noise at low-signal frequencies (e.g. less than 5 Hz), and when used in conjunction with shielded rooms can reduce noise by a factor of 10 [see Figure 2.5b]. However, these gradiometers also reduce sensitivity to deep sources, although Vrba & Robinson (2001) argue that signal attenuation is less for synthetic higher-order gradiometers than those *in situ*. Moreover, synthetic third-order gradiometers can eliminate the MEG systems sensitivity to vibrational noise such as head motion.

Noise cancellation by synthetic gradiometers is reversible and can be carried out in real-time or post-processing. Dependant on signal properties (e.g. frequency, depth of source), different gradiometers can therefore be synthesised to maximise signal to noise ratio's (Vrba, 2002).
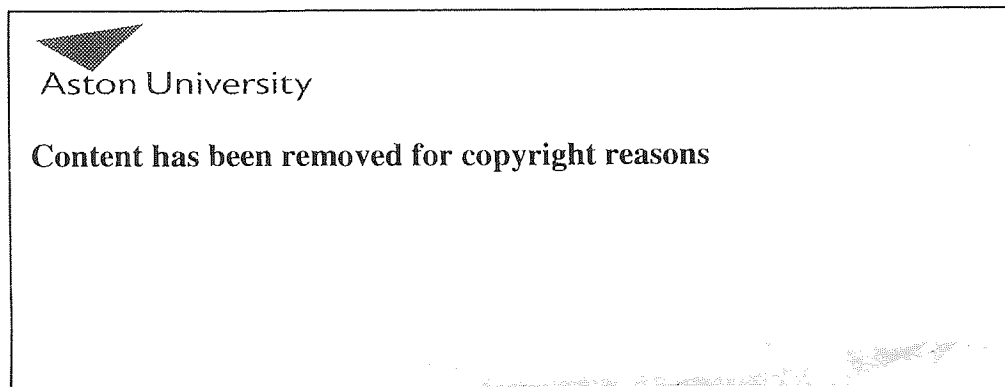
Figure 2.5: (a) Schematic of a first order axial gradiometer consisting of two oppositely wound coils inductively coupled to a SQUID sensor. (b) Reduction of environmental noise by a shielded room, synthetic gradiometers and adaptive methods (e.g. SAM) *[from Vrba, 2002]*.

2.3 Source Reconstruction and Synthetic Aperture Magnetometry

2.3.1 Introduction

The end product of a magnetoencephalographic scan is a 2-D temporal pattern of magnetic fields collated over the surface area of the scalp. To establish the source of the signals, one must solve what is termed the inverse problem. This is the spatial configuration, number, strength and temporal occurrence of neuronal currents from the magnetic field distribution (Hari, Levanen, & Raij, 2000). However, in the absence of any assumptions about the former parameters, the inverse problem is insoluble (i.e. there is no unique solution). Reducing the non-uniqueness of the problem is therefore usually achieved by adopting *a priori* assumptions. One common assumption, for instance, is that the source can be modeled as one or more equivalent current dipoles. This constraint can then be used in the formulation of algorithms to solve the forward problem and reconstruct the source location(s).

2.3.2 The forward problem

The forward problem involves determining what the output of the MEG sensors would be given activation within a certain cortical area. To resolve the inverse problem, the forward problem must first be solved.

To achieve mathematically viable solutions to the forward problem, common *a priori* constraints are the modelling of the head as a spherically symmetric volume conductor and the modelling of the current as an equivalent current dipole [ECD]. These constraints (outlined in the following sub-sections) simplify the problem, and the source(s) of the magnetic field patterns detected at the sensors can be computed using volume-conducting theory based on the Biot-Savart law. For an extensive mathematical computation of this law and its application to the solution of the inverse problem, see Sarvas (1987).

2.3.2.1: Source modelling

The relationship between neural activity and associated magnetic fields can be reconstructed using a model based upon current flow within neurons. Given that neuronal activation associated with an action potential can be modeled as a single dipole

[see section *2.2.1.2*], when an event is attended to, a large number of neurons and *n* current dipoles are synchronously activate. This total magnetic field can be expressed as the vector sum of the single fields. If these dipoles are located close to one another (i.e. within a few cubic millimeters) and oriented in the same direction, the total magnetic field can be considered as being generated by just one equivalent current dipole. Thus, a way to model the source of the MEG signal is by using an equivalent current dipole. Moreover, as it is known that pyramidal cells present a preferential alignment in a direction perpendicular to the cortex [see Section *2.2.1.3*], an ECD serves as a likely and feasible model of neuronal activation. Additionally, according to Snyder (1991), the assumption that a small area of cortex can be modeled as an ECD is reasonable given that the active area is small relative to the distance from which the signals are measured.

2.3.2.2: Volume conduction

Current opinion suggests that it is the intracellular primary currents that are responsible for producing a measurable magnetic field [see Section **2**, this Chapter]. However, this statement is only true when the cell medium is of infinite dimensions and uniform conductivity (Pizella & Romani, 1990); but the brain does not conform to these truisms. Therefore, to compute the pattern of magnetic signals distributed over the scalp, a model of volume conduction is needed to resolve these additional complexities.

One model commonly used with MEG involves representing the boundary of the skull as a sphere. This model is adopted because concentric spherical layers, such as those associated with the skull and scalp, do not disturb the magnetic field produced by the ECD (Williamson & Kaufman, 1981). Furthermore, when used in conjunction with a homogenous head model, the magnetic field does not depend on the conductivity of the medium (Romani & Pizella, 1990). Hence, the brain as an inhomogeneous medium consisting of cerebral tissue, scalp & skull is circumvented.

The pattern of a primary dipolar current is, however, perturbed at the point of the skull boundary [Figure **2.6a**]. To address this problem, the simulation of secondary volume currents is introduced. These current sources are oriented perpendicular to the boundary and, when combined with a model of the dipole in an infinite medium, simulate the perturbed dipolar current [Figure **2.6b**]. The problem of skull boundaries is therefore resolved, and the resultant magnetic field is modelled to reflect a combination of

primary and secondary sources (Lewine & Orrison, 1995). An advantage of this solution is that in a single spherical volume conductor model these secondary currents do not contribute to the measurable MEG signals (Cuffin, 1986). Therefore, the modelling of the head as a single homogenous volume sphere, although crude, greatly simplifies the evaluation of the measurable magnetic field.

a   b

Aston University

Illustration removed for copyright restrictions
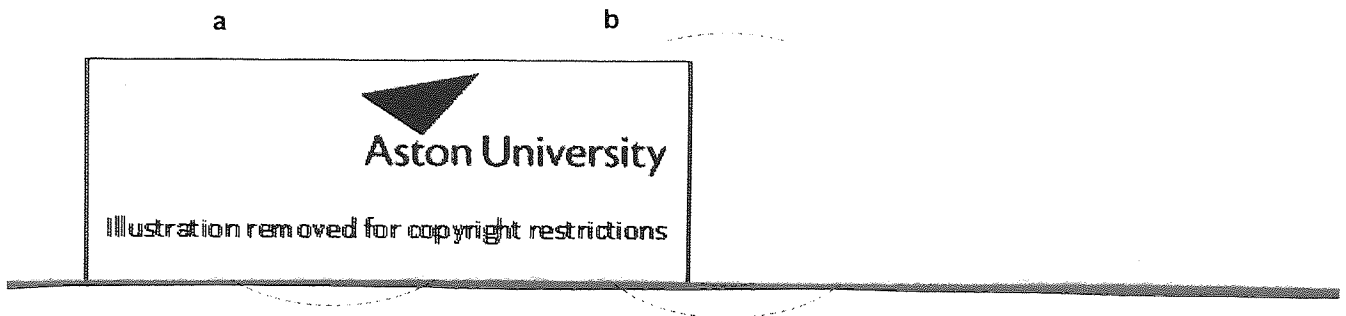
Figure 2.6: (a) The pattern of volume currents (dashed line) from a primary dipolar current is perturbed by electrical conductivity barriers. (b) This perturbed pattern is mathematically equivalent to that which would be produced in an infinite medium by the original impressed current (centre) plus the currents associated with secondary sources positioned at, and oriented perpendicular, to the barrier. *[Adapted from Lewis & Orrison, 1995]*

In recent years more realistic head models have been introduced, with MRI segmentation used to obtain meshes for real-shaped skulls, scalp and brain. This information can then be used in conjunction with finite element models [FEM] (e.g. van den Broek, Reinders, Donderwinkel & Peters, 1998), boundary element models [BEM's] (e.g. Crouzeix, Yvert, Bertrand & Pernier, 1999) or multi-sphere models in order to provide a more robust solution to the forward problem.

Modelling the brain as spherical, nonetheless, has implications related to the measurement of extracranial magnetic fields. It is assumed, for example, that due to symmetry, only tangential currents and not radial currents will produce an external magnetic field [Figure 2.7]. Additionally, a dipole located at the sphere's centre will not be detectable. As such, it has been argued that MEG is insensitive to both gyral and deep sources, these claims are however disputed. For example, Hillebrand & Barnes (2002) have demonstrated that thin strips of radially orientated neurons are abutted with nominal tangentially orientated neurons that do produce external magnetic fields. Additionally, as cited in Chapter 1, Section 1.4.3, Hari, Joutsiniemi & Sarvas (1988) and Lutkenhoner (1996) have demonstrated that deep sources can be localised, *albeit* with less accuracy.

Figure 2.7: (a) Coronal section of human brain. Cortex is indicated by dark colour. **(b)** The convoluted nature of the cortex (sulci and gyri) gives rise to both tangential and radial currents. Consequently only tangential currents **(c)** and not radial currents **(d)** will produce extracranial magnetic fields **(e)**. *[Vrba & Robinson, 2001].*

2.3.3 The inverse problem

The main confound of the inverse problem is that there is not a unique solution to the pattern of magnetic fields recorded at the scalp surface. To resolve the problem, once constraints like the modeling of the head as a homogenous sphere have been adopted, solutions to the problem are calculated using source reconstruction algorithms. Two such source reconstruction techniques are Equivalent Current Dipole Fitting and SAM (a beaming forming technique). These techniques differ with respect to both *a priori* information incorporated and assumption sets adopted.

2.3.3.1: Equivalent current dipole fitting

ECD fitting is one of several algorithms whose solution to the bioelectromagnetic inverse problem is based on the location of *discrete* sources. This method involves approximating the flow of electromagnetic current within a brain region, modeled using a single equivalent current dipole(s).

The process for locating a dipole(s) is iterative and based on a model of least-squares fit (Hämäläinen *et al.*, 1993; Romani & Pizella, 1990). The aim is to fit an ECD(s) to the observed magnetic field distribution. Using estimates of strength and orientation, the magnetic field map of a hypothetical dipole is compared to the actual magnetic field measured [see Equation **2.1** & Figure **2.8**]. This process is repeated until an optimal solution is found, that is, the dipole(s) with the minimum χ^2 value.

There are several disadvantages to the ECD model. For example, problems associated with the manual selection of starting parameters include, that if the first guess of dipole location and orientation lies in the local minimum, the global minimum may not be found. The ECD model further assumes that the recorded signal is the result of a single source and as such depends upon *a priori* assumptions as to the number of dipoles present.

$$\chi^2 = (B^{theor} - B^{meas})^2 / \sigma^2$$

Equation 2.1: Used to evaluate a model of least-square fit, where σ is the standard deviation of the measured field
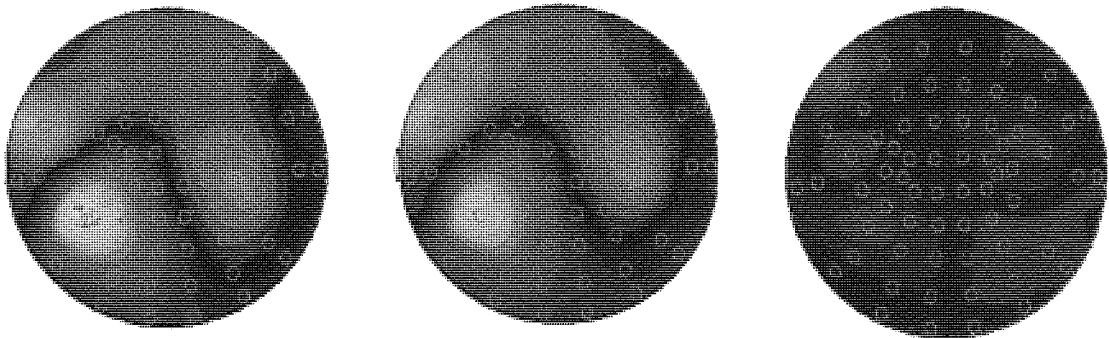
Figure 2.8: **(Left)** The distributed magnetic field of an auditory evoked potential. **(Centre)** The distributed magnetic field of the ECD. **(Right)** The difference between the actual field map and the ECD field map.

In recent years, a number of new algorithms have been proposed to refine the ECD fit and overcome such limitations. For instance, Lütkenhöner *et al.* (1998a; 1998b) provide a comprehensive overview of a current dipolar model that reduces standard deviations of the estimated dipole parameters by a factor of two, and Huang *et al.* (1998) put forward a 'multi-start method' that limits local minimum source errors. Additionally, Supek & Aine (1993) and Uutela, Hämäläinen & Somersalo, (1999) provide methods that require no explicit *a priori* assumptions about the source configuration, and Achim (1995) reviews multiple spatiotemporal source modeling methods that decompose spatiotemporal data into a number of source topographies (providing multiple dipole models). Nonetheless, despite these refinements, ECD methods rely on the averaging of many short epochs to distinguish evoked responses from background noise and

spontaneous brain activity. Unlike Synthetic Aperture Magnetometry, therefore, they **cannot** provide an estimate of induced (i.e. non-phased locked and poorly time-locked) activity.

2.3.3.2: Synthetic aperture magnetometry

Synthetic Aperture Magnetometry [SAM] is a beamforming technique that uses the same principle of fixed array weighted channels found in modern day radar systems to locate neural activity (Hillebrand, Singh, Holliday, Furlong & Barnes, 2005). A beamformer performs spatial filtering on data from a sensor array to discriminate between signals arising from a location of interest compared to those arising elsewhere. In modern day radar, a fixed array of spatially broadband selective filters is used to detect, identify, localize and track one or more objects (e.g. aircraft) of interest. At each point in space and time, a virtual antenna output is generated from the weighted sum of individual sensors to locate the object(s) (Shaw, 2002). The same principles are adopted in SAM: for any neuronal current source, an optimal set of weights can be calculated by selectively altering the contribution each gradiometer makes to the overall output of the spatial filter (Hillebrand & Barnes, 2003). In this respect, SAM differs from traditional source reconstruction techniques, such as dipole fitting, in that it does not attempt to solve the inverse problem *per se*. Traditional approaches model all contributors to the magnetic field pattern, including those that are the product of 'external world' noise. In SAM, however, the signals from such sources are ignored (Barnes & Hillebrand, 2003). Rather than try to account for all signal data, SAM selectively focuses on a region of magnetic signal for a specific location, spatial filter and time period (i.e. the forward problem).

In SAM, the spatial filter output can be thought of as a virtual electrode placed at the neural source location. To achieve the optimal weights for the virtual electrode, constraints of minimal power and unity gain are adopted. SAM minimises power (the variance of measured MEG signals), such that signals emitted from sources outside each specific voxel are suppressed, without attenuating power from the specific coordinate. Additionally, by limiting the power output of the filter, the gaussian passband curve is restricted and signal attenuation at non-source locations optimised [Figure **2.9**]. In SAM, a unique multi-dimensional solution for an equivalent current dipole is therefore

achieved by optimizing the beamformer output of the dense-array for a specific location in time and space (Tanguichi *et al.*, 2000).
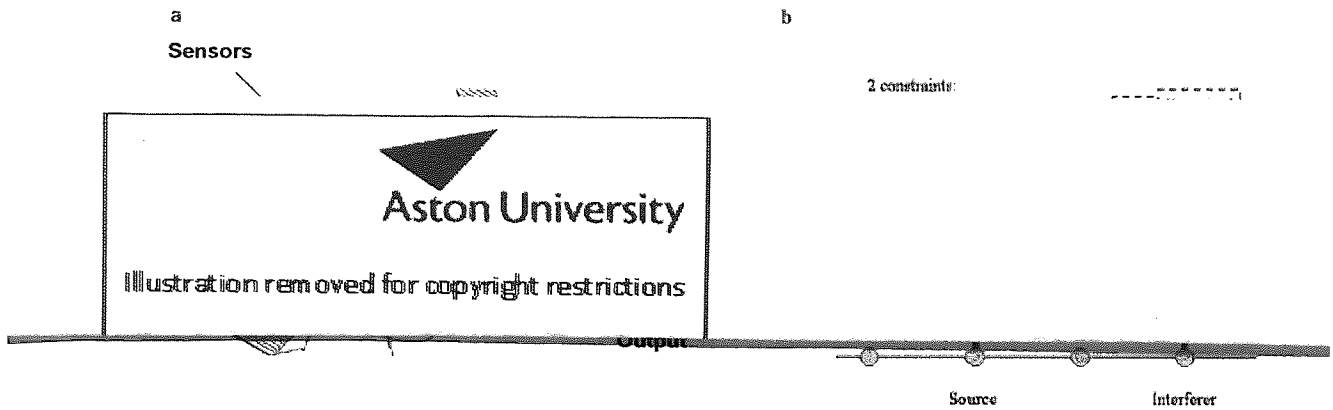
Figure 2.9: (a) A virtual electrode output is generated by the weighted sum of the gradiometers. (b) By restricting the power output of the filter the passband is restricted (adapted from *Hillebrand et al., 2005*).

A virtual electrode can be produced for all possible brain source locations and as the beamformer output is calculated using a weighted sum of the detectional array, it has the same precise millisecond time resolution as the original MEG signal (Singh, Barnes, Hillebrand, Forde & Williams, 2002). Additionally, multiple cortical sources at varying locations within the brain can be reconstructed without the need for any additional *a priori* spatial constraints, because the method exploits the spatial covariance of the source electrical activity (van Veen, van Drongelen, Yuchtman & Suzuki, 1997). Relatedly, the risk of being trapped in a local minimum is avoided by scanning a region for all possible sources. Adopting SAM as a source reconstruction technique therefore has numerous advantages over the dipole fit. Furthermore, SAM not only enables source changes as an estimation of time, but also the imaging of differences in power state for any VE location.

Essentially SAM involves dividing the time-series of a target voxel into passive and active states of predefined bandwidths and comparing power changes across the conditions [see Section 2.4]. In adopting this data analysis technique, averaging is not necessary and one can study brain responses that are poorly time locked to the stimulus presentation through utilizing box-car type experiments that do not rely on strict stimulus-response time locking. It is this that makes SAM especially suited for

measuring the non-phased locked events that are related to certain visual and motor phenomena discussed in Chapter **1** [Section **4**].

The main assumption adopted in beamformer techniques is that each cortical source has a time course that is not linearly correlated with any other source. The assumption is implicit in the minimum power and unity passband constraints adopted. A limitation of SAM, therefore, is that synchronous sources are self-cancelling and will not be detected by the sensors (Hillebrand *et al.*, 2004). Such sources would nevertheless need to maintain perfect synchrony throughout the entire time course of the task (Singh, Barnes, Hillebrand, Forde & Williams, 2002). Whilst this may prove problematic when studying conventional evoked-responses, it is precisely the reason why SAM is best suited for studying induced activity. That is, event related desynchronous activity [ERD] and event related synchronous activity [ERS] that are poorly time-locked and non-phased locked to the stimuli.

2.4: MRI Co-Registration & Complimentary Analysis Techniques

2.4.1 MRI co-registration

Co-registration of MEG and MRI data is based upon two techniques: the primary matching of discrete anatomical (fiducial) landmarks and the alignment of the two head surfaces defined in the respective co-ordinate systems. Fiducial points are based on easily recognisable landmarks, such as the nasion and bilateral pre-auricular points. With MEG, these fiducial points are determined by using a set of small localisation coils. These coils are attached to the head using a Velcro band, and a record of their positions (with respect to the MEG sensors) determined both pre- and post- recording. The average position of these landmarks forms the basis of the co-registration information (Adjamian, 2004). Subsequently, outside the shielded room, the participant's head is stabilised with a bite-bar and a digitizing pen is used to re-locate the same fiduciary points using a Polhemus Isotrak 3D digitizer (Kaiser Aerospace Inc.). The velcro band is then removed and a set of surface points representing the head-shape obtained by running the digitizing pen across the participant's scalp. These surface points are then co-registered with the segmented scalp surface obtained from the participant's MRI using Align software (www.ece.drexel.edu/ICVC/Align/align11.html). Align achieves the co-registration of the MRI and Polhemus headshape data by a least squares fitting procedure that minimises the Euclidean distance between the two surfaces (Kozinska, Tretiak, Nissanov & Ozturk, 1997) [Figure 2.10]. The MEG and Polhemus fiduciary points are then matched and the recorded MEG sensor data can be displayed on the volumetric MRI.

2.4.2 Single subject data analyses

2.4.2.1: Peak voxel analysis

Using SAM, systematic scanning on a voxel-by-voxel basis can be conducted to detect power changes within localised regions. If data contained active and passive periods (e.g. baseline vs. active period), the differences between related spectral power states can be assessed using a simple pseudo t-statistic calculation for each voxel. The volumetric images of peak power within predefined frequency ranges can then be represented on an individual's brain [Figure 2.11]. For these analyses, however, the pseudo t is not derived from the within-subject variance but a projection of the MEG
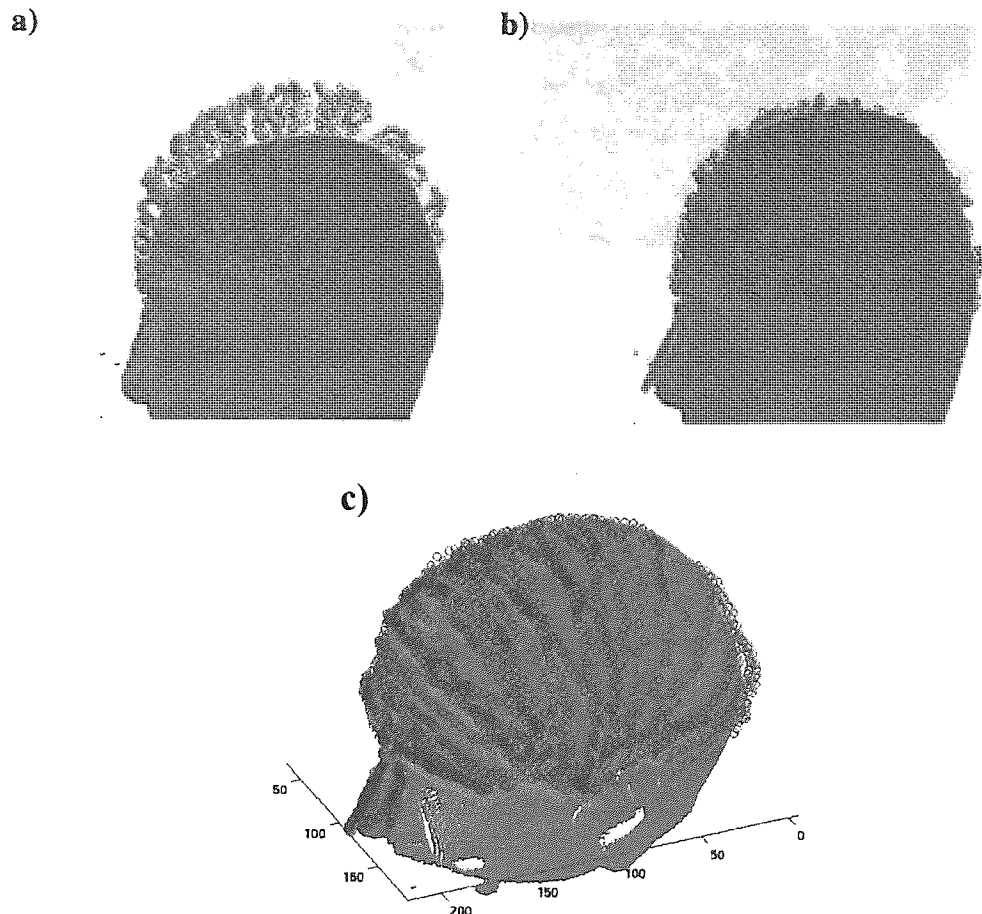
Figure 2.10: Co-registration of the MRI (red circles) and Polhemus (green circles) headshape data. **(a)** The points as first recorded. **(b)** Initial manual adjustment of data. **(c)** Minimising the squared Euclidean distance between the two surfaces using align software optimises the match. The blue circles depict the final co-registration calculated.

sensor noise (i.e. variance of MEG signals across trials). Thus to establish significance levels, once regions of interest [ROI's] have been identified, the timing/frequency data of these ROI's is investigated using transform methods.

2.4.2.2: Average time-frequency plots

To obtain time-frequency information for specific virtual electrodes, one must first filter the raw electrical current detected by the MEG sensors so that specific bounded frequencies (e.g. Alpha) and associated components can be detected. In this thesis a wavelet analysis was used to provide a time-varying energy signal in each frequency band. Until recently, the common method to study such brain rhythms had been to measure peak amplitudes through the use of Fourier Transform Methods [FTM's]. FTM's convert information from the time domain into the frequency domain by reconstructing an input wave into a series of sinusoids of various frequencies and
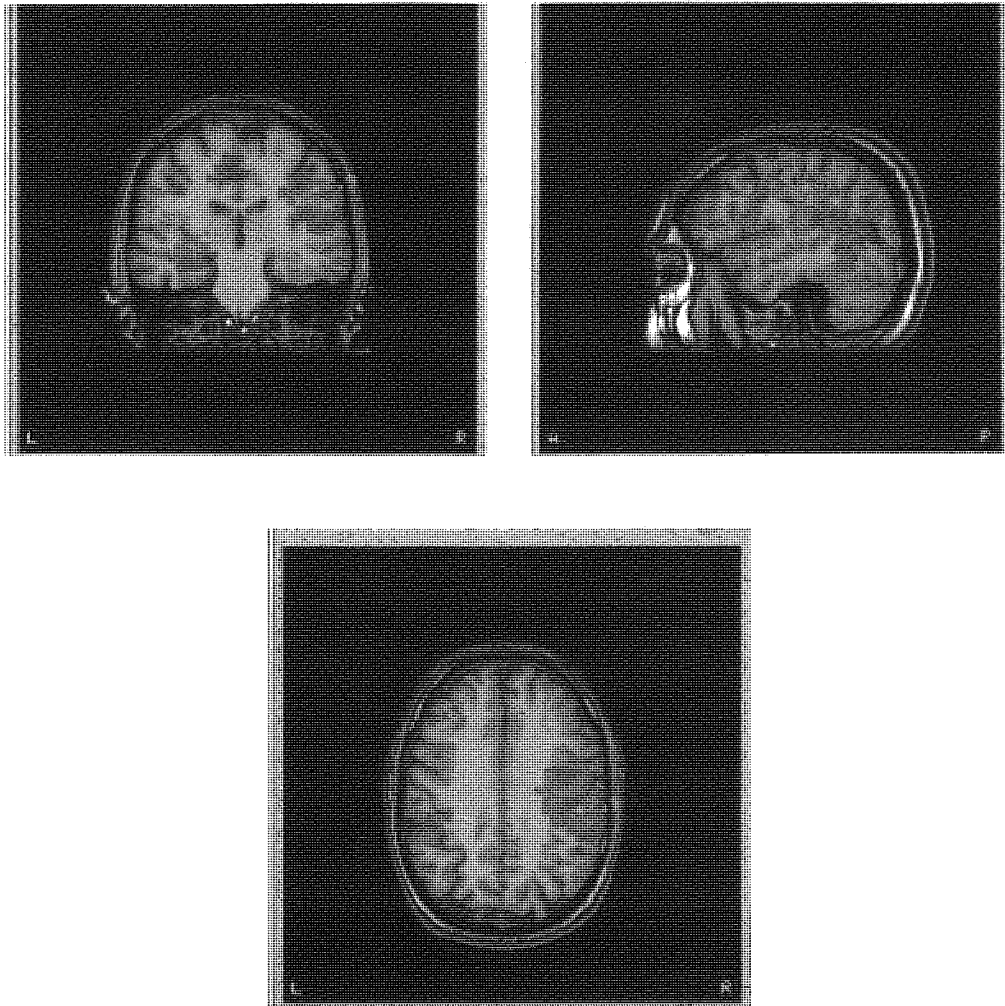
Figure 2.11: Virtual electrodes of peak power for predefined bandwidths can be displayed on an individual's co-registered MRI.

amplitudes. However, in consequence, at any given time, data is available in one modality only. Thus when component signal frequencies are investigated, the time course of the signal is lost or assumed constant (Sinkkonen, Tiitinen & Naatanen, 95). FTM's are therefore not suitable for studying non-phase locked signals.

In an effort to correct for this deficiency Gabor (1946) adapted the Fourier transform to analyze only a small section of the signal at a time; a technique called 'windowing'. This Short-Term Fourier Transform [STFT] provided a compromise between the time and frequency domain information, but with the drawback of a fixed window size [Figure **2.12a**]. Wavelet transform methods, however, use windows of different sizes and therefore offer a more flexible approach through which to investigate brain activity.

In the present analyses, an adaptation of Morlet's Waveform Transform [MWT] was used. In using a wavelet transform method, the analysis of transients differing on measures of amplitude, time-locking and phase-locking could be studied in detail.

The Morlet waveform was developed by Grossman and Morlet (1984) who noted that modulated pulses sent underground have a duration that is too long at high frequencies to separate the returns of fine, closely spaced layers (i.e. spatial information is lost). Instead of emitting pulses of equal duration, Morlet thought of sending shorter waveforms at high frequencies, and the concept of a wavelet function was borne. In its simplest form a Morlet wavelet is a Sinusoid multiplied by a Gaussian envelope, i.e. a Gabor function. In applying a 'Morlet' continuous wavelet to MEG data, the signal is multiplied by the wavelet and the transform is computed separately for different windows of the time-domain function. This is achieved by introducing a scale factor, a. As this scale factor varies, the width and height of the wavelet also vary (Polikar, 1996). When a decreases, the frequency support of the wavelet is shifted towards high frequency, and as a consequence time resolution increases but frequency resolution decreases. In contrast, when a increases, the frequency support of the wavelet is shifted towards low frequency, and the time resolution decreases but the frequency resolution increases (Tallon-Baudry, Bertrand, Delpuech & Pernier, 1997). Thus, frequency resolution of the wavelet reconstruction degrades as frequency increases, whilst the temporal resolution improves [Figure **2.12b**]. If at any point the spectral signal has a sinusoid signal that corresponds to the current scale factor value, the product of the wavelet at that location gives a relatively large value, comparative to a relatively low value (or zero) where the spectral component is not present [Figure **2.13**].

Once all regions in the time-frequency plane have been computed for a respective window size, s is increased and a new sampling at a new window size takes place. When the process is complete for all desired values of s, the waveform transform of the signal has been calculated.

In the present analyses, for a pre-defined passive time period, a baseline was computed by averaging information gained from a MWT analysis for a specific frequency band across time and epochs. Using this average as a reference, power changes relative to the baseline at any time point for the specific frequency band in the active (or passive)
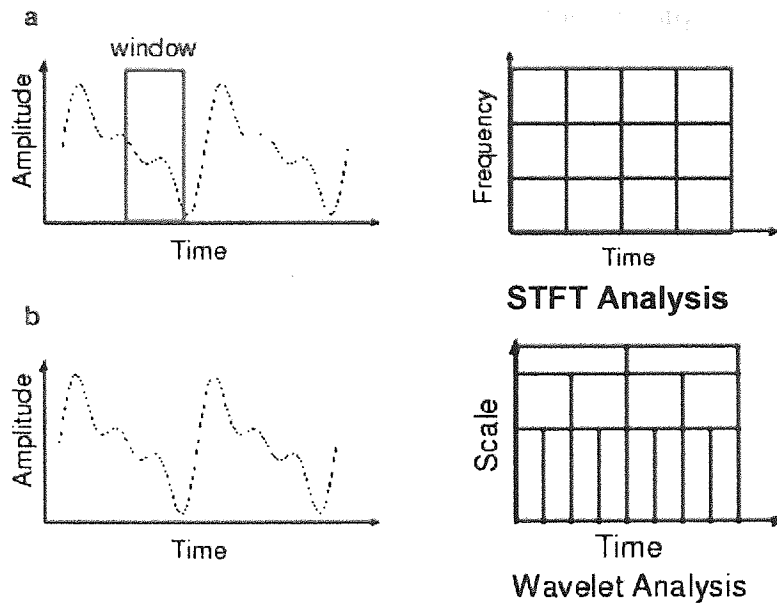
Figure 2.12: **(a)** In STFT's a window of fixed size is used and information, although limited, is available on both the time course and frequency of the constituent waves. **(b)** In a Morlet wavelet transform the introduction of a scale factor allows for adaptability of the function dependent upon frequency and temporal information. Information on the time course and frequency of the constituent waves is therefore more refined.
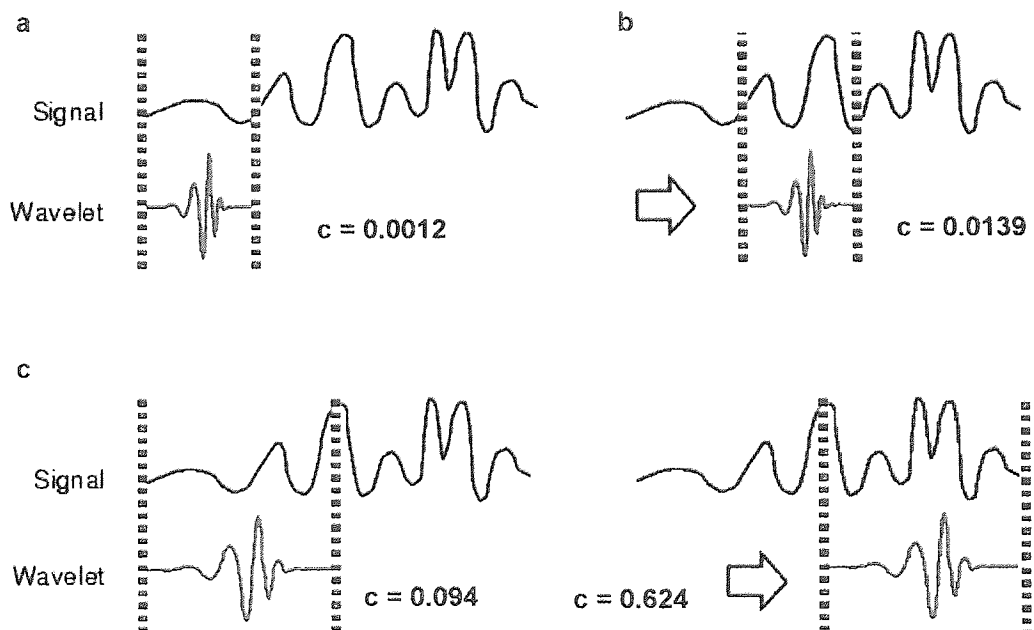
Figure 2.13: **(a)** A wavelet of scale a_1 is applied to the MEG signal and a value [c] representing how closely the wavelet correlates with that part of the signal recorded. The higher the value the higher the similarity. **(b)** The wavelet is shifted along the signal and the same procedure repeated. **(c)** A wavelet of scale a_2 is then applied and the same procedure adopted. These steps are repeated for all scales. By shifting the wavelet in time, the signal is localised in time. By changing the value of a, the signal is localised in scale (i.e. frequency). The resultant values can then be displayed on a time-frequency plot.

period can be calculated. This process is then repeated for further frequency/time ranges and the resulting power changes covering the entire frequency range can be presented in one single image. From this data, percent power changes can be calculated, giving a comprehensive overview of relative ERD/ERS activity across time and frequency [Figure **2.14**].

2.4.2.3: Bootstrapped time-frequency plots

To assess the statistical significance of the relative power changes, however, additional analyses are needed. In this thesis, a non-parametric method, *bootstrapping*, was used. Data analyzed with this method need not satisfy specific assumptions concerning population distributions (e.g. a normal distribution and/or homogeneity of variance). Bootstrapping is therefore suited to both the analysis of ERD/ERS (where more often than not outliers are apparent), and the analysis of data from randomised trial designs (where sample sizes may not be equivalent).

Bootstrapping is in idea similar to randomisation testing and involves randomly removing epochs of data and recomputing the metric of interest from these samples to draw conclusions about that metric (Fearon, 2003). The basic idea is to estimate the unknown population distribution from the known empirical distribution. For example, if one wished to estimate a parameter such as the standard error of a population, one method would be to draw repeated random samples from the data, calculate the mean of each sample, and examine the distribution of means across these samples (Burgess & Gruzelier, 1999). Thus, when estimating the standard error of ERD/ERS from a sample of *n* observations for a particular time-frequency point, a series of *n* random samples is taken, **with replacement**, from the observed data and the mean ERD/ERS value is calculated. This is repeated many times (e.g. 1000). The distribution of the mean ERD/ERS of these re-samplings can then be used to estimate standard error of mean ERD/ERS for a particular time-frequency point. This process is then repeated for all time and frequency points. In practice, however, rather than calculate standard error in this way, more accurate confidence intervals can be obtained using bootstrap samples to estimate the distribution of the t-values of a sample, or the *t* percentile bootstrap (Davidson & Hinckley, 1997). Such a method has been proposed by Graimann, Huggins, Levine & Pfurtscheller (2002) and is the method of bootstrapping adopted in this thesis for estimating confidence intervals for ERD/ERS.
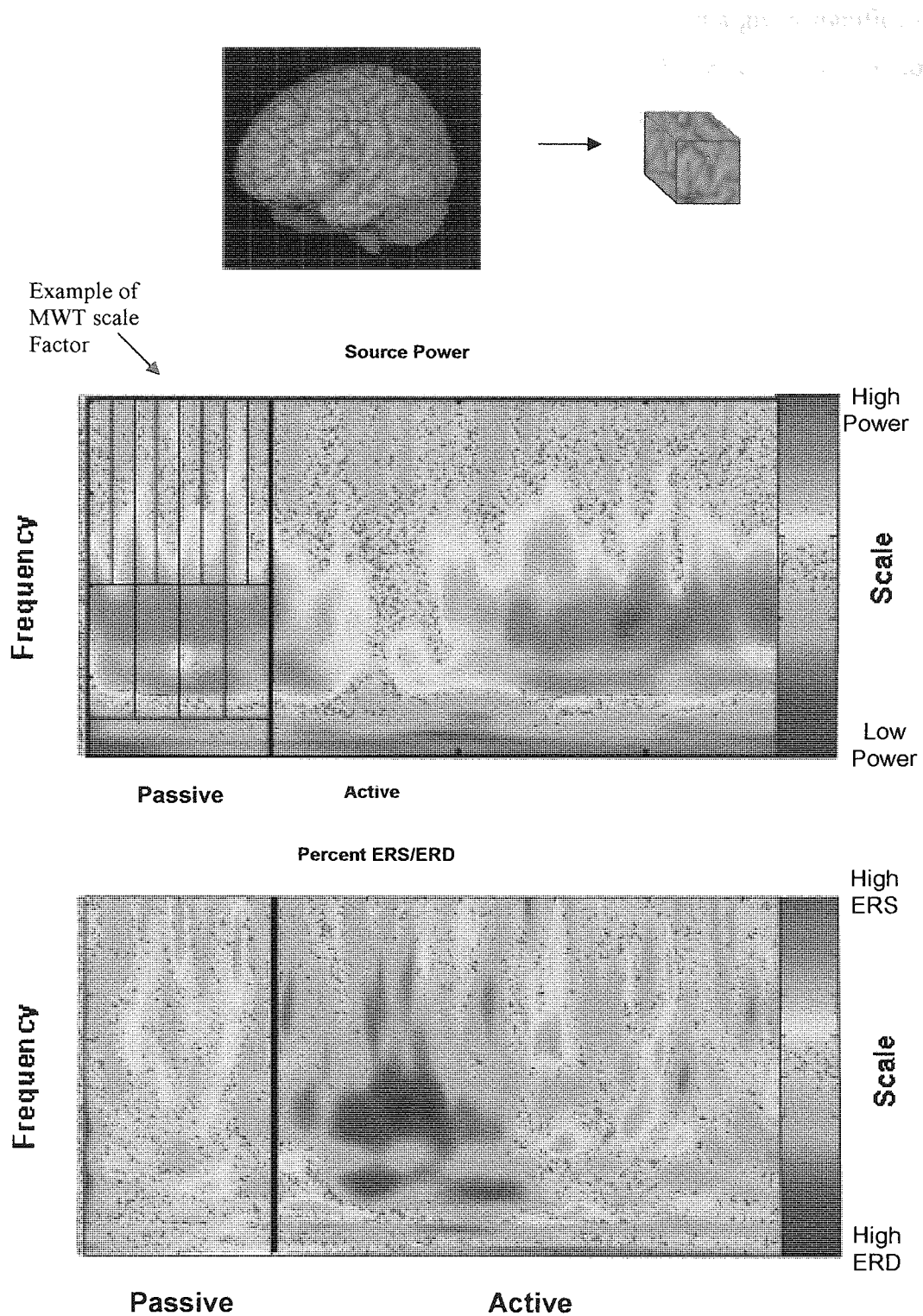
Figure 2.14: Top: An individuals MRI is divided into voxels of predetermined size (typically 0.5mm^3). Amplitude of the electrical current within each voxel is calculated as the weighted sum of the MEG sensors and ROI's established. Middle: For a pre-defined passive time region, using a Morlet wavelet transform, average baseline power changes across specific frequency bands, time and epochs are computed for an ROI. Power changes relative to this average baseline for specific time and frequency points across epochs can then be established for both the active and the passive time periods. Bottom: Based on the power change data established using a Morlet wavelet transform the % change in ERD/ERS relative to the baseline can be calculated

The bootstrap technique is used here to derive confidence levels at a given significance level for ERD/ERS obtained through the MWT and involves the selection of n random epochs of data, with replacement, from the MWT data. For these samples, the mean and standard deviations are calculated. This process is then repeated to obtain B bootstrap estimates that can be ordered to approximate the 'true' distribution for all samples from the subset used. The ERD/ERS can then be defined as the proportional power decrease (ERD) or power increase (ERS) in relation to this distribution [See Appendix I for exact mathematical formulae]. For any particular time-frequency point, if the 95% confidence interval boundaries are both positive (or both negative), then the associated ERS (or ERD) is significant. In adopting bootstrap analyses, any activity due to random fluctuations (or error) is minimized [Figure 2.15].
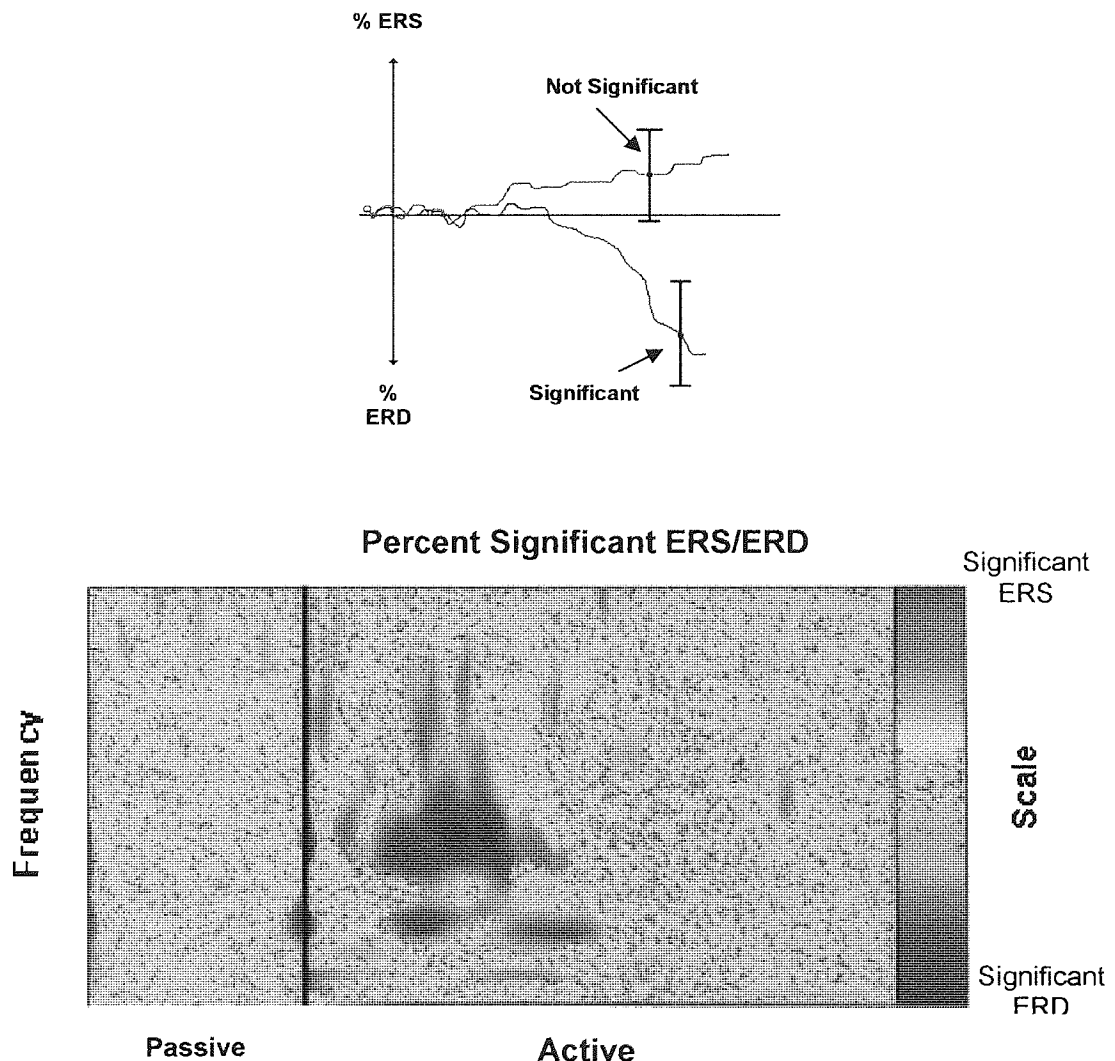
Figure 2.15. Top: Using data derived from the MWT, the bootstrap analyses gives the confidence intervals for ERD/ERS at a requested significance level (e.g. 0.05). Bottom: This information can be represented on a bootstrapped time-frequency plot. The resultant image is much 'cleaner' than in Figure 2.14 (Bottom Panel).

2.4.3 Group data analyses

2.4.3.1: Statistical parametric mapping analyses

The voxel-by-voxel scanning process used to detect power changes within an individual's brain allows for comparisons of brain activity across participants. A participant's peak voxel analysis data (once co-registered with their individual MRI) can be spatially normalised into the 3-dimensional anatomical co-ordinate space of Talairaich and Tournoux (1998). If this procedure is repeated for all subjects, t images of group activation can be constructed on the spatially normalised brain using SPM99 (Singh, Barnes, Hillebrand, Forde & Williams, 2002).

Two types of model exist for producing this statistic, the fixed-effect model and the random-effects model (Friston, Holmes, Worsley, Poline, Frith & Frackowiak, 1995). If a fixed-effect model is adopted the group data is collated and a t test based on the amplitude normalised by the variance of the effect conducted (i.e. *between-subject* differences). Assuming that the data is normally distributed, the t scores can then be transformed to z-scores and probabilities against the null hypothesis calculated. As only intra-subject variances are used to assess significance, this method has the advantage of being sensitive to small numbers of participants. A disadvantage is, however, that because only the between-subject differences are used to calculate the effects, data from one individual could dominate the resulting image. To overcome this limitation a random-effects model can be computed. In this model, before the data is pooled, *within-subject* variations are assessed and the data from individual activation maps also entered into a t-test. In this approach the final z-score is based on both inter- and intra- subject differences and the estimated activations are assessed against their variance across participants (Holmes & Friston, 1998). The random-effects model therefore allows for a quantitative inference of the average effect in the population. Despite these advantages, Singh, Barnes & Hillebrand (2003) argue that it is a less sensitive technique that requires high participant numbers (e.g. >10). This, they claim, is because of both the high inter-subject variances that occur in group neuroimaging studies and the model's sensitivities to possible deviations from normality that occur with low degrees of freedoms. For these reasons, Singh advocate the use of nonparametric permutation testing [e.g. SnPM] where the assumption of normality is not required.

70

2.4.3.2: Nonparametric permutation testing analyses

Rather than making inferences about samples and their relations to populations, permutation tests are based purely on the sample themselves (Fearon, 2003). Essentially, permutation testing presumes a null result and that data from two conditions (e.g. baseline vs. active) is from the same population. In assuming this, scores from the two populations can be collated and recombined in all possible (*n*) ways. For example, regardless of the metric of interest, if condition one contained the scores 2,4,6 and condition two contained the scores 1,3,5, the n_1 recombination of the samples could be 2,3,6 and 1,4,5. In permutation testing the original result is compared to the *n* permutation results and the probability of getting the result by chance alone calculated. Permutation testing therefore offers a method of statistical testing in which minimal assumptions (about *n*) are made.

The specific nonparametric permutation method adopted in this thesis is explained in detail by Nichols & Holmes (2002). In essence, the procedure is comparable to the random effects analysis, but when calculating the voxel-wise T image using the pooled inter-subject variance data, a normal distribution is not assumed. Instead, to assess the statistical significance of the *t*-score at each voxel, permutation testing is adopted and significance assessed by comparing the un-permuted *t* value against the permuted distribution. Additionally, for each iteration, the largest *t* value can be recorded and used to generate a probability distribution for *t* across the entire volume. By using this maximum probability distribution as the metric of interest, the problem of multi-comparisons is circumvented. Aside from assessing significant voxels (the maximum *t* values in the volume of interest), one can also assess cluster significance. A cluster is a region of interest that contains many active adjoining voxels. Although none of the individual voxels may reach significance, the summation of the connected cluster may be statistically significant. The procedure for cluster analysis, described by Singh *et al.* (2002), involves calculating a *t*-map for the volume, assigning a threshold and finding the largest voxel cluster that exceeds this threshold. This then acts as the permutation statistic and is tabulated in the normal distribution. At the end of the permutations, a cluster-size threshold is set and the probability of finding a cluster greater than this size calculated.

SnPM analyses provide a reliable statistical method for assessing group activity and rely on minimal data assumptions. The metric of interest can be manipulated dependant upon the needs of the researcher and correcting for multiple comparisons controls for type 1 errors. Results of group-imaging analyses techniques should, nonetheless, be interpreted with caution as a highly significant activation may represent a region of cortex that is **weakly** activated across all participants rather than a region that is fundamental to the task/stimulus. Furthermore, when using cluster analysis, because the assignment of the primary threshold is an arbitrary choice, the size and number of significant voxel clusters can vary immensely. Steinmetz, Furst, Freund (1990) also note that, because of the non-linear normalisation procedures adopted in SMP/SnPM, a match of local structures such as individual sulci and gyri can vary in position across individuals by several tens of mm [see also Figure **2.16**]. They suggest that such methods can only provide a good match for low frequency data, such as the gross outline of the brain.

Aston University

Content has been removed for copyright reasons
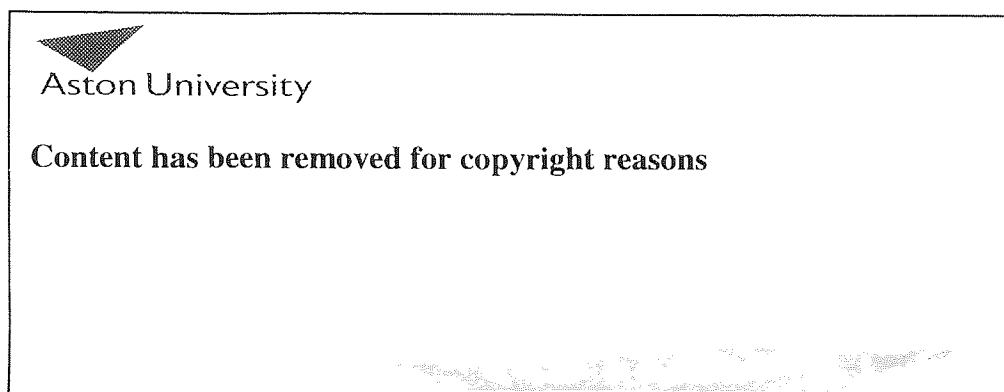
Figure 2.16: Variability of cortical landmarks after normalisation using the method described by Talairach and Tournoux, 1988. [*From Woods, 1996*]

Finally, it is now recognised that the Talairach co-ordinate reference system is not representative of the neuroanatomy of the general population. It is based upon the post-mortem brain of a single individual with an unusually shaped cerebellum (e,g. Carmack, Spence, Gunst, William, Schucany, Woodward & Haley, 2004). To align an individual's brain to this template, the brain is divided into 12 regions using one horizontal plane and three vertical planes. Each region is scaled, separately for

direction, to match the template atlas. This piecewise linear scaling, provides a simple method of converting an individual's brain into Talairach space. However, a criticism of this metric is that transformation into talairach space is unreliable, with no guarantee that a transformed brain will completely match either the shape or the anatomical features of the Talairiach reference system (Chau & McIntosh, 2005).

To allow for a better representation of average neuroanatomy, the Montreal Neurological Institute (MNI) developed an average brain template based on MRI scans from several individuals (http://www.mni.mcgill.ca/.). Whilst this reference system has been incorporated into several brain-imaging normalisation programmes (e.g. SPM99), the fact remains that the Talairach atlas is still considered the standard reference. Hence, co-ordinates transformed in MNI space are typically mapped into Talairach space, often resulting in further unreliability (see for example Hammers *et al*, 2002).

It is for these reasons, that a combination of single-subject data analyses and group data analyses have been undertaken in this thesis. In incorporating both methodologies, a more thorough and reliable investigation of the temporal, spectral and **spatial** neuronal activity of the brain can be achieved.

Chapter 3

Passive Perception and Sensori-motor Activation

3.1 Introduction

The efficiency with which we are able to grasp objects can be attributed, at least in part, to a repertoire of motor signals derived directly from vision. The evidence for this assertion comes from single cell studies on monkeys and behavioural and neuroimaging studies on humans. In monkeys, neurons in the anterior intraparietal sulcus and ventral pre-motor cortex are known to discharge not only during actual grasping movements but also during the passive perception of graspable objects [see Chapter 1 Section 1.2.3]. The latter supports the hypothesis that motor programmes associated with graspable objects are automatically generated whenever the monkey views them (Jeannerod *et al.*, 1995).

Comparatively, in humans, recent PET and fMRI studies have demonstrated that the passive perception of graspable tools elicits 'excitation' in a range of areas including sensori-motor and parietal cortex (Grafton, Fadiga, Arbib & Rizzolatti, 1997; Chao & Martin, 2000; Grezes & Decety, 2002; Grezes *et al.*, 2003; Grezes, Tucker, Ellis & Passingham 2003; Handy *et al.*, 2003; Kellenbach, Brett & Patterson, 2003; Creem-Regehr & Lee, 2004). Subsequently, it has been proposed that object affordances potentiate motor codes. These codes are postulated to provide information about the visual features and attributes of graspable tools and/or objects with the appropriate hand and finger movements necessary for using them [see Chapter 1 Section 1.3.3]. However, it has been known for sometime that shifts of attention may also contribute to the automatic generation of motor signals (e.g. Simon, 1969; Nicoletti & Umilta, 1989, 1994; Stoffer, 1991; Tipper *et al.*, 1992, 1998; Proctor & Lu, 1994; Rizzolatti *et al.*, 1994; Rubichi *et al.*, 1997; Sheliga *et al.*, 1997; Anderson *et al.*, 2002). For example, Anderson *et al.* (2002) have shown that attentional shifts within both object and non-object patterns are correlated with movement response advantages for one hand or the other, depending on the direction of the attentional shift.

It is also known that a number of action-related tasks result in oscillatory changes in beta frequency ranges within sensori-motor areas. For instance, a reduction in beta amplitude within such areas is not restricted to actual voluntary limb movement [see Chapter 1 Section *1.4.2.1*] but has also been found to occur when planning a hand action (e.g. Endo *et al.*, 1999; Guie *et al.*,1999; Szurhaj *et al.*, 2003), anticipating the need to make a movement (e.g. Bastiaansen *et al.*, 1999; Leocani, Magnani & Comi, 1999), observing another's actions (e.g. Hari *et al.*, 1998; Avikainene *et al.*, 2002), or when merely imagining making a movement (Pfurtscheller & Neuper, 1997; Neuper & Pfurtscheller, 1999). The basis of sensori-motor signals generated by the perception of graspable objects, however, remains unclear. If object affordances are important for action potentiation (e.g. e.g. Craighero *et al.*, 1996, 1998; Tucker & Ellis, 1998, 2001, 2004; Rumiati & Humphreys, 1998; Gentilucci, 2002; Hommel, 2002; Ellis & Tucker, 2000), then as with the above studies, a similar pattern of induced ERD in sensori-motor (and parietal) areas may occur when viewing graspable stimuli [see also Chapter 1 Section **1.4**]. Alternatively, if such motor codes are a consequence of attentional modulation, ERD in sensori-motor areas may be expected upon viewing a range of visual stimuli, irrespective of whether or not such stimuli afford action.

3.2 METHODS

3.2.1 Participants

Ten participants (4 males and 6 females, aged 23-52 years) with no history of neurological dysfunction or injury consented to participate in the study. All participants had previously undergone an anatomical MR volume scan, and were right-handed with normal visual fields and normal or corrected-to-normal (with contact lenses) visual acuity. The experimental procedures were in accordance with the tenets of the Declaration of Helsinki and received local ethical committee approval.
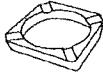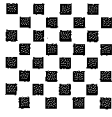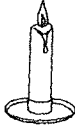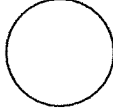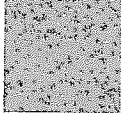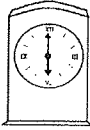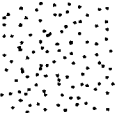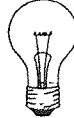
3.2.2 Stimuli

Achromatic images of object and abstract/geometric patterns were displayed on an Eizo T562-T monitor at a frame rate of 100 Hz, with a resolution of 589 lines by 816 pixels, using a VSG2/3 graphics card (from Cambridge Research Systems, Rochester, Kent, UK). Each image was viewed against a featureless background of mid-grey (mean luminance = 12 cd/m^2). The object stimuli were taken from a standardized set produced by Snodgrass & Vanderwart (1980) and were divided into *graspable-* and *standard-object* groups. Graspable objects were defined as those requiring a well defined single-handed grasping action during normal usage (e.g. cup, scissors and hammer). Standard objects were defined as those requiring minimal or no hand contact during normal usage (e.g. spectacles, ashtray and candle). The *abstract/geometrical* patterns were considered to have no cognitive association with a grasping action. They included non-patterned luminance patches (square, circular, or irregular), one-dimensional patterns (sine- or square-wave gratings of 1.0 c/deg periodicity, parallel lines), two-dimensional patterns (dartboard or checkerboard), and random-element displays (dots or lines). Each stimulus condition: (**GO**) '*graspable objects*', (**SO**) '*standard objects*' and (**AG**) '*abstract/geometric*' contained 10 stimuli. Examples of each stimulus-type are shown in Table **3.1**. The surface area of each stimulus (approximately 91 mm^2) did not vary across or within groups ($P_{(2,27)}$ = 1.207, p = NS).

3.2.3 Procedure

For each participant, extracranial magnetic signals were recorded in a magnetically shielded room using a 151-channel, whole-head biomagnetic imaging system (from CTF Systems Inc., Port Coquitlam, Canada). Participants were seated in an upright position and

76

Table 3.1: The 30 Stimulus Images Utilised

GO Stimuli		SO Stimuli		AG Stimuli*	
Cup		Ashtray		Checks	
Fork		Box		Dartboard	
Door Handle		Candle		Circle	
Hairbrush		Chain		Square	
Hammer		Clock		Parallel Lines	
Saucepan		Cotton Spool		Random Lines	
Scissors		Crown		Random Dots	
Spanner		Light Bulb		Random Shape	
Pen		Spectacles		Sine Wave	
Pliers		Vase		Square Wave	

* *As the AG stimuli were produced using a VSG graphics card, the corresponding images presented above are replicas, and unlike the GO & SO stimuli, not the actual images participants viewed.*

electromagnetic head coils attached to determine head position within the MEG helmet [see Chapter 2 Section 2.4.1]. The room illumination was low photopic and uniform, achieved through the use of 32 fibre optic lights directed around the room. The display monitor was positioned outside the shielded room and viewed through a window using a front-silvered mirror. The stimuli were viewed binocularly at an optical viewing distance of 2m, and a small blue central fixation target remained on-screen throughout each recording block. During a recording process the participants head was stabilized within the liquid helium dewar using an inflatable head-cuff.

There were 150 trials in each experimental block. Every trial consisted of a single stimulus presentation (150 ms) and an inter-stimulus interval (4000 ms) [see Figure 3.1]. The stimulus type was randomised between trials such that within any one block approximately 50 graspable object patterns, 50 standard object patterns and 50 non-object patterns were presented. This resulted in approximately five viewings of any single pattern per experimental block. Viewing was entirely passive - the only instruction given to participants was to maintain central fixation throughout the recording session. Repeatability measures were completed on five subjects.

4000 ms ⎯⎯⎯⎯⎯⎯⎯⟶ 150 ms ⎯⎯⎯⎯⎯⎯⎯⟶ 4000 ms
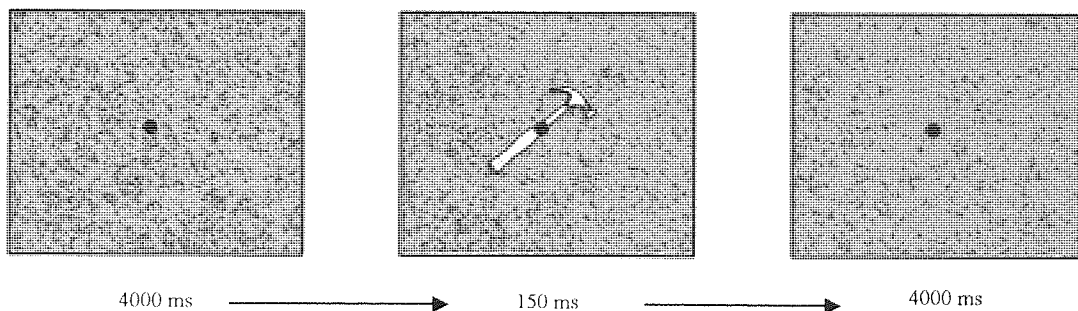
Figure 3.1: Stimulus Presentation Paradigm

Data were recorded in a single unaveraged run of duration 624.5 s at a sampling rate of 625 Hz, beginning 2 s before the onset of the first stimulus. The data were DC corrected and an antialiasing filter with a cutoff of 200 Hz was used. Immediately after data acquisition, the Polhemus Isotrak 3D digitizer was used to map the surface shape of each subject's head and localise the electromagnetic head coils with respect to that surface. Using the software *Align* (www.ece.drexel.edu/ICVC/Align/align11.html), this surface was matched to the

head shape extracted from MRI scans of each participant, enabling the co-registration of MEG and MRI data to form a functional brain image.

In order to determine accurately the position of the primary motor cortex, a control study examined the magnetic responses to slow movement of one observer's (SJA) right index finger. With the exception of epoch length (1000 ms only) single-subject analysis details for this paradigm were as reported below.

3.3.4 Data analysis

MEG data were analyzed using Synthetic Aperture Magnetometry (SAM), the adaptive beamforming technique discussed in Chapter 2 Section **2.2.2**. In the present analyses, each individual's MRI was divided into voxels of 5 mm^3, with a 'box-car' experimental design used to determine spectral power changes between matching pre-stimulus ('passive' state) and post-stimulus ('active' state) time windows (of 500 ms, 1000 ms and 2000 ms) for several frequency bands (5-15Hz, 10-20Hz, 15-25Hz, 20-30Hz, 25-35Hz and 30-40Hz) [1].

Each participant's individual anatomical MR was resliced in the same orientation and position as the SAM functional volume and spatially normalized into the same standard space as the MRI datasets using SPM99 (Holmes & Friston, 1998). Non-parametric permutation analyses (Nicholas and Holmes, 2001; Singh *et al.*, 2003) were then used to assess significant group effects for both voxel- and cluster-level inferences. Probability maps for significant effects (p < 0.05, corrected) were computed and visualised as group Statistical non-Parametric Maps (SnPM) using mri3dX (http://www.aston.ac.uk/lhs/staff/singhkd/mri3dX). The neuroanatomical locations of significant effects were determined using a Talairach database (Lancaster *et al.*, 2000). For detailed information concerning voxel and cluster level analyses techniques refer to Chapter 2 Section **2.4.3**.

Regions-of-interest (ROI) were determined from peak *t*-values on individual SAM images and from the Talairach coordinates of significant voxels in SnPM group SAM results. To examine the temporal sequencing of activity within a ROI, time-frequency spectrograms

---

[1] These frequency bands were adopted as it has been demonstrated that individual brain activity does not always conform to traditional brain rhythm nomenclature (e.g. Basar, Schurmann, Basar-Eroglu, Karaskas, 1997).

were calculated for a representative individual using a Morlet wavelet transform [See Chapter 2 Section 2.4.2]. Two types of spectrograms were created: (1) total average spectrograms were created from the average of the activation waveforms for a given ROI to reveal the level of evoked activity; and (2) bootstrapped spectrograms were created from single-trial activation waveforms for a given ROI to determined significance ($p < 0.5$) of induced (plus evoked) activity [refer to Chapter 2 Section 2.4.2.3]. Note that for the bootstrap analyses, a re-sample rate of 500 was adopted as it provided the optimal approximation of the 'true' distribution when considering computational limitations. It was decided upon by analysing a ROI in a single individual for re-sample rates of 100, 200, 500, 1000 and 2000.

3.3 Results

3.3.1. Localisation of primary motor cortex – single participant data

To determine the position of the primary motor cortex, SAM was used to spatially map event-related oscillatory changes to slow index finger movement of the right (dominant) hand for observer SJA. A standard active-passive boxcar design with an epoch length of 1000 ms was employed. Figure **3.2** shows sagittal (left hemisphere), coronal and surface-rendered (right hemisphere) MRI-SAM images of statistical estimates (t > 3) of power changes between the passive and active phases within the frequency band 10-20 Hz; no power changes were evident in either lower or higher frequency bands. The colour scale shows a neural activity index of oscillatory power changes: white-purple colours indicate a relative decrease in signal power during the active phase (i.e. ERD), while yellow-orange colours indicate a relative increase (i.e. ERS). Power decreases (ERD) were evident just anterior to the central sulcus when the active phase was compared with the passive phase, consistent with activity in the primary motor cortex (see Pfurtscheller & colleagues, 1997, 1999a; 1999b; 2001; Brunia, 2001). The power decreases tended to be left lateralised, consistent with finger movement of the right hand. The neuroanatomical locations of peak voxel activity were determined using a Talairach database (Lancaster *et al.*, 2000), and are shown in Table **3.2**.

3.3.2 Passive perception of object and abstract patterns – single participant data

In the same observer [SJA], SAM was used to map oscillatory power changes in the cortex to the passive perception of visual patterns. Figure **3.3** shows sagittal (left hemisphere), coronal and surface-rendered (right hemisphere) MRI-SAM images for SJA when viewing (a) graspable objects, (b) standard objects and (c) abstract/geometric patterns. The images depict statistical estimates (*t* > 3) of power changes between a pre- and post-stimulus time window of 1000 ms within the frequency band 10–20 Hz. Preliminary analyses showed that, for this observer, activity was maximal within this time period and frequency band. For each stimulus type, the activated areas show decreases in signal power (ERD) during the post-stimulus time window compared with the pre-stimulus window. No power increases were evident under any condition. The spatial distribution of ERD was similar for each stimulus type: for graspable objects [Figure **3.3a**], standard objects [Figure **3.3b**] and abstract/geometric patterns [Figure

t = -5.5   t = 0.0   t = 5.5
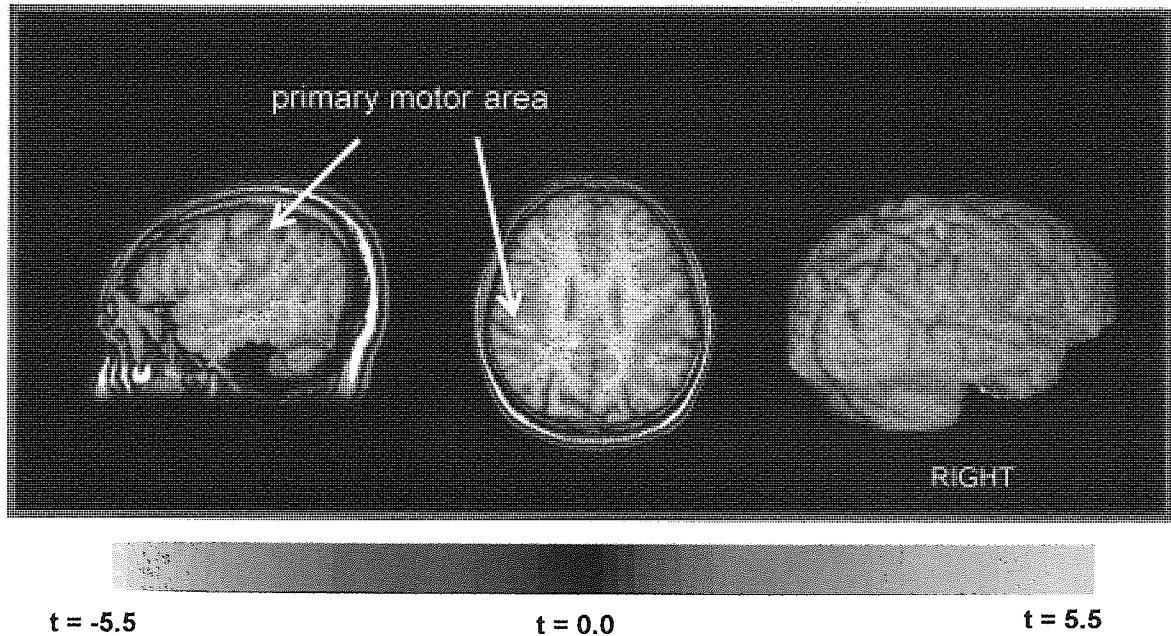
Figure 3.2: : Sagittal (left hemisphere), coronal and surface-rendered (right hemisphere) MRI-SAM images depicting statistical estimates ($t > 3$) of power changes within the 10-20 Hz frequency band between active and passive phases of the index finger movement task for participant SJA. The colour scale shows a neural activity index of oscillatory power changes: white-purple colours indicate a relative decrease in signal power during the active phase (i.e. ERD), while yellow-orange colours indicate a relative increase (i.e. ERS). Note that a power decrease (ERD) was evident just anterior to the central sulcus.

Brain Region	Talairach Coordinates	T value
Precentral gyrus (L), Frontal lobe	-42, -12, 45	-6.34
Postcentral gyrus (R), Parietal lobe	48, -27, 36	-6.07
Precentral gyrus (R), Frontal lobe (Ba4)	45, -15, 48	-5.98
Inferior parietal lobule (L), Parietal lobe (Ba40)	-39, -54, 45	-5.17
Superior temporal gyrus (L), temporal lobe (Ba22)	-60, -18, 0	-4.22
Middle temporal gyrus (L), temporal lobe	-36, -75, 21	-3.53

Table 3.2: Peak voxels of power changes in talairach coordinates depicting statistical estimates ($t > 3$) of power changes within the 10-20 Hz frequency band between active and passive phases of the index finger movement task for participant SJA. Negative t values indicate a decrease in signal power (ERD) during the post-stimulus phase, compared to the pre-stimulus phase. In all cases: a) only activity exceeding a t value of 3 was considered reliable; and b) the distance between peak voxels exceeded 7.5mm^3.

3.3c], bilateral activity was evident within extrastriate visual areas (BA19), occipito-temporal cortex (Ba37), superior parietal cortex (BA7), sensori-motor cortex (BA1-3), and within the central sulcus extending anteriorally into the primary motor cortex (BA4). The neuroanatomical locations of peak voxel activity determined using a Talairach database are shown in Table **3.3**. Note that, although not apparent on the surface-rendered images of the cerebellum in Figure **3.3**, ERD effects were evident within the posterior lobe of the cerebellum [see Table **3.3**]. Note also, that for the five
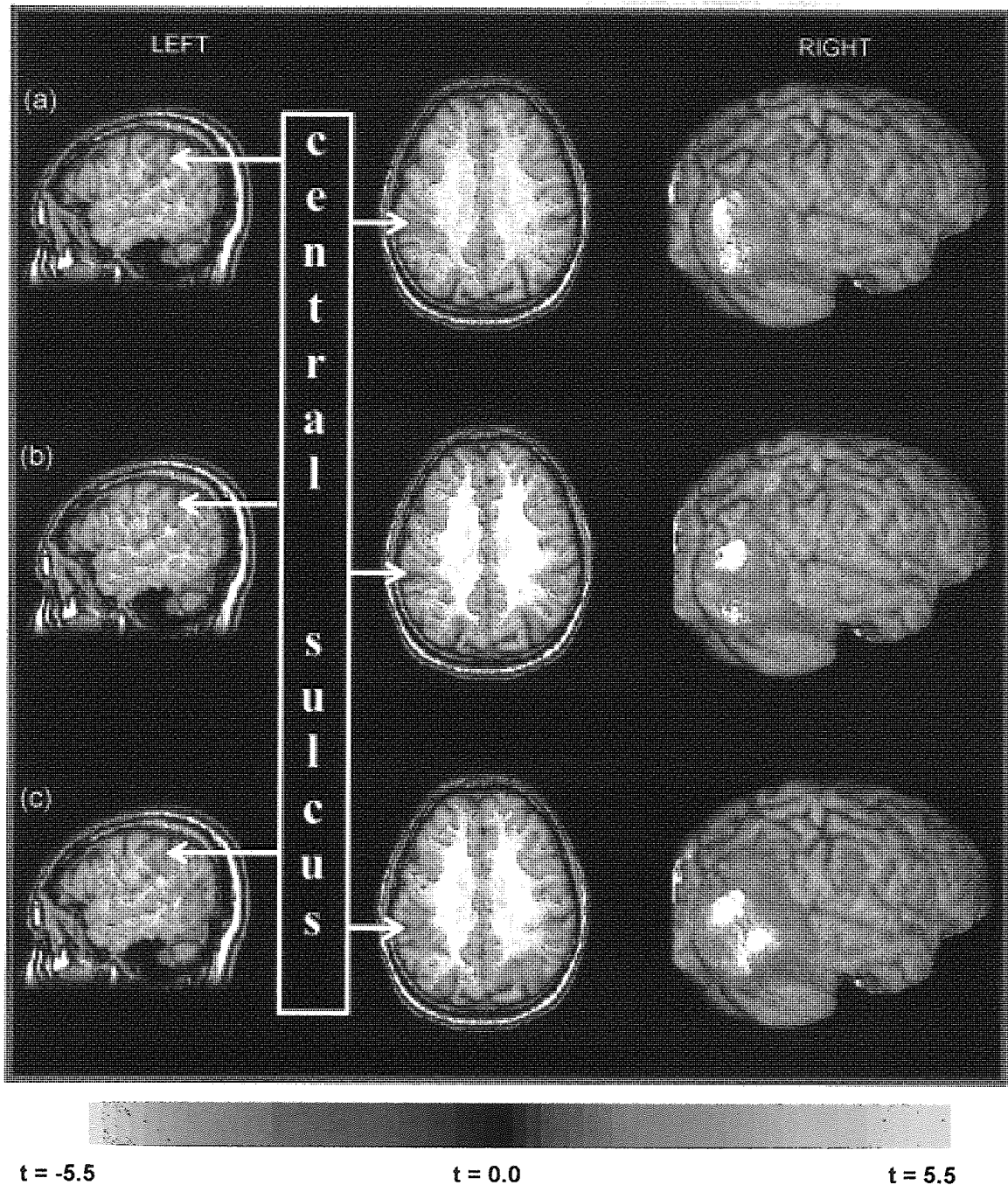
Figure 3.3: Saggital (left hemisphere), coronal and surface rendered (right hemisphere) MRI-SAM images depicting statistical estimates ($t > 3$) of power changes between a pre- and post-stimulus time window of 1000 ms within the frequency band 10–20 Hz for a single participant [SJA] passively viewing images of: (a) graspable objects, (b) standard objects, or (c) abstract/geometric patterns. The colour scale shows a neural activity index of oscillatory power changes: white-purple colours indicate a relative decrease in signal power during the post-stimulus window (i.e. ERD), while yellow-orange colours indicate a relative increase (i.e. ERS). For each stimulus type, bilateral ERD (10-20 Hz band) was evident within extrastriate cortex (Ba19), occipito-temporal cortex (Ba37), superior parietal cortex (Ba7), sensori-motor cortex (Ba1-3), and within the central sulcus extending anteriorally into the primary motor cortex (Ba4). The neuroanatomical locations of peak voxel activity are shown in Table **3.3**. Note that, although not apparent on the surface-rendered images of the cerebellum, ERD effects were evident within the posterior lobe of the cerebellum [see Table **3.3**]. Additionally, ERD is evident just anterior to the central sulcus, consistent with activation of the primary motor cortex in Figure **3.2**.

Brain Region	Talairach Coordinates	T value
Graspable Objects		
Middle temporal gyrus (L), Temporal lobe	-42, -72, 9	-12.8
Middle occipital gyrus (R), Occipital lobe	24, -87, 18	-9.10
Sub-gyral (R), Occipital lobe	24, -81, -6	-8.52
Superior parietal lobule (R), Parietal lobe (Ba7)	33, -57, 57	-5.60
Postcentral gyrus (R), Parietal lobe (Ba2)	54, -30, 39	-5.41
Postcentral gyrus (L), Parietal lobe	-57, -27, 36	-4.59
Inferior parietal lobule (L), Parietal lobe, (Ba40)	-30, -54, 57	-3.04
Standard Objects		
Sub-gyral (L), Occipital lobe	-27, -84, 21	-9.52
Sub-gyral (L), Occipital lobe	-30, -75, -6	-7.88
Middle temporal gyrus (L), Temporal lobe	-42, -72, 9	-7.38
Middle occipital gyrus, (R) Occipital lobe (Ba19)	30, -84, 18	-7.31
Lingual gyrus (R), Occipital lobe	27, -81, -9	-7.07
Superior parietal lobule (R), Parietal lobe (Ba7)	33, 60, 60	-6.22
Postcentral gyrus (R), Parietal lobe (Ba3)	39, -21, 48	-5.68
Inferior parietal lobule (R), Parietal lobe (Ba40)	51, -33, 39	-5.33
Precuneus (R), Parietal lobe (Ba7)	18, -48, 57	-4.69
Sub-gyral (L), Parietal lobe	-24, -60, 57	-3.70
Precentral gyrus (L), Frontal lobe (Ba4)	-60, -21, 39	-3.53
Inferior parietal lobule (L), Parietal lobe	-45, -39, 57	-3.22
Abstract/Geometric Patterns		
Sub-gyral (L), Occipital lobe	-27, -84, 21	-14.9
Middle occipital gyrus (R), Occipital lobe	24, -87, 15	-8.74
Middle occipital gyrus (R), Occipital lobe	36, -78, -3	-8.13
Inferior parietal lobule (L), Parietal lobe	-51, -39, 27	-5.74
Supramarginal gyrus (L), Parietal lobe	-45, -54, 27	-5.70
Postcentral gyrus (L), Parietal lobe	-54, -21, 36	-5.00
Inferior parietal lobule (R), Parietal lobe (Ba40)	60, -30, 27	-4.74
Declive, Posterior lobe (R), Cerebellum	30, -60, -27	-4.49
Inferior parietal lobule (L), Parietal lobe (Ba40)	-30, -54, 57	-4.45
Postcentral gyrus, (L) Parietal lobe	-42, -36, 54	-3.96
Inferior frontal gyrus (R), Frontal lobe (Ba10)	42, 39, 15	-3.62

Table 3.3: Peak voxels of power changes in talairach coordinates between a pre- and post-stimulus time window of 1000 ms within the frequency band 10–20 Hz for a single participant [SJA] passively viewing images of: (a) graspable objects, (b) standard objects, or (c) abstract/geometric patterns. Negative t values indicate a relative decrease in signal power (i.e. ERD) during the post-stimulus window. In all cases: a) only activity exceeding a t value of 3 was considered reliable; and b) the distance between peak voxels exceeded $7.5mm^3$. Note that whilst ERD is not apparent on the surface-rendered images of the cerebellum in Figure **3.3**, power decreases in this region were evident.

participants for whom repeatability measures were obtained, neuronamatomical locations of peak power were similar across runs. For data pertaining to this measure see Maratos, Anderson & Barnes (2002).

3.3.3 Passive perception of object and abstract patterns – group data

Figure 3.4 shows the group [n=10] normalised RFX surface-rendered images for the passive perception of (a) graspable objects, (b) standard objects and (c) abstract/ geometric patterns. The images depict statistical estimates ($t > 3$) of power changes between a pre- and post-stimulus time window of 1000 ms within the frequency band 10–20 Hz. Comparable to the single participant data, preliminary analyses showed that power changes were maximal within this time period and frequency band. For each stimulus type, the activated areas show either a decrease in signal power (ERD) or an increase in signal power (ERS) during the post-stimulus time window, compared with the pre-stimulus window. Again, the spatial distribution of ERD was similar for each stimulus type: for graspable objects [Figure 3.4a], standard objects [Figure 3.4b] and abstract/geometric patterns [Figure 3.4c], bilateral activity was evident within the cerebellum (e.g. declive and cerebellar tonsil) extrastriate visual areas (BA19), occipito-temporal cortex (BA37), superior parietal cortex (BA7), sensori-motor cortex (BA1-3), and within the central sulcus extending anteriorly into the primary motor cortex (BA4). Note that activity in all these regions predominated as ERD. The neuroanatomical locations of peak power changes are shown in Table 3.4

In assessing group effects for small numbers of subjects (e.g. ≤ 10), to avoid possible statistical distortion of the data from strong activation in any one individual, nonparametric permutation analyses are preferred [see Chapter 2 Section 2.4.2]. Therefore, probability maps for voxel-level effects ($p < 0.05$, corrected) were also computed for several frequency bands (5-15 Hz, 10-20 Hz, 15-25 Hz, 20-30 Hz, 25-35 Hz, and 30-40 Hz) and visualised as group Statistical non-Parametric Maps (SnPM) using mri3dX (www.aston.ac.uk/lhs/staff/singhkd/mri3dX). The SnPM group data analyses, displayed in Figures 3.5 – 3.7, provide evidence that the passive perception of each stimulus type resulted in pockets of desynchronised (but no synchronised) activity within the cortex and cerebellum, consistent with the general pattern of results shown in Figures 3.3 and 3.4. The locations of significant ERD group effects, as determined using a Talairach database, are shown in Table 3.5. The SnPM group SAM results are reported below for each of the frequency bands analysed.

3.3.3.1 5 – 15 Hz frequency band

Figure 3.5 shows the SnPM voxel-level results for (a) graspable objects, (b) standard
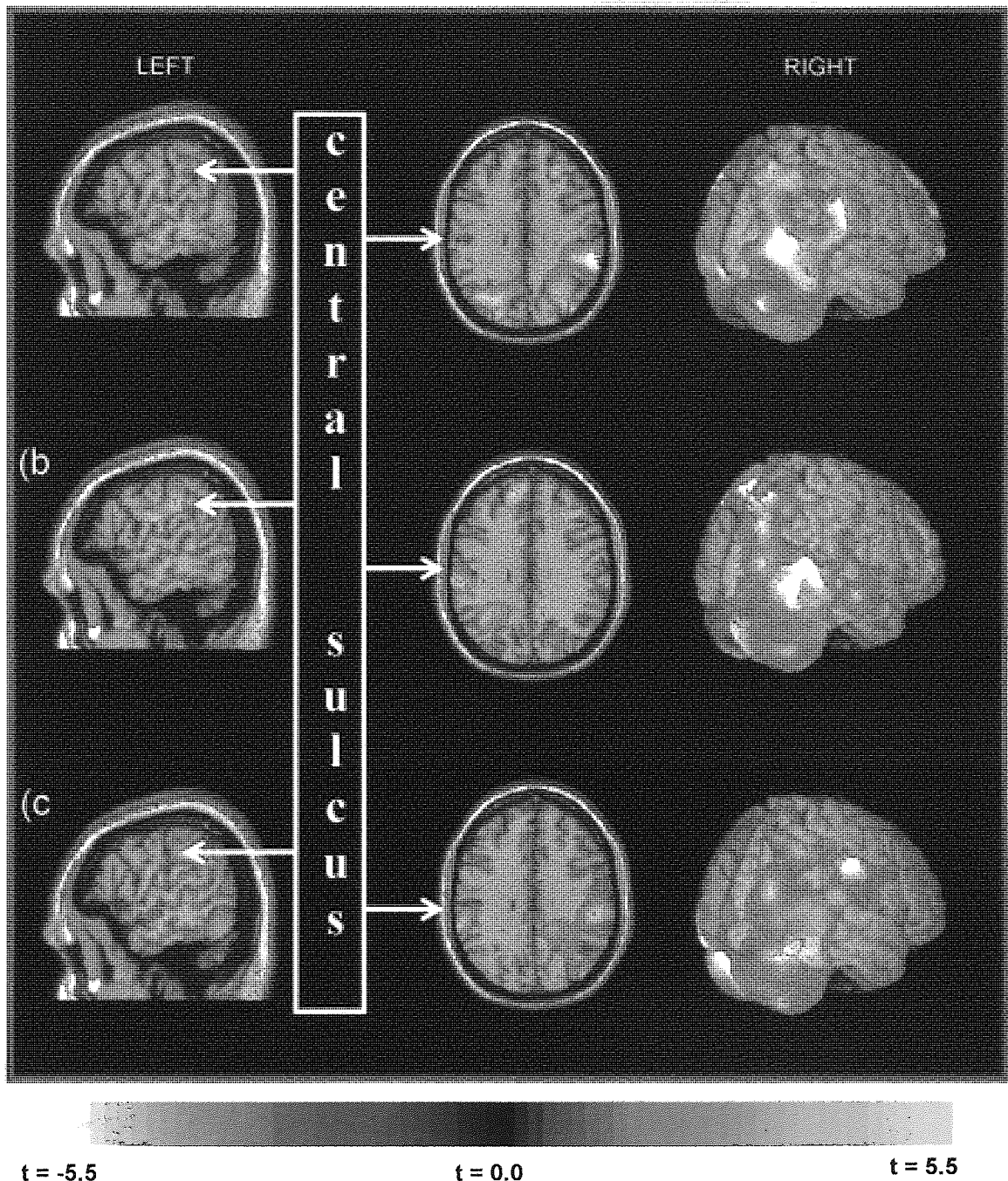
Figure 3.4: Saggital (left hemisphere), coronal and surface rendered (right hemisphere) normalized RFX MRI-SAM images depicting statistical estimates ($t > 3$) of power changes between a pre- and post-stimulus time window of 1000 ms within the frequency band 10–20 Hz for all participants [n=10] passively viewing images of: (a) graspable objects, (b) standard objects, or (c) abstract/geometric patterns. The colour scale shows a neural activity index of oscillatory power changes: white-purple colours indicate a relative decrease in signal power during the post-stimulus window (i.e. ERD), while yellow-orange colours indicate a relative increase (i.e. ERS). The images demonstrate similar patterns of ERD and ERS change for all three stimulus patterns including bilateral ERD (10-20 Hz band) within cerebellum, extrastriate cortex (Ba19), occipito-temporal cortex (Ba37), superior parietal cortex (Ba7), sensori-motor cortex (Ba1-3), and within or near the central sulcus (e.g. Ba4). The neuroanatomical locations of peak voxel activity are shown in Table **3.4**. Note that the distribution of activity across participants during perception of the three stimulus patterns is similar to that observed in the single participant images [Figure **3.3**].

Brain Region	Talairach Coordinates	T value
Graspable Objects		
Superior temporal gyrus (L), Temporal lobe	-72, -33, 6	-8.03
Inferior semi-lunar lobe (L), Cerebellum	-39, -66, -48	-6.78
Middle temporal gyrus (R), Temporal lobe	48, -60, 12	-5.48
Middle temporal gyrus (L), Temporal lobe (Ba21)	-63, -39, -15	-5.38
Superior frontal gyrus (R), Frontal lobe	30, 39, 45	4.79
Middle temporal gyrus (R), Temporal lobe (Ba37)	54, -60, -15	-4.73
Superior temporal gyrus (L), Temporal lobe (Ba42)	-66, -21, 9	-4.57
Angular gyrus (L), Parietal lobe	-36, -69, 30	-4.14
Middle temporal gyrus (L), Temporal lobe	-45, -75, 24	-4.10
Inferior temporal gyrus (R), Temporal lobe	51, -33, -24	-4.01
Middle occipital gyrus (L), Occipital lobe (Ba19)	-60, -69, - 9	-4.01
Postcentral gyrus (L), Parietal lobe (Ba2)	-24, -39, 75	-3.63
Lingual gyrus (L), Occipital lobe	- 6, -93, -12	-3.39
Postcentral gyrus, (R), Parietal lobe (Ba5)	6, -48, 66	-3.27
Middle frontal gyrus (R), Frontal lobe (Ba10)	45, 60, - 6	-3.24
Standard Objects		
Superior frontal gyrus (R), Frontal lobe	18, 51, 24	7.53
Precuneus (L), Parietal lobe (Ba7)	-27, -51, 54	-7.50
Medial frontal gyrus (L), Frontal lobe	-12, -51, 54	7.31
Middle frontal gyrus (R), Frontal lobe	33, 36, 24	6.85
Superior temporal gyrus (R), Temporal lobe (Ba22)	60, -60, 12	-6.43
Sub-gyral (r), Temporal lobe	42, -63, 0	-6.00
Superior parietal lobule (L), Parietal lobe (Ba7)	- 9, -72, 60	-6.00
Superior temporal gyrus (L), Temporal lobe	-66, -39, 3	-5.27
Inferior frontal gyrus (R), Frontal lobe	39, 30, 6	5.25
Declive (L), Cerebellum	-48, -81, 27	-5.21
Middle occipital gyrus (R), Occipital lobe (Ba19)	42, -87, 15	-4.98
Middle temporal gyrus (R), Temporal lobe	63, -30, - 6	-4.85
Postcentral gyrus (L), Parietal lobe	-66, -12, 24	-4.82
Inferior semi-lunar lobule (R), Cerebellum	51, -72, -45	-4.61
Lentiform nucleus (L), Cerebellum	-12, - 3, - 6	-4.49
Inferior parietal lobule (L), Parietal lobe	-54, -27, 30	-4.42
Inferior temporal gyrus (R), Temporal lobe	63, - 3, -16	-4.27
Inferior frontal gyrus, (L), Frontal lobe	-33, 33, 51	4.01
Superior frontal gyrus (R), Frontal lobe	18, 36, 51	3.88
Medial frontal gyrus (R), Frontal lobe	9, 33, 45	3.64
Inferior parietal lobe (R), Parietal lobe	63, -33, 27	-3.45
Cerebellar lingual (L), Cerebellum	- 9, -48, -18	-3.41
Abstract/Geometric Patterns		
Cerebellar tonsil (L), Cerebellum	- 9, -54, -42	-5.83
Middle occipital gyrus (R), Occipital lobe	39, -72, -15	-5.72
Postcentral gyrus (R), Parietal lobe (Ba1)	60, -27, 39	-5.49
Superior frontal gyrus (L), Frontal lobe	- 6, 60, -21	5.43
Paracentral lobule (R), Frontal lobe (Ba5)	15, -42, 54	-5.28
Culmen (L), Cerebellum	-42, -42, -30	-5.12
Medial frontal gyrus (R), Frontal lobe	9, 33, -18	-5.06
Superior occipital gyrus (R), Occipital lobe (Ba19)	42, -81, 24	-4.96
Middle occipital gyrus (R), Occipital lobe (Ba19)	54, -84, 3	-4.58
Declive (L), Cerebellum	-45, -69, -21	-4.48
Superior temporal gyrus (R), Temporal lobe (Ba22)	54, -51, 9	-4.38
Sub-gyral (L), Temporal lobe	-48, - 6, -12	-4.30
Inferior frontal gyrus (L), Frontal lobe	-48, 30, 15	3.98
Middle frontal gyrus (R), Frontal lobe	24, 54, 21	3.72
Medial frontal gyrus (L), Frontal lobe	9, 60, 15	3.57
Inferior frontal gyrus (L), Frontal lobe (Ba47)	-18, 12, -21	-3.37

Table 3.4: As in Table **3.3** but for all participants [n=10]. Negative RFX *t* values indicate a relative decrease in signal power (i.e. ERD) during the post-stimulus window

objects and (c) abstract/geometric patterns revealed by a pre-post stimulus comparison over 1000 ms in the 5-15 Hz frequency band. Voxels that are significantly activated (p <0.05) are shown as dark areas on sagittal and axial 'glass-brain' views, and as white-purple areas on surface-rendered images of the rear of the brain/cerebellum. Note that on glass-brain views, activation is integrated throughout the brain as if it were a transparent structure. The activated areas displayed on each image in Figure 3.5 indicate significant regions of power decreases. For this frequency range, the passive perception of both standard object patterns [Figure 3.5b] and abstract/geometric patterns [Figure 3.5c] resulted in significant power decrease effects within the sensori-motor cortex (*sm*) and occipito-temporal cortex (*ot*). In addition, significant power decrease effects in the 5 – 15 Hz frequency range were observed in the cerebellum (*c*) for all three stimulus types. However, within the cerebellum, differences were observed in the number of significant voxels reported; more significant voxels were recorded for graspable-object pattern viewing compared with standard-object pattern viewing, and for standard-object pattern viewing compared with abstract/geometric pattern viewing [see Table 3.5]. Additionally, for the abstract/geometric patterns [Figure 3.5c] the locus of significant activity was outside the brain. This aberrant localisation result is likely due to the normalisation procedures adopted and is discussed in more detail in Section 3.4.2.

The SnPM group SAM results shown in Figure. 3.5 were lateralised, though not consistently to any one hemisphere. Within the sensori-motor cortex, power changes were lateralised to the left hemisphere for standard-object patterns [Figure 3.5b], and to the right hemisphere for abstract/geometric patterns [Figure 3.5c]. Within the occipito-temporal cortex, power changes were lateralised to right hemisphere for both standard- [Figure 3.5b] and abstract/geometric patterns [Figure 5.3c]. And within the cerebellum, power changes were lateralised to the right hemisphere for object patterns [Figures 5.3a and 5.3b] but to the left hemisphere for abstract/geometric patterns [Figure 5.3c]. The analyses of MRI-SAM images using RFX analyses [see Figure 3.4 and Table 3.4] showed that the reductions in oscillatory power within the areas identified above were bilateral. The aberrant lateralisation result is possibly due to the normalisation procedures adopted [see Section 3.4.2].

3.3.3.2 10 – 20 Hz frequency band

Figure 3.6 shows the results of the same analyses as that reported in Figure 3.5 for the
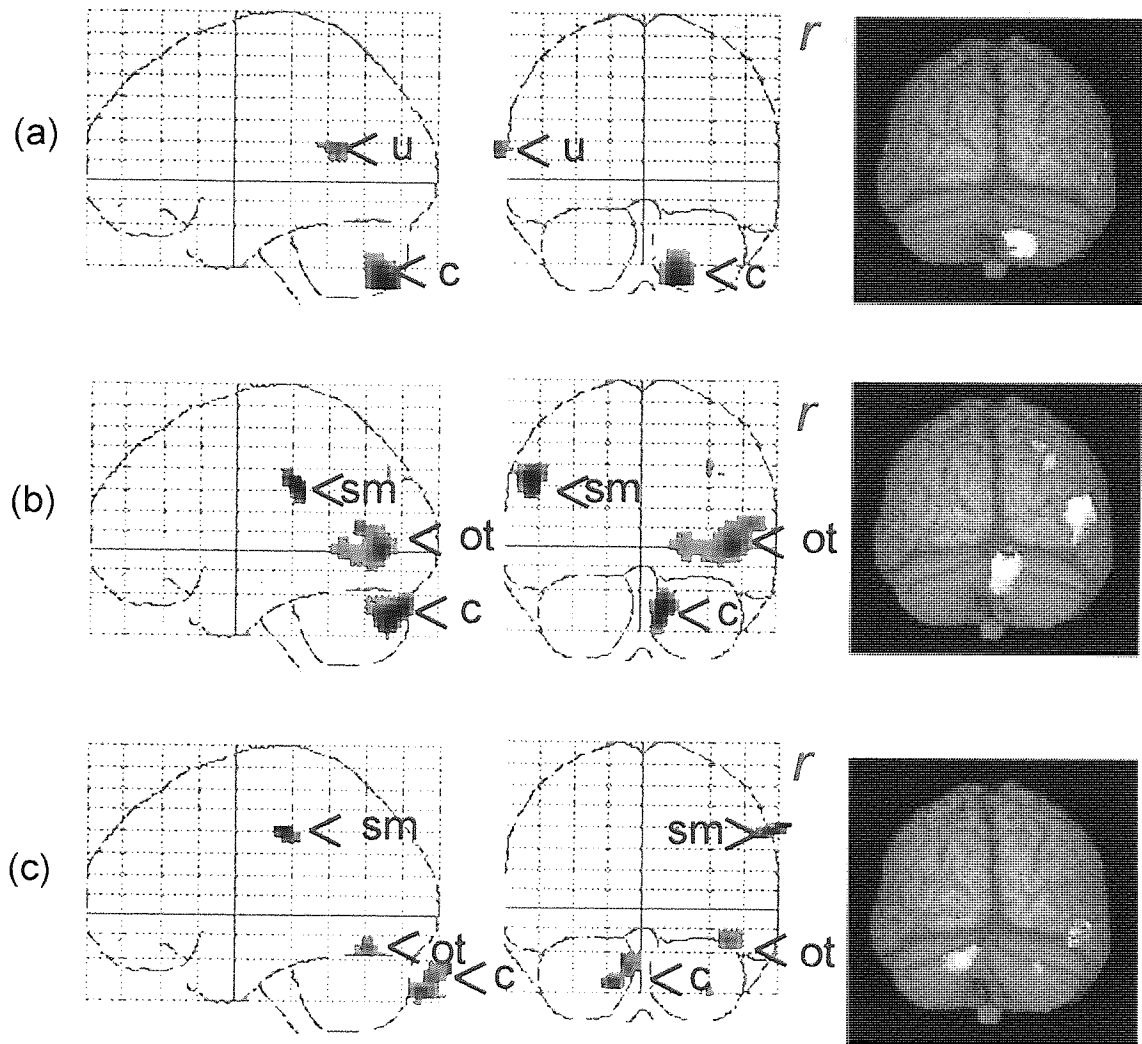
Figure 3.5: Group [n=10] SnPM voxel-level results for (a) graspable-object patterns, (b) standard-object patterns and (c) abstract/geometric patterns revealed by a pre-post stimulus comparison over 1000 ms in the 5-15 Hz frequency band. Activated voxels (p < 0.05, corrected) are shown as dark areas on sagittal and axial 'glass-brain' views, and as white-purple areas on surface-rendered images of the rear of the brain/cerelbellum. The red 'r' alongside axial glass-brain views indicates the *right* hemisphere. The activated areas displayed on each image indicate regions of desynchronisation (ERD). Significant ERD effects are evident within the sensori-motor cortex (*sm*), occipito-temporal cortex (*ot*), cerebellum (*c*), and one unidentified (*u*) area. The Talairach coordinates of significant ERD group effects are shown in Table 3.5.

passive perception of each stimulus type resulted in desynchronised activity within the sensori-motor cortex (*sm*) and occipito-temporal cortex (*ot*). Within occipito-temporal cortex differences were observed in the number of significant voxels recorded, with more significant voxels recorded for graspable-object pattern viewing compared with standard-object pattern viewing, and for standard-object pattern viewing compared with abstract/geometric pattern viewing [see Table 3.5]. Additionally, both graspable- and

Stimulus Type, Frequency & Brain Region	Talairach Coordinates	p	No of voxels
Graspable object stimuli, 5-15 Hz			
Posterior lobe, Cerebellum	**15, -75, -51**	0.006	141
Unidentified (L)	**-72, -51, 15**	0.017	31
Graspable object stimuli, 10-20 Hz			
Inferior temporal gyrus (Ba 19/37)	**51, -60, -12**	0.012	319
Middle occipital gyrus	*48, -75, 3*	*0.023*	
Inferior parietal lobe/Sensori-motor cortex (Ba40/2)	**57, -36, 30**	0.031	54
Middle temporal gyrus (L)	**-57, -57, -6**	0.035	90
Unidentified (L)	*-69, -60, 6*	*0.043*	
Parietal lobe, precuneus (Ba7)	**24, -72, 51**	0.035	31
Graspable object stimuli, 15-25			
Parietal lobe, Superior parietal lobule (Ba7)	**27, -66, 51**	0.010	36
Standard object stimuli, 5-15 Hz			
Inferior parietal lobe/Sensori-motor cortex (Ba40/1/2) (L)	**-54, -30, 33**	0.009	65
Posterior lobe, Cerebellum	**12, -78, -30**	0.010	114
Middle occipital gyrus	**45, -72, 0**	0.015	213
Middle Temporal gyrus (Ba19/37)	*54, -63, 12*	*0.021*	
Parrahipocampal gyrus (Ba10)	*21, -54, 0*	*0.026*	
Precuneus, Parietal lobe	**33, -75, 39**	0.038	3
Precuneus, Parietal lobe (Ba7)	**39, -84, 36**	0.041	1
Standard object stimuli, 10-20 Hz			
Precuneus, Parietal lobe (Ba7) (L)	**-27, -54, 54**	0.025	33
Posterior lobe, Cerebellum	**12, -81, -45**	0.027	27
Inferior parietal lobe/Sensori-motor cortex (Ba40/2) (L)	**-57, -27, 33**	0.027	21
Middle temporal gyrus (Ba37)	**48, -65, 3**	0.029	25
Posterior lobe, cerebellum	**15, -84, -36**	0.033	8
Abstract/geometric stimuli, 5-15 Hz			
Sensori-motor cortex (Ba1-3)	**69, -24, 42**	0.016	38
Posterior lobe, Cerebellum (L)	**-15, -90, -36**	0.022	63
Unidentified (L)	*-9, -105, -27*	0.024	
Unidentified (L)	*-6, -96, -30*	0.025	
Sub-gyral, Occipital lobe	**42, -66, -15**	0.024	27
Posterior lobe, Cerebellum	**33, -90, -39**	0.044	2
Abstract/geometric stimuli, 10-20 Hz			
Sensori-motor cortex (Ba1/2)	**57, -30, 39**	0.018	22
Sub-gyral, Occipito-temporal lobe	**48, -57, -12**	0.041	10

Table 3.5: Talairach co-ordinates of SnPM significant voxels upon the passive perception of the three different stimulus types for the 5-15 Hz, 10-20 Hz and 15-25 Hz frequency bands. **Bold type** represents the location of the most significant voxel within a cluster; *italic type* represents the most significant voxel of an additional adjoining sub-clusters of voxels. In all cases the distance between significant peak voxels exceeded $10mm^3$.

10-20 Hz frequency range. Significant (p < 0.05) power decrease effects are shown as dark areas on sagittal and coronal glass-brain views, and as white-purple areas on surface-rendered brain images of either the right or left hemisphere (depending on the lateralisation of activation for sensori-motor cortex). For this frequency range, the
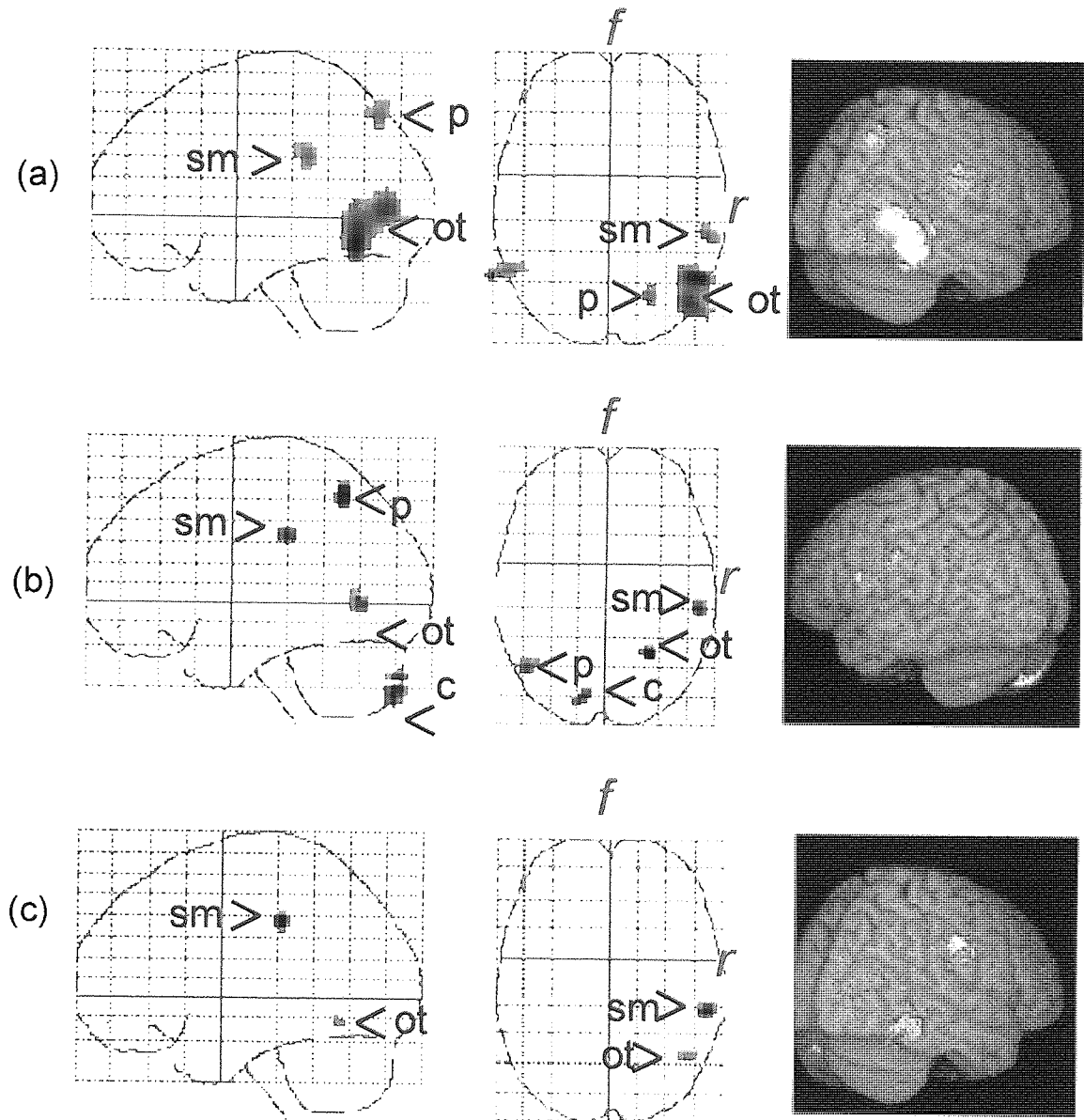
Figure 3.6: Group [n=10] SnPM voxel-level results in the 10-20 Hz frequency band for (a) graspable-object patterns revealed by a pre-post stimulus comparison over 250-750 ms, (b) standard-object patterns revealed by a pre-post stimulus comparison over 1000 ms and (c) abstract/geometric patterns revealed by a pre-post stimulus comparison over 1000 ms. Activated voxels (p < 0.05, corrected) are shown as dark areas on sagittal and coronal 'glass-brain' views, and as white-purple areas on surface-rendered images of the brain. The red 'r' and 'f' next to coronal glass-brain views indicate the right hemisphere and front of brain, respectively. The activated areas displayed on each image indicate regions of desynchronisation (ERD). Significant ERD effects are evident within the sensori-motor cortex (sm), parietal cortex (p), occipito-temporal cortex (ot), and cerebellum (c). The Talairach coordinates of significant ERD group effects are shown in Table 3.5.

standard-object patterns yielded significant power decrease effects in the superior-parietal cortex (labelled p in Figures **3.6a** and **3.6b**). For standard-object patterns alone [Figure **3.6**], significant ERD effects in the 10 – 20 Hz range were also observed in the (right) cerebellum (c).

Similar to the results reported above for the 5-15 Hz range, the SnPM group results for 10-20 Hz were always lateralised, though not consistently to any one hemisphere. Within the sensori-motor cortex, power changes were lateralised to the right hemisphere for graspable-object patterns [Figure **3.6a**] and abstract/geometric patterns [Figure **3.6c**], but to the left hemisphere for standard-object patterns [Figure. **3.6b**]. Within the occipito-temporal cortex, power changes were lateralised to the right hemisphere for each stimulus type. And within the parietal cortex, power changes were lateralised to the right hemisphere for graspable-object patterns [Figure **3.6a**] and to the left hemisphere for standard-object patterns [Figure **3.6b**]. Again, this aberrant lateralisation result could be due to the normalisation procedures adopted [see Section **3.4.2**].

3.3.3.3 15 – 25 Hz frequency band

Figure **3.7** shows the SnPM voxel-level results for graspable objects patterns revealed by a pre-post stimulus comparison over 1000 ms in the 15-25 Hz frequency band. Within this frequency range, there were no significant powers decreases or increases for either standard object patterns or abstract/geometric patterns. However, for graspable-object patterns significant power decreases were evident in the superior parietal lobe (BA7), lateralised to the right hemisphere.
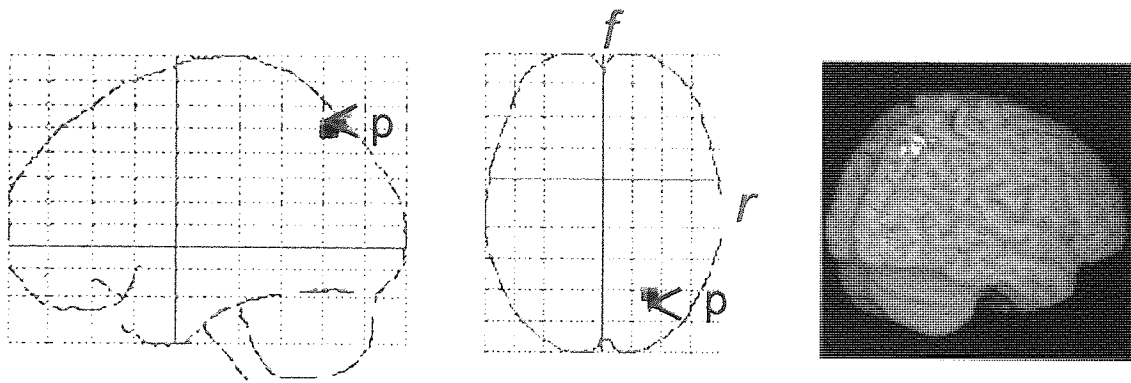
Figure 3.7: Group [n=10] SnPM voxel-level results for graspable-object patterns revealed by a pre-post stimulus comparison over 1000 ms in the 15-25 Hz frequency band. Activated voxels ($p < 0.05$, corrected) are shown as dark areas on sagittal and coronal 'glass-brain' views, and as white-purple areas on a surface-rendered image of the brain. The red 'r' and 'f' next to the coronal glass-brain view indicate the *right* hemisphere and *front* of brain, respectively. Significant ERD effects are evident in the parietal cortex (p), lateralised to the right hemisphere. The Talairach coordinates of this area are given in Table **3.5**.

3.3.3.4 20 – 40 Hz frequency bands

For voxel-level tests, there were no significant power increases or power decrease revealed by a pre-post stimulus comparison over 1000 ms within 20-30 Hz, 25-35 Hz or 30-40 Hz frequency bands.

Summary of significant group effects

The passive perception of graspable-object patterns, standard-object patterns and abstract/geometric patterns resulted in significant power decreases in a number of cortical areas, though no significant power increases were observed. For each stimulus category, power decreases were evident in the sensori-motor cortex, occipito-temporal cortex and the cerebellum. In addition, for both graspable- and standard-object patterns, significant power decreases were evident in the superior parietal cortex. The extent to which these areas were affected, in terms of the number of significant voxels activated, varied with frequency range and stimulus category. Most ERD effects were observed for the frequency ranges 5-15 Hz and 10-20 Hz [Figure **3.5** and Figure **3.6**]. In the 15-25 Hz range, the superior parietal cortex was activated by the passive perception of graspable objects, though not by standard objects or abstract/geometric patterns [Figure **3.7**]. Figure **3.8** shows the number of significant (p < 0.05) voxels in each activated area for each stimulus category. In all cases, data are shown for the frequency band that contained the maximum number of activated voxels (see figure caption for details). Within the sensori-motor cortex, the number of significant voxels activated was similar for each stimulus category. For all other identified areas, the number of significant voxels activated was always greatest for graspable object patterns and least for abstract/geometric patterns.

3.3.4 Regions of Interest Spectrograms

For each stimulus type, the regions-of-interest (ROI) determined from peak *t*-values on the MRI-SAM images for observer SJA [Figure **3.3**; Table **3.2**] are in close agreement with those determined from the Talairach coordinates of significant voxels in the SnPM group SAM results [Figures **3.5** - 7; Table **3.4**]. The principal ROI common to both individual and group data included sensori-motor cortex, superior parietal cortex, occipito-temporal cortex, and cerebellum. Additionally, although not evident in the SnPM group results, a significant reduction in oscillatory power within extra-striate cortex (BA19) was evident in the RFX group SAM images [e.g. Figure **3.4** and Table

☐ c ■ ot ☐ p ▨ sm
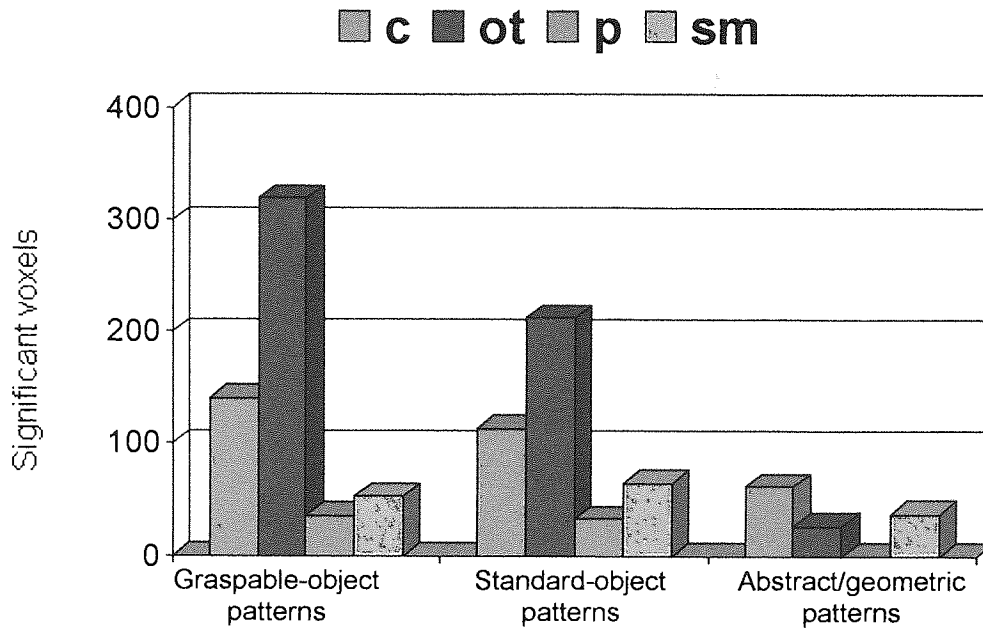
Figure **3.8**: Summary of significant ERD effects. Number of significant (p < 0.05, corrected) voxels, as determined from group SnPM analyses, within activated areas of the cortex and cerebellum for each stimulus category. In all cases, data are shown for the frequency band that contained the maximum number of activated voxels [*cerebellum* (c), 5-15 Hz for all stimulus types; *occipito-temporal cortex* (ot), 5-15 Hz for standard- and abstract/geometric patterns, 10-20 Hz for graspable-object patterns; *parietal cortex* (p), 10-20 Hz for standard-object patterns, 15-25 Hz for graspable-object patterns; *sensori-motor cortex* (sm), 5-15 Hz for standard- and abstract/geometric patterns, 10-20 Hz for graspable-object patterns].

3.4]. To examine the temporal sequencing of activity within each ROI, including the extra-striate cortex, time-frequency spectrograms were calculated for observer SJA using a Morlet wavelet transform. To reveal the level of *evoked* activity, spectrograms were created from the average of the activation waveforms for each ROI. To reveal the level of *induced* (plus evoked) activity, bootstrapped spectrograms were created from single-trial activation data [see Chapter 2 Section *2.4.2.3*]. The resulting time-frequency plots showed that, for each ROI and for both evoked and induced activity, the principal effects were bilateral. Therefore, to minimise repetition and allow for a more direct pictorial comparison between the levels of evoked and induced activity within each ROI, only data for the right hemisphere are shown.

Figure **3.9** shows the time-frequency wavelet plots for evoked activity (left-hand panels) and evoked plus induced activity (right-hand panels) within the sensori-motor cortex, representing frequencies from 5 to 40 Hz over the time scale -1.0 s to 2.8 s, for graspable objects [Figure **3.9a**], standard objects [Figure **3.9b**] and abstract/geometric patterns [Figure **3.9c**]. All the results are for the right hemisphere. The dashed vertical
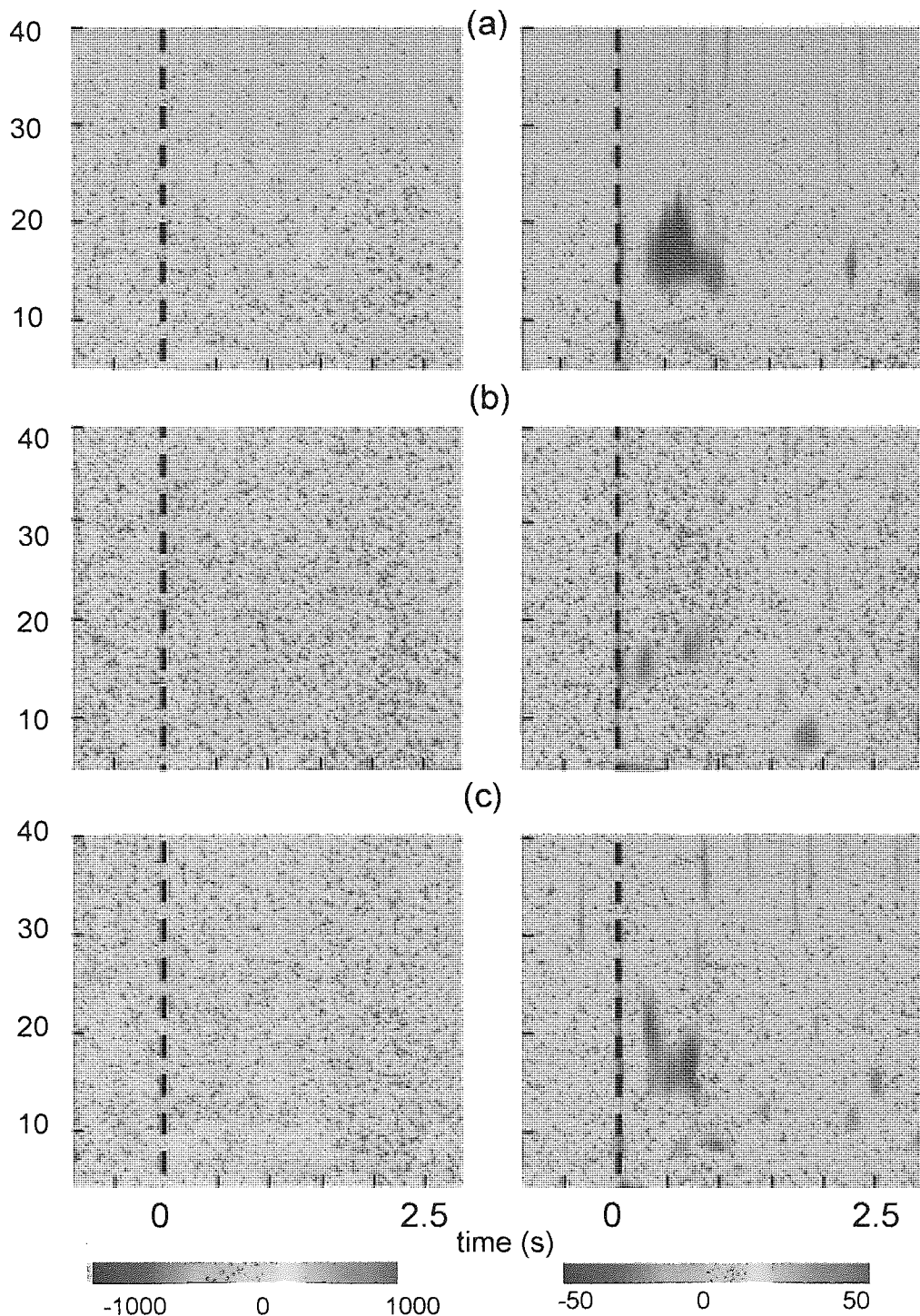
Figure 3.9: Time-frequency wavelet plots computed for a Region-Of-Interest (ROI) within the sensorimotor cortex, as determined from peak *t*-values on the MRI-SAM images for participant SJA [Figure **3.3**; Table **3.3**]. The colours represent significant decreases in power (ERD, blue/purple) or increases in power (ERS, orange/red), with average plots shown for evoked activity (left panels) and bootstrapped plots shown for evoked plus induced activity (right panels) for (a) graspable-object patterns, (b) standard-object patterns and (c) abstract/geometric patterns. All results are for the right hemisphere. The dashed vertical line at *t=0* s in each plot indicates the stimulus onset. Note the absence of any significant *evoked* power changes (left panels), but the presence of significant *induced* power changes (right panels). For each stimulus type, the induced activity was manifest as a reduction in oscillatory power (ERD) in the 15-25 Hz frequency band, beginning approximately 200 ms post-stimulus onset and lasting for 600-800 ms.

line at $t = 0\ s$ in each plot indicates the time at which the stimulus appeared on-screen, and the red and blue colours represent power increases and decreases, respectively. As can be seen in Figure **3.9**, no prominent *evoked* power changes were evident under any experimental condition [Figure **3.9a-c**; left-hand panels]. However, the passive perception of all three stimulus types yielded significant *induced* power changes within the sensori-motor cortex [Figure **3.9a-c**; right-hand panels]. For each stimulus type, the induced activity was manifest as a reduction in oscillatory power (ERD) in the 15 - 25 Hz frequency band, beginning approximately 250 ms post-stimulus onset and lasting for 600 – 800 ms.

Figure **3.10** shows the time-frequency wavelet plots for evoked activity (left-hand panels) and evoked plus induced activity (right-hand panels) within the superior parietal cortex (Ba7), representing frequencies from 5 to 40 Hz over the time scale -1.0 s to 2.8 s, for [**3.10a**] graspable objects, [**3.10b**] standard objects and [**3.10c**] abstract/geometric patterns. All the results are for the right hemisphere. The time-frequency plots for activity within the superior parietal cortex are similar to those for the sensori-motor cortex, with a sustained decrease in oscillatory power in the 15 – 25 Hz range evident under all experimental conditions, beginning approximately 250 ms after stimulus onset. In addition, however, within the parietal cortex the perception of each stimulus type yielded a significant reduction in alpha activity (8 – 13 Hz) from approximately 250 ms to 1000 ms post-stimulus onset.

Figure **3.11** shows the time-frequency wavelet plots for evoked activity (left-hand panels) and evoked plus induced activity (right-hand panels) within extrastriate cortex (BA19, right hemisphere) for [**3.11a**] graspable objects, [**3.11b**] standard objects and [**3.11c**] abstract/geometric patterns. Unlike the results for sensori-motor and parietal cortex, significant *evoked* power increases (coloured red) were evident in extrastriate cortex for all stimulus types [Figure **3.11a-c**; left-hand panels]. For each stimulus category, the evoked power increase occurred soon after stimulus onset and was confined to frequencies in the 5 - 10 Hz range. All three stimulus types also yielded a sustained reduction in oscillatory power (coloured blue) across a broad range of frequencies (5 –25 Hz) within this area, beginning approximately 150 ms after stimulus onset [Figure **3.11a-c**; right-hand panels]. Note that a near identical pattern of evoked
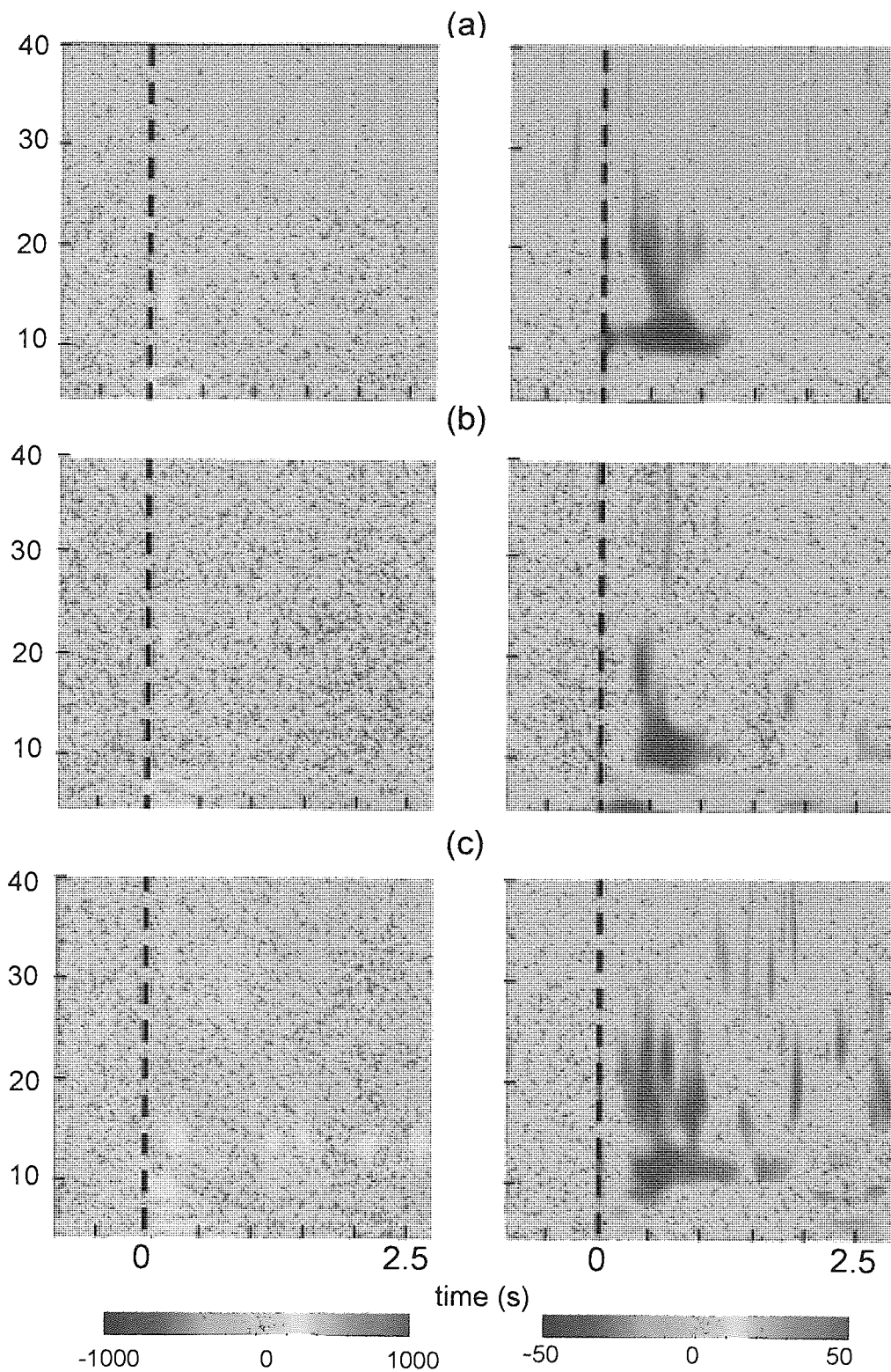
Figure 3.10: As in Figure **3.9** for a region-of-interest within posterior parietal cortex area Ba7 identified from peak t-values on the MRI-SAM images shown in Figure **3.3** and Table **3.3** for participant SJA. Note that significant ERD (12-20 Hz range) is evident bilaterally in all ROIs from approximately 0.25-0.75 s post-stimulus onset. Note also that whilst evoked activity increases (coloured red, left-hand panels) occurring soon after stimulus onset in the 5-10 Hz range are evident, this result is not robust across stimulus types.
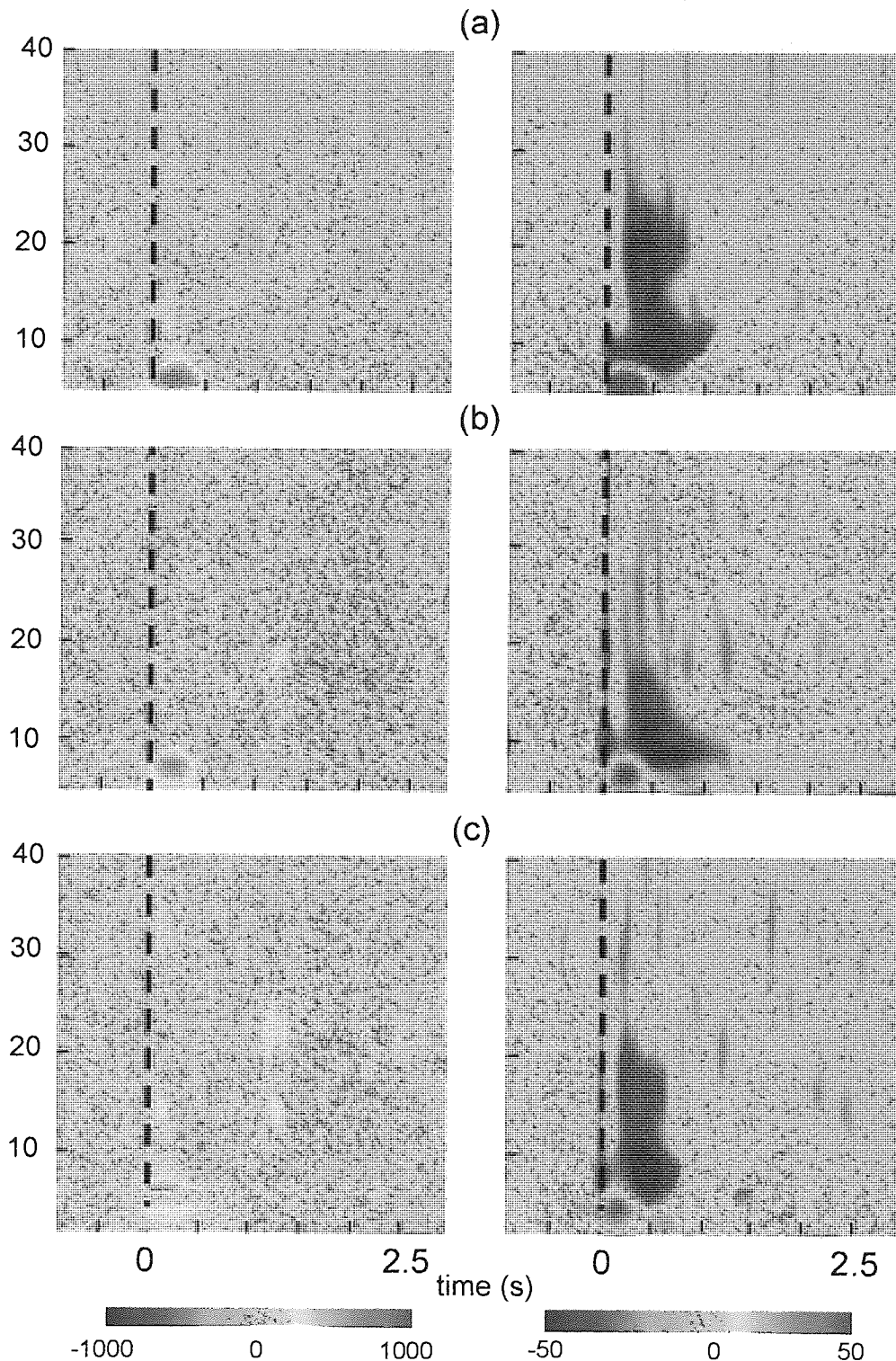
Figure 3.11: As in Figure **3.9** for a region-of-interest within extrastriate visual area Ba19 identified from peak t-values on the MRI-SAM images shown in Figure **3.3** and Table **3.3** for participant SJA. Note the presence of significant *evoked* power increases (coloured red, left-hand panels) occurring soon after stimulus onset in the 5-10 Hz range. Note also the presence of *induced* power decreases (coloured blue, right-hand panels) across a broad range of frequencies (5–25 Hz), beginning about 200 ms post-stimulus onset and lasting for 600–800 ms.
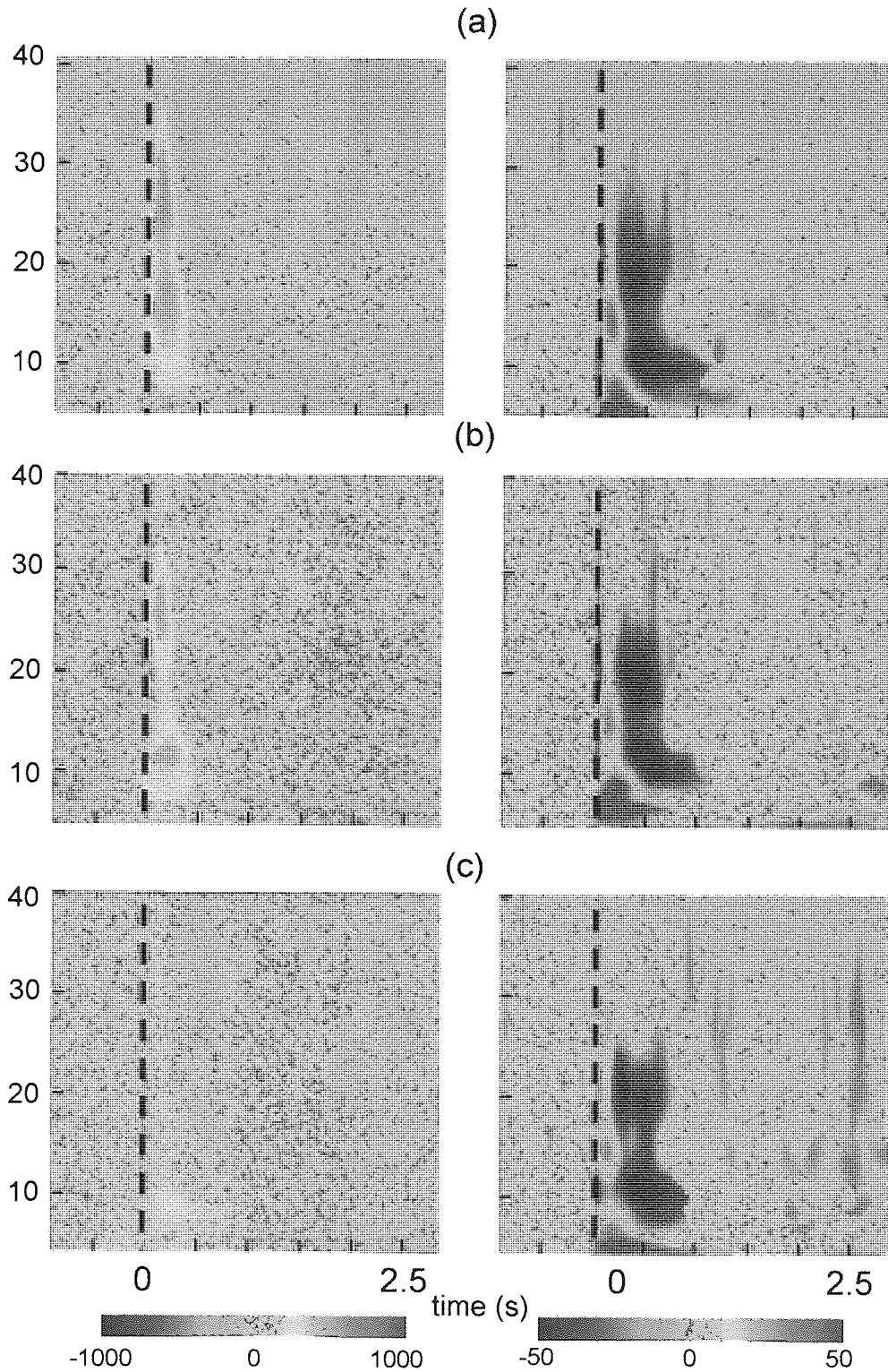
Figure 3.12: As in Figure **3.9** for a region-of-interest within occipito-temporal cortex identified from peak *t*-values on the MRI-SAM images shown in Figure **3.3** and Table **3.3** for participant SJA. Note the presence of significant *evoked* power increases (coloured red, left-hand panels) occurring soon after stimulus onset in the 5 - 10 Hz range. Note also the presence of *induced* power decreases (coloured blue, right-hand panels) across a broad range of frequencies (5–25 Hz), beginning about 200-250 ms post-stimulus onset and lasting for 600–800 ms.
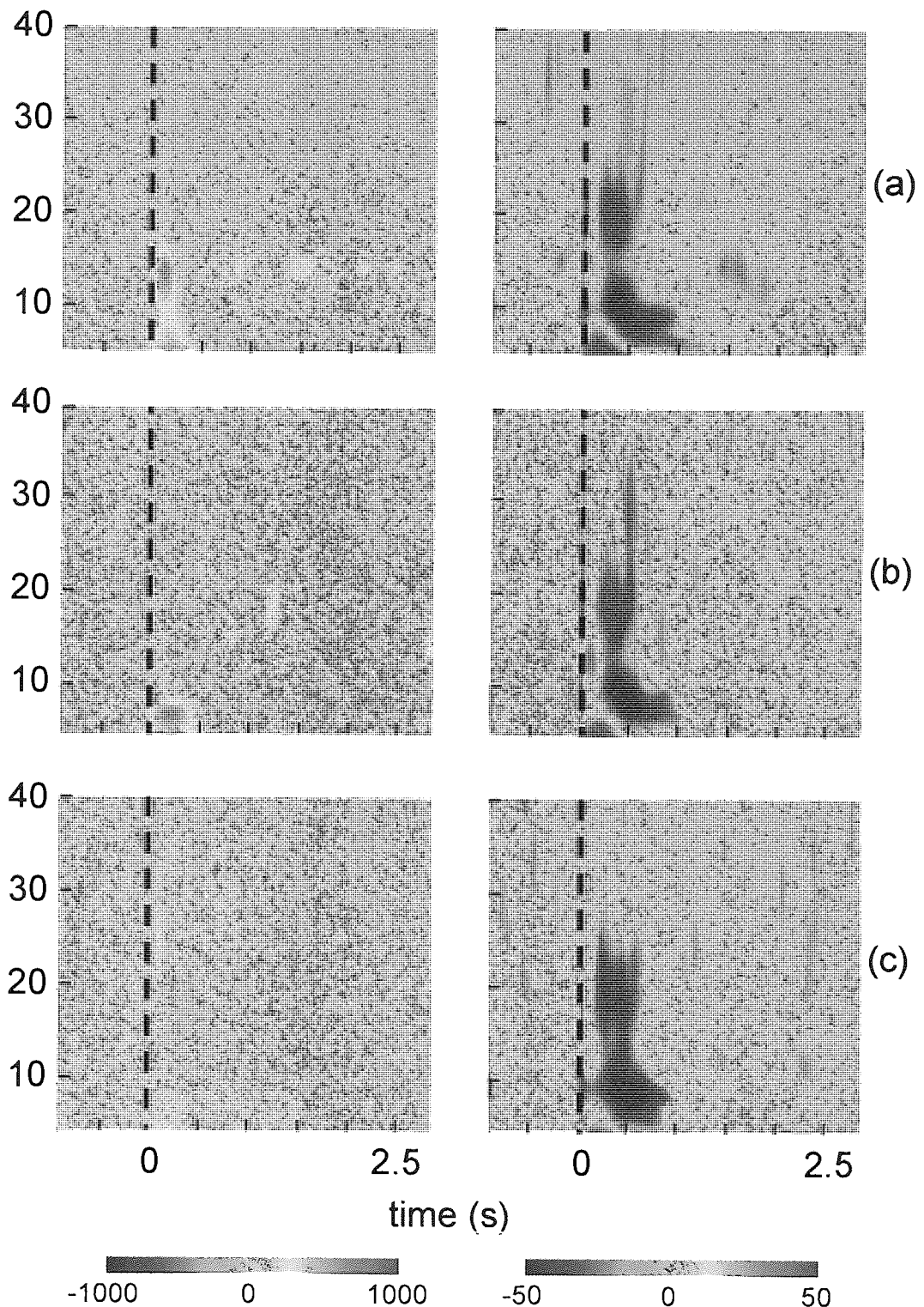
Figure 3.13: As in Figure **3.9** for a region-of-interest within middle temporal gyri identified from peak *t*-values on the MRI-SAM images shown in Figure **3.3** and Table **3.3** for participant SJA. Note the presence of significant *evoked* power increases (coloured red, left-hand panels) occurring soon after stimulus onset in the 5 - 10 Hz range for object patterns. Note also the presence of *induced* power decreases (coloured blue, right-hand panels) across a broad range of frequencies (5–25 Hz), beginning about 200-250 ms post-stimulus onset and lasting for 600–800 ms.
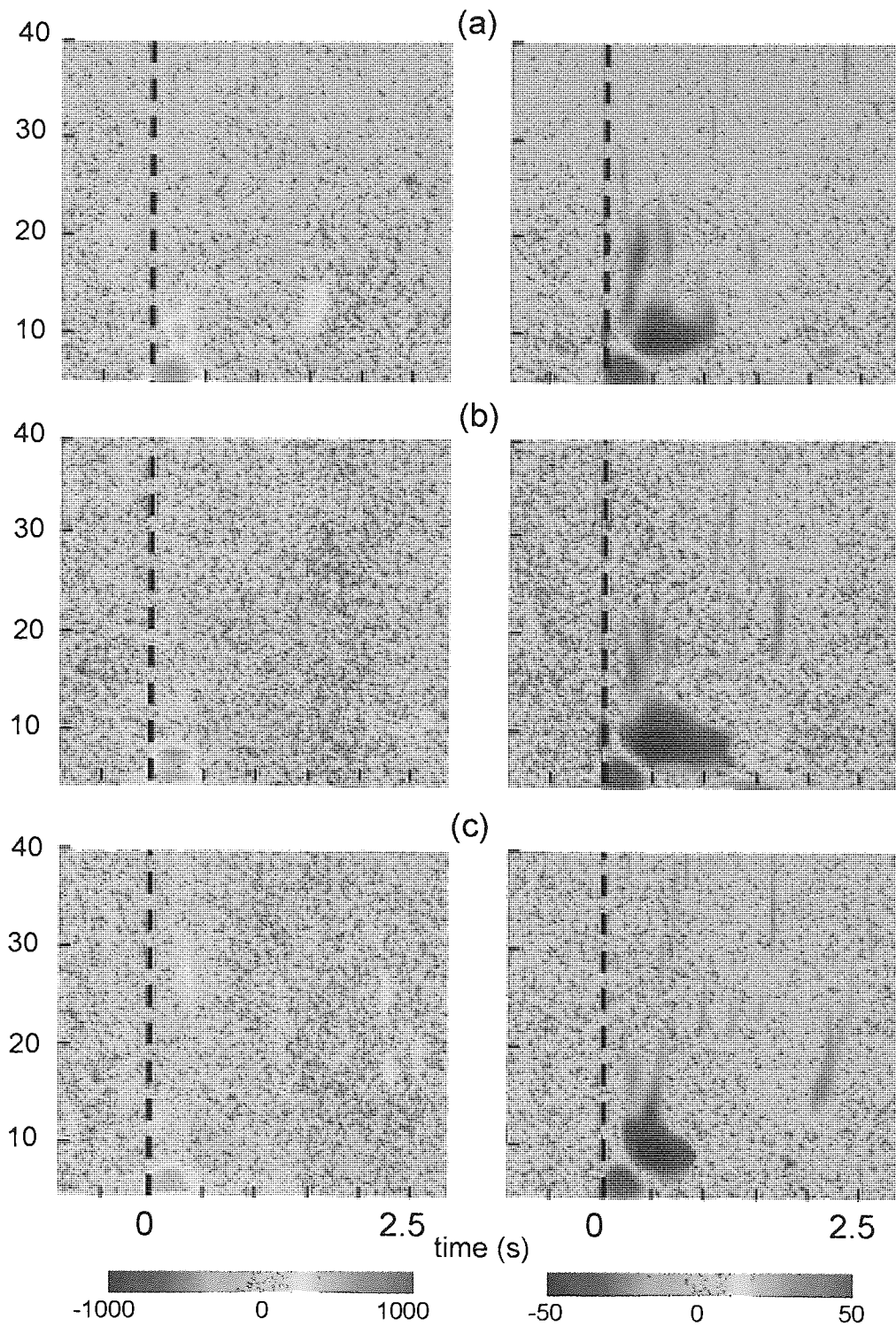
Figure 3.14: As in Figure **3.9** for a region-of-interest within the cerebellum (determined from peak *t*-values on the MRI-SAM images shown in Figure **3.3** and Table **3.3**) for participant SJA. Note the presence of significant *evoked* power increases (coloured red, left-hand panels) occurring soon after stimulus onset in the 5 - 10 Hz range. Note also the presence of *induced* power decreases (coloured blue, right-hand panels) in the 5-15 Hz band, beginning about 200 ms post-stimulus onset and lasting for 600 –1000 ms.

and induced power changes was obtained for both occipito-temporal cortex [Figure 3.12] and middle temporal gyri [Figure 3.13].

As with the cortical areas identified above, a sustained reduction in oscillatory power approximately 200 ms after the onset of each stimulus type was also evident in the cerebellum [Figure. 3.13 a-c, right-hand panels], though at a lower frequency range (5 – 15 Hz) than that generally observed in the cortex. Additionally, a significant evoked power increase was also evident in the cerebellum immediately after stimulus onset, confined to frequencies between 5 – 10 Hz [Figure 3.13 a-c, left-hand panels].

3.3.5 Comparison of activity for object and abstract pattern viewing

The SnPM pre-post comparisons of activations revealed several differences between stimuli, for example significant activation tended to encompass more voxels for the passive perception of graspable-object patterns and significant parietal activity was absent for the abstract/geometric patterns [refer to Figures 3.6-3.8]. However, pair-wise SnPM post-post comparisons across stimulus types revealed no differences at either the voxel- or the cluster-levels (p < 0.05, corrected) for the chosen frequency bands and time-periods. In a final analysis, the object stimuli were combined and probability maps for voxel- and cluster-level effects (p < 0.05, corrected) computed for the 10-20Hz frequency band over the 250-750ms post-stimulus onset, for 'object' compared with abstract/geometric patterns. This frequency range and post-stimulus onset time period were adopted because within these comparison windows, power decreases observed were of the largest magnitude. The comparison yielded a positive cluster-level effect in the right pre-central gyrus, extending anteriorally to encompass Ba6 [see Figure 3.14]. The significant cluster is shown as dark areas on sagittal, coronal and axial 'glass-brain' views, and as a yellow region on the surface-rendered image of the brain/cerebellum. That the effect was positive indicates that the reduction in oscillatory power in the 10-20 Hz range was greatest for 'object patterns'. The neuroanatomical locations of significant effects, using a Talairach database, are presented in the accompanying Figure table.
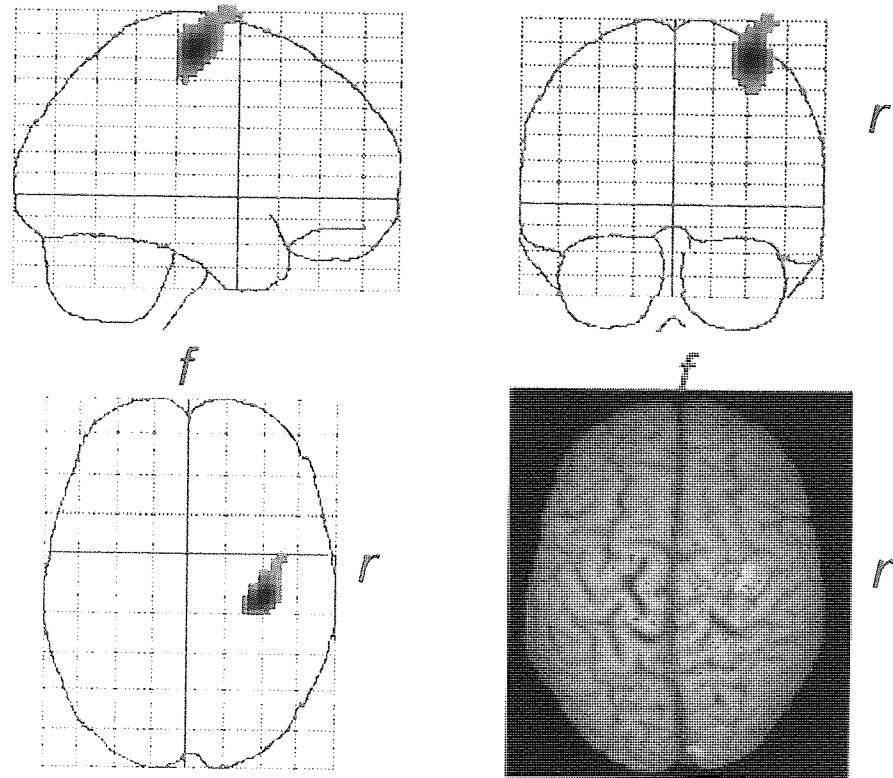
Brain Region	Talairach Coordinates	p	Cluster Size
Right pre-central gyrus (e.g. Ba6)	33,-21,66	$p = 0.049$	208

Figure 3.15: SnPM cluster-level comparison between the effects of 'object patterns' (averaged data from graspable- and standard-object patterns) and 'abstract/geometric patterns', completed for the 10 – 20 Hz frequency range and for a post-stimulus onset time range of 250 ms – 750 ms. The results are shown on three orthogonal glass-brain views and on a surface-rendered image of the brain. Note that this analysis yielded a significant positive effect in the right pre-central gyrus, extending anteriorally to encompass Ba6 ($p < 0.05$, corrected), indicating that the reduction in oscillatory power in the 10-20 Hz range was greatest for 'object patterns'.

3.4 Discussion

3.4.1 Experimental findings

Consistent with the idea that usable tools potentiate action, it has been revealed that the passive perception of graspable object stimuli is associated with activity in dorsal stream and pre-motor regions implicated in tasks involving perception for action and the imagined manipulation of object stimuli (e.g. Grafton *et al.*, 1997; Binkofski *et al.*, 1999; Chao & Martin, 2000; Grezes & Decety, 2002; Grezes *et al.*, 2003a; 2003b; Handy, Grafton, Shroff, Ketay & Gazzaniga, 2003; Kellenbach *et al.*, 2003; Creem-Regehr & Lee, 2004). However, the novel contribution of this research was to examine whether the pattern of cortical activity demonstrated for stimuli which afforded a reaching and grasping action was distinct from that observed for stimuli which did not afford such action. Achieved through a combination of single-subject and group data analyses, it has been shown that the passive perception of both object and abstract/geometric stimuli results in neuronal activity within sensori-motor regions the cerebellum and the occipital lobes. The implications of these findings are discussed below.

Of critical importance, neuronal activity in sensori-motor regions was found when viewing stimuli with no cognitive associations with a grasping action (i.e. abstract/geometric stimuli). This activity was manifest as a power decrease in the beta band, and was similar in location to that observed when a single participant produced voluntary finger movements (see also Pfurtscheller & colleagues, 1997, 1999; 2000; 2003). It was, in addition, comparable to that demonstrated for a number of action-related tasks (see Endo *et al.*, 1999; Guie *et al.*, 1999; Szurhaj *et al.*, 2003; Bastiaansen *et al.*, 1999; Leocani *et al.*, 1999; Pfurtscheller & Neuper, 1997).

Given that sensori-motor activation is not unique to the perception of usable tools versus other object categories it is unlikely that affordance *per se* is responsible for the potentiation of motor codes. Moreover, as no evoked responses were recorded in regions of sensori-motor cortex [see Figure **3.9**], luminance effects related to the rapid onset of the stimulus patterns can also be ruled out. A more feasible alternative is that

the perception of stimuli automatically resulted in an attentional modulation. This theory is in general agreement with the research of Anderson *et al.*, (2002).

The cerebellum, postulated to be important for the skilled control of movement (see Doyon, 1994; Horne & Butler, 1995; Laforce & Doyon, 2001; Saab & Willis, 2003; Jueptner & Weiller, 1998), was also found to be commonly activated across conditions. This activation was manifest as a power decrease in the alpha band and corresponded with the timing of sensori-motor activity, although its duration appeared slightly longer than that of activity in sensori-motor cortices [see Figures **3.9** and **3.13**].

A principal function of the cerebellum is to process visual feedback signals (e.g. Miall, Weir & Stein, 1987; Stein & Glickstein, 1992; Van Donkelaar & Lee, 1994), including visual information related to the control of visually guided movements (see also Glickstein & May, 1982). For instance, in primates with severed cortico-cortical fibres, visual guidance of the limbs still occurs, with Glickstein (2002) providing evidence that dorsal stream and parietal areas project heavily to the cerebellum. Relatedly, it has been suggested that, via connections to the primary motor cortex, the cerebellum receives a 'movement efference copy' (i.e. a blueprint of the movement) to ensure fast, appropriate motor responses are produced (Vercher & Gauthier, 1988; Kawato & Gomi, 1992; Miall & Reckess, 2002; Ohyama, Nores, Murphy & Mauk, 2003; see Horne & Butler, 1995 for a review). Activation of cerebella regions on the passive perception of a range of visual stimuli may therefore be important for ensuring efficient responses are produced if a situation necessitated. Indeed, a number of recent studies have demonstrated that induced oscillatory alpha and beta band networks composed of sensori-motor, premotor, parietal and cerebellum areas do subserve motor tasks (e.g. Salenius & Hari, 2003; Courtemanche & Lamarre, 2004; Pollok, Gross, Muller, Aschersleben & Schnitzler, 2004). Additionally, as cerebellum and parietal cortex contribute to the shifting of attention, oscillations in these regions could indicate a 'readiness' of the motor system (see Mackay & Mendonca, 1995; Courtemanche & Lamarre 2004).

Regions of occipito-temporal pathway (or ventral stream) are consistently reported as critical for visual processing (e.g. Dubner & Zeki, 1971; Zeki, 1973; Perett *et al.*, 1987; Gulyas *et al.*,1993; Zeki, 1993; Ahlfors *et al.*, 1999). In accordance with this finding,

activation in early visual areas was common to all stimulus types. Moreover, whilst the alpha and beta power decreases were of a similar duration to those evident in sensori-motor regions, activity in early occipital regions slightly preceded the onset of sensori-motor activity [see Figures **3.9** and **3.11**], consistent with the idea of hierarchical visual streams (e.g. Zeki & Bartels, 1999; Felleman & Van Essen, 1990; Müller, Lutzenberger, Preibl, Pulvermüller & Birbaumer, 2003; Vanni *et al.*, 2003). Of importance, the group analyses further revealed the locus of visual activity to differ between stimulus types, with only activations for the graspable object stimuli and standard object stimuli encompassing 'higher order' ventral stream regions such as the lateral occipital complex (area LO), the middle temporal gyrus and Ba37.

Regions of occipito-temporal gyrus include area LO. Area LO is located posteriorly on the lateral borders of the fusiform gyrus, extending ventrally to the anterior borders of Ba19 and dorsally to the anterior borders of Ba37 (Pins, Meyer, Fourcher, Humphreys & Boucart, 2004). This area is consistently reported to respond preferentially to pictures of objects with a clear, three-dimensional shape (e.g. Malach *et al.*, 1995, Grill-Spector, Kourtzi & Kanwisher, 2001). Limited activation of this region on the passive perception of abstract/geometric stimuli is consistent with these findings. Activation in (left) Ba37 has recently been associated with object naming, with Stewart, Meyer, Frith & Rothwell (2001) revealing a deficit in object naming when TMS is applied to this brain area. Power decreases in this region on the perception of standard and graspable object stimuli, but not abstract/geometric stimuli [see Table **3.5**], matches well with this described function of the area. Middle temple gyri activation has been associated with representations of tools and non-biological motion (e.g. Martin & Wiggs, 1996; Chao, Haxby & Martin, 1999; Joseph, 2001; Beauchamp, Lee, Haxby & Martin, 2002; Kable, Lease-Spellmeyer & Chatterjee, 2002). Thus, activation of this region for object stimuli, especially the graspable object stimuli, is again consistent with previous literature.

Group data analyses further revealed that for graspable and standard object stimuli, significant power decreases were also evident in the 10-20 Hz range within regions of superior/posterior parietal cortex. Additionally, for the graspable object stimuli, a significant power decrease in these regions was also found in the 15-25 Hz band.

In primate neurophysiology, it is well documented that anterior IntraParietal Sulcus [IPS] neurons respond to both visual and motor aspects of grasping, as well as visually guided hand movement (e.g. Sakata *et al.*, 1997; Kalaska *et al.*, 1997; Gold & Mazurek, 2002). In consequence, parietal neurons are argued to play an essential role in the visual guidance of hand actions (see Sakata and colleagues, 1997, 1998). In human, posterior parietal cortex is known to be active when a wide variety of tool-specific grasp information is retrieved (e.g. Binkoski *et al.*, 1998; 1999; Inoue *et al.*, 2001), including information concerned with the manipulability of objects for grasping (i.e. canonical neurons). Thus, it has been proposed that this area may be the homologue of monkey anterior IPS and that regions of posterior parietal cortex are critical for the pragmatic description of objects for action (Jeannorod, Arbib, Rizzolatti & Sakata, 1995). Activation in superior/posterior parietal regions for the graspable object stimuli provides convincing support for these arguments. The finding of activation in this region upon the perception of standard object stimuli is returned to later.

Pair-wise SnPM post-post comparisons across stimulus types revealed no differences at either the voxel- or cluster-level (p < 0.05, corrected). Therefore, in a final exploratory analysis, activity for object stimuli was averaged and compared with abstract/geometric stimuli activity. This revealed a greater reduction in 10-20 Hz power for the object stimuli compared with the abstract/geometric stimuli in a region encompassing Ba6 of the ventral premotor cortex [Figure **3.14**]. Ventral premotor cortex (specifically area Ba6) is known to be active during tasks of perception for action (e.g. Grezes *et al.*, 2003b; Handy *et al.*, 2003), passive perception of action-related stimuli and gestures (Grafton *et al.*, 1997; Chao & Martin, 2000; Grezes & Decety, 2002; Grezes *et al.*, 2003b; Kellenbach *et al.*, 2003; Creem-Regehr & Lee, 2004), and motor imagery (e.g. Decety *et al.*, 1994; Geradin *et al.*, 2000; Grafton, Arbib, Fadiga & Rizzolatti, 1996). In consequence, Ba6 has been argued to be the human homologue of primate area F5 (Chao & Martin, 2000), which is reciprocally connected to anterior IPS (see Wise *et al.*, 1997; Sakata *et al.*, 1998; Quintana & Fuster, 1999) and also contains canonical neurons (Rizolatti *et al.*, 2000). Comparatively, Ba6 is proposed to be reciprocally connected to posterior parietal cortex and is also believed to contain canonical neurons (Rizzolatti *et al.*, 2002). Simultaneous activation of these areas during the passive perception of tools has been suggested to provide strong neurophysiological evidence for visual routes to action and, specifically, the concept of object affordance (e.g. Grezes & Decety, 2002;

Grezes *et al.*, 2003a; 2003b). Indeed, activation of premotor and superior parietal regions is thought to be tightly coupled (see Svoboda, Sovka & Stancak, 2002).

Of relevance, Kellenback *et al.* (2003) have observed activations of ventral premotor cortex for stimuli that are not manipulable and, in consequence, do not afford action (e.g. shelves, speaker, stop sign). In trying to reconcile their findings with theories of affordance (and the data of Chao & Martin, 2000), a suggestion proposed was that '*non-manipulable stimuli are somehow more similar to tools than buildings are...*' (pp38) resulting in a similar, if attenuated, pattern of activity in premotor regions. In the present investigation, whilst the standard object stimuli utilised did not afford specific grasping responses they were all manipulable. Thus, it is possible that the affordant 'manipulability' of a visually presented stimulus and not the affordant 'graspability' of a stimulus is important in eliciting neuronal activity in premotor and parietal areas. This hypothesis can also accommodate the similar levels of power decrease in superior/posterior parietal cortex for both types of object stimuli.

In sum, differential networks of induced neuronal activity were apparent when individuals viewed stimuli ranging in their associations with a grasping action. For all visual stimuli, activity in regions of sensori-motor cortex, occipital cortex and cerebellum was apparent. This activity, manifest as event-related desynchronisations in alpha and beta band frequencies, was largely correlated in timing onset and duration. Given the connectivity of these regions in primates and associated functions, it is suggested that simultaneous activity in such regions could serve as a base framework from which fast, coordinated responses could be produced. For stimuli with increasing cognitive association with a grasping action (or manipulability), three further activation patterns were apparent. Firstly, power decreases in regions of superior/posterior parietal cortex of comparable frequencies were also recorded. Secondly, within sensori-motor cortex, cerebellum and occipital-temporal gyri, the oscillatory activity encompassed more neurons. Thirdly, comparative analyses of activation across stimulus types revealed that the perception of object stimuli compared with the perception of abstract/geometric stimuli was associated with a greater augmentation of power decreases (again in alpha and beta band ranges) in ventral premotor cortex. This extensive network of areas activated when viewing graspable/manipulable stimuli is

consistent with research indicating that such stimuli elicit a function-specific representation for action[1].

3.4.2 The importance of employing both group and single-subject analyses

The group and individual findings were not always congruent. In individual and RFX analyses, activations were always bilateral, whereas in SnPM analyses they tended to be lateralised. Secondly, in SnPM analyses, activations in regions of superior parietal cortex and middle-temporal gyri were significant for object stimuli only, whereas in individual wavelet analyses, activation in these regions was significant across stimulus types.

Steinmetz, Furst, Freund (1990) have demonstrated that the non-linear normalisation procedures adopted in group analyses can result in a poor match of local structures, with individual sulci and gyri varying in position across individuals by several tens of millimetres [see Chapter 2 Section 2.4.3]. Therefore, when considering the SnPM analyses results, it is possible that activity across participants did not localize to the same $5mm^2$ of cortex used to assess significance. This would explain the inconsistent lateralisations of activity reported for the SnPM analyses (e.g. the left lateralisation of activity within sensori-motor cortex, and cerebella, for standard object patterns and abstract/geometric patterns, respectively). These findings illustrate a major limitation of group imaging techniques, namely that homologous sites of significant change may become lost in stringent group analyses by being spread out anatomically with little or no overlap (Woods, 1996).

The second discrepant result (i.e. activity in parietal cortex and middle temporal gyri for the single participant when observing abstract/geometric patterns) is likely to be a consequence of participant idiosyncrasies. For example, Creem-Regehr *et al.* (2004b) have provided evidence that when individuals are given experience of manipulating novel graspable objects, passive viewing of the stimuli post-training results in differential brain regions activated compared with passive viewing pre-training. Thus, if observer SJA had previously experienced similar stimuli where a response was required

---

[1] See Singh, Barnes, Hillebrand, Forde & Williams (2002) for a review of task-related related changes using MEG (and SAM) compared with hemodynamic measures.

this could have affected brain activity associated with this stimulus type. Alternatively, the parietal and middle temporal responses seen in this participant could reflect a non-specific attentional orienting. Indeed, regions of extrastriate visual cortex and parietal cortex are known to be modulated by directed attention (e.g. Foxe, Simpson & Alhlfors, 1998; Martinez *et al.*, 2001; Rushworth, Krams & Passingham, 2001). Whilst it is not possible to verify whether either of these hypotheses is correct, the findings do demonstrate that activation patterns differ dependent upon the level of analysis adopted.

In sum, the present imaging results further demonstrate that an optimum investigation of neuroimaging data is best achieved through a combination of both single and group data analysis techniques.

Chapter 4

Visual Attention, Affordance and Movement Construction

4.1 Introduction

The MEG investigation reported in Chapter 3 provided evidence that the passive perception of familiar objects and abstract patterns activates an extended network of cortical areas encompassing regions believed to be involved in the planning and production of action. However, the contributory roles of directed visual attention within objects and/or affordance upon action production remain unknown.

In the following chapters, both the planning and control of goal directed pointing movements will be investigated in a group of normal participants [Chapters 6 and 7] and in a single deafferented participant [Chapter 8]. This will be undertaken in order to assess the relative importance of both visual attention and affordance upon movement construction.

In this chapter a theory of movement production based upon distinct planning and control phases is briefly reviewed, together with an overview of how this system maps onto proposed visual processing streams [Section 5.2]. The known affects of perception upon planning and control movement phases are also reviewed [Section 5.3].

4.2 The Planning and Control of Goal Directed Movements

There is a general consensus that the production of goal-directed movement is the result of distinct planning and control movement phases (e.g. Jeannerod, 1986, 1988; Desmurget & Grafton, 2000; Sabes, 2000; Glover 2002). Glover (2004) has recently provided a comprehensive model of movement construction based upon these separate phases. Centred on a systematic review of behavioural and neuroimaging data of movement in healthy and brain-damaged participants, he proposes that the planning and control of action each serve a specialized purpose. This model, outlined in the following sub-sections, forms the basis on which the effects of visual attention and affordance upon action construction were investigated [see Chapters 5 to 8].

4.2.1 The planning system

To produce a planned movement, a target must be localised in space and the initial state of an individual's arm and hand (or other body-parts) defined. This information is then assimilated to form a path trajectory program (see Desmurget, Pelisson, Rossetti & Prablanc, 1998). In consequence, a wide variety of visual and cognitive information is utilised by the planning system. This information includes not only the characteristics of the target and the surrounding medium but also the goal(s) of the individual.

In accordance with the roles of the planning system, Glover (2004) suggests that planning is closely related to cognitive processes (e.g. memory) and requires a relatively long processing time to allow for the integration of cognitive and visual information related to the action. This information is then used to compute a range of movement kinematics (e.g. velocity, force, movement time, hand shaping and object semantics such as fragility/temperature/hazards). Consistent with the idea that planning encompasses a wide variety of movement kinematics, research has demonstrated that both spatial (e.g. grip-aperture) and non-spatial (e.g. force) characteristics of a target are operationalised well before a movement is complete (see Gordon, Forssberg, Johannson & Westling 1991; Jakobson & Goodale, 1991; Klatzky, Fikes & Pellegrino, 1995; Flemming, Klatzky & Behrmann, 2002). For example, Klazky *et al.* (1995) have demonstrated that shaping the hand appropriately for functional interaction with a target object decreases the time needed to initiate a movement (i.e. arm-lift off). Similarly,

Gordon *et al.* (1991) have shown that, when initiating lifting movements to boxes of increasing size (but equal weight), grip force, vertical lifting force, force rates and vertical movement also increase.

In support of the idea that planning relates closely to cognitive processes, Kunde, Hoffmann & Zellemann (2002) have demonstrated that the computation of actions towards a target are prone to interference effects from cognitively relevant variables. They demonstrated that the preparation and initiation of even simple actions was mediated by an anticipation of their effects (i.e. their 'reafferences'). That is, a to-be-executed motor response was initiated more quickly when it resulted in the same auditory tone as a preceding (but different) prepared motor response than when it did not. Additionally, Gentilucci and colleagues (1998; 2000; 2003) have revealed interference effects of semantics on action. In these studies, the word printed on an object (e.g. small, large, short or long) affected the kinematics of a participant's goal-directed movement towards the object. For example, when reaching for an object with the word 'long' printed on it, peak acceleration, velocity and deceleration were greater than for the same object when the word 'short' was printed on it. According to Gentilucci *et al.* (2003), this finding suggests that participants automatically associated the words with the distance of the target object. Thus, they concluded that motor acts can be cognitively represented and as such movement construction can be facilitated or impeded by cognitive information.

Glover (2004) further proposes that the planning system governs movement time. Dependent upon the degree of movement complexity required to complete an action, the planning system adjusts the time dedicated to each movement phase appropriately [see Section **5.2.3**]. However, this idea is not without its critics (see Bootsma, Marteniuk, Mackenzie & Zaal, 1994; Tresilian & Stelmach, 1997; see Plamondon & Alimi, 1997 for a review).

In sum, the planning system is proposed to operate prior to movement onset and during movement initiation. Based on feedforward models of action (see Sabes, 2000 for a review), its requirement is to select an adaptive motor program given the environment and goals of the individual.

4.2.2 The control system

Once a movement has been selected and initiated, an on-line control system is believed to become operationalised, responsible for monitoring and if necessary adjusting motor programs 'in flight' (Pisella *et al.*, 2000). Glover (2004) suggests the control system is subject to two constraints. Firstly, that it is limited to visual information concerned with the spatial characteristics of a target (as these are the most likely to be erroneously planned or subject to change; e.g. catching a moving ball). Secondly, that it operates outside of conscious awareness. In support of these conjectures, there is some evidence that visual feedback, proprioceptive feedback and efference copy (i.e. a blueprint of the movement plan obtained from the planning system prior to movement initiation) are all used during the on-line control of action (e.g. Zelaznik, Hawkins & Kisselburgh, 1987; Gentilucci, Toni, Cieffi & Pavesi, 1994; Jackson *et al.*, 2000; Jackson, Jackson, Newport & Harvey, 2002; Miall & Reckess, 2002). These systems are postulated to have properties that allow for the fast computation of movement parameters/kinematics. For example, visual and proprioceptive feedback can operate in under 200ms (see Carlton, 1981; Elliott & Allard, 1985; Jeannerod, 1988; Jackson *et al.*, 2000), and as such can be used to quickly update movement kinematics such as velocity, direction and force during an action. When such feedback is removed, the use of efference copy is utilised to ensure fast (corrective) movements are still constructed. This has been demonstrated in deafferented individuals who have no sense of proprioception (i.e. limb position and movement). For example, Bard *et al.* (1999) demonstrated that a deafferented individual could quickly correct aiming movements to a target, even without vision of her moving limb. Employing a double-step paradigm, they demonstrated that the individual could quickly update an aiming movement when the location of the target was perturbed (i.e. changed) after movement onset. Bard *et al.* (1999) suggested that 'internal feedback-loops of central origin' provide information about the current spatial goal of a programmed movement (see also Jones, 1974, Kawato & Gomi, 1992a; 1992b; Ohyama, Nores, Murphy & Mauk, 2003). Moreover, in the study conducted by Bard *et al.* (1999), the target location was perturbed during saccadic suppression. In consequence, their participant was unaware that the target's location had changed or that she had updated her motor programme. This supports the assumption that the control system operates outside of conscious awareness. Findings that the control system is impervious to visual illusions (e.g. Glover, 2002) whereas the

planning system is not (e.g. Glover & Dixon, 2002; Westwood & Goodale, 2003) also support this assumption.

In sum, the control system is proposed to operate during movement execution, and its influence is believed to be greatest during the middle and final stages of movement. Based upon feedback models of action (see Sabes, 2000 for a review), the requirement of the control system is to minimise the spatial error of a movement.

4.2.3 Neurophysiology of the planning-control system and perception-action system links

The neural network defining the 'planning system' is believed to encompass the inferior parietal lobule, the frontal lobes and the basal ganglia (e.g. Adam & Keulen, 2004; Seidler, Noll & Thiers, 2004), whereas that defining the 'control system' is believed to encompass the superior parietal lobules and the cerebellum (e.g Nair, Purcott, Fuchs, Steingberg & Kelso, 2003). This division has prompted some to link Glover's model of action to the perception-action model of Goodale & Milner (1992; Milner & Goodale, 1995). Glover himself proposes that *'...dissociations between perception and action might more accurately be described as dissociations between perception and on-line control'* [Glover, 2002 pp 290].

This proposition has resulted in new lines of investigation with findings broadly falling into one of four categories. These are:
1) Research in support of the planning-control model over the perception-action model (e.g. Coello & Rossetti, 2004; DeLoache, 2004; Phillips, Triggs & Meehan, 2004)
2) Research in support of the action-perception model over the planning-control model (e.g. Goodale & Westwood, 2004; Goodale & Milner, 2004)
3) Research against the planning control model (e.g. Brouwer, Brenner & Smeets, 2004; Coslett & Buxbaum, 2004; Johnson-Frey, 2004; Wright & Chubb, 2004)
4) Research not consistent with either model (e.g. Handlovsky, Hansen, Lee & Elliott, 2004; Elliott & Meegan, 2004).

Bridgemann (2002; 2004) argues, however, that the basic tenets of the planning-control model and the perception-action model can be united in a three-way model encompassing planning, perception and control functions [see also Figure **4.1**].

Additionally, a planning-control model of action allows for the study of both planned movements and the study of unplanned movements. This model therefore provides a detailed basis from which to study visual precursors of action.

Illustration removed for copyright restrictions

Illustration removed for copyright restrictions
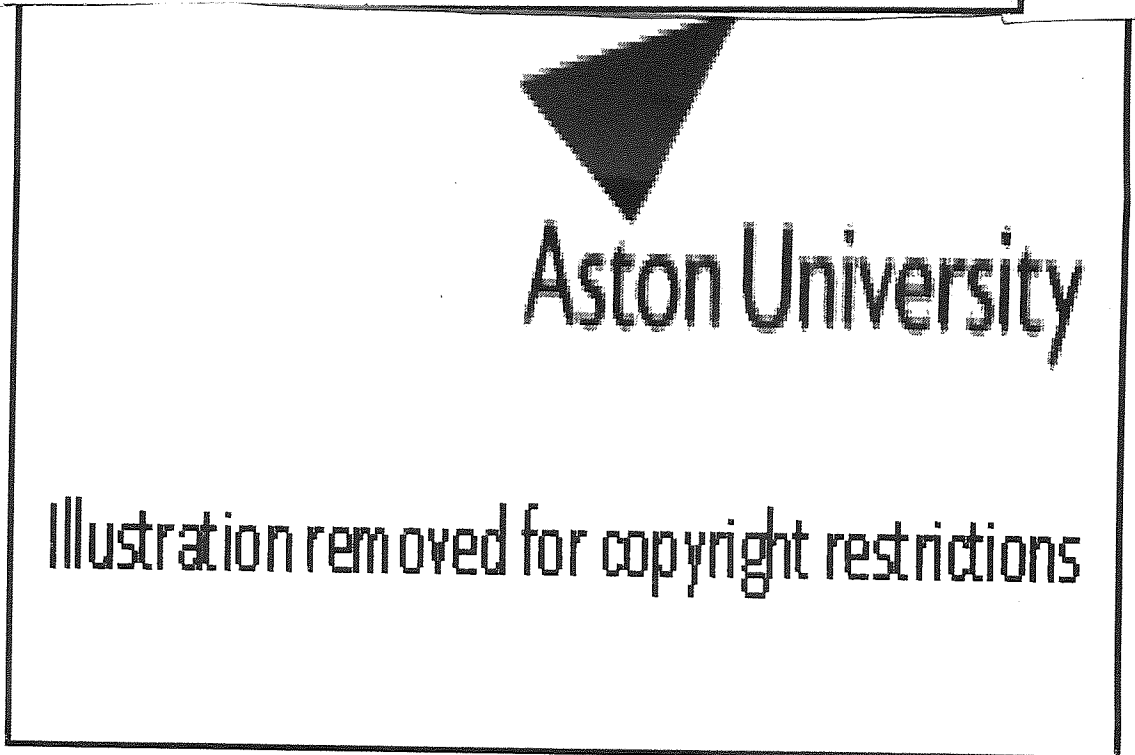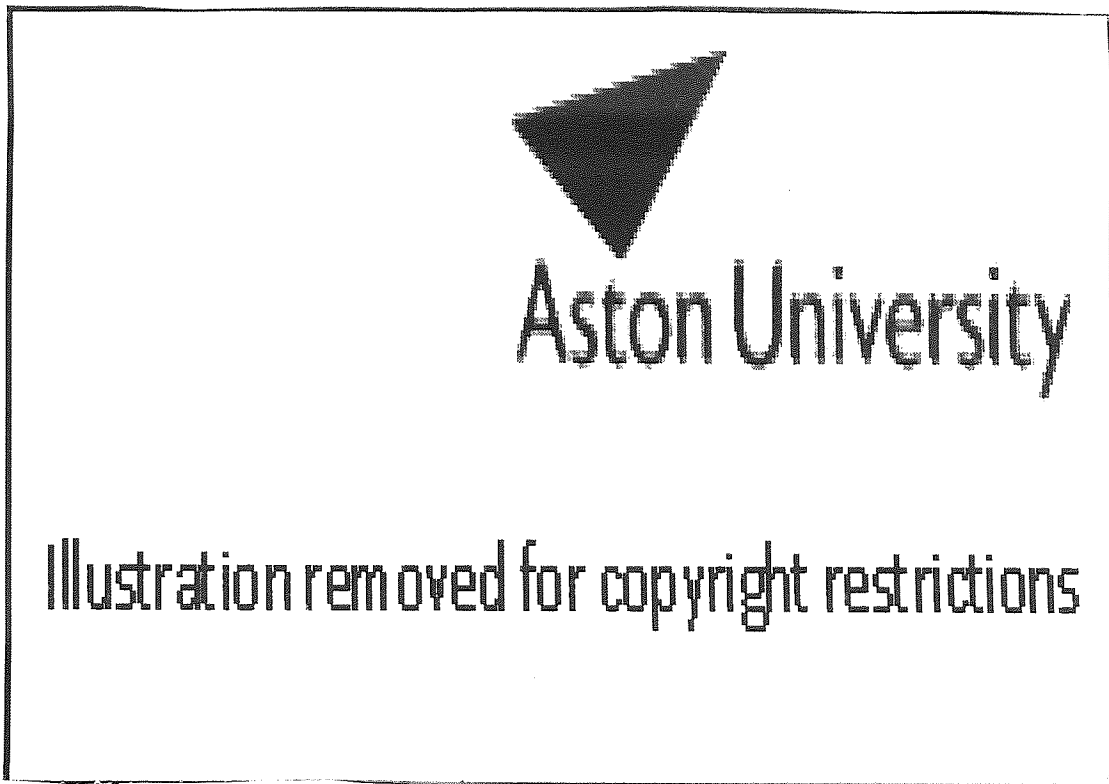
Figure 4.1 Theories of visual perception and action and how the planning-control model can be encompassed. (**A**) The 'what' and 'where' pathways of Ungerleider & Mishkin (1982). (**B**) The 'what' and 'how' pathways of Goodale & Milner (1992, Milner & Goodale, 1995). (**C**) The 'planning' and 'control' model of Glover (2004), where a third visual stream of 'planning' is introduced.

4.3 The Influence of Perception upon Planning and Control

There is evidence to suggest that the more predictable a movement is, the more it will rely on planning (e.g. Seidler, Noll & Thiers, 2004), whereas the more complex a movement is, the more it will rely on control (e.g. Wolpert & Gharamani, 2000). Thus, the time course of planning and control are not definitive and can overlap (see also Desmurget & Grafton, 2000; Sheth & Shimojo, 2002). In the following section, a review of the effects of visual attention and affordance upon planning and control movement stages is provided. To investigate planning, studies are presented where the to-be-executed-action is simple and known prior to movement initiation. Conversely, to investigate control, studies are presented whereby information regarding the to-be-executed-action is complex and altered after movement initiation.

4.3.1 Planning movements

To evaluate the effects of visual attention and affordance upon planning, much of the behavioural research investigating visual routes to action presented in Chapter 1 [Section 1.3] is relevant. This research provided evidence for both the importance of object affordances and visual attention upon reaction times. In brief, advocates of affordance theories demonstrated that, when information between a planned movement and an object-related parameter (e.g. grip-aperture, action relevant properties and stored knowledge) was congruent, reaction times decreased. Advocates of theories of visual attention, nonetheless, purported that the majority of the affordance findings could be a consequence of the attentional bias intrinsic to an object. In one study, for example, the attentional bias of non-affordant stimuli was also found to influence reaction times (Anderson *et al.*, 2002).

Based on several research experiments, however, Pavese & Buxbaum (2002) have argued that the planned response-mode (e.g. button press or pointing) can differentially affect the extent of interference caused by irrelevant object properties or distractor stimuli. They propose that, to comprehensively investigate visual routes to action, tasks requiring direct action towards stimuli should be adopted, rather than tasks which require simple responses such as button presses. This, they note, is because ecological perspectives hold that such direct action is necessary if the relationship between objects,

goals, and actions is to be well understood. In line with such arguments, movement planning has also been investigated using measures of path trajectory (e.g. Wolpert, Ghahramani & Jordan, 1994; Flanagan and Rao, 1995).

When pointing towards a target, individuals typically demonstrate an efficient movement trajectory that approximates a linear trace from start to finish (Jackson & Hussain, 1997; Desmurget, Pelison, Rosetti & Prablanc, 1998). However, Tipper and colleagues (1997a, 1997b) have demonstrated that the presence of distracting objects in a display can affect path trajectory efficiency. They noted an 'attentional repulsion' effect whereby path trajectories curved away from distractor objects and locations. Comparatively, studies of patients with left visual neglect have revealed that path trajectories generally deviate to the right (e.g. Goodale *et al.*, 1990; Harvey, Milner & Roberts, 1994). Interestingly, such path trajectories appear to mimic the trajectories of saccadic eye movements, which also curve away from visual distractors (see Doyle & Walker, 2001; 2002; Tipper, Howard & Paul, 2001; McSorley, Haggard & Walker, 2004). In accounting for these eye-movement findings, McSorley *et al.* (2004) suggested that the initial saccade direction is modulated by the inhibition of distractor locations within a 'motor map' specifying saccade directions. This motor map encodes the location of all visual stimuli. Saccade direction can then be programmed by calculating the weighted average of neural activity in relation to the different stimuli perceived. Therefore, when a target and distractor are present two separate populations of activity result where activity associated with the distractor is inhibited.

In explaining their curved path trajectory findings, Tipper, Meegan & Howard (2002) also suggested a model for selection based upon inhibitive mechanisms. They proposed that reaching movements are planned within a hand-centred frame of reference, and when attention is anchored to a target object, inhibition acts on the representation of a potential distractor. Moreover, Castiello (1996; 1999) proposed that both the target and the distractor evoke parallel actions and that competition between these simultaneous responses is resolved by inhibitive mechanisms. Such models have been useful in accounting for reach paths that veer towards non-target items (see for example Tipper and colleagues, 1998; 1999).

In contrast, Tresilian (1999) argues that deviant path trajectories may be explained as 'avoidance manoeuvres', in that non-target items might not only be potential distractors but also potential obstacles. Tresillian states that in order for the nervous system to treat something as a distractor it must have been noted and attended too. Thus, obstacle avoidance will only be observed when a non-target object is an 'attended' object. Tresillian explains the effects of a non-target object on performance as a consequence of planning a response to this distractor. He notes, nonetheless, that such a theory cannot account for data showing path trajectories towards a non-target item. Consistent with Tresilian's (1999) theory, however, eye movement research has demonstrated that salient external events can capture attention despite instructions not to attend to such locations/event (e.g. Müller & Rabbit, 1989; Theeuwes, Kramer, Hahn, Irwin & Gregory, 1999; Remington, Folk & McLean, 2001).

In sum, reaction time studies reveal that visual attention and affordance affect movement efficiency. However, the effects of visual attention and affordance upon movement time and path trajectories are unknown. Additionally, whilst it is known that non-target items can also influence these parameters, the attentional or affordance biases of such distractors has not been investigated.

4.3.2 The on-line control of movement

Perturbation (or double-step) paradigms have been utilised to evaluate the effects of movement parameters related to visual perception upon control. These paradigms involve suddenly changing a characteristic of the to-be-grasped or hit target, either coincident with or briefly after movement onset (see Rossetti, 1998 for a review). To date, the majority of such research has focused on perturbations of an object's size (i.e. grasp kinematics) or perturbations of an object's location (i.e. reach/pointing kinematics). However, an object's inherent affordance or attentional properties have been largely ignored. For example, whereas several studies have investigated parameters of monocular/binocular vision and congruency of grip type upon grasp kinematics and movement time (see for example Castiello, Bennett & Stelmach, 1993; Castiello, Bennet & Chambers, 1998; Dubrowski, Bock, Carnahan, Jüngling, 2002; Jackson, Newport & Shaw, 2002), none have considered the attentional biases of a to-be-grasped stimulus and only one has investigated object affordances (e.g. Castiello, Bonfigioli & Bennett, 1998). Additionally, in this latter study only perceived 2-D/3-D

object appearance was examined. This study revealed that the motor patterns used for object interactions were primarily influenced by the way the object was perceived in real time (i.e. 2-D or 3-D), with these perceptions overriding influences exerted by existing cognitive representations. However, the intrinsic affordance properties of the stimuli (e.g. association with a grasping response) were not investigated.

Studies of object-location change have revealed that for target position movements of up to a distance of 4cm, responses are neither significantly slower nor less efficient than responses on unperturbed trials, with path trajectories displaying a smooth curvilinear trace towards a perturbation target (e.g. Smeets & Brenner, 1995; Brenner & Smeets, 1997). In manipulating stimulus attributes of colour and location, Pisella, Arzi & Rosetti (1998) further found that modifications of path trajectories were approximately 80ms faster for perturbations of object location than object colour. They also found that whereas individuals do not make unwanted movement corrections for perturbations of object colour they often cannot avoid automatically correcting fast aiming movements for perturbations of object position (Pisella *et al.*, 2000). Pisella *et al.* (2000) hence suggest that an 'automatic pilot' drives fast corrective arm movements. Consistent with theories of on-line control (Goodale & Milner 1992; Milner & Goodale, 1995; Glover 2004), this system is proposed to rely on spatial vision and can escape intentional control. Certainly, for path trajectories to be efficiently corrected, target displacements do not need to be consciously perceived (see Fecteau, Chua, Franks & Enns, 2001).

Nonetheless, to date, studies of object location change (see also Desmurget *et al.*, *1999*; Fourneret & Jeannerod, 1998; Boulinguez, Blouin & Nougier, 2001; Grea *et al.*, 2002; Lee & van Donkelaar, 2002; Johnson, van Beers, Haggard, 2002; Bedard & Procteau, 2003; Nijhof, 2003) have been of limited use in addressing perturbations related to an object's intrinsic spatial characteristics (e.g. asymmetry). Although Procteau & Masson (1997) have investigated perturbations of an object's surrounding medium and demonstrated that visual background changes affect aiming accuracy. Additionally, work by Boulinguez and Nougier (1999) has revealed that both the time-to-correction and mean movement time to perturbed targets decreases when the probability of a perturbed response being in a given direction increases.

In sum, whilst it is known that perturbations of object size, location, background information and perturbation probability influence the on-line control of action towards a target, the influences of attentional and/or affordance biases in mediating such processes have received limited, if any, investigation.

Chapter 5

General Behavioural Methods

5.1. Assessments of Visual Attention and Affordance upon Movement Construction

The behavioural studies reported in Chapters 6 to 8 were designed to investigate the effects of visual attention and/or affordance upon both planned and unplanned movements. A range of measures including movement time, path trajectory and hit error were used to determine movement efficiency for pointing manoeuvres towards a target. Stimulus parameters and general experimental procedures are reported in this chapter. Details pertaining to specific experiments are reported in the relevant experimental chapters.

5.2 Stimuli and Equipment

5.2.1 Stimulus generation

Four different categories of stimuli were utilised. Each category comprised ten stimulus images, five of which were mirror images of the original. All stimulus images were achromatic and differed with respect to their associated attentional and/or affordance properties.

To investigate the influence of visual attention upon planning and control, images of geometric stimuli were used [Figure **5.1**]. These stimuli contained a single conspicuous feature on either their left or right edge, giving them a degree of attentional bias towards the left or right side of object-space, respectively (see Anderson *et al.*, 2002). To investigate the shared contributory influence of visual attention and affordance upon action, images of 'coherent' object stimuli were used [Figure **5.2**]. The single conspicuous feature of these objects was also that which afforded action (e.g. the handle of a mug). This resulted in a combined attentional and affordance bias (see Tucker & Ellis, 1998) towards this feature/side of object-space. To investigate the unique contributory roles of visual attention and/or affordance upon action, images of 'incoherent' object stimuli were used [Figure **5.3**]. In these stimuli, the conspicuous feature and the object's graspable handle were separated in object-space (e.g. a razor). The incoherent object stimuli were therefore deemed to have opposing attentional and affordance biases. In a fourth (control) condition, images of fruit and vegetables were utilised [Figure **5.4**]. These stimuli were designed to neither encompass a salient left/right attentional bias nor a salient left/right affordance bias. Moreover, for these stimuli, the presence of any biases was irrelevant.

The geometric stimuli were generated using a VSG 2/5 graphics card (from Cambridge Research Systems [CRS], Rochester, Kent). A Sony Digital Mavica Camera was used to photograph various control and object stimuli, which were then copied to the graphics card for display purposes. The pixel resolution was set to 1.6 Mega Pixels, the capture size to 1024 x 768mm and the image type to achromatic. To ensure a homogenous background all stimuli were positioned in a white screen medium. To ensure measures of hue, luminance, contrast and background canvas colour were consistent, all control

and object stimuli were adjusted using Jasc Paint Shop Pro 7. The canvas colour adopted was a featureless mid-grey [R=157,G=157,B=157], which matched the background display page generated using the VSG graphics card (mean luminance = 14 cd/m^2). The surface area of each stimulus (approximately 94 mm^2) did not vary within or between conditions ($F_{(2, 29)} = 1.357, p = 0.274$).
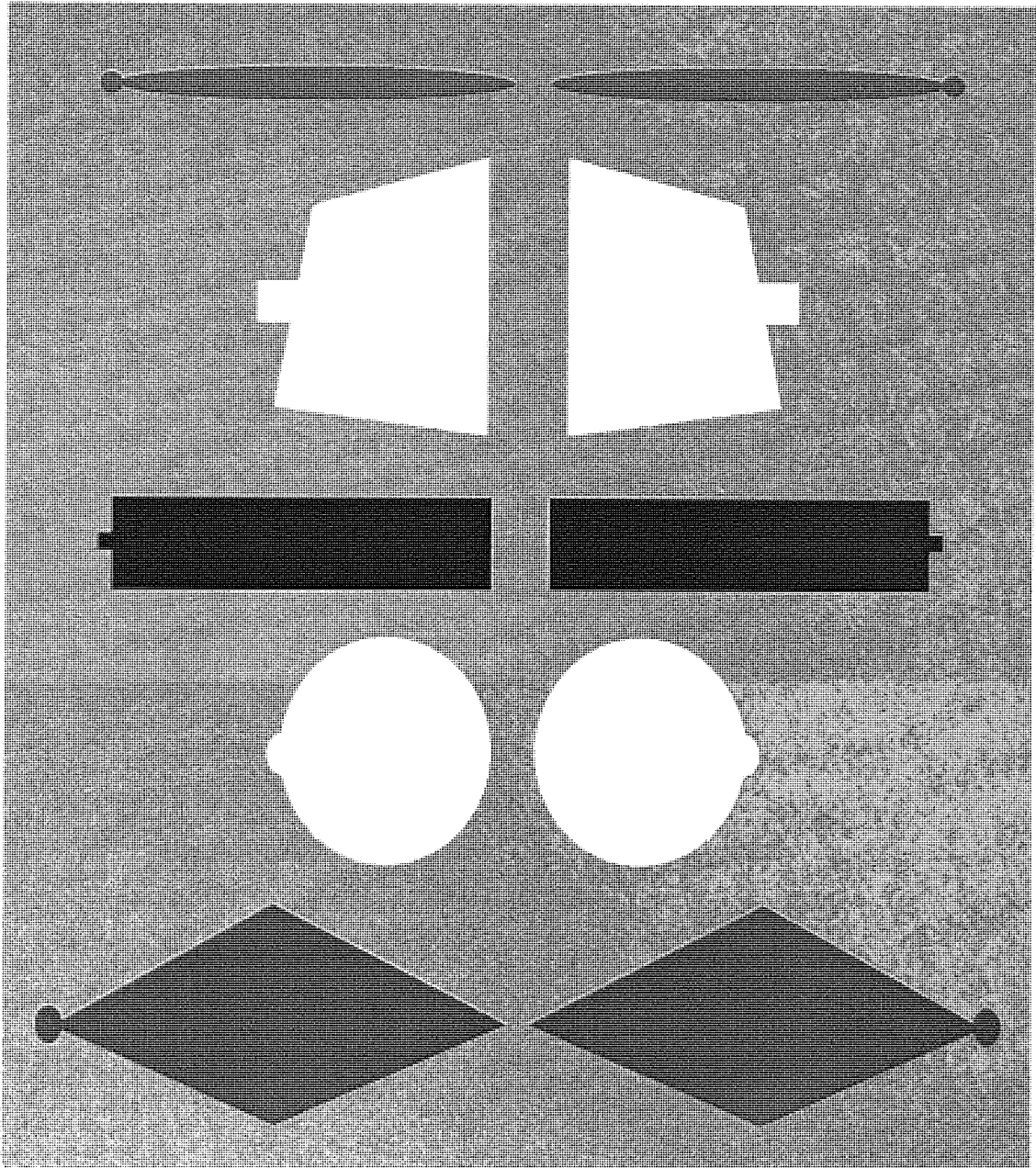
Figure 5.1: The 10 stimuli used in the geometric condition. From top left to bottom right: Elipse L, Elipse R, Trapezium L, Trapezium R, Rectangle L, Rectangle R, Circle L, Circle R, Diamond L, Diamond R. The stimuli in this condition were all asymmetrical, with a left or right attentional bias.
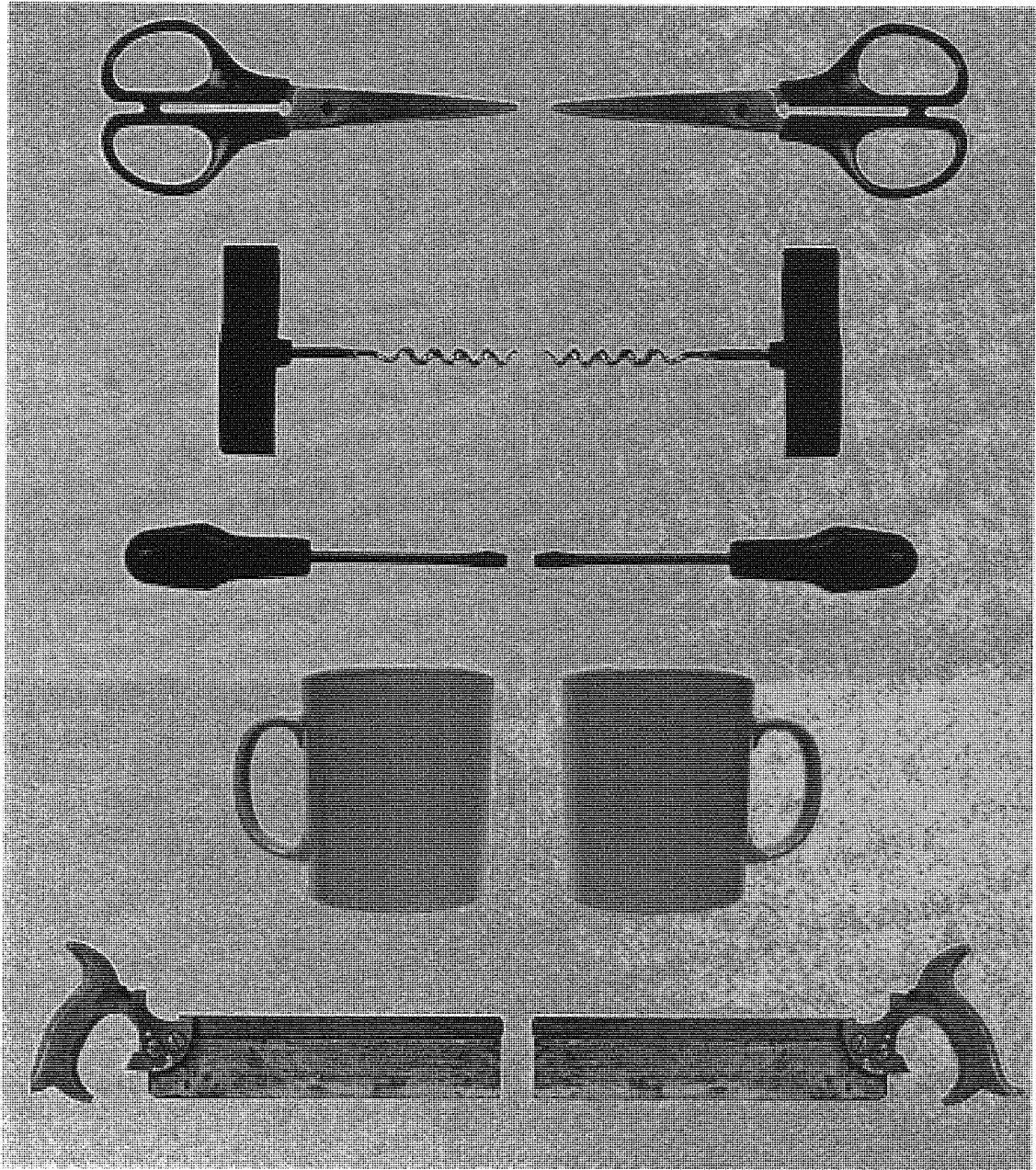
Figure 5.2: The 10 stimuli utilised in the coherent object condition. From top left to bottom right: Scissors L, Scissors R, Corkscrew L, Corkscrew R, Screwdriver L, Screwdriver R, Cup L, Cup R, Saw L, Saw R. The stimuli in this condition were all asymmetrical and had a shared left/right attentional/affordance bias.
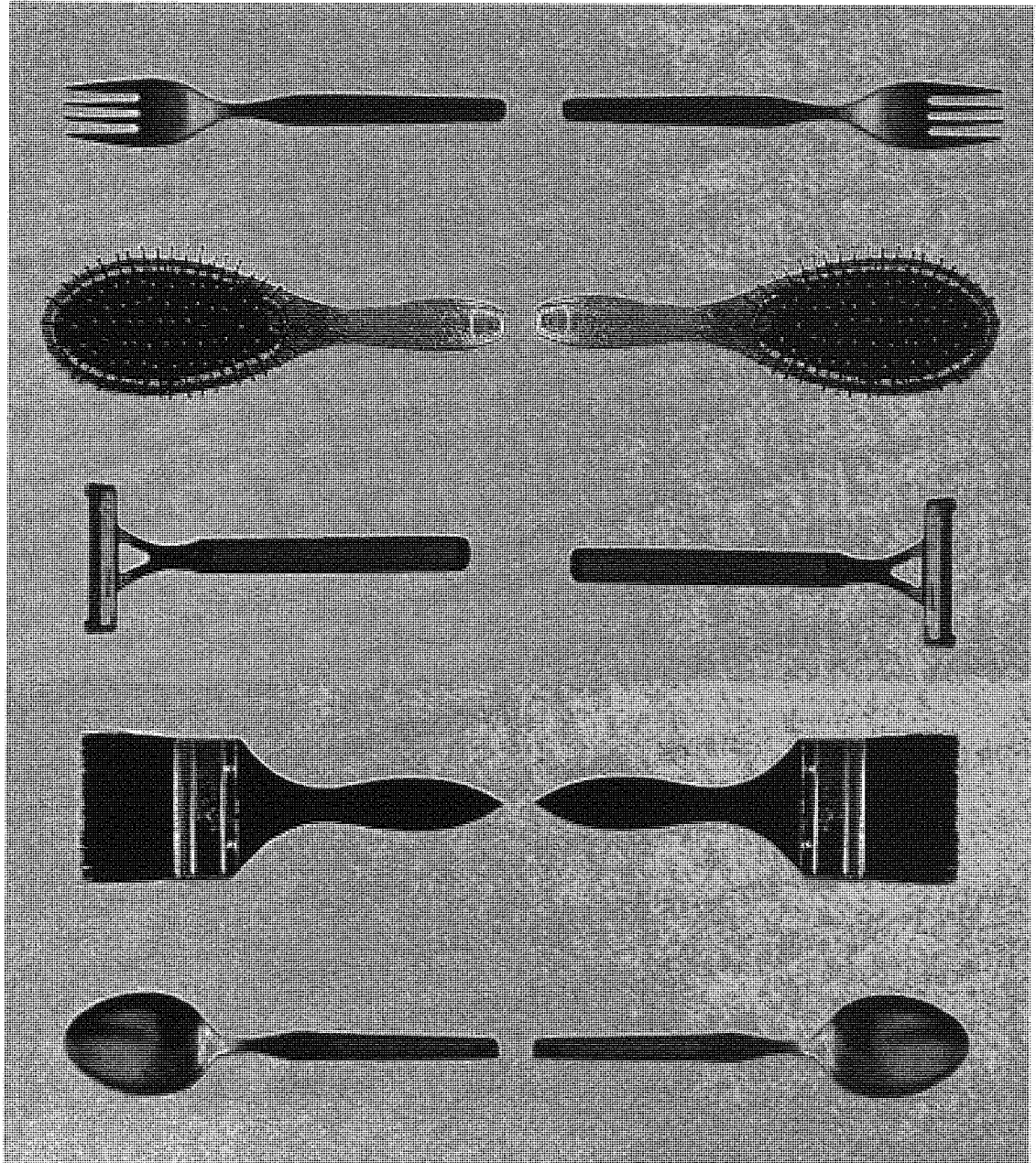
Figure 4.3: The 10 stimuli utilised in the incoherent object condition. From top left to bottom: Fork L, Fork R, Hairbrush L, Hairbrush R, Razor L, Razor R, Paintbrush L, Paintbrush R, Spoon L, Spoon R. The stimuli in this condition were all asymmetrical and had opposing left/right attention/affordance biases.
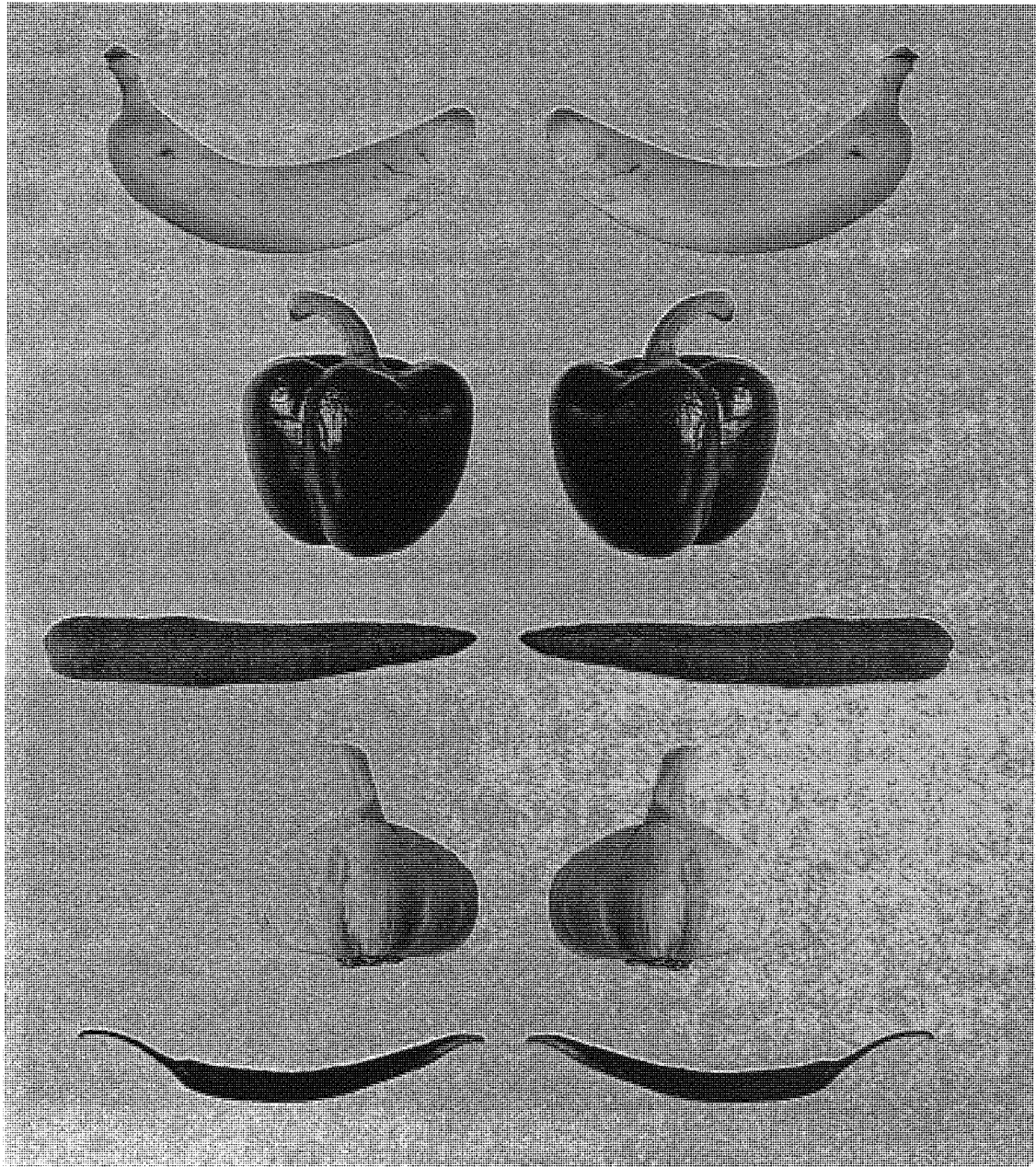
Figure 5.4: The 10 fruit and vegetable stimuli utilised in the control condition. From top left to bottom right: Banana L, Banana R, Pepper L, Pepper R, Carrot L, Carrot R, Garlic L, Garlic R, Chilli L, Chilli R. For the stimuli in this condition any left/right attentional or affordance bias were irrelevant.

5.2.2 Equipment

All stimuli were presented in the centre of a Sony FD Triniton 16 x 12 inch monitor using a VSG graphics card housed in a Dell Workstation PW56SO computer. The monitor had a 1024 x 768 pixel resolution and 100hz frame rate. Attached to the monitor control panel (below the screen) was a button box [B0]. Attached to the monitor casing was a clear perspex screen and two reflective 19mm spherical reference markers at the top left and right corners [Figure 5.5]. The perspex screen covered the entire monitor screen and the button box. On applying pressure to the perspex screen (e.g. with a pointing action), the button box was depressed and a button press triggered.
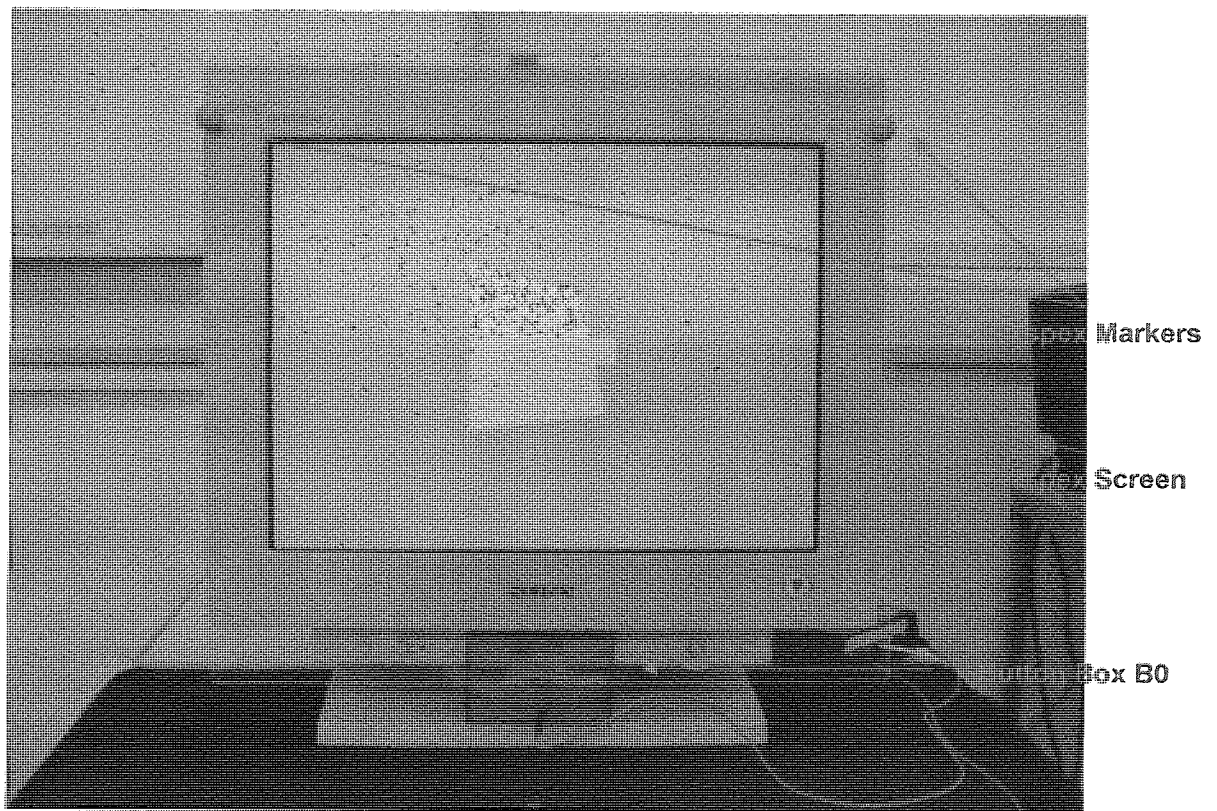
Figure 5.5: Stimulus Display on VSG Monitor

The Qualisys Track Manager (QTM) motion capture equipment consisted of three ProReflex MCU120 cameras and a range of different sized spherical reflective markers. The system software was housed in a Crest Ability 510 computer. The motion capture equipment enabled the reconstruction of movements in 3-D space through the detection of light reflected from the markers. This was achieved by exposing the markers to infrared light emitted by the ProReflex cameras. The cameras' recorded the 2-D

coordinates of each marker as a data stream. When data from two or more MCU cameras were combined (as in the present experiments), 3-D marker positions were established at a rate of up to 120 frames per second.

5.2.3 Experimental set-up

The stimulus display monitor was situated on a non-reflective table. A second button box [B1] was positioned in front of the monitor at a distance of 40cm. Mounted to the edge of the table, and in central alignment with B1 and the monitor, was a chin rest. The viewing distance from eye to target (i.e. chin rest to monitor) was approximately 56cm, and the movement distance from start to target (i.e. button box to monitor) was approximately 40cm. To record movements in 3-D volume space between B1 and the monitor, participants used a cylindrical hand-held stylus (153 X 8mm) that had a 4mm half sphere reflective marker attached to its tip. The experimental work space is depicted in Figure 5.6.
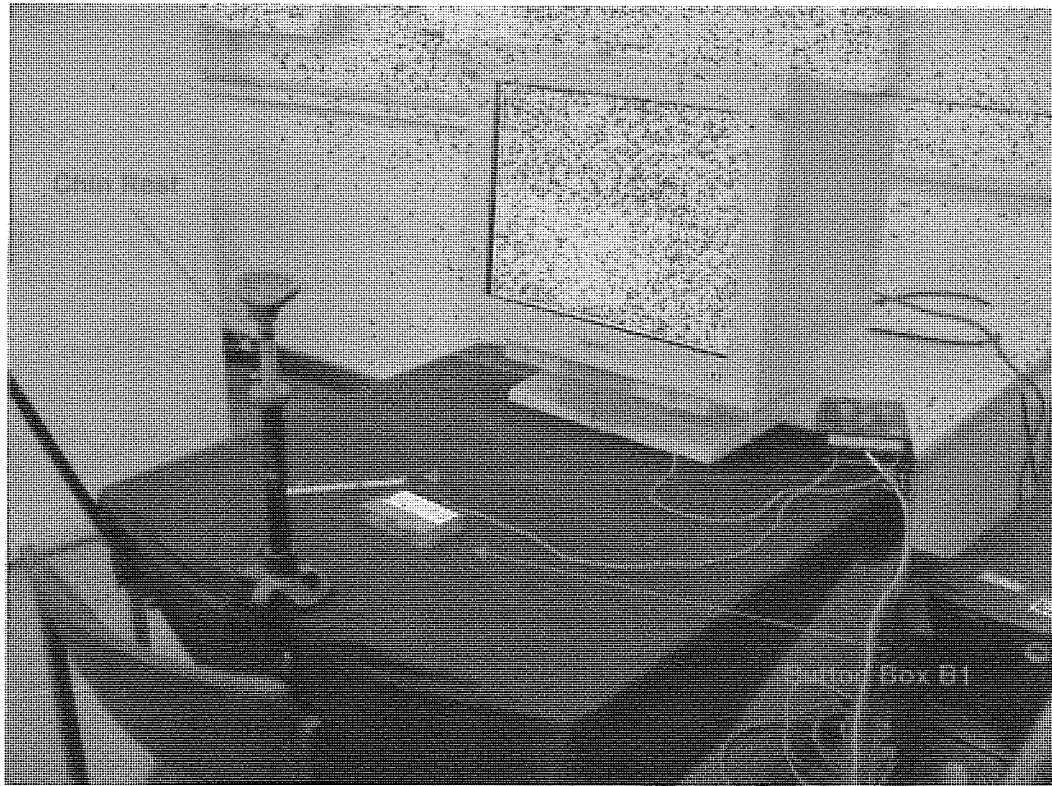
Figure 5.6: Experimental Work Space

To ensure efficient 3-D motion capture, the reflective markers attached to the stylus and the monitor had to be within the capture area (i.e. viewing region) of at least two motion capture cameras. For ease of comparison, B1 was used as the focal landmark. The experimental set-up is depicted in Figures **5.7**.

In x and y Cartesian co-ordinates, camera 1 was positioned to the left of B1 at a distance of 111cm and angle of 10^0, camera 2 was positioned to the left-behind of B1 at a distance of 131cm and angle of 60^0 and camera 3 was positioned to the right of B1 at a distance of 90cm and angle of 178^0. In the z co-ordinate, Camera 1 was positioned at a distance of 90cm and angle of 40^0, camera 2 was positioned at a distance of 84cm and angle of 30^0 and camera 3 was positioned at a distance of 75cm and angle of 35^0.
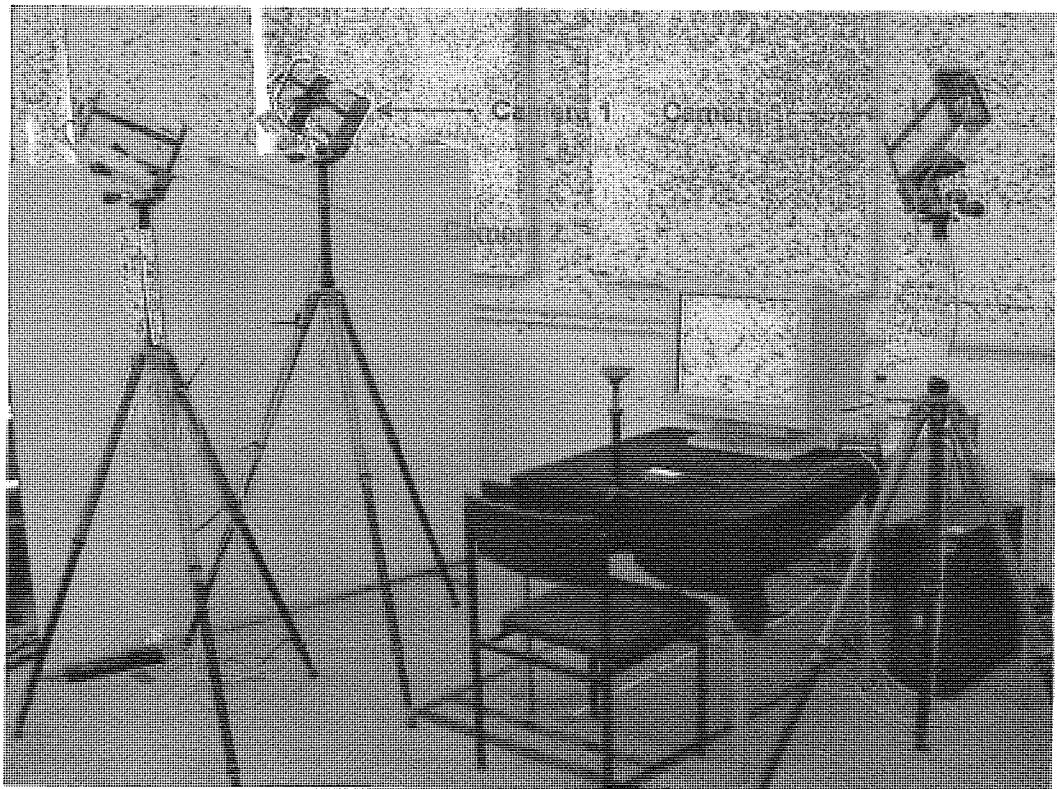
Figure 5.7: Experimental Set-Up

5.2.4 Calibration of the QTM equipment

In order to track and perform calculations on the 3D data the QTM software required information about the position and orientation of each camera. This was achieved using

a calibration procedure, whereby the volume of space in which a movement could occur was mapped out prior to recording.

To conduct the calibration procedure, a stationary L-shaped reference structure with four reflective markers attached to it was positioned in the experimental work-space. This reference structure defined the origin and orientation of the coordinate system to be used with the camera system. Once this structure was in position, a second reference structure (wand) was moved through the experimental work space volume. This structure had two markers located at a fixed distance from each other and provided data that determined the locations and orientations of the cameras.

Prior to experimentation it was necessary to capture frames (n = 500 per marker) of the calibration wand structure in as many different positions as possible within the work space volume. Calibration measures were only accepted as reliable if the number of points used to calculate the x, y and z distances (in mm) between the origin of the co-ordinate system to the optical centre of the camera(s) exceeded 750 out of a maximum of 1000. This was in accordance with QTM operation guidelines[1].

---

[1] Further information on QTM motion capture software is found at www.qualysis.com

5.3 General Procedure

Each experiment included an initial control training phase and a second test phase. In the control training phase, the fruit and vegetable stimuli were utilised. In the test phase, the geometric stimuli, coherent object stimuli and incoherent object stimuli were utilised. Only data from the test phase was analysed.

In both the training and test phases, the order of stimuli and trial type was randomised. Dependent upon trial type, either a 'standard' movement (standard trials) or a 'corrective' movement (perturbed trials) was required. Standard movements were used to investigate the influence of visual attention and/or affordance upon planning. Corrective movements were used to assess the influence of visual attention and/or affordance upon on-line control.

5.3.1 Experimental task

5.4.1.1: Standard trials

On standard trials a centrally presented arrow cue (10 x 5mm), was elicited by depressing B1. The direction of the arrow cue indicated to the participant which edge of the stimulus (i.e. left or right) the pointing movement should be made towards. After a random interval of between 750-2250ms, a visual stimulus was presented and the participant was required to point towards (and hit) the (perspex) screen in the corresponding position [see Figure **5.8a**]. The trial was terminated by the depression of B0, which occurred whenever the perspex screen was hit.

5.4.1.2: Perturbed trials

A perturbed trial was initiated in the same way as a standard trial. However, movement onset (i.e. the release of B1) triggered the appearance of a small red circular target (8 mm diameter) at one edge of the stimulus. The task of the participant on these trials was to hit the circular target. This target could be compatible or incompatible with the direction of movement indicated by the initial cue-arrow presentation. If it was compatible, the edge of a stimulus the movement was towards was still indicated by the initial arrow cue [see Figure **5.8b**]. If it was incompatible a corrective movement towards the opposite stimulus edge was required [see Figure **5.8c**].
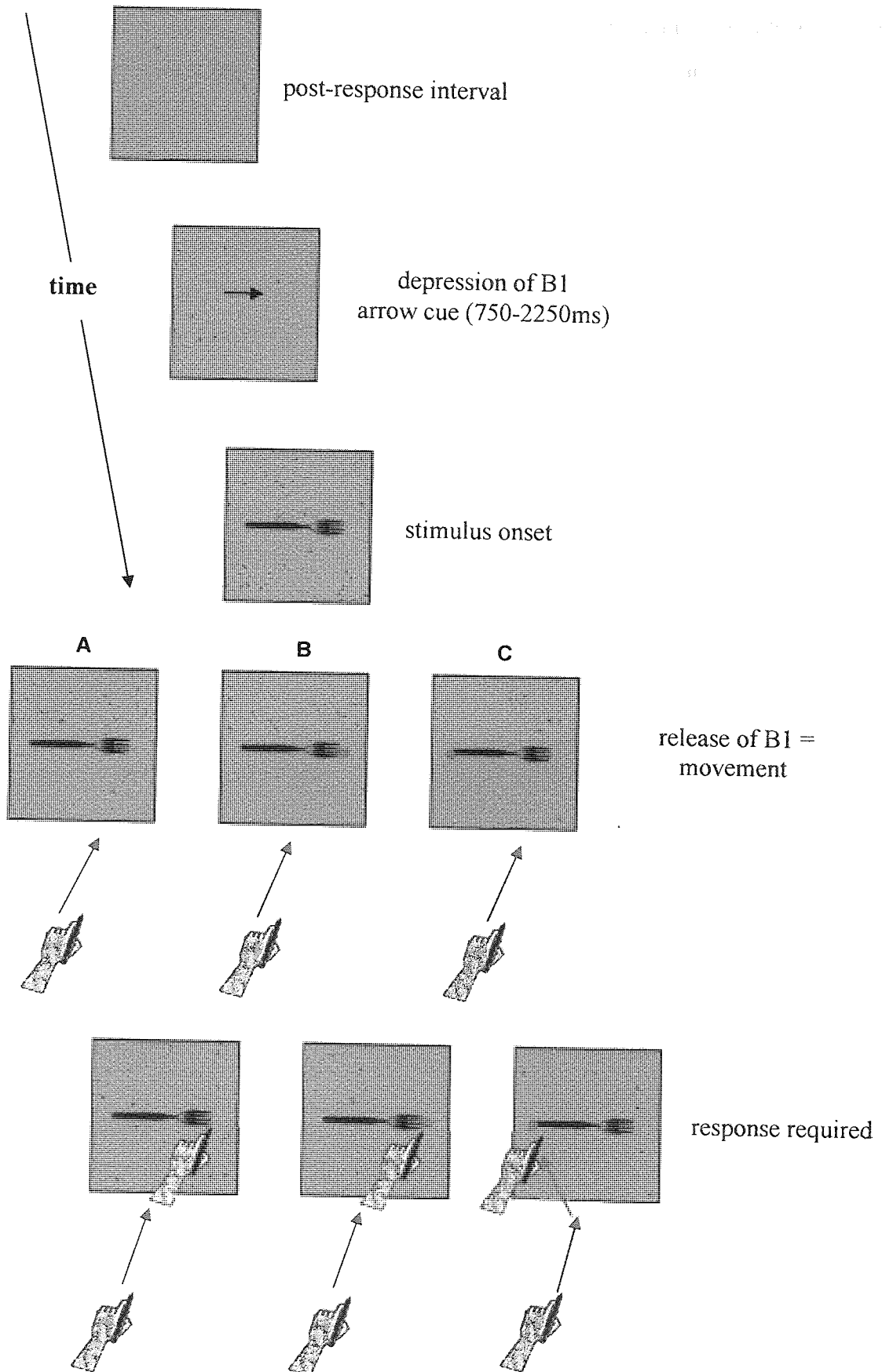
Figure 5.8: Examples of responses required dependent upon trial type. **(A)** The response required on a standard trial is straight forward as is the response required on a compatible perturbation trial **(B)**. **(C)** The response required on an incompatible perturbation trial is complex and requires on-line movement planning. Standard trial, compatible perturbation trials and incompatible perturbation trials accounted for 80%, 10% and 10% of trials, respectively.

To summarise, whereas on standard trials the response-to-made was always known prior to movement onset, on perturbation trials this was not necessarily the case.

5.3.2 Experimental procedure

5.3.2.1: Experimental instructions & consent form

Prior to participating in the study, each participant was provided with a combined experimental instruction and consent form [Appendix II]. This stated the requirements of the participant, the experimental procedure and the ethical issues concerning the research. In brief, this documentation informed the participant that they would be required to point to either the far left or right edge of a stimulus, or a red circular target that appeared coincident with movement onset. It also informed the participant that they must respond quickly but accurately as soon as the stimulus appeared on screen, and that a time-limit of 2.5 minutes would be imposed for the completion of experimental blocks. It stated that experimental blocks contained 40 trials, but that a period of practice would be incorporated to ensure that they could complete this number of trials within the 2.5 minute time-limit. The form additionally explained the basic mechanics of the experimental task and that the depression of button box B1 initiated a trial. Finally, it informed participants of their right to withdraw participation from the experiment at any time.

5.3.2.2: Control training phase

In the training phase of the experiment, the ratio of standard to perturbed trials was 60:40. This ratio of trials was adopted to ensure participants had thorough practice of both response types.

Each participant was taught how to hold the stylus so that the reflective marker was visible to the three cameras. They were further shown how a trial was elicited by the depression of B1 and how it was terminated when the stylus hit the screen (i.e. depression of B0). The participant was not informed that the release of B1 would, on occasion, also trigger the appearance of the perturbation signal.

Once a participant had mastered the basic elements of the task, they were asked to complete a block of 20 trials. During this first block it was checked that the reflective marker on the stylus-tip was visible to all three cameras, and that the participant

understood the task and was seated in a comfortable position. The participant was then asked to complete a second block of 40 trials. After this block it was again verified that the reflective marker on the stylus-tip was visible to all three cameras and that the participant was seated in a comfortable position. The participant was then asked to complete a further block of 40 trials, for which a time-limit of 2.5 minutes (signalled by a high-pitched tone) was imposed. This completed the control training phase. However, if a participant did not complete this practice block within the time-limit, further practice blocks of 40 trials were undertaken until this criterion was met. Details relating to each participant's performance in the control training phase are reported in the relevant experimental chapters [Chapters **6-8**, Section **2**].

5.3.2.3: Test phase

In the experimental test phase, the ratio of standard to perturbed trials was 80:20. This ratio of trials was adopted to ensure participants did not prepare responses to perturbation trials (see Boulinquez & Nougier, 1999).

Participants were reminded that a time limit of 2.5-minutes would be imposed per experimental block. They were also informed that they were required to complete *n* experimental blocks (reported in the methodology sections of the relevant experimental chapters). After each experimental block, a rest period of approximately two minutes was allowed.

5.4 Performance Measures

The measures of performance were movement time, path trace and hit error.

Movement time data was recorded using the VSG timer, which has a resolution of 100 microseconds. The timer was initiated by the release of B1 (i.e. movement onset) and terminated by the depression of B0 (i.e. movement termination). This data (to the nearest millisecond), along with all trial details (e.g. arrow direction, stimulus displayed, trial type) was automatically recorded in a separate text file and was later analysed using statistical software packages (e.g. SPSS).

Path trace data was recorded using the motion capture system, which has a resolution of one thousandth of a millimetre. When using the hand-held stylus, the constant stream of light reflected from the stylus tip marker to each of the cameras allowed both hand and arm movements to be recorded. The path trace data of interest was a participant's movement(s) from B1 to the perspex screen. These movements were recorded at a frame rate of 60 Hz and to an accuracy of one millimetre. This data was analysed using QTM Software which enabled the visualisation of 3-D marker movement in real time. The starting point of a movement was defined as five consecutive sampling points where the value of the stylus tip in the y co-ordinate (i.e. anterior-posterior axis) increased in value by at least 4mm between sampling points. The end point of a movement was defined as the peak y co-ordinate (see below). QTM Q-tools software was used for the graphical presentation of the data.

Hit error data was also recorded using the motion capture equipment, and was a measure of the discrepancy between the stimulus edge/perturbation target and the point of contact between the stylus and perspex screen. Hit error was rounded to the nearest millimetre, with a hit accuracy of 0mm denoting no error. Measurements of hit accuracy were made using the Qualysis Track Manager. This was achieved by recording the value of the stylus tip marker in the x co-ordinate (i.e. medio-lateral axis) when the value of this marker in the y co-ordinate was at its peak[2]. The x movement co-ordinate of the stylus tip marker was then compared with the actual stimulus edge/circular

---

[2] This was because when y was at its peak, the stylus was pressed against the screen

137

perturbation target measurement. These measurements were obtained prior to experimentation by placing a reflective marker on the stimulus edge/perturbation target and recording the x co-ordinate of this marker with reference to the x co-ordinates of each marker attached to the top of the monitor.

When analysing movement time and hit accuracy data, the 0.05-trimmed mean was adopted. The trimmed mean controls for the presence of outliers having an undue influence on results. Therefore in comparison to the standard mean, when used with inferential statistics, the trimmed mean typically yields fewer Type-1 and Type-2 errors (Burgess & Gruzelier, 1999).

Chapter 6

The Influence of Visual Attention and Affordance on Planned Movements

6.1 Introduction

Reaction time studies have revealed that both visual attention and affordance affect movement efficiency [see Chapter's 1 and 4]. However, it has not been determined whether the influences of these precursors to action are mutually exclusive or a consequence of a common visual stimulus property (e.g. object asymmetry). Additionally, the roles of visual attention and/or affordance upon movement construction have not been investigated using ecologically valid paradigms (see Pavese & Buxbaum, 2002).

These issues were addressed here by assessing the efficiency of pointing manoeuvres to a wide variety of stimuli varying in their attentional and affordance attributes. The measures of movement efficiency utilised were movement time, path trajectory and hit error. Participants were required to point to the left or right edge of a stimulus. Similar to reaction time studies, the 'to-be-executed response' was known prior to movement onset (i.e. it was planned) [1].

To investigate the effects of visual attention, geometric stimuli were used. These stimuli were asymmetric due to the presence of a single conspicuous feature in either the left or right side of object-space. To investigate the combined effects of visual attention and affordance, coherent object stimuli were used. These stimuli were also asymmetric due to the presence of a graspable handle, which formed the object's conspicuous feature. To investigate the unique effects of visual attention and affordance, incoherent object stimuli were used. These stimuli were again asymmetric. However, the conspicuous

---

[1] On approximately 10% of trials a participant had to alter their movement to point towards the opposite edge of a stimulus. The inclusion of such trials ensured the participants did not selectively process the parts of an object the movement was towards (see Vecera, Behrmann & Filapek, 2001).

feature and the object's graspable handle were on opposing sides of object-space. The rationale for employing these stimulus types to assess the effects of visual attention and affordance is provided in Chapter 5, Section 2.

Consistent with reaction time findings, it was hypothesised that if attentional properties of an object are represented automatically during visual perception, then decreased movement times are expected when pointing towards the conspicuous feature of geometric stimuli, the conspicuous feature of coherent object stimuli and the conspicuous feature of incoherent object stimuli. However, if the action-relevant (i.e. affordance) properties of an object are represented automatically during visual perception, then decreased movement times are expected when pointing towards the handle of coherent and incoherent object stimuli. For coherent object stimuli, the handle is also the conspicuous feature. For incoherent object stimuli, the handle opposes the conspicuous feature.

Little is known about the effects of visual attention and affordance upon path trajectories [see Chapter 4]. Applying the same arguments, however, it was hypothesised that if attentional properties of an object are represented automatically, then path trajectory efficiency should be greater (i.e. fewer path deviations) when an individual has to point towards the conspicuous feature of the three stimulus types. Yet, if the action-relevant properties of an object are represented automatically then path trajectory efficiency should be greater when an individual has to point towards the handle of coherent and incoherent object stimuli.

Deviations in path trajectory might also lead to comparable differences in hit error when striking a stimulus edge. If attentional properties of an object are represented automatically, hit accuracy should be greatest (i.e. minimal hit error) when pointing towards the conspicuous feature edge of the three stimulus types. If, however, the action-relevant properties of an object are represented automatically, for coherent and incoherent object stimuli, hit accuracy should be greatest when pointing towards the graspable handle.

6.2 Participant Information and Experimental Details

Only details specific to the completion of planned movements are reported here. Planned movements were investigated using 'standard' trials. On these trials the pointing movement was directed towards a given stimulus edge (i.e. left or right) by an arrow cue presented at the start of each trial.

Twenty, right-handed participants (14 male, 6 female) took part in the investigation. The mean age of the participants was 32 years 4 months (range 24 to 47 years). In the training phase of the experiment, every participant completed one control block of 20 trials and two additional control blocks of 40 trials each. Two participants (AHa & BW) completed a third control block of 40 trials to ensure that they could complete the task within the 2.5 minute time period. In the test phase, all participants completed eight blocks of 40 trials each. The experiment was conducted in a semi-darkened room. All participants held the stylus in their right-hand.

Where applicable, parametric statistics were adopted to analyse the data. These analysis methods were used as both the (trimmed) movement time data and (trimmed) hit error data conformed to the underlying assumptions of normality and homogeneity of variance. For clarity, the results presented for each stimulus type are colour coded: blue is used for geometric stimuli; red is used for coherent object stimuli; and green is used for incoherent object stimuli. Raw data for all performance measures are reported in Appendix III. Refer to Chapter 5 for all other experimental details.

6.3 Results

6.3.1 Movement time data

Movement time was a measure of the time it took a participant to complete a pointing manoeuvre (i.e. one trial) and was recorded from the release of B1 to the depression of B0.

Figure **6.1** shows movement times to geometric stimuli, coherent object stimuli and incoherent object stimuli. For each stimulus type the shaded bar represents movement times towards the edge with the conspicuous feature. For geometric stimuli, movement times differed dependent upon whether the pointing manoeuvre was directed towards the edge with the conspicuous feature or towards the edge without this feature [t = -1.793, df = 19, p = 0.045, one-tailed]. For this stimulus type, movement times were reduced when an action was directed towards the edge with the conspicuous feature. Movement times towards or away from the edge with the conspicuous feature were not significantly different for either coherent or incoherent object stimuli [t = -0.149, df = 19, p = 0.442, one-tailed and t = 1.260, df = 19, p = 0.223, two-tailed, respectively]. For coherent object stimuli, the edge with the conspicuous feature was the edge with the graspable handle. For incoherent object stimuli, the edge with the conspicuous feature opposed the edge with the graspable handle.

A repeated measures ANOVA of stimulus type (i.e. geometric, coherent object and incoherent object) x edge property (i.e. with or without a conspicuous feature) further revealed a significant interaction between stimulus type and edge property (F $_{(2, 38)}$ = 3.871, p = 0.041, partial η^2 = 0.17). Namely, whilst action directed towards the edge with the conspicuous feature facilitated movement on geometric stimuli trials, this was not the case on coherent object trials. Moreover, on incoherent object trials the reverse was true. This interaction effect is evident in Figure **6.1**.

Discussion

In accordance with the idea that visual attention potentiates motor codes (Anderson *et al.*, 2002), the task-irrelevant direction of a single attentional bias affected movement times. Movements corresponding with the direction of a single attentional bias were

Mean Movement Time (ms)

580
575
570
565
560
555
550
545
540
535
530

Geometric
Stimuli

Coherent
Object Stimuli

Incoherent
Object Stimuli
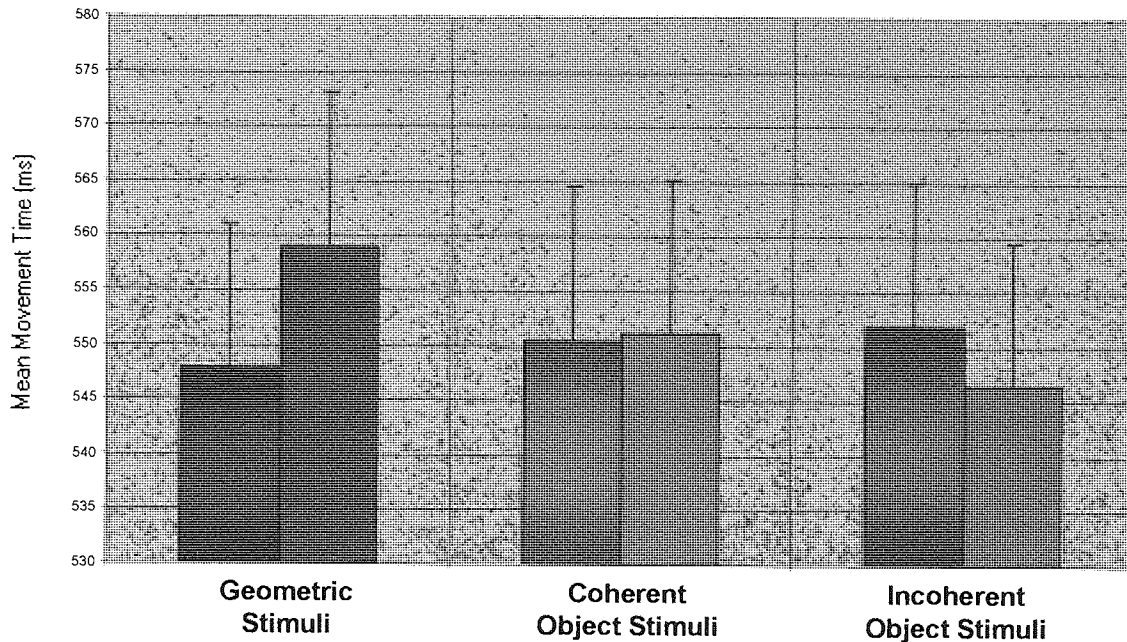
Figure 6.1: Mean movement times for geometric stimuli, coherent object stimuli and incoherent object stimuli. The shaded bars represent movement times towards the edge with the conspicuous feature. The vertical bars show one standard error of the mean [SEM]. The vertical bars show one standard error of the mean [SEM].

significantly faster than those opposing this bias. However, if only the attentional properties of a stimulus influenced the automatic potentiation of motor codes, the presence of a competing affordance bias should have been negligible. This was not verified. For stimuli with an opposing affordance bias, no movement time differences were reported irrespective of whether a manoeuvre corresponded with this bias or the attentional bias. This result would appear to demonstrate that affordance biases can also influence the potentiation of motor codes (e.g. Craighero *et al.*, 1996, 1998; Tucker & Ellis, 1998, 2001, 2004; Rumiati & Humphreys, 1998; Ellis & Tucker, 2000; Gentilucci, 2002; Humphreys, 2001; Hommel, 2002; Phillip & Ward, 2002). Indeed, the observation of increased movement times towards the conspicuous feature on incoherent object trials compared with geometric stimuli trials (i.e. the interaction effect) could reflect response competition effects (see Tipper, Lortie & Baylis, 1992; Pratt & Abrams, 1994; Tipper *et al.*, 1997; 1998) between opposing affordance and attentional biases when movements were directed towards incoherent object stimuli. Finally, contrary to both predictions and previous literature [refer to Chapter 1, Section 1.3; Chapter 4, Section 4.3; this Chapter, Section 6.1], the presence of a shared attentional and affordance bias did not affect movement times. A possible explanation for this null result is provided from the analysis of the path trace data.

6.3.2 Path trace data

Path trace was a measure of path trajectory efficiency for a given trial and was recorded from the release of B1 to the depression of B0. Independent of stimulus type or whether movement was directed towards or away from the conspicuous feature of a stimulus, participants demonstrated efficient movement trajectories that approximated a diagonal trace in x-y space on 95.9% of trials. An efficient movement trajectory was defined as a movement that did not deviate from a start-to-target diagonal by more than 7% in the x co-ordinate plane. For two participants, examples of these traces are provided in Figure 6.2. The red lines represent their path trajectories from B1 to the perspex screen plotted in x and y cartesian planes. In each case, efficient diagonal path traces are evident.
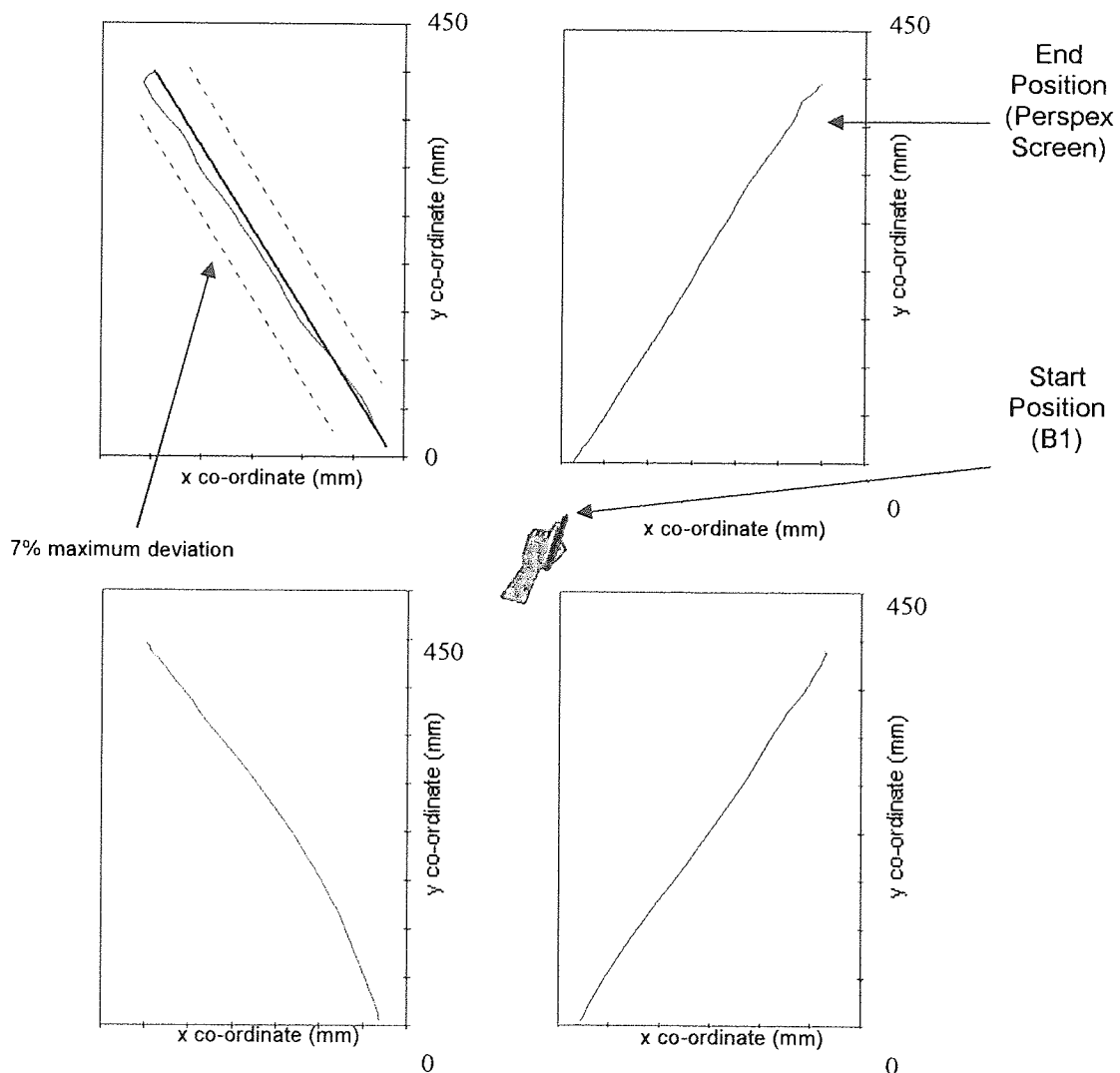
Figure 6.2: Examples of normal path trajectories irrespective of stimulus type or associated edge properties. The red lines represent the participant's path trajectories from B1 to the perspex screen. The broken orange lines in the top left panel represent the maximum 7% departure from a diagonal (not to scale) accepted as an efficient path trajectory. Traces are plotted in the x and y cartesian planes. Top Panels = Participant AH; Bottom Panels = Participant NM.

Major path deviations were evident on 1.49% of trials. These were defined as a movement in x and y cartesian planes that did not approximate a diagonal trace for a period of more than 25% of the whole movement. For six participants, examples of trials on which such deviations occurred are presented in Figure **6.3**. For pointing manoeuvres towards the left stimulus edge (from top-to-bottom, participants JL, FMc and JW, respectively), major path deviations towards the non-target edge in the right-side of space are evident [left panels]. For pointing manoeuvres towards the right stimulus edge (from top-to-bottom, participants SH, LM and AZ, respectively), major path deviations towards the non-target edge in the left side of space are evident [right panels].

Figure **6.4** shows the frequency of major path deviations for each stimulus type. The shaded bars represent major path deviations towards the edge with the conspicuous feature. Note that major path deviations always veered towards the non-target edge. For geometric stimuli, major path deviations differed dependent upon whether the non-target edge coincided with the conspicuous feature or the edge without this feature [$\chi^2 =$. 49.07, df = 1, p < 0.001]. For this stimulus type, path trace efficiency was greatest when a movement was directed towards the edge with the conspicuous feature. When a movement was directed towards the opposing edge (i.e. the edge without the conspicuous feature), path deviations towards the non-target edge were significantly more likely to occur. For coherent and incoherent object stimuli, major path deviations towards the non-target edge did not differ dependent upon whether a pointing manoeuvre corresponded with or without the edge with the conspicuous feature [coherent object stimuli χ^2 = 0.333, df = 1, p = 0.564; incoherent object stimuli χ^2 =0.037, df = 1, p = 0.847].

An analysis of stimulus type (i.e. geometric, coherent object and incoherent object) additionally revealed that major path deviations towards the non-target edge were most likely to occur on geometric stimuli trials [χ^2 = 12.636, df = 2, p = 0.002]. This was a consequence of the high number of path deviations towards the edge with the conspicuous feature on these trials. This effect is clearly evident in Figure **6.4**.
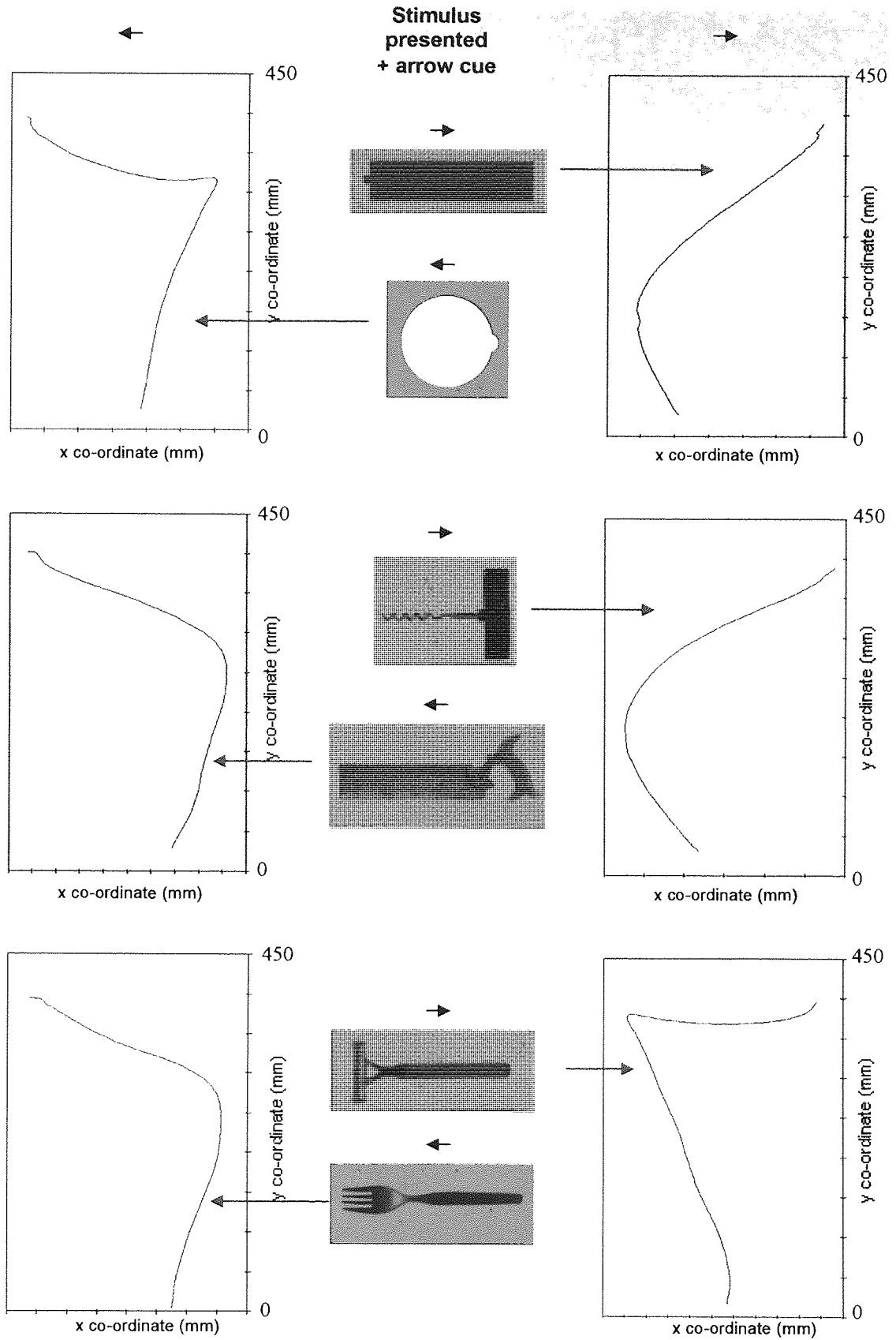
Figure 6.3: Examples of trials on which participants made major path deviations. The red lines represent the participant's path trajectories from B1 to the perspex screen. These are plotted in the x and y cartesian planes. Deviations toward the non-target edge are evident.
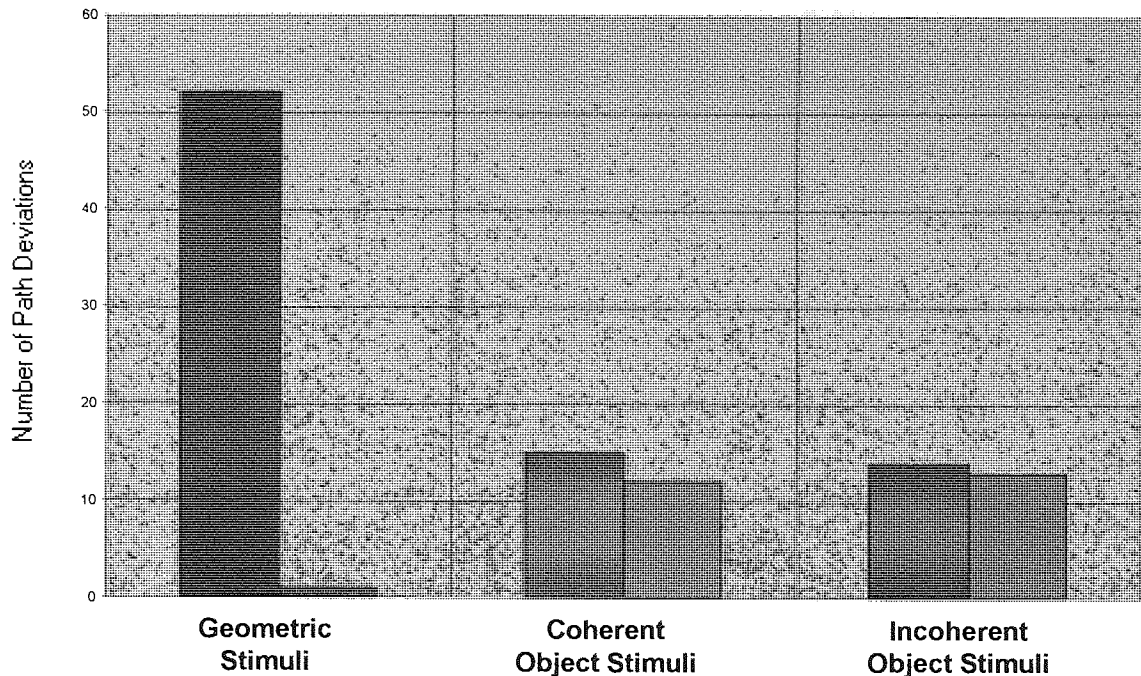
Figure 6.4: Distribution of major path deviations for geometric stimuli, coherent object stimuli and incoherent object stimuli. The shaded bars represent deviations towards the non-target edge when it coincided with the conspicuous feature.

Discussion

Similar to the movement time data it is apparent that the direction of a single attentional bias was important in determining the efficiency of an individual's path trajectory. For geometric stimuli, interference effects manifest as path deviations towards the conspicuous feature[2] demonstrate that the single attentional bias of this stimulus type potentiated salient motor response codes (see also Castiello, 1996; 1999; Tresillian, 1999; Meegan & Tipper, 1999; Tipper *et al.*, 2002). Moreover, path deviations corresponding with the direction of a single attentional bias outnumbered path deviations corresponding with all other biases summed together. This result, in itself, demonstrates the powerful response saliency of attentional biases.

The path trajectory data further revealed that for stimuli with a shared attentional and affordance bias, path deviations towards the non-target edge did not differ dependent upon whether this edge corresponded with, or opposed, the direction of shared bias. Subsequently, it would appear that the edge opposing the direction of shared bias

---

[2] It is possible that path deviations also veered away from the 'distractor' edge (see Harvey, Milner & Roberts, 1994; Tipper and colleagues, 1997a; 1997b; 1998; 1999; 2002; McSorley *et al.*, 2004) but that these deviations were too subtle to be detected. This does not, however, impact upon theories proposed.

elicited a degree of automatic response capture (e.g. Müller & Rabbit, 1989; Theeuwes et al, 1999; Remington *et al.*, 2001). Opposing the object's graspable handle, this response saliency is likely to reflect an unpredictable attentional capture and could explain why null movement time results were observed for this stimulus type. Namely, if the edge opposing the direction of shared bias elicited a response saliency, it is likely that pointing manoeuvres towards it would have been facilitated, influencing movement efficiency.

For stimuli with competing attentional and affordance biases, deviations towards the non-target edge were also similar irrespective of whether this edge corresponded with the direction of attentional bias or the direction of affordance bias. The sensitivity of this measure, nonetheless, reveals that as path trajectories did deviate towards the direction of an object's graspable handle, the affordance bias of a stimulus must have resulted in the automatic potentiation of motor codes. Therefore, consistent with the movement time findings, it is likely that for stimuli with opposing attentional and affordance biases, an element of response competition was present.

6.3.3 Hit error data

Hit error was defined as the distance between the target edge and the hand-held stylus tip upon 'striking' the perspex screen. A hit error of zero was recorded when the stylus tip was aligned with the target edge. Positive errors were defined as hits inwards of the stimulus edge (i.e. somewhere on the stimulus). Negative errors were defined as hits beyond the stimulus edge.

Figure **6.5** shows mean hit error for geometric stimuli, coherent object stimuli and incoherent object stimuli. For each stimulus type the open square shows mean hit error when the movement was directed towards the edge with the conspicuous feature. Note that, independent of whether movement was directed towards or away from the conspicuous feature of a stimulus, hit error was always positive. For coherent and incoherent object stimuli, hit error differed depending upon whether a movement was directed towards the edge with the conspicuous feature or the edge without this feature [$t = 2.268$, df $= 19$, p $= 0.035$, two-tailed and $t = -7.200$, df $= 19$, p < 0.001, two-tailed, respectively]. For coherent object stimuli, hit error was greatest when pointing towards the edge with the conspicuous feature (i.e. coinciding with the location of the object's

graspable handle). For incoherent object stimuli, hit error was greatest when pointing towards the edge without the conspicuous feature (i.e. towards the object's graspable handle). For geometric stimuli, mean hit error did not differ dependent upon whether the movement was directed towards the edge with the conspicuous feature or the edge without this feature [$t = -0.181$, df $= 19$, p < 0.858, two-tailed].
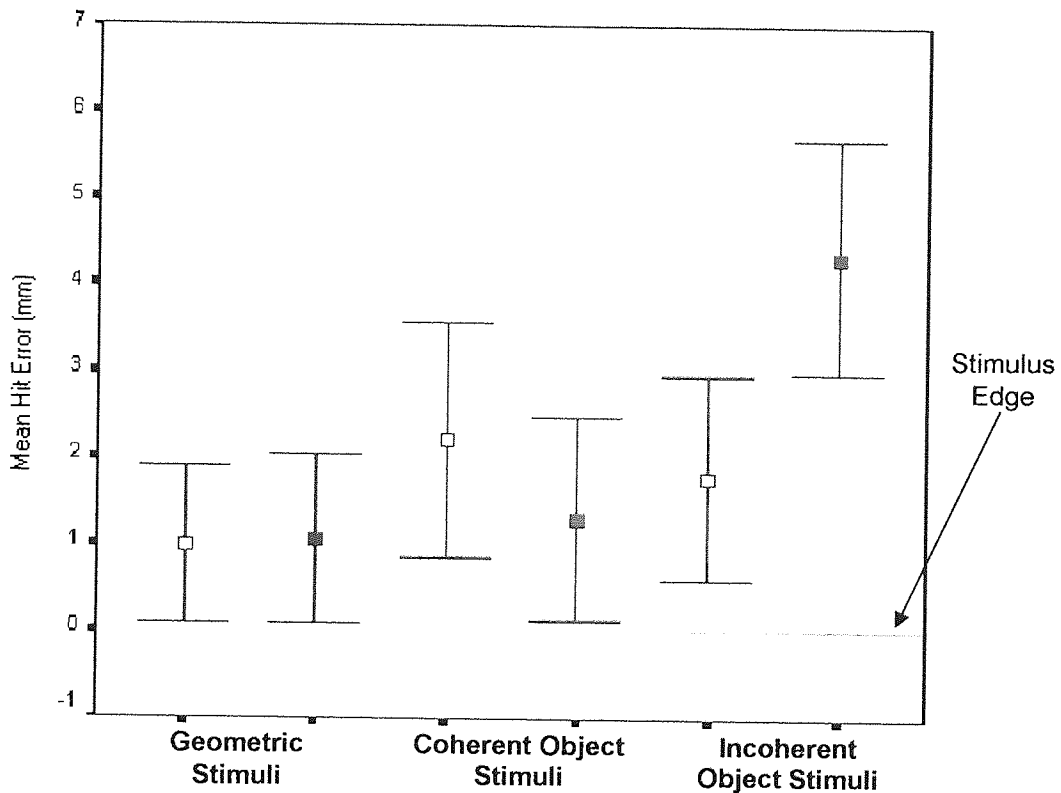
Figure 6.5: Mean hit error for geometric stimuli, coherent object stimuli and incoherent object stimuli. For all stimulus types the open squares shows mean hit error when the movement was directed towards

A repeated measures ANOVA of stimulus type (i.e. geometric, coherent object and incoherent object) x edge property (i.e. with or without a conspicuous feature) further revealed a main effect of stimulus type ($F_{(2, 38)} = 28.44$, p < 0.001, partial $\eta^2 = 0.60$; linear trend $F_{(1, 19)} = $, p < 53.28, partial $\eta^2 = 0.74$). Namely, movement accuracy was most efficient on geometric stimuli trials and least efficient on coherent object trials. This effect is evident in Figure **6.5**.

Discussion

It was expected that if attentional biases were of key importance in determining hit error, then hit accuracy should have been greatest when pointing manoeuvres were

directed towards an edge with a conspicuous feature. This theory was not supported. The key predictor of hit accuracy was the direction of affordance bias. However, contrary to predictions, hit accuracy was greatest when a movement opposed an object's graspable handle. When a movement corresponded with a graspable handle participants tended to 'undershoot' the target edge and strike the object's handle. This effect was greatest when a movement corresponded with the direction of a single affordance bias and likely reflects functional knowledge related to graspable object stimuli (e.g. Ellis & Tucker, 2000; Tucker & Ellis, 2004). This hypothesis is discussed in more detail in Section **6.4**.

6.3.4 Trial error data

A *trial error* was recorded for any trial whereby the participant hit the stimulus edge opposite to that directed by the arrow cue. Participants made errors on 0.8% of trials.

The number of trial errors for each stimulus type is displayed in Figure **6.6**. The shaded bars show trial errors towards the edge with the conspicuous feature. For geometric stimuli, trial errors differed dependent upon whether a pointing manoeuvre was directed towards or away from the edge with the conspicuous feature [$\chi^2 = 11.56$, df $= 1$, p $= 0.002$]. For this stimulus type, trial errors were significantly more likely to occur when the movement was directed towards the edge without the conspicuous feature. In consequence, there were more trial errors towards the non-target edge when it corresponded with the conspicuous feature edge. Trial errors towards or away from the edge with the conspicuous feature were not significantly different for either coherent or incoherent object stimuli [$\chi^2 = 1.68$, df $= 1$, p $= 0.197$ and $\chi^2 = 3.28$, df $= 1$, p $= 0.071$, respectively].

An analysis of edge property (i.e. with or without a conspicuous feature) additionally revealed that more errors were made when a non-target edge coincided with a conspicuous feature than when it did not [$\chi^2 = 14.00$, df $= 1$, p < 0.001].

Figure **6.7** shows the distribution of path deviations [left bars] and trial errors [right bars] to the left and right side of space. White bars represent trial errors and path deviations towards the left side of space, whereas black bars represent trial errors and path deviations towards the right side of space. Independent of stimulus type, or

whether movement was directed towards or away from the conspicuous feature of a given stimulus, path deviations towards the right side of space [n = 74] were more common than those towards the left side of space [n= 31] [χ^2 = 17.28, df = 1, p < 0.001]. However, for the trial error data the side of space a movement was towards made no difference [χ^2 = 0.037, df = 1, p = 0.789], with 29 and 27 trial errors to the right and left side of space, respectively.
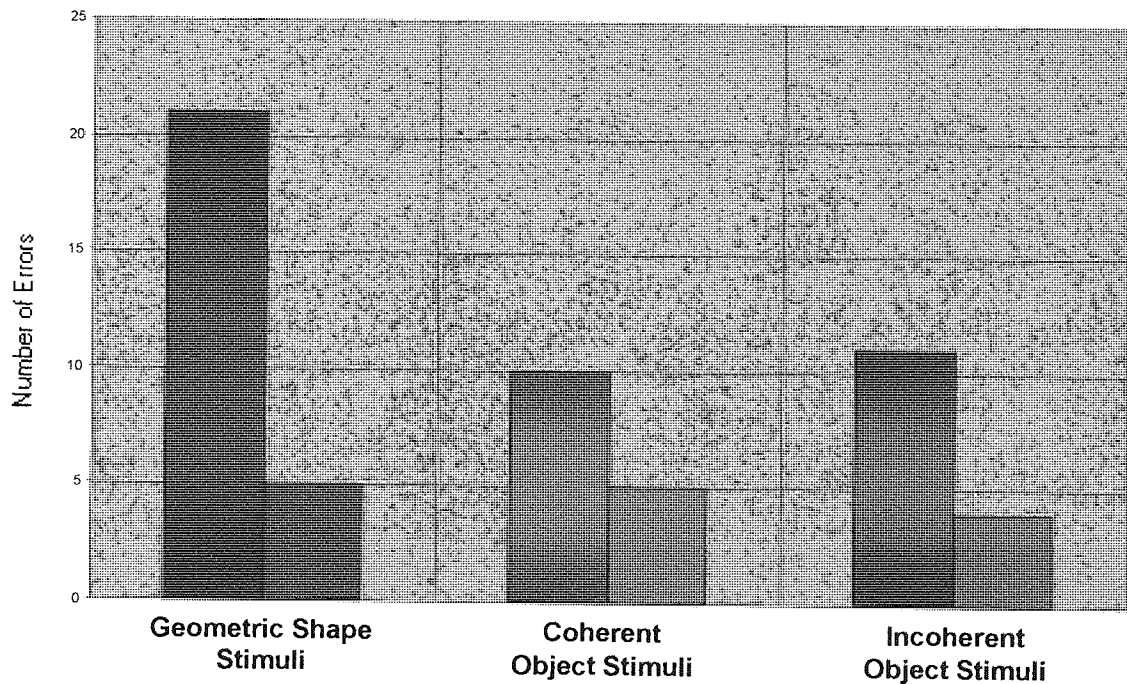
Figure 6.6: Distribution of errors for geometric stimuli, coherent object stimuli and incoherent object stimuli. For all stimulus types the shaded bars represent errors when the non-target edge concurred with the conspicuous feature.

Discussion

Of importance, the trial error data reveals that the direction of attentional bias was the critical variable in determining error rates. That is, foremost, the attentional bias of stimuli influenced the potentiation of motor codes. However, whilst infrequent, trial errors did correspond with the direction of a single affordance bias. This result reaffirms the hypothesis that the affordance bias of stimuli can result in the automatic potentiation of motor codes. For coherent object stimuli, trial errors directed towards the edge opposing the direction of shared attentional and affordance bias were observed. This finding is consistent with the theory that this edge elicited a degree of response saliency.
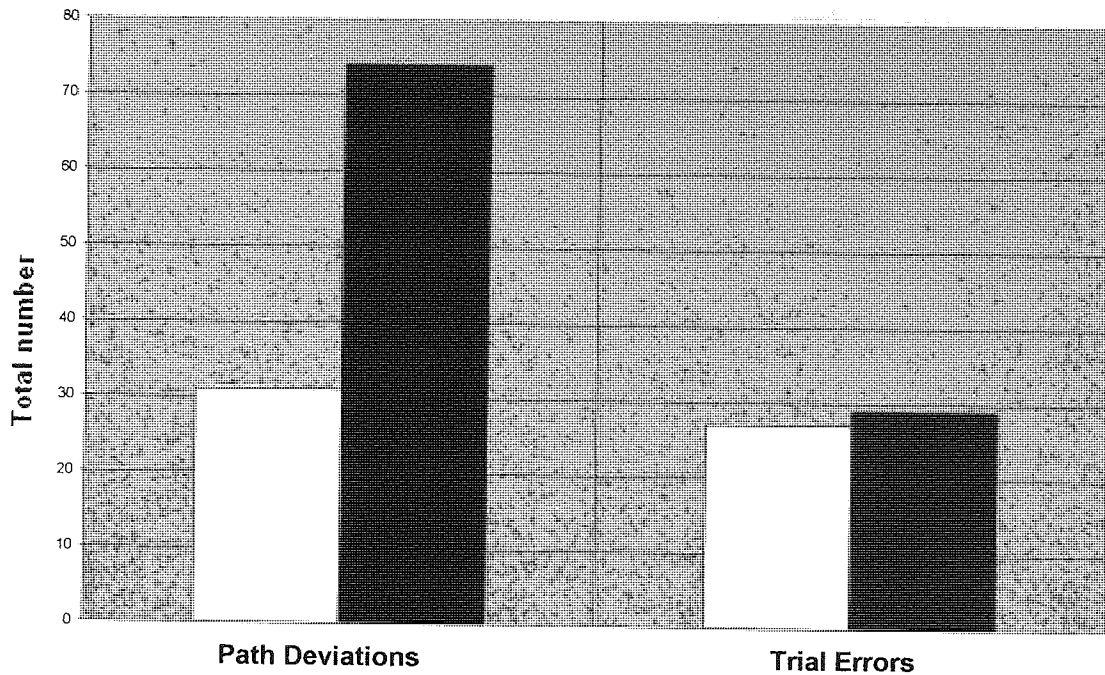
Figure 6.7: Distribution of path deviations and trial errors on standard trials. The white bar represents path deviations/trial errors to the left side of space. The black bar represents path deviations/trial errors to the right-side of space.

In an analysis of 'side of space' a movement was towards, it was revealed that major path deviations towards the right-side of space were more common than those towards the left-side of space. This finding is consistent with a rightward attentional bias in right-handed individuals (e.g. Reuter-Lorenz, Kinsbourne, Moscovitch, 1990; Corbetta, Miezin, Shulman & Peterson, 1993; but see Barthelemy & Boulinguez, 2001; Barthelemy & Boulinguez, 2002).

6.4 Discussion

The results provide evidence to suggest that the visual attributes of a stimulus can affect the efficiency with which planned arm/hand movements towards it are produced. Of importance, the research reveals that action potentiation was foremost influenced by directed visual attention. This was evident from the high number of path deviations and trial errors observed when a movement opposed the direction of attentional bias. These findings have implications for theories of affordance (e.g. Craighero *et al.*, 1996, 1998; Tucker & Ellis, 1998, 2001, 2004; Rumiati & Humphreys, 1998; Ellis & Tucker, 2000; Gentilucci, 2002; Humphreys, 2001; Hommel, 2002; Phillip & Ward, 2002). Namely, they demonstrate that 'slips of action' (see Reason, 1991) are likely to be primarily influenced by attentional biases.

However, whilst the attentional bias of a stimulus appeared to be the critical prerequisite for the potentiation of motor codes, it was observed that effects of this bias were often attenuated when a stimulus had a shared or opposing affordance bias. For example, contrary to predictions and previous research, it was found that for stimuli with a shared attentional and affordance bias, pointing manoeuvres were no less efficient when they opposed the direction of shared bias. From the path trajectory and trial error results it was evident that these aberrant results were most likely due to the edge opposing the direction of shared attentional and affordance bias also eliciting a degree of attentional capture. Credence for this idea is provided from the research of Anderson *et al.* (2002). When investigating attentional biases, they noted that what captures attention can be both highly idiosyncratic and unpredictable. In the current investigation, this unpredictable and idiosyncratic attentional capture likely confounded results. Nonetheless, this result again demonstrates the salience of attentional biases in potentiating motor response codes.

For stimuli with competing attentional and affordance biases, movement efficiency was also similar irrespective of whether a pointing manoeuvre corresponded with the direction of attentional bias or the direction of affordance bias. Such null results could reflect stimulus differences of attentional focus; that is, whereas for geometric stimuli attentional bias was spatially focused, for object stimuli attentional bias was spread over

a large surface area [see Figure **6.8**]. For incoherent object stimuli, however, the null results are likely due to response competition effects (see Tipper, Lortie & Baylis, 1992; Pratt & Abrams, 1994; Tipper *et al.*, 1997; 1998) and the potentiation of motor codes by both attentional and affordance biases. Support for this theory is evinced from findings of path deviations and trials errors corresponding with the direction of a single affordance bias. Thus, whilst not critical for the potentiation of motor response codes, the current findings do lend support for theories of visual routes to action through object affordances (e.g. Craighero *et al.*, 1996, 1998; Tucker & Ellis, 1998, 2001, 2004; Rumiati & Humphreys, 1998; Ellis & Tucker, 2000; Gentilucci, 2002; Humphreys, 2001; Hommel, 2002; Phillip & Ward, 2002). Indeed, affordance biases were of importance in determining hit error. Whereas movements towards all stimuli typically undershot the target edge, this effect was greatest for object stimuli when the pointing manoeuvre corresponded with the direction of an object's graspable handle.
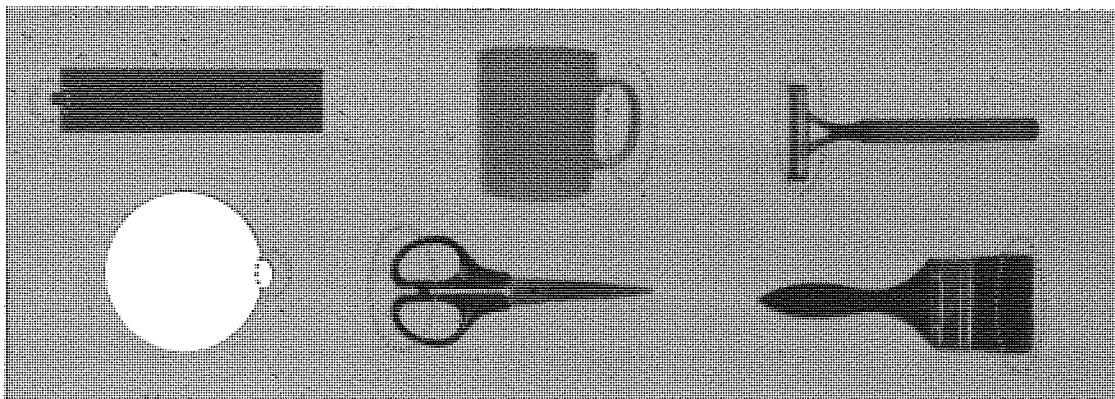
Figure 6.8: Rough estimates of attentional focus required to strike the edge with the conspicuous feature. For geometric stimuli (left images) attention is spatial focused compared with coherent (central images) and incoherent (right images) stimuli. In these stimuli, the attentional bias is spread over a larger surface area.

In previous research, 'hit error' as a measure of movement efficiency has not been investigated. However, from the observation of hitting an object's graspable handle rather than the stimulus edge, it is apparent that this measure provides convincing support for three affordance arguments. Firstly, the hit error results are indicative of the idea of 'micro-affordances' (Ellis & Tucker, 2000; Tucker & Ellis, 2004). These are affordances that result in subconscious motor plan repertoires that provide basic information on how to utilise object stimuli with known affordances (e.g. where/how to grasp objects). Secondly, the results are consistent with primate and neuroimaging

findings that dorsal stream parietal neurons have response selectivity for visual qualities of an object that link information about the visual features and attributes of objects with the appropriate hand and finger movements necessary for using them (e.g. Sakata *et al.*, 1997; Kalaska *et al.*, 1997; Chao & Martin, 2000; Rizzolatti *et al.*, 2000; 2002; Gold & Mazurek, 2002; Grezes & Decety, 2002; Handy *et al.*, 2003; Grezes *et al.*, 2003). Thirdly, they reveal that the motor patterns one uses to interact with an object are influenced by existing affordance representations (e.g. Hommel, 2002; Tucker & Ellis, 2004) and not how an object is perceived in real time (i.e. 2-D or 3-D). This third finding casts doubt on the arguments of Castiello *et al.* (1998; Chapter **4** Section **4.4**) who proposed that, primarily, the way an object is perceived in real time will override influences exerted by existing (cognitive) representations.

In sum, the results demonstrate that both the attentional and affordance attributes of visual stimuli influence movement construction and, subsequently, the potentiation of motor response codes. These findings are consistent with well documented theories of visual routes to action (e.g. Gibson, 1979; Michaels & Carello, 1981; Michaels 1988; Goodale & Milner, 1992; Milner & Goodale, 1995; Glover, 2004; see also Mattingly & Driver, 1997; Behrmann & Meegan, 1998; Craighero *et al.*, 1996, 1998; Tucker & Ellis, 1998, 2001, 2004; Rumiati & Humphreys, 1998; Anderson *et al.*, 2002; Ellis & Tucker, 2000; Humphreys, 2001; Gentilucci, 2002; Hommel, 2002; Philip & Ward, 2002; Marotta *et al.*, 2003). Additionally, by utilising an ecologically valid response of pointing (see Pavese & Buxbaum, 2002) and adopting a wide-range of movement efficiency measures, it has been revealed that the influences of affordance and directed attention upon movement construction are, to an extent, separable. Whereas affordance was of foremost importance in determining the action properties of an object that enabled its correct use (e.g. grasp type), directed visual attention was critical for fast, correct actions. Such findings could be of invaluable practical significance in applied situations. For example, in situations where fast, efficient movements are required, an optimum design would encompass a lay-out where the to-be-executed response is composed of one salient 'event' (i.e. an affordance bias or, better still, an attentional bias) in the right-side of space with no opposing bias. A poor design would encompass a lay-out where a number of distractors, attached to the salient 'event' or otherwise, are within close proximity of the event and/or in the right-side of space. Not surprisingly,

reaching for the wrong control in such situations is a common phenomenon (see for instance Bradley, 1969; Glendon, 1993).

Chapter 7

The Influence of Visual Attention and Affordance on the On-line Control of Movements

7.1 Introduction

It is known that perturbations of object size, location and background information influence the on-line control of action towards a target [see Chapter 4]. However, little is known regarding the effects of attention and/or affordance upon the control of action.

These issues were addressed by assessing the on-line control of action to a wide variety of stimuli varying in their attentional and affordance properties. The measures of movement efficiency utilised were movement time, path trajectory and hit error, and the participant response required was a pointing manoeuvre towards a perturbation target. The perturbation target was a small red circular target that appeared at either the left or right edge of a stimulus coincident with movement onset on approximately 20% of trials[1]. Similar to previous perturbation studies (e.g. Brenner & Smeets, 1997; Fourneret & Jeannerod, 1998; Pisella *et al.*, 1998; Desmurget *et al.*, 1999; Pisella *et al.*, 2000; Boulinguez *et al.*, 2001; Grea *et al.*, 2002; Lee & van Donkelaar, 2002; Johnson *et al.*, 2002; Bedard & Procteau, 2003; Nijhof, 2003), when this target was incompatible with the arrow cue, movement re-planning was required.

To investigate effects of visual attention, geometric stimuli were used. These stimuli were all asymmetric due to the presence of a single conspicuous feature in either the left or right side of object-space. To investigate the combined effects of visual attention and affordance, coherent object stimuli were used. These stimuli were also asymmetric due to the presence of a graspable handle, which formed the object's conspicuous feature. To investigate the unique effects of visual attention and affordance, incoherent object

---

[1] The occurrence of perturbation targets was infrequent to avoid participants preparing responses to such targets (see Boulinquez & Nougier, 1999).

157

stimuli were used. These stimuli were again asymmetric. However, the conspicuous feature and the object's graspable handle appeared in opposing sides of object-space. For all stimulus types, the perturbation target could appear at either edge of the stimulus (i.e. the edge with the conspicuous feature or the edge without this feature). The rationale for employing the three stimulus types to assess effects of visual attention and affordance is provided in Chapter 5, Section 2.

Studies of object location change have revealed that when an individual alters a movement on-line they can respond both quickly and efficiently, with movement times and path trajectories comparable to performances upon unperturbed trials, provided the perturbed target is located no more than approximately 4cm from the original target [See Chapter 4]. In general, such studies have utilised simple circular/cylindrical targets and not stimuli varying in their affordance or attentional attributes. However, based on previous findings [see Chapters 1, 3, 4 & 6], it is likely that the manipulation of where a perturbation signal appears will accord or conflict with the attentional and/or affordance biases coded for. Thus, it is predicted that:

1) If attentional biases potentiate motor codes, then on geometric stimulus trials, a response directed towards the conspicuous feature is likely to be primed irrespective of whether a movement is primarily directed towards it or not. In consequence, on the appearance of a perturbation target corresponding with this feature, on-line movement re-planning towards it will be initiated both quickly and efficiently. Namely, movement time, path trajectories (i.e. smoothness of trace) and hit accuracy will be of greater efficiency when a perturbation target coincides with the conspicuous feature edge than when it does not. These arguments should also apply when a corrective manoeuvre is required towards the conspicuous feature of incoherent object stimuli.

2) If affordance biases potentiate motor codes, then for incoherent object stimuli, a response directed towards an object's graspable handle is likely to be primed irrespective of whether a movement is primarily directed towards it or not. Therefore, on-line corrections to perturbation targets appearing at the edge with the graspable handle, rather than the edge with the conspicuous feature, should be most efficient. This is with the exception of hit error where a pattern of striking the object's handle may be observed [see Chapter 6].

3) If both attentional and affordance biases contribute to the potentiation of motor codes, on-line responses should be most efficient when a perturbation target coincides with the conspicuous feature edge of the coherent object stimuli (given the shared attentional/affordance bias of this edge)[2]. However, hit accuracy may be variable for the reasons stated above.

4) Finally, due to the experimental design, the perturbation target could also be compatible with the initial arrow cue. It was reasoned that performance on these trials would be comparable to that demonstrated on trials where the to-be-executed response was known prior to movement onset [i.e. standard trials; Chapter 6]. This hypothesis was based on similarities between the response required on both compatible perturbation trials and standard trials. Namely, the response necessary always accorded with the direction of the initial arrow cue.

---

[2] NB: In acknowledgement of the results of investigation two it should be noted that what is deemed to be salient (i.e. the conspicuous feature) can be highly idiosyncratic - this may affect results [refer to Chapter 6 Section 6.4].

7.2 Participant Information and Experimental Details

Only details specific to the completion of unplanned movements (i.e. performance on perturbation trials) are reported here. On these trials the pointing manoeuvre was directed towards a given stimulus edge by a circular perturbation target that appeared at movement onset. This target could be either *compatible* or *incompatible* with the arrow cue. Additionally, its appearance could correspond with the conspicuous feature edge or correspond with the opposing stimulus edge.

Twenty, right-handed participants [14 male, 6 female] took part in the investigation. The mean age of the participants was 32 years 4 months [range 24 to 47]. In the training phase of the experiment, every participant completed one initial block of 20 trials and two additional blocks of 40 trials each. Two participants [AHa & BW] completed a third additional control block of 40 trials to ensure that they could complete the task within the 2.5 minute time period. In the test phase, all participants completed eight blocks of 40 trials each. The experiment was conducted in a semi-darkened room. All participants held the stylus in their right-hand. Three participants, AHa, JS & SJA, deduced that the release of button box B1 triggered the appearance of the perturbation target. The remaining participants assumed that the perturbation target appeared sometime after movement onset.

Where applicable, parametric and/or non-parametric statistics were adopted to analyse the data. For clarity, the results presented for each stimulus type are colour coded: blue is used for geometric stimuli results; red is used for coherent object stimuli results; and green is used for incoherent object stimuli results. Raw data for all performance measures are reported in Appendix IV. Refer to Chapter 5 for all other experimental details.

7.3 Results

7.3.1 Incompatible perturbation trial findings

On incompatible perturbation trials the appearance of a perturbation target did not accord with the direction of the arrow cue. In consequence, a participant was required to alter their movement towards the opposite stimulus edge.

7.3.1.1: Movement time data[1]

Figure 7.1 shows movement times towards perturbation targets. For each stimulus type, the shaded bar represents movement time towards perturbation targets that coincided with the conspicuous feature edge. For all stimulus types, movement times towards perturbation targets did not differ dependent upon whether the target appeared at the edge with the conspicuous feature or the edge without this feature [geometric stimuli $t = -1.356$, df $= 18$, p $= 0.096$, one-tailed; coherent object stimuli $t = 0.341$, df $= 18$, p $= 0.369$, one-tailed; incoherent object stimuli $t = 0.690$, df $= 18$, p $= 0.499$, two-tailed].

Figure 7.1: Mean movement times for perturbation targets appearing on geometric stimuli, coherent object stimuli and incoherent object stimuli on incompatible perturbation trials. The shaded bars represent mean movement times towards perturbation targets when they appeared at the edge with the conspicuous feature. The vertical bars show one standard error of the mean [SEM].

---

[1] For incompatible perturbation trials, due to a computing error, movement time data is only available from 19 participants.

However, a movement time analysis of stimulus type (i.e. geometric, coherent object and incoherent object) x edge property at which the perturbation target appeared (i.e. with or without a conspicuous feature) did reveal a trend towards significance for the effect of stimulus type ($F_{(2, 32)}$ = 2.651, p = 0.086, partial η^2 = 0.14; linear trend $F_{(1, 16)}$ = 5.346, p = 0.034, partial η^2 = 0.25). This effect, evident in Figure **7.1**, demonstrates that movements towards perturbation targets were fastest when the targets appeared on geometric stimuli and slowest when the targets appeared on incoherent object stimuli.

Discussion

Given the literature demonstrating the importance of attentional and affordance biases in potentiating motor codes [see Chapter **1**, Sections **1.3** & **1.4** and Chapter **4**, Section **4.3** & **4.4**], the null movement time findings for stimuli with either a single attentional bias or shared attentional and affordance bias were unexpected. An explanation for these results is that the sudden appearance of a perturbation target automatically captured attention (e.g. Müller & Rabbit, 1989; Theeuwes *et al.*, 1999; Remington *et al.*, 2001) and, subsequently, elicited a degree of response saliency towards the edge at which it appeared. However, whilst such an effect was probable it was unlikely to influence results. This is because the response saliency of a perturbation target was constant irrespective of the edge at which it appeared. A more detailed discussion of this issue, including alternative explanations for the null results, is returned to in Section **7.4**.

For stimuli with competing affordance and attentional biases, the null movement time results could be taken as evidence that both attention and affordance potentiate motor codes [see Chapter **6**, Section **6.3.1** for relevant arguments]. Additional support for this idea is observed from the finding of increased movement times towards this stimulus type. This is indicative of response competition (e.g. Tipper and colleagues, 1992; 1997; 1998; 2002; Pratt & Abrams, 1994; Castiello, 1996; 1999; Jackson & Hussain, 1997; Meegan & Tipper, 1998; Tresillian, 1999; McSorley *et al.*, 2004). Namely, if both directed attention and affordance automatically elicit response saliencies, then when producing a movement corresponding with the direction of either bias, neural activity associated with the bias of the opposing stimulus edge is likely to be inhibited. In consequence, when a perturbation target suddenly appears at this latter edge, movement towards it will be impeded. This would result in corrective movements of comparable,

162

but increased, movement durations towards perturbation targets appearing at either edge, consistent with the findings.

7.3.1.2: Path trace data

To analyse path trajectory efficiency on incompatible perturbation trials, measures of movement transition type (i.e. non-smooth vs. smooth) and time-to-movement-transition (early vs. late) were used.

Examples of the two types of transition movement participants adopted when pointing towards perturbation targets are displayed in Figure **7.2**. The blue traces demonstrate non-smooth movement transitions plotted in x and y cartesian co-ordinates. Non-smooth movement transitions were composed of a corrective manoeuvre of sudden onset that appeared to be composed of two separate, co-joined movements. A trial was classed as demonstrating a non-smooth movement transition if the 'axis-of-rotation' at the turn-point was less than 45^0 or greater than 135^0. The red traces demonstrate smooth movement transitions plotted in x and y cartesian co-ordinates. A smooth movement transition was composed of a corrective manoeuvre with no sudden directional change in stylus motion. A trial was classed as demonstrating a smooth movement transition if the angle-of-rotation at the turn-point was between 45^0 and 135^0. In total, the ratio of smooth to non-smooth movement transitions on incompatible trials was 11:14, respectively. Additionally, on trials where a smooth movement transition was demonstrated, movement times were approximately 100ms faster [$t = 12.852$, df = 19, p < 0.001]. This finding is displayed in Figure **7.3**, where the white bar represents smooth movement transitions and the black bar represents non-smooth movement transitions.

Figure **7.4** shows the percentage of smooth-to-non-smooth transitions towards perturbation targets dependent upon the stimulus type at which they appeared. For each stimulus type, the shaded bar represents smooth (red) and non-smooth (blue) transition movements towards perturbation targets when they appeared at the edge with the conspicuous feature. For geometric stimuli, the movement transition type differed dependent upon the edge at which the perturbation target appeared [$\chi^2 = 9.785$, df = 1, p = 0.002 two-tailed, Cramer's V = 0.229]. For this stimulus type, when a perturbation target appeared at the edge with the conspicuous feature, a participant was significantly more likely to demonstrate a smooth movement transition. Movement transition type for
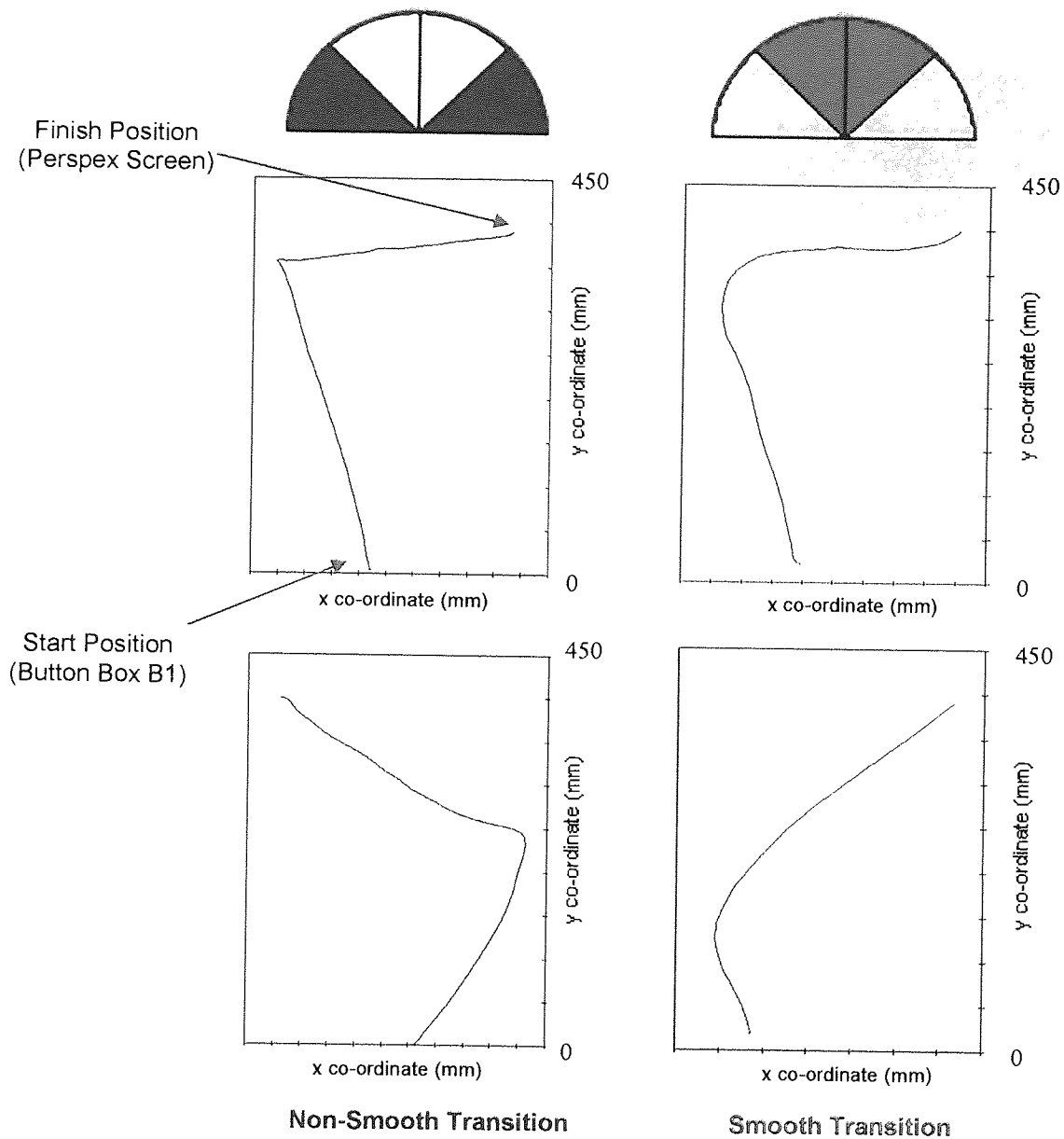
Figure 7.2: Examples of the two modes of response evident on incompatible perturbation trials. Non-smooth movement transitions are represented by a blue path trace and smooth movement transitions by a red path trace. The shaded areas of the top panels represent the angle-of-rotation at the turn point.

coherent and incoherent object stimuli did not differ dependent upon whether the perturbation target appeared at the edge with the conspicuous feature or the edge without this feature [coherent object stimuli $\chi^2 = 0.221$, df $= 1$, p $= 0.676$ two-tailed, Cramer's V $= 0.032$; incoherent object stimuli $\chi^2 = 1.982$, df $= 1$, p $= 0.187$ two-tailed, Cramer's V $= 0.102$].

Examples of early and late transition manoeuvres are presented in Figure **7.5**. The blue trace demonstrates a late transitions manoeuvre. A trial was classed as displaying a late transition manoeuvre if the turning manoeuvre was initiated after the mid-point of the
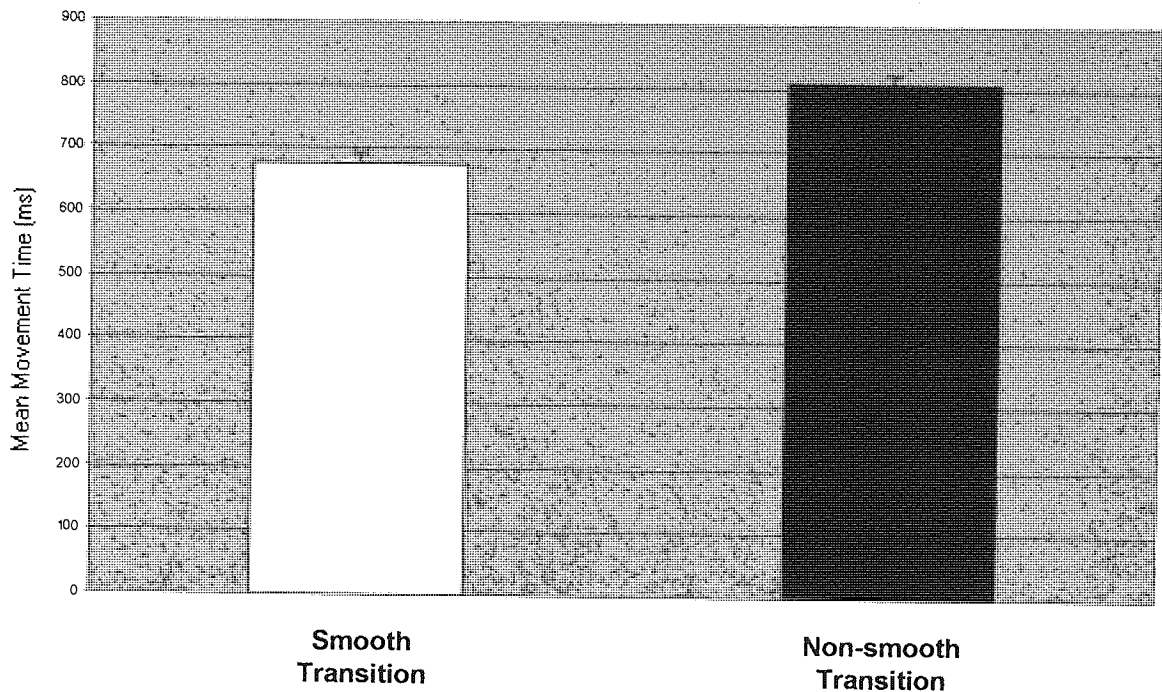
Figure 7.3: Mean movement time (ms) on trials where the movement towards perturbation targets consisted of a smooth movement transition (white bar) and where it consisted of a non-smooth movement transition (black bar). The vertical bars show one standard error of the mean [SEM].
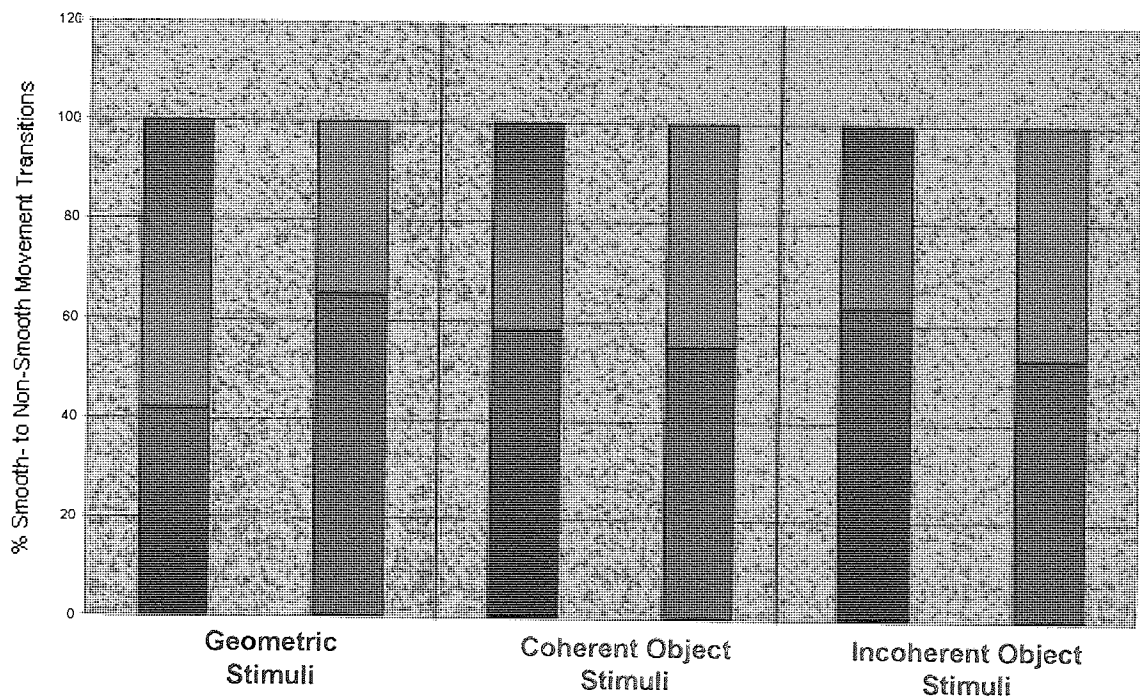
Figure 7.4: Percentage of smooth (red) to non-smooth (blue) transition movements toward perturbation targets dependent upon the stimulus at which they appeared. The shaded bars represent movement transitions towards perturbation targets when they appeared at the edge with the conspicuous feature.
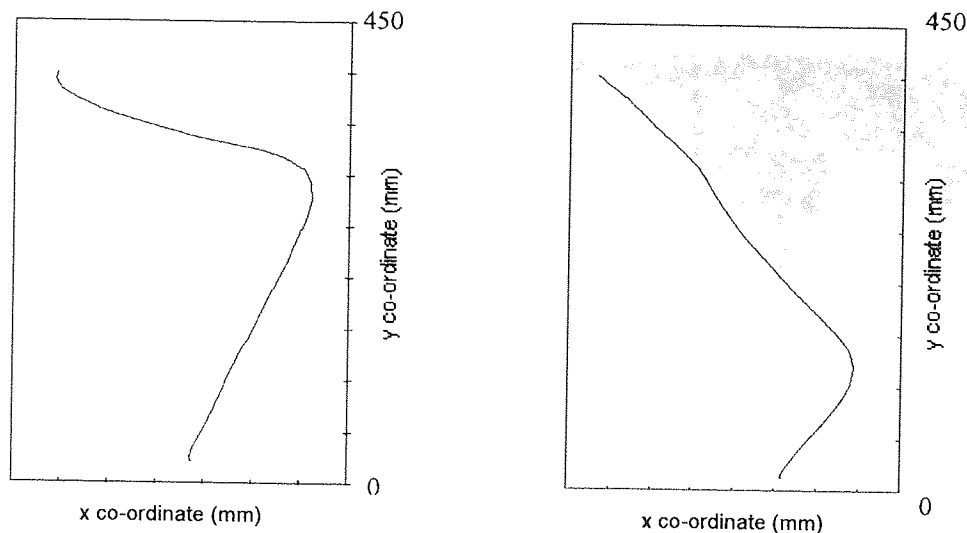
Figure 7.5: Examples of early and late transition manoeuvres. Late movement transitions are represented by a blue path trace and early movement transitions by a red path trace.

movement in the y cartesian plane. The red trace demonstrates an early transition manoeuvre. A trial was classed as displaying an early transition manoeuvre if the turning manoeuvre was initiated before the mid-point of the movement in the y Cartesian plane. In total, the ratio of early to late transition movements on incompatible trials was 3:17 respectively.

In Figure **7.6** the percentage of early to late transitions towards perturbation targets for each stimulus type is displayed. The shaded bars represent early (red) and late (blue) transition movements towards perturbation targets that appeared at the edge with the conspicuous feature. For geometric stimuli, the time-to-transition differed dependent upon the edge at which the perturbation target appeared [$\chi^2 = 8.237$, df = 1, p = 0.006 two-tailed, Cramer's V = 0.210]. That is, when a perturbation target appeared at the edge with the conspicuous feature, a participant was significantly more likely to initiate a transition manoeuvre before the mid-way point. Time-to-transition for coherent and incoherent object stimuli did not differ dependent upon whether a perturbation target appeared at the edge with the conspicuous feature or the edge without this feature [coherent object stimuli $\chi^2 = 0.088$, df = 1, p = 0.840 two-tailed, Cramer's V = 0.021; incoherent object stimuli $\chi^2 = 0.451$, df = 1, p = 0.637 two-tailed, Cramer's V = 0.049].

Discussion

The measures of path trajectory efficiency reveal that responses were facilitated when a corrective manoeuvre corresponded with the direction of attentional bias. When this

166
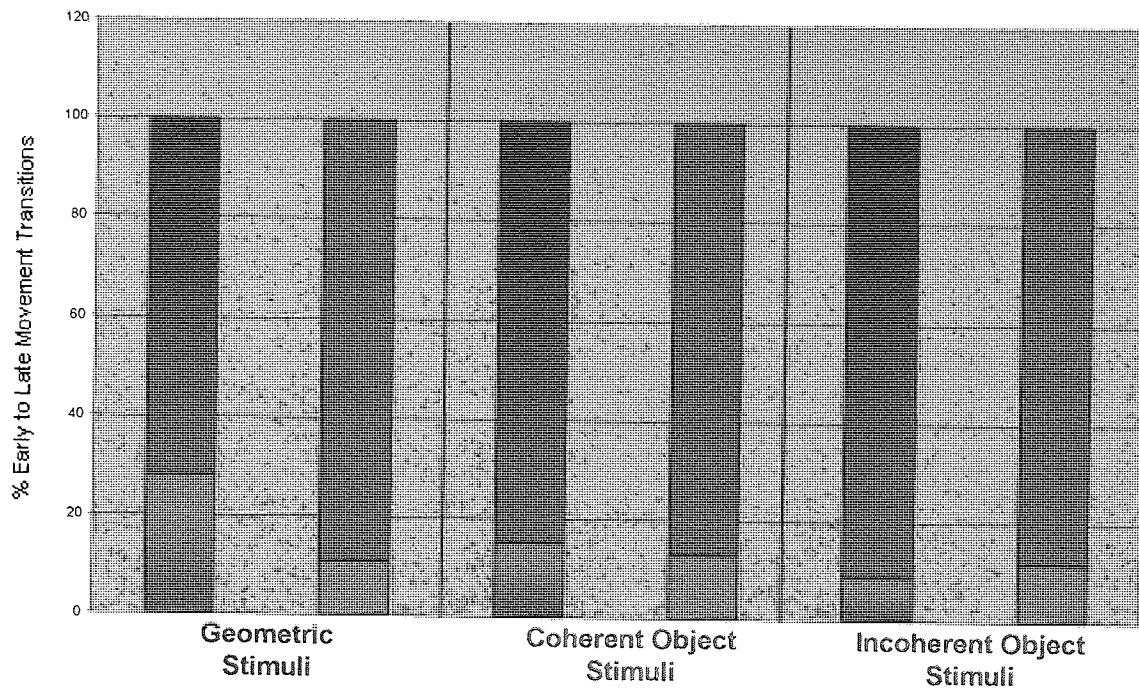
Figure 7.6: Percentage of early (red) versus late (blue) transition movements towards perturbation targets dependent upon the edge properties of the stimulus at which they appeared. The shaded bars represent movement transitions towards perturbation targets when they appeared at the edge with the conspicuous feature.

response criterion was met, corrective movements tended to be initiated sooner and were more likely to display a smooth path trajectory trace. Contrary to scientific opinion (Bremner, 2004; personal communication), this smooth path trajectory trace was correlated with increased movement time efficiency. Thus, these findings are consistent with the theory that attentional biases potentiate motor codes (Anderson *et al.*, 2002). However, similar to findings of planned pointing manoeuvres [Chapter 6], the attentional bias of a stimulus was only a significant predictor of path trajectory efficiency when it was the only bias present. For stimuli with either a shared or opposing attentional and affordance biases, measures of path trajectory efficiency did not differ depending upon the edge the corrective movement was towards. For stimuli with a shared attentional and affordance bias, the null result was likely due to the edge opposing the direction of shared bias also eliciting an idiosyncratic attentional response saliency [see Chapter 6 Section's 6.3 & 6.4]. This is surmised from the similar number of early and smooth corrective manoeuvres towards perturbation targets appearing at this edge compared with the edge with the shared attentional and affordance bias. For stimuli with opposing biases, the result is consistent with the idea that both affordance and attention potentiate motor codes.

7.3.1.3 Hit error data

Hit error was defined as the distance between the perturbation target and the hand-held stylus tip upon 'striking' the perspex screen. Positive errors were defined as hits inward of the perturbation target (i.e. somewhere on the stimulus). Negative errors were defined as hits beyond the perturbation target.

Figure **7.7** shows mean hit error towards perturbation targets for each stimulus type. The open squares show mean hit error when perturbation targets appeared at the edge with the conspicuous feature. For coherent object stimuli, hit error differed dependent upon whether the perturbation target appeared at the edge with the conspicuous feature or the edge without this feature [z = -2.012, N-ties = 20, p = 0.044, two-tailed]. For this stimulus type, when a perturbation target appeared at the edge with the conspicuous feature, hit error was greatest. For geometric and incoherent object stimuli, hit errors tended to be negative. Additionally, for these stimulus types, mean hit error did not differ dependent upon whether the perturbation target appeared at the edge with the conspicuous feature or the edge without this feature [geometric stimuli t = 0.259, df = 19, p = 0.799, two-tailed; incoherent object stimuli z = -1.489, N-ties = 20, p = 0.136, two-tailed].

A hit error analysis of stimulus type (i.e. geometric, coherent object and incoherent object) x edge property at which the perturbation target appeared (i.e. with or without a conspicuous feature) additionally revealed a trend towards significance for the main effect of stimulus type ($F_{(2, 32)}$ = 2.729, p = 0.08, partial η^2 = 0.15; quadratic trend $F_{(1, 16)}$ = 4.074, p = 0.061, partial η^2 = 0.20), and a significant quadratic trend for the stimulus type x perturbation-edge property interaction ($F_{(1, 16)}$ = 6.386, p = 0.022, partial η^2 = 0.29) [2]. For the effect of stimulus type, whereas average hit error for geometric and incoherent object stimuli was negative, average hit error for coherent object stimuli was positive. For the stimulus type x perturbation-edge property interaction, whilst hit error was of a lower value when perturbation targets appeared at an edge with a conspicuous feature compared with the opposing stimulus edge for geometric and incoherent object stimuli, the opposite pattern of results was observed for coherent object stimuli. These ANOVA findings are evident in Figure **7.7**.

---

[2] The analysis was employed as the F max value for homogeneity of variance was not contravened.

Mean Hit Error (mm)

6

4

2

0

-2

-4

-6

Geometric
Stimuli

Coherent Object
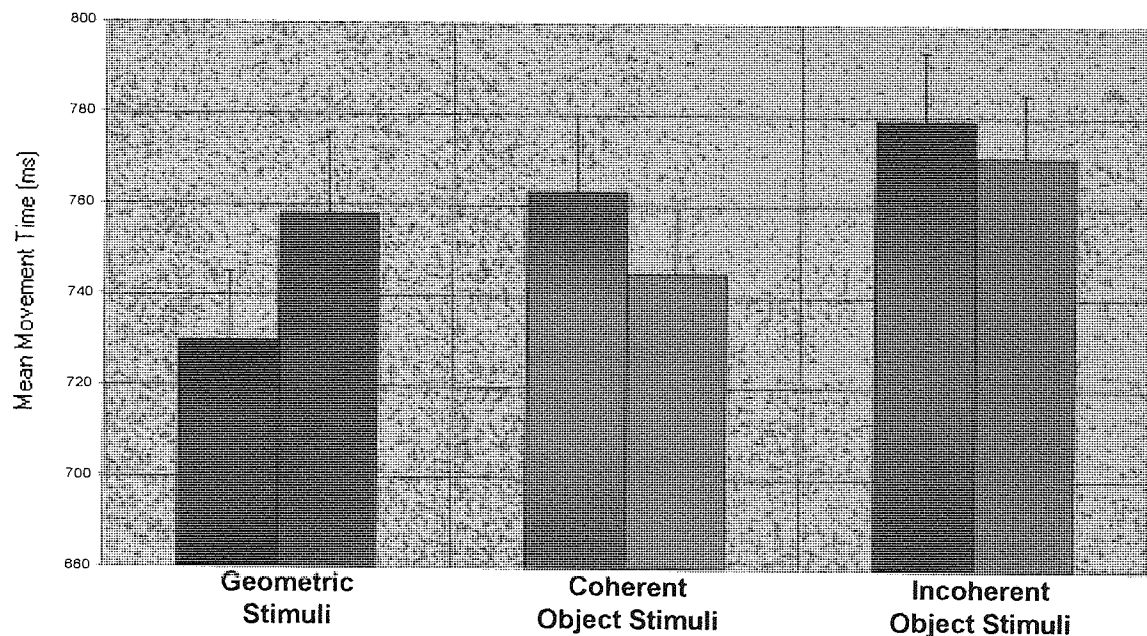Stimuli

Incoherent Object
Stimuli

Perturbation
Target
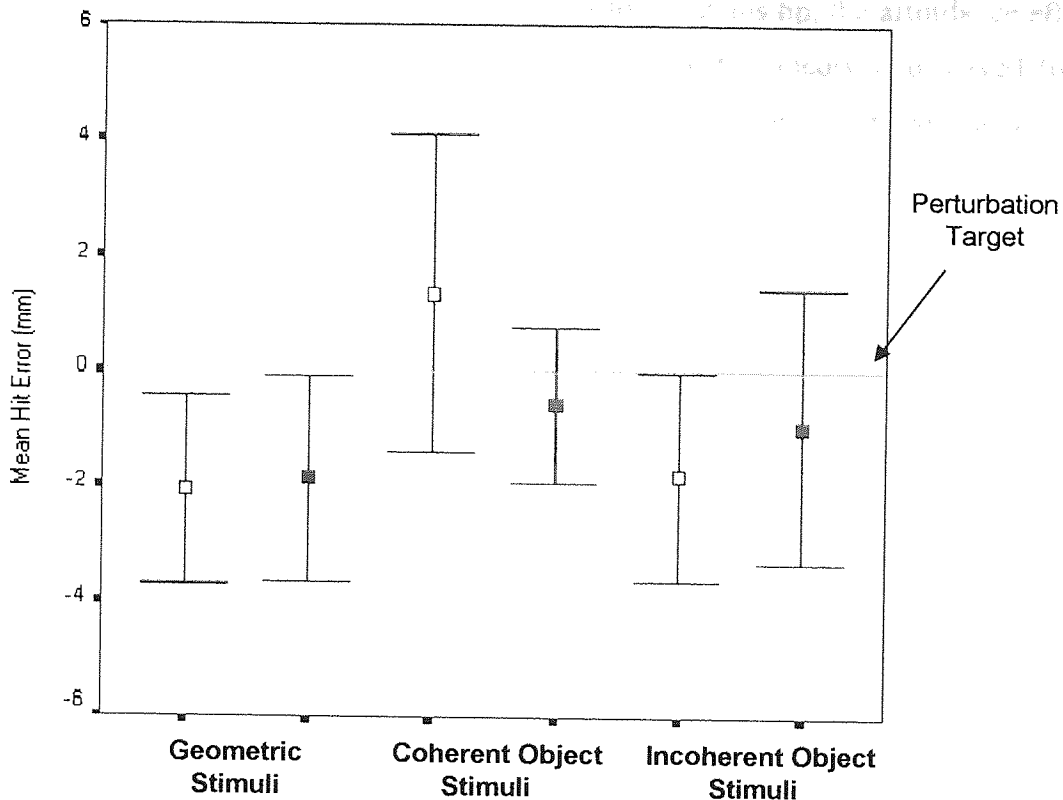
Figure 7.7: Mean hit error for perturbation targets appearing on geometric stimuli, coherent object stimuli and incoherent object stimuli on incompatible perturbation trials. The open squares show mean hit error towards perturbation targets when they appeared at the edge with the conspicuous feature. The vertical bars show 95% confidence limits.

Discussion

For stimuli with a shared attentional and affordance bias, corrective movements towards this shared bias (i.e. towards an object's graspable handle) tended to undershoot perturbation targets[3]. This result is in accordance with both theories of micro-affordances (Ellis & Tucker, 2000; Tucker & Ellis, 2004) and the idea that dorsal stream parietal neurons have response selectivity for visual qualities of an object that link information about the visual features of this object with appropriate hand actions (e.g. Sakata *et al.*, 1997; 1998; Kalaska *et al.*, 1997; Chao & Martin, 2000; Rizzolatti *et al.*, 2000; 2002; Gold & Mazurek, 2002; Grezes & Decety, 2002; Handy *et al.*, 2003; Grezes *et al.*, 2003). However, contrary to predictions, the positive hit error effect was not replicated on incoherent object stimuli trials when the corrective manoeuvre also corresponded with the graspable handle. One possible explanation for this aberrant result is that as the to-be-executed response was a pointing manoeuvre towards a clearly

[3] This effect additionally resulted in hits towards coherent object stimuli tending to be inward of the target edge (i.e. the main effect of stimulus type).

defined perturbation target of similar proportions to the stylus tip, the affordance effect of striking an object's handle was negated. Support for this theory is observed from greater hit accuracy *per se* when pointing towards perturbation targets compared with either the left or right edge of stimuli on standard trials [refer to Figures **6.5** and **7.7**].

7.3.1.7 Perturbation trial error data

A perturbation trial error was recorded when a participant struck the stimulus edge opposite to that of the perturbation target, which occurred on 8.5% of trials.

Figure **7.8** shows the number of perturbation trial errors for each stimulus type. The shaded bars represent perturbation trial errors towards the edge with the conspicuous feature. Irrespective of stimulus type [geometric stimuli: χ^2 =0.043, df = 1, p = 0.835; coherent object stimuli: χ^2 =0.333, df = 1, p = 0.564; incoherent object stimuli: χ^2 =1.000, df = 1, p = 0.317] or edge property [χ^2 = 0.970, df = 1, p = 0.325], no patterns of errors was evident. Namely, the presence or absence of a conspicuous feature at the edge where a perturbation target appeared did not influence trial error rates.
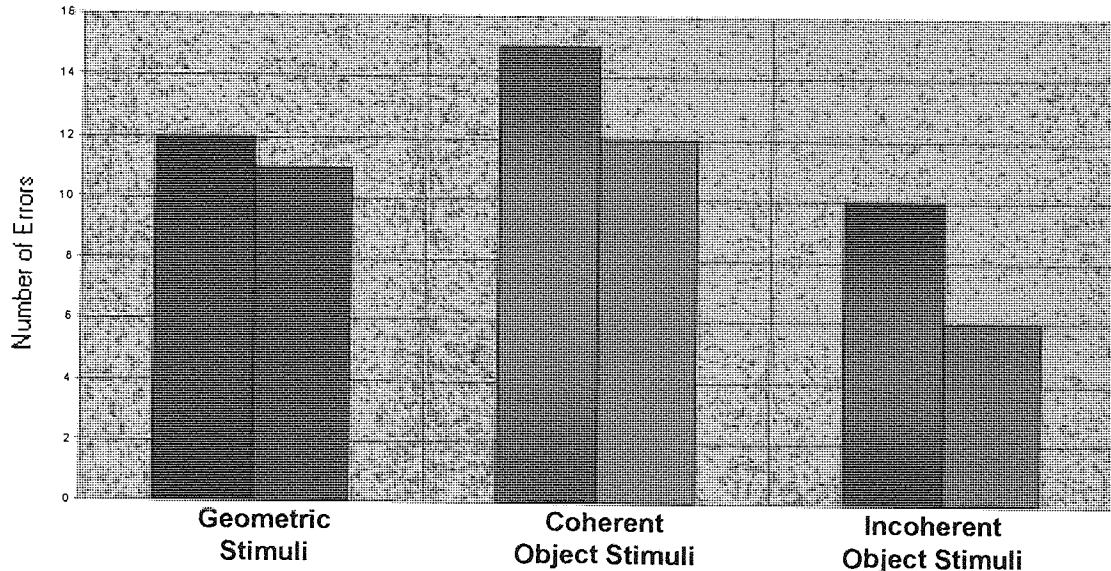
Figure 7.8: Distribution of errors for the geometric stimuli, coherent object stimuli and incoherent object stimuli on incompatible perturbation trials. For all stimulus types the shaded bars represent errors when the non-target edge was the edge with the conspicuous feature.

Discussion

Whilst no effects of edge property at which the perturbation target appeared were evident, the finding that participants did occasionally fail to respond to perturbation

targets has implications for the idea of an 'automatic pilot' (Pisella *et al.*, 2000). This is discussed in greater detail in Section **7.4**.

7.3.2. Compatible perturbation trial findings

On compatible perturbation trials, the appearance of a perturbation target always corresponded with the direction of the arrow cue. In consequence, the response required resembled that produced on standard trials [Chapter **6**].

7.3.2.1 Movement time data

For each stimulus type, movement times towards perturbation targets are displayed in Figure **7.9**. For geometric and incoherent object stimuli, results were similar to those demonstrated on standard trials. That is, for geometric stimuli, movement times towards perturbation targets were fastest when they appeared at the edge with the conspicuous feature [$t = -3.507$, df = 19, p = 0.001, one-tailed], and for incoherent object stimuli, movement times did not differ dependent upon which edge the perturbation target appeared at [$t = -0.340$, df = 19, p = 0.787, two-tailed]. Unlike standard trial findings, however, for coherent object stimuli a trend was noted whereby movements were fastest when perturbation targets appeared at the edge with the conspicuous feature [$t = -1.649$, df = 19, p = 0.058, one-tailed].

A movement time analysis of stimulus type (i.e. geometric, coherent object and incoherent object) x edge property at which the perturbation target appeared (i.e. with or without a conspicuous feature) revealed a main effect of edge property (F $_{(1, 19)}$ = 7.740, p = 0.012, partial $\eta^2 = 0.29$). Namely, when perturbation targets appeared at an edge with a conspicuous feature, movement times were faster than when they appeared at the opposing stimulus edge (i.e. an edge without a conspicuous feature).

Discussion

The results are consistent with the hypothesis that both attention and affordance influence the potentiation of motor codes [See Chapters **1**, **4** & **6**]. The main effect of edge property further reveals that, irrespective of stimulus type, pointing manoeuvres were faster when they corresponded with the direction of attentional bias even when this bias opposed the direction of affordance bias. Thus, the results again appear to indicate
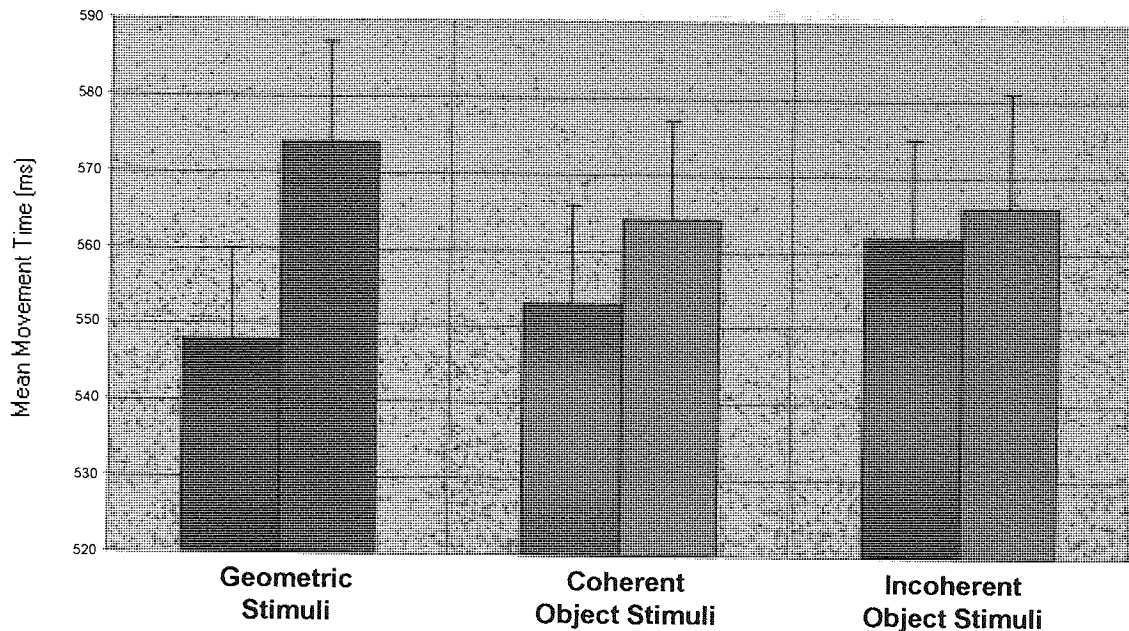
Figure 7.9: Mean movement times for perturbation targets appearing on geometric stimuli, coherent object stimuli and incoherent object stimuli on compatible perturbation trials. The shaded bars represent mean movement times towards perturbation targets when they appeared at the edge with the conspicuous feature. The vertical bars show one standard error of the mean [SEM].

that for 'planned' manoeuvres, the attentional bias of a stimulus was of primary importance for the potentiation of motor codes.

7.3.2.1 Path trace data

On compatible perturbation trials, participants demonstrated efficient movement trajectories that were comparable to those produced on standard trials [see Chapter 6 Section **6.3.2**]. These traces all approximated a diagonal trace from start to target, and as no path deviations were recorded no further analyses were undertaken.

7.3.2.3 Hit error data

Mean hit error towards perturbation targets are shown in Figure **7.10**. Again, similar to standard trial findings, for geometric stimuli, mean hit error did not differ dependent upon whether the perturbation target appeared at the edge with or without the conspicuous feature [geometric stimuli $t = -1.263$, df $= 19$, p $= 0.222$, two-tailed]. However, unlike standard trial findings, a null result was also demonstrated for coherent object stimuli [$z = -0.429$, N-ties $= 20$, p $= 0.668$, two-tailed]. For incoherent object stimuli, when perturbation targets appeared at the edge opposing the conspicuous feature (i.e. the graspable handle), hit error was greater and tended to be positive [$z = -$

2.725, N-ties = 20, p = 0.006, two-tailed]. This latter finding mirrored standard trial results.
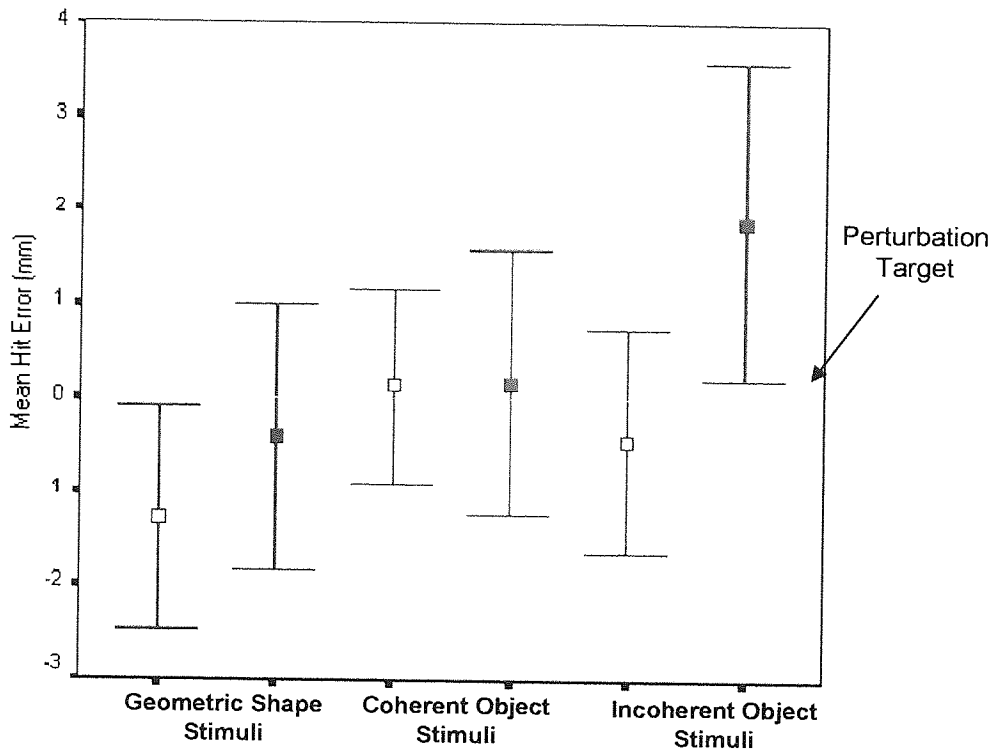
Figure 7.10: Mean hit error for perturbation targets appearing on geometric shape stimuli, coherent object stimuli and incoherent object stimuli on compatible perturbation trials. The open boxes represent movement times towards perturbation targets when they appeared at the edge with the conspicuous feature. The vertical bars show 95% confidence limits.

A hit error analysis of stimulus type x edge property at which the perturbation target appeared additionally revealed a trend towards significance for the main effect of stimulus type ($F_{(2, 38)}$ = 2.848, p = 0.070, partial η^2 = 0.13; linear trend ($F_{(1, 19)}$ = 5.798, p = 0.026, partial η^2 = 0.23)[4]. Namely, when perturbation targets appeared on geometric stimuli, mean hit error was negative whereas when they appeared on incoherent object stimuli, mean hit error was positive. The ANOVA further revealed a main effect of edge property ($F_{(1, 19)}$ = 7.069, p = 0.016, partial η^2 = 0.27) and a trend towards significance for the stimulus type x edge property interaction ($F_{(2, 38)}$ = 2.975, p = 0.063, partial η^2 = 0.14; quadratic trend ($F_{(1, 19)}$ = 3.571, p = 0.074, partial η^2 = 0.16). For the main effect of edge property, when a perturbation target appeared at an edge with a conspicuous feature, a lower hit error value was recorded than when it appeared at an edge opposing this feature. However, this difference was minimal for coherent object stimuli (i.e. the

---

[4] The analysis was employed as the F max value for homogeneity of variance was not contravened.

stimulus type x edge property interaction). All ANOVA findings are evident in Figure
7.10.

Discussion

For stimuli with opposing attentional and affordance biases, corrective movements
towards an object's graspable handle tended to undershoot perturbation targets. Once
again this result is in accordance with both theories of micro-affordances and proposed
properties of dorsal stream neurons [see Section *7.3.1.3*]. Indeed, whilst this effect was
not observed for stimuli with a shared affordance and attentional bias, the opposite
pattern of results observed on incompatible perturbation trials (i.e. the effect of striking
an object's graspable handle on coherent object stimuli trials but not incoherent object
stimuli trials) supports the idea that the null results were a consequence of pointing
towards a clearly defined perturbation target. Thus, taken together, the hit error
findings are consistent with the argument that affordances result in motor plan
repertoires that provide basic information on how to utilise known object stimuli [see
Chapter **6** Section **6.4**].

7.3.2.6. Perturbation trial error data

No perturbation errors were evident on compatible perturbation trials.

7.3.3. Compatible vs. incompatible perturbation trial findings

Figure **7.11** shows that movement times towards perturbation targets depended upon the
trial type, i.e. compatible perturbation (white bar) or incompatible perturbation (black
bar). Pointing movements on incompatible perturbation trials took approximately
200ms longer to complete than pointing movements on compatible perturbation trials [t
= -11.318, df = 19, p < 0.001, one-tailed]. Figure **7.12** and **7.13** show that mean hit error
and mean hit accuracy towards perturbation targets were dependent upon trial type.
Mean hit accuracy was a measure of total error. Note that movements towards
perturbation targets were less accurate on incompatible perturbation trials compared
with compatible perturbation trials [t = -3.065, df = 19, p = 0.006, two-tailed].

Discussion

In contrast to previous research (e.g. Smeets & Brenner, 1995; Brenner & Smeets,
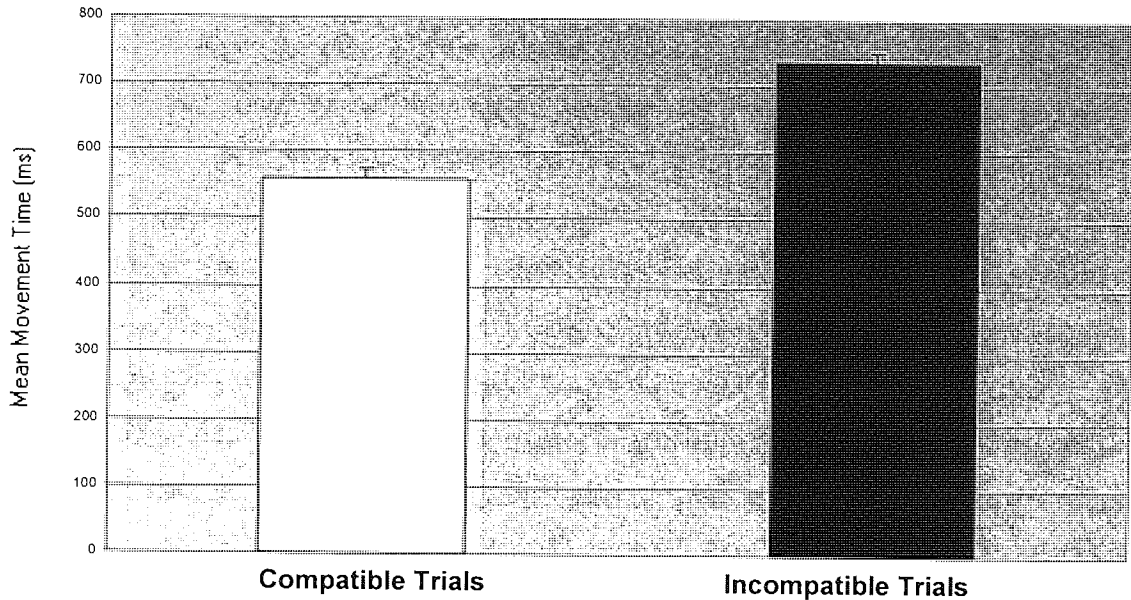
Figure 7.11: Mean movement time (ms) on trials where perturbation targets and arrow cues were compatible (white bar) and where perturbation targets and arrow cues were incompatible (black bar). The vertical bars show one standard error of the mean [SEM].
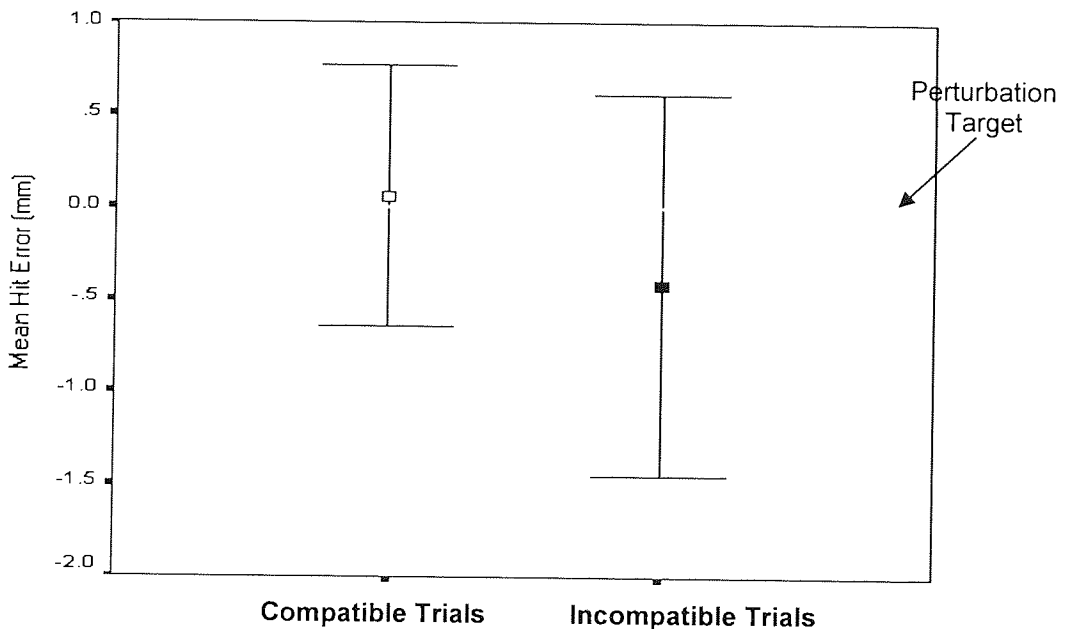
Figure 7.12: Mean hit error differences when perturbation targets and arrow cue were compatible (white box) and when perturbation targets and arrow cue were incompatible (black bar). The vertical bars show 95% confidence limits.

1997), the present results demonstrate inferior movement efficiency on trials where a corrective manoeuvre was required. However, given that the distance between the original target and a perturbation target was approximately 9.5cm, the movement time difference was not entirely unexpected. Comparative movement times on trials where a
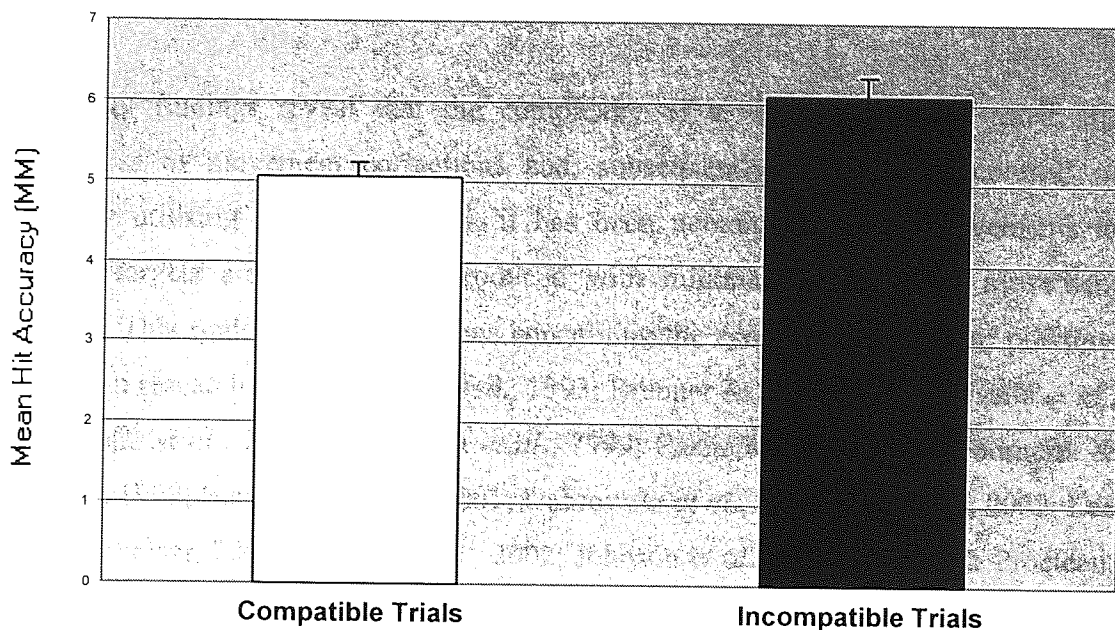
Figure 7.13: Mean hit accuracy differences when perturbation targets and arrow cues were compatible (white box) and when perturbation targets and arrow cues were incompatible (black bar). The vertical bars show one standard error of the mean [SEM].

corrective manoeuvre is required have only been demonstrated for target location changes of up to approximately 4cm (see Rossetti, 1998 for a review).

The inferior end-point accuracy on trials where a corrective manoeuvre was required possibly reflects increased movement complexity on these trials (see Wolpert & Gharamani, 2000; Desmurget & Grafton, 2000; Sheth & Shimojo, 2002; Seidler *et al.*, 2004). To elaborate, on incompatible perturbation trials the pointing manoeuvre required on-line movement re-planning. Therefore, whilst on compatible perturbation trials the end-point movement stage could have been influenced by information calculated by both 'planning' and 'online control' systems (see Glover, 2004), on incompatible perturbation trials the end-point of a movement could only be influenced by information computed on-line.

7.4 Discussion

The present findings reveal that the complexity of a visual target can affect the effectiveness of movement corrections and, subsequently, the 'on-line control' of action. By utilising complex stimuli, it has been demonstrated that movements to perturbed targets are not always produced with minimal disruption to movement efficiency. This finding raises questions concerning the ecological validity of previous perturbation research (e.g. Castiello *et al.*, 1993; Brenner & Smeets, 1997; Pisella *et al.*, 1998; Pisella *et al.*, 2000; Desmurget *et al.*, *1999*; Castiello *et al.*, 1998; Fourneret & Jeannerod, 1998; Boulinguez *et al.*, 2001; Dubrowski *et al.*, 2002; Grea *et al*, 2002; Lee & van Donkelaar, 2002; Jackson *et al.*, 2002; Johnson *et al.*, 2002; Bedard & Procteau, 2003; Nijhof, 2003) as it is apparent that both attentional and affordance properties of stimuli interfere with the on-line control of action. Relatedly, the results additionally demonstrate that directed visual attention and affordance are associated with the potentiation of motor codes, a finding consistent with results from reaction time studies [see Chapter 1 & 4]. Moreover, comparable to the findings of planned movements [Chapter 6] it is evident that the influences of affordance and directed attention upon on-line movement construction are, to an extent, separable. That is, whereas the attentional bias of stimuli was key in determining the efficiency of corrective manoeuvres, the affordance bias of stimuli was important in determining end-point accuracy.

To review, when a corrective manoeuvre corresponded with the direction of a single attentional bias, the turning manoeuvre tended to be initiated earlier and composed of a smooth turning transition. However, for stimuli with either a shared or opposing affordance bias, this effect was negated. For stimuli with opposing attentional and affordance biases, these findings were taken as evidence that affordance can also potentiate motor codes. For stimuli with a shared attentional and affordance bias, the null result was argued to reflect an idiosyncratic attentional capture of the edge opposing the direction of shared bias [see also Chapter 6 section 6.4]. This result further demonstrates the saliency of attentional biases in potentiating motor response codes.

Inconsistent with findings of path trajectory efficiency, nevertheless, the measure of movement time revealed no differences dependent upon whether a corrective manoeuvre corresponded or opposed the direction of attention and/or affordance. One possible explanation for this result is that the sudden appearance of a perturbation target automatically captured attention [see Section 7.3.1.2]. However, as perturbation targets were red circular targets of fixed proportions (i.e. 8mm diameter), the combined response saliency of a perturbation target corresponding with an attentional and/or affordance bias would still have been greater than that associated with a perturbation target opposing such a bias. Thus, it is unlikely that the null results were a consequence of this confound. A more feasible alternative is that for stimuli with a single attentional bias, or shared attentional and affordance bias, the null results reflected participant idiosyncrasies and/or the insensitivity of the movement time measure. Indeed, as significant movement time differences reported on planned movement trials were only in the order of 15ms [see Chapter 6 Section 6.3.1], it is possible that the additional time required to complete a trial on which a corrective movement was necessary (approximately 200ms; see Figure 7.11) masked any movement time differences. This theory is supported by the fact that differences in movement efficiency were observed for both the measures of path trajectory and hit error (discussed below)[1].

No differences dependent upon whether a corrective manoeuvre corresponded or opposed the direction of attention and/or affordance were further observed for the measure of perturbation trial error. Although, given that participant's did occasionally fail to respond to perturbation targets, this finding has implications for the idea of an 'automatic pilot' (Pisella et al., 2000). This system, proposed to rely on spatial vision, is reported to drive fast corrective movements to perturbations of object location, whether the target change is consciously perceived or otherwise. From the trial error data reported, however, it is apparent that corrective movements were not initiated automatically. Furthermore, participants were often aware of the appearance of a perturbation target but could not inhibit their planned movements; this was evinced from their spontaneous expression of frustration upon making a trial error. Theories regarding the automaticity of on-line control (e.g. Goodale & Milner, 1992; Milner & Goodale, 1995; Pisella et al., 2000; Glover, 2004) therefore, may need to be revised.

---

[1] NB: For geometric stimuli, a computing error meant that data was available from only 19 participants, this confound could also have affected the movement time result.

Additionally, as the majority of path trajectories to perturbation targets tended to be both non-smooth and late (an effect of the complex stimuli used), concerns are again raised regarding the ecological validity of previous perturbation studies where simple cylindrical or circular targets have been employed [see Chapter 4].

Finally, whilst affordance bias was not critical in determining efficient corrective manoeuvres, it was key in determining end-point accuracy. On incompatible and compatible perturbation trials, the end-point of a movement was typically inward of perturbation targets when it corresponded with the graspable handle of coherent or incoherent object stimuli, respectively. These findings are in agreement with theories of micro-affordance (Ellis & Tucker, 2000; Tucker & Ellis, 2004) and theories related to visuomotor properties of dorsal stream and parietal neurons (e.g. Sakata *et al.*, 1997; Kalaska *et al.*, 1997; Chao & Martin, 2000; Rizzolatti *et al.*, 2000; 2002; Gold & Mazurek, 2002; Grezes & Decety, 2002; Handy *et al.*, 2003; Grezes *et al.*, 2003). Moreover, when considering that individuals were required to point towards a clearly defined target, the observation that this confound did not fully negate hit-error effects demonstrates that influences exerted by function-related object knowledge can override current task objectives (see Goodale & Milner 1992; Milner & Goodale, 1995; Agliotti, Goodale & DeSouza, 1995; Haffenden & Goodale, 1998; Holmes, 1998; Pisella *et al.*, 2000; Bridgeman, 2002; Glover, 2002; Glover 2004).

To sum, by assessing the efficiency of corrective pointing manoeuvres it has been established that the attentional and affordant attributes of visual stimuli influence on-line movement control. It has further been revealed that whereas the attentional bias of a stimulus is the critical prerequisite in determining path trajectory efficiency, the affordance bias of a stimulus is key in determining end-point accuracy. These findings have both significant theoretical implications concerning theories of on-line control and significant practical implications in real-world situations where sudden, fast observer responses are required.

Chapter 8

The Influence of Visual Attention and Affordance on Movement Efficiency in a Deafferented Individual

8.1 Introduction

To allow for the accurate construction of movement, information concerned with a range of cognitive, spatial and non-spatial parameters must be calculated [See Chapter 4]. Whilst the importance of these parameters differs dependent upon the movement phase under construction, information on spatial parameters (e.g. object location, object size, object shape) is utilised during both the planning and online phase of action. In addition to visual information, proprioceptive information is also used to calculate such spatial parameters. For instance, several studies have demonstrated that when individuals (or animals) devoid of proprioceptive abilities are required to move their hand towards a visible object, accurate movement and/or grasp kinematics are reduced, or even impossible, in the absence of visual feedback (see for example Jackson, Jackson, Newport & Harvey, 2002; Farrer, Franck, Paillard & Jeannerod, 2003; Messier, Adamovich, Berkinblit, Tunik, Poizner, 2003; for a review see Jeannorod 1988). Deafferentation has therefore provided a key means to investigate how visual and proprioceptive information aid movement construction. Thus, in studying an individual devoid of proprioceptive abilities (i.e. feelings of limb position and movement), it is reasoned that a unique insight into the roles of visual attention and/or affordance upon action may be provided.

The efficiency of pointing manoeuvres to a wide variety of stimuli varying in their attentional and affordance attributes were assessed in a deafferented individual [I.W.]. The measures of movement efficiency utilised were movement time, path trajectory and hit error, and the response required was either a pointing manoeuvre towards the left or right edge of a stimulus, or a pointing manoeuvre towards a perturbation target that appeared at the left or right edge of a stimulus coincident with movement onset. The design employed enabled the investigation of visual attention and/or affordance upon

both planned movement construction (where the to-be-executed response was known prior to movement onset) and unplanned movement construction (where the to-be-executed response was altered after movement initiation).

In studying the effects of visual information on planned movements in deafferented individuals, Ghez, Gordon & Ghilardi (1995) have demonstrated that vision of a limb at rest, prior to movement onset, can reduce directional errors and improve path trajectories towards a target even if vision is removed during the actual movement. Ghez *et al.* (1995) suggested that vision of the arm may provide configurative information used by the planning system to update internal models of the limb (but see Scarchilli, Vercher, Gauthier & Cole, 1999). With continuous vision of the limb, however, movement efficiency in deafferented individuals is further improved. For example, Bard, Fleury, Teasdale, Paillard & Nougier (1995) have demonstrated that for slow movements towards fixed targets, movement times, hit error rates and velocity profiles are comparable across both deafferented individuals and control individuals. Nonetheless, in deafferented individuals, these movements require conscious effort and the substitution of proprioceptive information with on-line visual feedback.

Nougier *et al.* (1994) have also revealed that attentional processes are more controlled and less automatic in deafferented individuals than in control participants. In a cued response task, they demonstrated that deafferented individuals were more cautious with low validity cues, preferring to allocate attentional resources to uncued locations and 'to expect the unexpected'. This skilled allocation of attentional resources requires cognitive effort. Certainly, the combination of moving without proprioception coupled with an added cognitive task significantly reduces movement accuracy (see Ingram *et al*, 2000).

In studying the online control of action, Bard *et al.* (1999) have demonstrated that a deafferented individual could make efficient movements to a target perturbed in location at movement onset, independent of whether this perturbation was consciously acknowledged or not. The deafferented individual demonstrated similar movement times, smooth path trajectory traces and smooth velocity profiles compared with controls when pointing at circular targets perturbed by an amplitude of 6^0. Thus, Bard *et al.* (1999) suggested that corrective movement processes are based on an internal eye-

efference copy, with visual feedback utilised when producing fast, on-line movements (see also Fleury, Bard, Teasdale, Michaud & Lammare, 1999).

In sum, devoid of proprioceptive abilities, deafferented individuals must rely on visual-feedback mechanisms, increased cognitive effort and increased attentional resources to produce efficient movements. However, little is known regarding how the attentional and/or affordant attributes of a to-be-pointed-at stimulus might affect movement efficiency in these individuals. To investigate this, geometric stimuli, coherent object stimuli and incoherent object stimuli were again used to examine the shared and unique effects of visual attention and/or affordance upon action.

For I.W., on trials where a simple planned response was required, it was reasoned that because deafferented individuals require increased concentration, attention and cognitive effort to produce and monitor movements [see also section **8.2**], the effects of the affordant and/or attentional attributes of a to-be-pointed at stimulus might be negated. In consequence, movement times, path trajectories and hit accuracy measures would not differ dependent upon which edge of a stimulus I.W. produced a movement towards. Conversely, it was also reasoned that if the visual properties intrinsic to a stimulus are automatically coded for, then the saliencies of such visual precursors to action might be difficult to inhibit, even in an individual who has to consciously plan his every move. If this were the case then movement times, path trajectories and hit accuracy measures would be expected to resemble those of the control participants on standard trials.

In considering trials where the movement is more complex (i.e. requires on-line control), it was reasoned that if deafferented individuals do develop superior control of attentional resources (e.g. Nougier *et al.,* 1994) then this could lead to the earlier perception of perturbation targets. I.W. may therefore be expected to display more early transition manoeuvres to perturbed targets than control participants, irrespective of the attentional and/or affordance properties of stimuli. This would additionally lead to null results being observed for the other measures of movement efficiency. However, if the visual properties of stimuli are automatically coded for, then their response saliencies might be difficult to inhibit regardless of any superior allocation of attentional resources. The movement times, path trajectories and hit accuracy responses of I.W.

towards perturbation targets should, as such, resemble those of control participants. Alternatively, it was hypothesised that a superior allocation of attentional resources could lead to an effective inhibition of the non-target edge when it contains a salient bias (see Tipper *et al.*, 2002 for a review). Consequently, if an on-line correction is required towards this salient bias, movement efficiency will be impeded. Assuming this is the case, I.W.'s movements towards perturbation targets that appear at an edge with an attentional/affordance bias may be less efficient than movements towards perturbation targets appearing at the opposite stimulus edge.

8.2 Participant Information and Experimental Details

8.2.1 Participant information

Data was collected from one deafferented individual I.W. [male; aged 52; left-handed] and two-aged matched controls; J.C. [male; aged 53; right-handed] and L.C. [female; aged 54; left-handed].

8.2.1.1: Patient case history

At the age of 19 I.W. suffered a severe loss of peripheral sensory nerve functioning (i.e. an acute sensory neuropathy). At the time microbiological tests revealed him to be infected with the glandular fever virus (infectious mononucleosis) and it was inferred that I.W.'s immune system had produced cells that both reacted against the foreign virus, and attacked the specific nerves involved in cutaneous and muscular sensation[1].

The physiological loss was manifest in the large myelinated sensory nerves supplying information from the body and limbs (i.e. the periphery) to the central nervous system [CNS]. The motor peripheral nerves supplying information from the CNS to the periphery remained intact. The specific nerves affected were those associated with fast conduction velocities and included muscle spindles, tendon receptors and cutaneous receptors. These nerves, destroyed from the neck down, left I.W. with no sensation of touch or proprioception below the neck. However, the smaller unmyelinated sensory fibres were not damaged. Subsequently, I.W. had similar perceptions of pain, heat and cold over his unaffected head as in his affected body. Additionally, as I.W.'s motor fibres were not affected by the neuropathy, both muscle power and bulk were normal, as were perceptions of muscle fatigue and ache (Cole & Sedgewick, 1992). At the time of the incident I.W. was an individual who could produce power in his muscles yet with no control over the command. For example, when asked to move his left arm one way, it might go the other way, or his right arm might move as well (Cole, 1991).

Presently, to move and conduct a multitude of everyday tasks, I.W. has to continuously substitute visual feedback for proprioceptive feedback (see Cole, 1991, for a detailed

---

[1] Neuropathies have also been described in association with viral diarrhoea, thus it is possible that the glandular fever was coincidental (Cole, 1991).

case-history of I.W.'s rehabilitation). This requires immense concentration. Moreover, I.W.'s reliance on vision is so profound that when deprived of light he is unable to move.

8.2.1.2: Age-match control details

Both age-matched control participants had corrected-to-normal visual acuity and neither had a history of neurological dysfunction or motor impairment. J.C is I.W.'s consultant neurophysiologist.

8.2.2 Experimental details

Details specific to both the completion of planned and unplanned movements are reported here. Planned movements were investigated using 'standard trials', whereby the pointing movement was directed towards a given stimulus edge (i.e. left or right) by an arrow cue presented at the start of each trial. Unplanned movements were investigated using 'perturbation trials'. On these trials the pointing manoeuvre was directed towards a given stimulus edge by the circular perturbation target that appeared at movement onset. This target could be *compatible* or *incompatible* with the arrow cue. Additionally, its appearance could correspond with the conspicuous feature edge or oppose this stimulus edge. Refer to Chapter 5 for all other task details.

In the training phase of the experiment, each participant completed one initial block of 20 trials and two additional blocks of 40 trials each. In this phase, the ratio of standard to perturbed trials was 60:40. In the testing phase, the ratio of standard to perturbed trials was 80:20. I.W. and L.C. completed eight blocks of 40 trials, whereas J.C. completed 10 blocks of 40 trials. This strategy was adopted as it was evident that for I.W. to return the stylus to B1 (the start position for a new trial) a constant eye-stylus gaze was required. For I.W., this additional demand may have limited resources available to studying the arrow cue of the forthcoming trial and, subsequently, limited time devoted to planning the next pointing manoeuvre. Thus, for J.C., a design of ten randomly intermixed blocks was applied, where for five blocks a 'return-task constraint' was imposed where the stylus had to be returned to a specific location on B1. This was a central colour coded region (dimensions 20mm x 10mm) and ensured J.C. maintained a constant eye-stylus gaze on returning the stylus to B1. In the remaining five blocks a 'free-return' approach was adopted. In these blocks, J.C. did not

maintain a constant eye-stylus gaze when returning the stylus to B1. The return-task constraint was not enforced on participant L.C. as this participant always returned the stylus to the colour coded region of B1. Therefore, L.C. automatically maintained an eye-stylus gaze when returning the stylus to the start position for a new trial.

The experiment was conducted in a semi-darkened room. All participants held the stylus in their dominant hand (for I.W. and L.C. this was their left-hand, and for J.C. this was his right-hand). According to post-experimental reports, none of the participants deduced that the release of B1 triggered the appearance of a perturbation target on perturbation trials.

For clarity, results presented for each stimulus type are colour coded: blue is used for geometric stimuli results; red is used for coherent object stimuli results; and green is used for incoherent object stimuli results. To gain an indication of I.W.'s general ability on the tasks, additional analyses of movement efficiency on the different trial types (i.e. standard, incompatible perturbation and compatible perturbation) were undertaken independently of stimulus attributes. This approach was pursued to determine whether any confounds of the experimental task (e.g. task logistic difficulties) were likely to mask effects of the stimulus attributes. The results of these analyses are reported at the beginning of the appropriate movement efficiency sections before performance dependent upon stimulus attributes is reported.

8.3 Results

8.3.1 Standard trial findings

For the two age-matched control participant's findings of stimulus properties [see Appendix V] replicated those of the 20 unselected control participants [see Chapters 6 & 7]. Therefore, to minimise repetition, where applicable, only data pertaining to I.W. is presented.

8.3.1.1 Movement time data

Movement time was a measure of the time it took I.W. to complete a pointing manoeuvre (i.e. one trial) and was recorded from the release of B1 to the depression of B0. Table **8.1** shows general movement time performances for I.W. and all control participants. For I.W., whilst movement times were within the normal range, it is evident that the imposition of a return-task constraint for participant J.C. (J.C. Task) increased movement times. Thus, it is possible that this task confound increased the time it took I.W. to complete a pointing manoeuvre on standard trials.

Table 8.1: Mean Movement Time on Standard Trials

	I.W.	J.C.	J.C. Task	L.C.	Control Participants
Standard Trials	$\underline{X} = 684$ SE = 5.10	$\underline{X} = 497$ SE = 4.16	$\underline{X} = 511$ SE = 3.39	$\underline{X} = 516$ SE = 4.65	$\underline{X} = 552$ $\sigma = 120$

Figure **8.1** shows movement times towards geometric stimuli, coherent object stimuli and incoherent object stimuli for I.W. Similar to the control participant data [see Figure **6.1**], I.W demonstrated increased movement efficiency on geometric trials when a pointing manoeuvre was towards the edge with the conspicuous feature. However, unlike the control participants, I.W. demonstrated increased movement efficiency towards the edge with the conspicuous feature *per se*, irrespective of stimulus type.
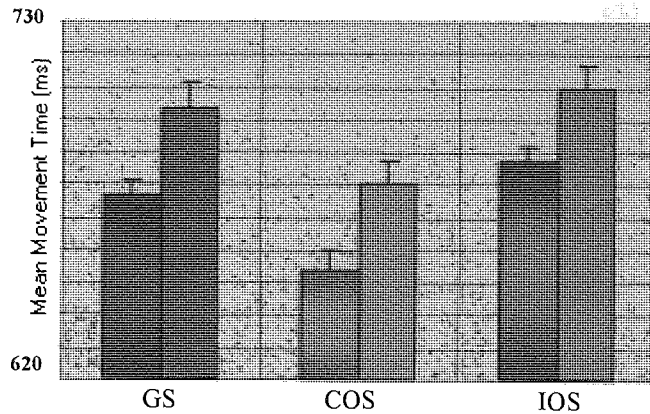
Figure 8.1: Mean movement times for I.W. when pointing towards geometric stimuli [GS], coherent object stimuli [COS] and incoherent object stimuli [IOS] on standard trials. The shaded bars represent movement times towards the edge with the conspicuous feature. The vertical bars show one standard error of the mean [SEM].

8.3.1.2 Path trace data

Path trace was a measure of the path trajectory efficiency of I.W. on a given trial and was recorded from the release of B1 to the depression of B0. On standard trials J.C. and the twenty control participants demonstrated efficient path trajectories that approximated a diagonal trace from start-to-target on 96% of trials [see Figure **6.2**]. This was true even when for participant J.C. a return-task constraint was imposed. I.W., however, demonstrated such movement efficiency on less than 25% of trials. The majority of his path traces were composed of two movement stages that contained separate mediolateral plane and anterior-posterior plane movements. Furthermore, these trajectories varied dependent upon the side of space the movement was towards. Examples of such traces are provided in Figure **8.2**.

Comparative to I.W., the age-matched control L.C. also demonstrated unusual path trajectories for pointing manoeuvres towards the left-side of space. For this participant, whereas over 90% of movements towards the right-side of space approximated a diagonal start-to-target trace, only 23% of those towards the left-side of space approximated this stereotypical trace. Examples of this participant's traces are provided in Figure **8.3**. Similar to I.W., movements to the left-side of space are composed of an initial mediolateral plane movement and a secondary anterior-posterior plane movement. An explanation for these unanticipated path trajectory results is discussed in Section **8.4.3**.

400

y co-ordinate (mm)

x co-ordinate (mm)

0

400

Finish Position
(Contact with
Perspex Screen)

y co-ordinate (mm)

Start Position
(Button Box b1)

x co-ordinate (mm)

0

400

y co-ordinate (mm)

x co-ordinate (mm)

0

400

y co-ordinate (mm)

x co-ordinate (mm)

0
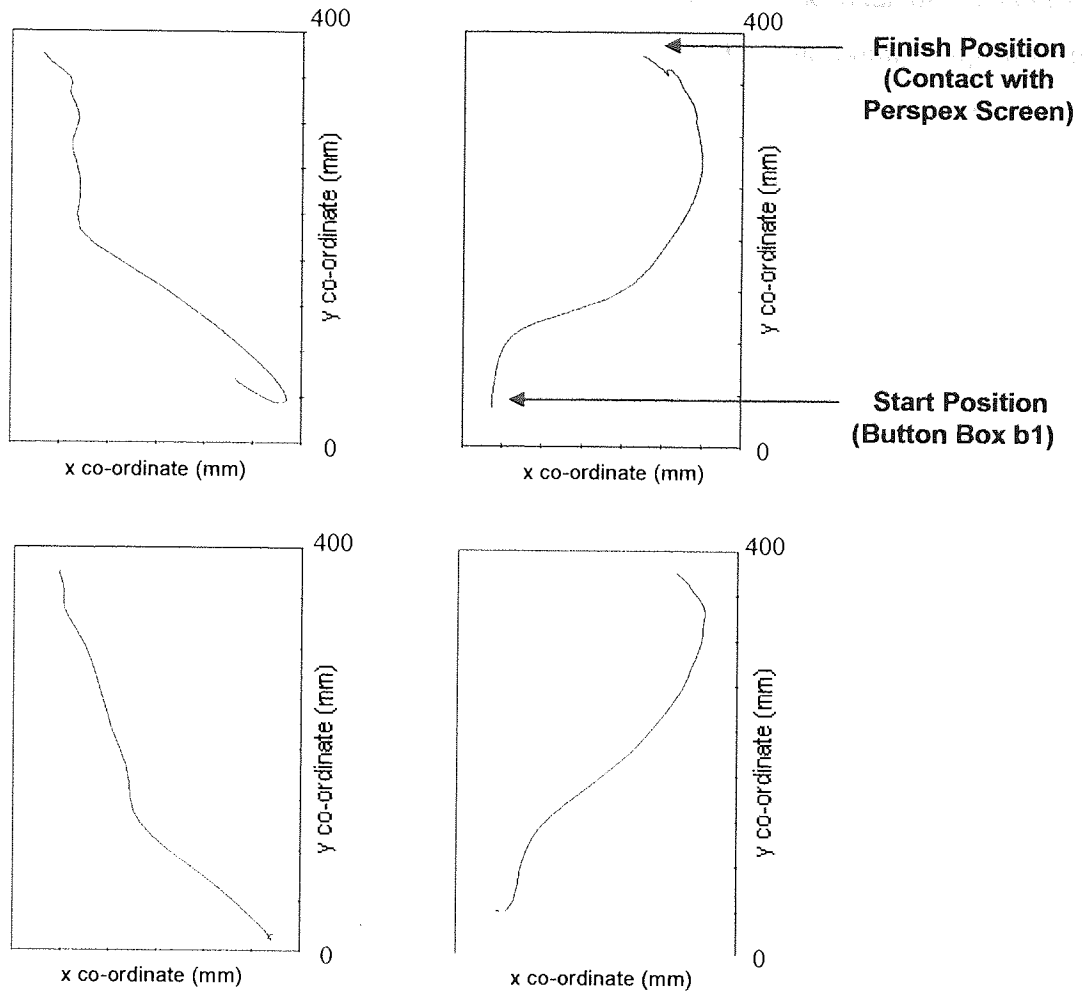
Figure 8.2: Typical path trajectories of I.W. on standard trials. The top panel represents his performance on early trials and the bottom panel represents his performance on later trials. The red lines represent his path trajectories from B1 to the perspex screen, these are plotted in the x and y cartesian planes.

400

y co-ordinate (mm)

x co-ordinate (mm)

0

400

y co-ordinate (mm)

x co-ordinate (mm)

0
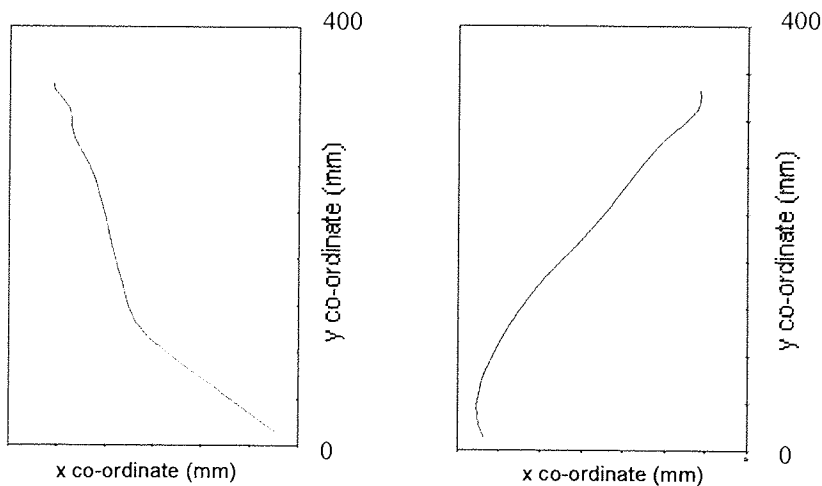
Figure 8.3: Typical path trajectories of L.C. on standard trials. The red lines represent her path trajectories from B1 to the perspex screen, these are plotted in the x and y cartesian planes. For L.C. hits to the left-side of space are comparable to those of I.W.

A second difference in the path trajectory data of I.W. and the data of all control participants was the number of end-point readjustments made. End-point readjustments concerned the repositioning of the stylus in the latter stages of movement. A movement was classed as displaying an end-point readjustment, if a stylus repositioning occurred in the last 75mm of movement in the y plane and involved a movement of the stylus in the x plane of a magnitude greater than 10mm. On average, the standard and age-matched control participants (including J.C. Task) displayed end-point readjustments on less than one percent of trials. I.W., however, made end-point readjustments on over 20% of trials. Examples of such readjustments are presented in Figure **8.4**. The red lines show I.W.'s path trajectories as the stylus approaches the perspex screen.
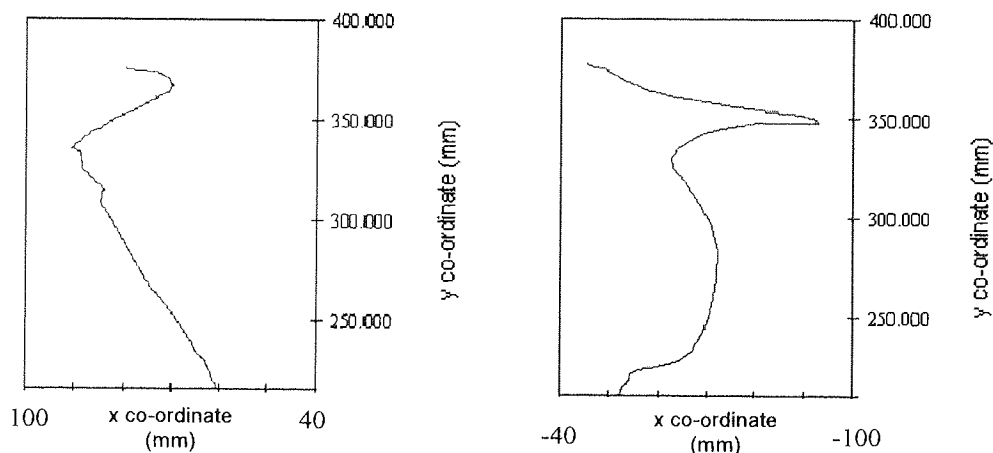
Figure 8.4: Examples of the end-point re-adjustments I.W. made. These involved a repositioning of the stylus tip in the last 75mm of the movement in the y axis of a magnitude of greater than 10mm in the x-axis.

Despite the irregular path trajectories I.W. displayed, major path deviations were still evident. For I.W. these were defined as movements in x and y cartesian planes that veered towards the non-target edge for more than 25% of the whole movement[1]. Examples of traces on which such deviations occurred are presented in Figure **8.5**.

I.W. made major path deviations towards the non-target edge on 2.8% of trials. This figure was comparable to that of control and age-matched control participants who displayed major path deviations on approximately 1.49% of trials [see Chapter 7 Section **7.3.2** for the appropriate definition]. The pattern of path deviations I.W.

---

[1] For L.C., when pointing towards the left-side of space, this definition was also adopted

190

400   400

y co-ordinate (mm)   y co-ordinate (mm)

0   0

x co-ordinate (mm)   x co-ordinate (mm)
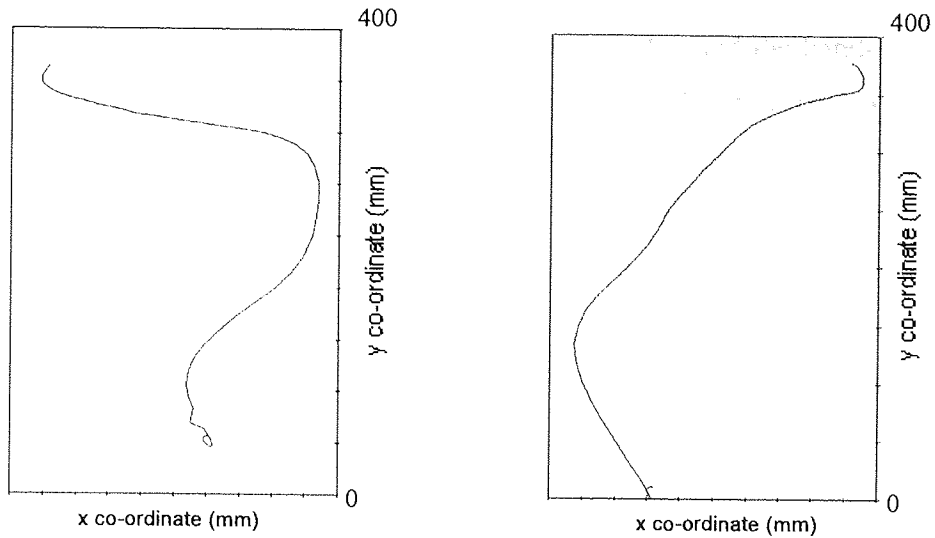
Figure 8.5: Examples of trials on which I.W. made major path deviations. The red lines represent his path trajectories from B1 to the perspex screen. These are plotted in the *x* and *y* cartesian planes. Deviations toward the non-target edge are evident.

displayed is shown in Figure **8.6**. Comparable to all control data [see Figure **6.4**], for geometric stimuli, I.W. displayed more path deviations towards the non-target edge when this coincided with the conspicuous feature. Additionally, I.W., demonstrated more path deviations towards geometric stimuli *per se*. This was a consequence of the high number of path deviations towards the non-target edge when it coincided with the conspicuous feature, and is also in agreement with control participant data.

4.5

Number of Path Deviations

0

GS   COS   IOS
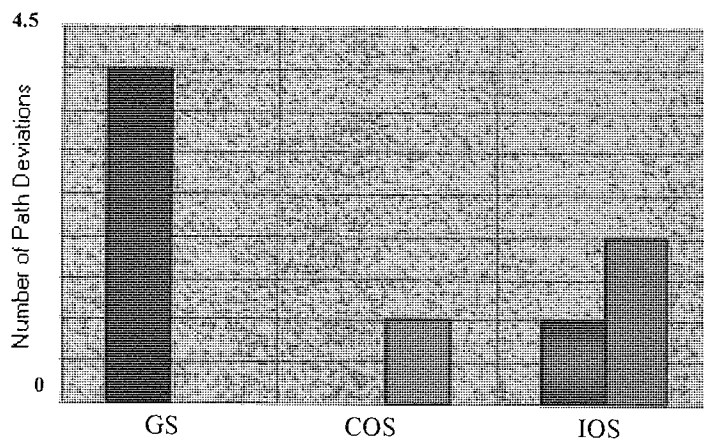
Figure 8.6: Distribution of path deviations towards the non-target edge on standard trials for I.W. when pointing towards geometric stimuli [GS], coherent object stimuli [COS] and incoherent object stimuli [IOS]. The shaded bars represent path deviations towards the non-target edge when it coincided with the conspicuous feature.

191

8.3.1.3 Hit error data

Hit error was defined as the distance between the target edge and the hand-held stylus tip when I.W. 'struck' the screen. Positive errors revealed I.W. had hit inward of the stimulus edge (i.e. somewhere on the stimulus), whereas negative errors revealed I.W. had hit beyond the stimulus edge. In Table **8.2** general hit accuracy (i.e. total error) for I.W. and all control participants is displayed. For I.W. mean hit accuracy was within the normal range. Additionally, for participant J.C., the imposition of a return-task constraint (i.e. J.C. Task) did not affect hit accuracy.

Table 8.2: Mean Hit Accuracy on Standard Trials

	I.W.	J.C.	J.C. Task	L.C.	Control Participants
Standard Trials	$\underline{X} = 6.38$ SE = 2.24	$\underline{X} = 7.38$ SE = 2.96	$\underline{X} = 5.78$ SE = 2.46	$\underline{X} = 8.49$ SE = 2.22	$\underline{X} = 6.19$ $\sigma = 1.73$

Figure **8.7** shows mean hit error for all stimulus types for I.W. Consistent with control participants [see Figure **6.5**], I.W. displayed more positive hit error for coherent and incoherent object stimuli when the movement was towards an object's graspable handle.
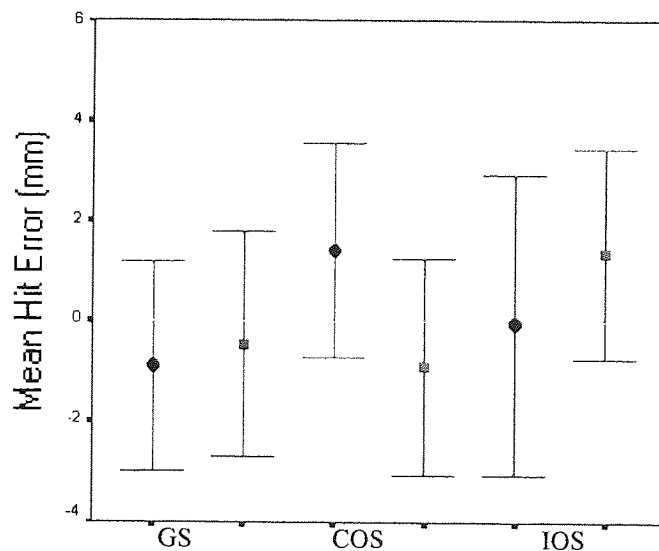
Figure 8.7: Mean hit error for I.W. when pointing towards the geometric stimuli [GS], coherent object stimuli [COS] and incoherent object stimuli [IOS]. The diamond represents mean hit error when the movement was directed towards the edge with the conspicuous feature. The vertical bars show 95% confidence limits.

8.3.1.4 Trial error data

A trial error was recorded for any trial whereby I.W. hit the stimulus edge opposite to that directed by the arrow cue. I.W. made trial errors on 1.9% of trials, while unselected control participants made trial errors on approximately 0.8% of trials. The age-matched control participants made no errors, even when for J.C. a return-task constraint was imposed.

Figure **8.8** shows the number of trial errors for geometric stimuli, coherent object stimuli and incoherent object stimuli for I.W. Comparative to the unselected control participants, I.W. made errors when the non-target edge coincided with a conspicuous feature on geometric stimuli trials. Moreover, I.W. only made errors when the non-target edge coincided with a conspicuous feature, a finding also similar to that of the unselected control participants, who produced more errors when the non-target edge coincided with the conspicuous feature *per se*, irrespective of stimulus type.
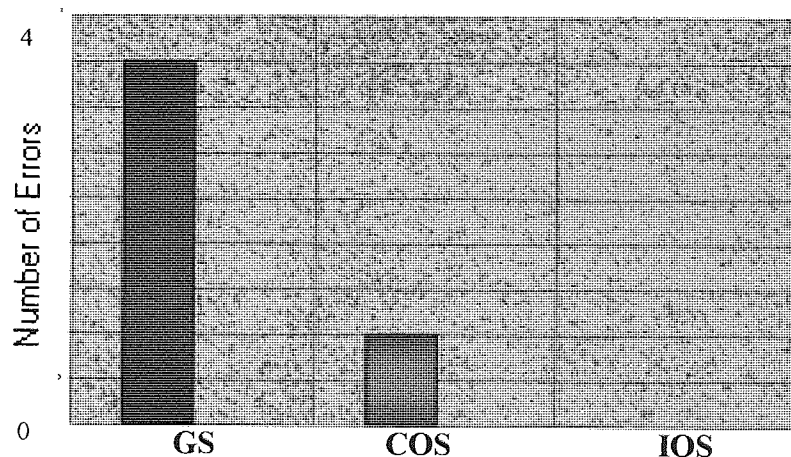
Figure 8.8: Distribution of errors for geometric stimuli [GS], coherent object stimuli [COS] and incoherent object stimuli for I.W. on standard trials. The shaded bars represent errors when the non-target edge coincided with the conspicuous feature

8.3.1.5 Additional findings

In Figure **8.9** z-score measures for mean hit accuracy (i.e. total error) and mean movement time for I.W., the unselected control and age-matched control participants J.C. and L.C., are displayed. With the exception of I.W., all participants demonstrated either a speed-accuracy trade-off or increased efficiency (i.e. negative z-score) for both measures. This was true even when for J.C. a return-task constraint was imposed (i.e. J.C. Task). I.W., however, performed poorly and displayed positive z-scores for both

hit accuracy and mean movement time. Therefore, although his movement times and hit accuracy performance were within the normal range, movement efficiency differences on these measures were observed.

Figure 8.9: Distribution of participant's mean Z-scores for movement time (MT) and hit accuracy (HA) on standard trials. For I.W. no speed-accuracy trade-off is demonstrated. The positive z-scores reveal his performance on both measures was below average

8.3.1.6 Discussion: standard trial findings

For I.W. the effects of attentional and/or affordance stimulus properties upon planned action are comparable to those reported for the control participants. Namely, whereas measures of movement time, path trace and trial errors reveal the attentional bias of a stimulus to be critical for ensuring fast, target-directed actions are produced, the measure of hit error reveals that the affordance bias of a stimulus was critical in determining end-point accuracy.

However, unlike control participants, for I.W., movements corresponding with an attentional bias were not impeded when a stimulus had an opposing affordance bias. Moreover, I.W. made no trial errors corresponding with the direction of affordance bias. This finding reveals that the attentional bias of a stimulus was the primary prerequisite for fast, efficient actions for I.W. Indeed, considering I.W. has to consciously plan and

visually monitor all his movements, the results provide evidence that motor response codes associated with attentional biases are difficult to inhibit.

8.3.2 Incompatible perturbation trial findings

For the age-matched control participants, findings of stimulus properties [see Appendix VI] replicated those of the 20 unselected control participants [see Chapters 6 & 7]. Therefore, where applicable, only data pertaining to I.W. is presented.

8.3.2.1 Movement time data

Table **8.3** shows general movement time performances for I.W., the unselected control and the aged-matched control participants. For I.W. mean movement time was within the standard range, additionally, the imposition of a return-task constraint for participant J.C. did not affect movement times towards incompatible perturbation targets.

Table 8.3: Mean Movement Times on Incompatible Perturbation Trials

	I.W.	J.C.	J.C. Task	L.C.	Control Participants
Incompatible Perturbation Trials	$\underline{X} = 931$ SE = 26.18	$\underline{X} = 646$ SE = 28.62	$\underline{X} = 667$ SE = 22.90	$\underline{X} = 620$ SE = 13.66	$\underline{X} = 734$ $\sigma = 124$

Figure **8.10** shows movement times towards perturbation targets, for I.W., dependent upon the stimulus type at which they appeared. A pattern of **increased** movement time is evident when perturbation targets coincided with an edge with a conspicuous feature *per se*. This result was dissimilar to all control participant data [see Figure **7.1**] where **decreased** movement times were observed when this criterion was met. Additionally, whereas for control participants corrective movements towards geometric stimuli were the fastest, whilst those towards incoherent object stimuli were the slowest, for I.W. the reverse was true. Namely, for I.W., corrective movements towards incoherent object stimuli were the fastest, whereas those towards geometric stimuli were the slowest.

Figure 8.10: Mean movement times towards perturbation targets for I.W. when they appeared on the geometric stimuli [GS], coherent object stimuli [COS] and incoherent object stimuli [IOS]. The shaded bars represent movement times towards the perturbation targets when they appeared at the edge with the conspicuous feature. The vertical bars show one standard error of the mean [SEM].

8.3.2.2 Path trace data

To analyse I.W.'s path trajectory efficiency on incompatible perturbation trials, measures of movement transition type and time-to-movement-transition were used [refer to Chapter 7, Section *7.3.1.2* for appropriate definitions and pictorial examples]. Figure **8.11** demonstrates the number of non-smooth movement transitions for all participants, once the variable of late responses[2] had been factored out. For participant J.C., the imposition of a return-task constraint did not affect the movement transition type displayed. Additionally, although I.W. displayed a high number of non-smooth movement transitions, three unselected control participants also demonstrated a high number of non-smooth movement transitions.

Figure **8.12** shows, for I.W., the percentage of smooth-to-non-smooth movement transitions towards perturbation targets dependent upon the stimulus type at which they appeared. Compared with the data of all control participants [see Figure **7.4**], I.W. displayed more smooth movement transitions towards geometric stimuli when perturbation targets appeared at the edge with the conspicuous feature.

---

[2] On all trial containing a late response (i.e. a turning manoeuvre initiated in the last 50mm of the *y*-axis movement) the manoeuvre was non-smooth. This was not a consequence of the stimulus properties but a consequence of engineering a turn late into the movement.
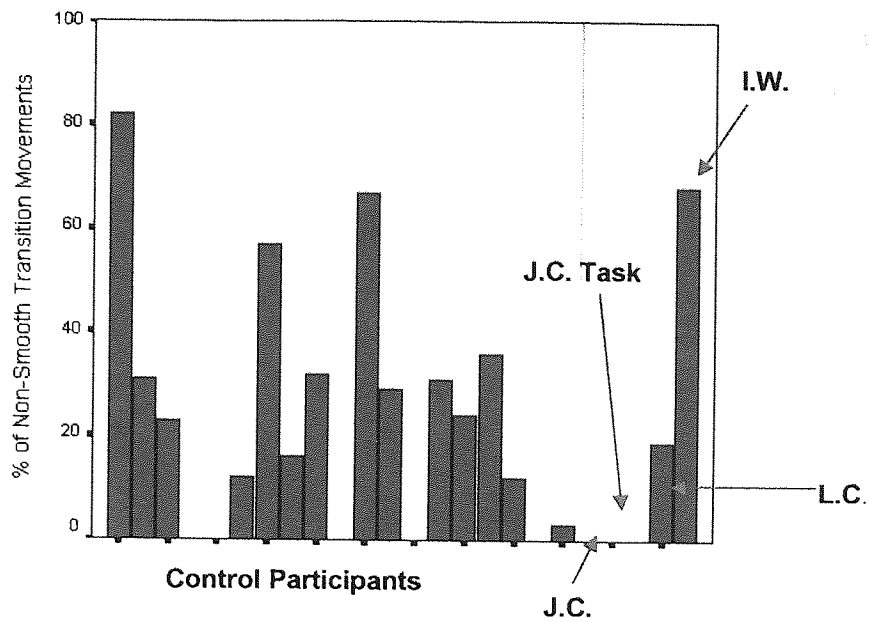
Figure 8.11: Percentage of non-smooth path corrections to perturbation targets for I.W., the control and age-matched control participants.
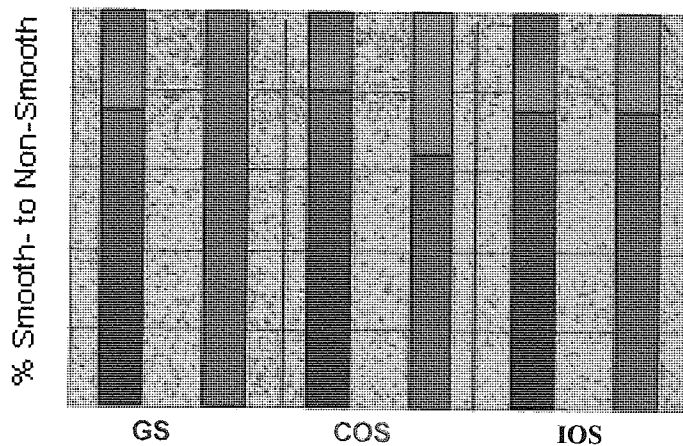
Figure 8.12: Percentage of smooth (red) to non-smooth (blue) transition movements towards perturbation targets dependent upon the stimulus type at which they appeared, for I.W. The shaded bars represent movement transitions towards perturbation targets when they appeared at the edge with the conspicuous feature. Key: GS = Geometric Stimuli; COS = Coherent Object Stimuli; and IOS = Incoherent Object Stimuli.

Examples of early and late transition manoeuvres I.W. displayed are presented in Figure 8.13. I.W. demonstrated early transition movements on approximately 23% of incompatible perturbation trials. This figure was comparable to the control and age-matched control participants who demonstrated early transition movements on approximately 16% of such trials.

197

450

450

y co-ordinate (mm)

y co-ordinate (mm)

x co-ordinate (mm)

x co-ordinate (mm)

0

0
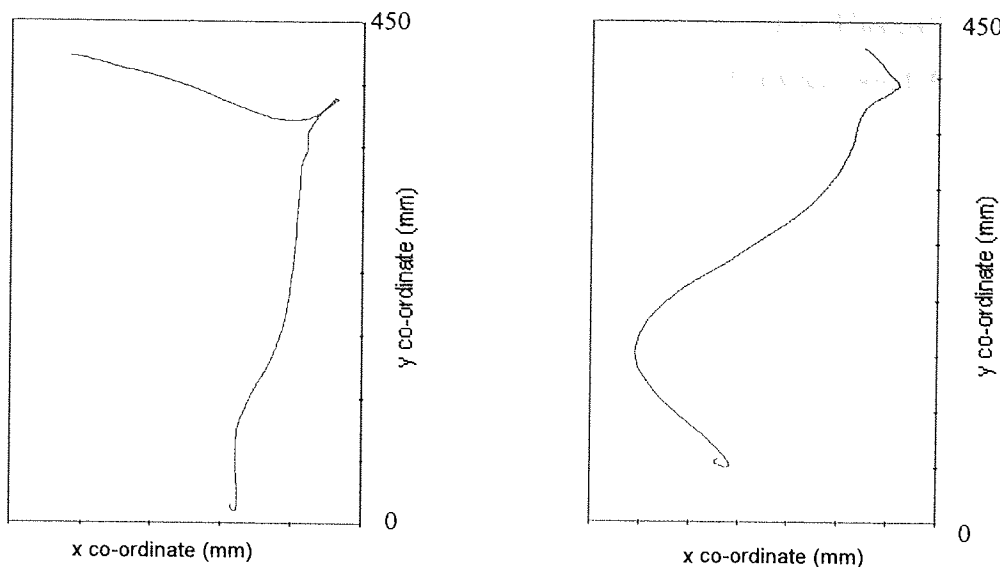
Figure 8.13: Examples of early and late transition manoeuvres. Late movement transitions are represented by a blue path trace and early movement transitions by a red path trace.

Figure **8.14** shows the percentage of early to late transitions towards perturbation targets dependent upon the stimulus type at which they appeared for I.W. Similar to the data of control participants [see Figure **7.6**], I.W. displayed more early transitions manoeuvres towards geometric stimuli when a perturbation target appeared at the edge with the conspicuous feature.

% Early to Late Corrective Manoeuvres

GS   COS   IOS
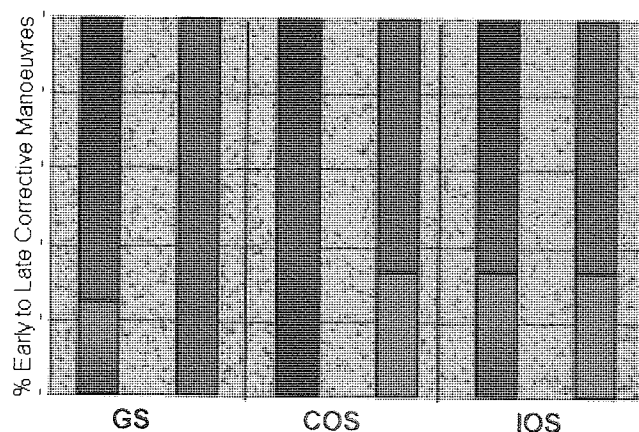
Figure 8.14: Percentage of early (red) to late (blue) transition movements towards perturbation targets dependent upon the stimulus type at which they appeared for I.W. The shaded bars represent movement transitions towards perturbation targets when they appeared at the edge with the conspicuous feature. Key: GS = Geometric Stimuli; COS = Coherent Object Stimuli; and IOS = Incoherent Object Stimuli.

On incompatible perturbation trials I.W. made one major path deviation. This path deviation involved two turning transitions in the mediolateral plane. This path deviation is displayed in Figure **8.15**, where movement time duration between point A and point B was approximately 250ms. Neither the unselected controls nor the age-matched control participants demonstrated similar errors.

a) ———▶

b)

c)

Point B

Point A
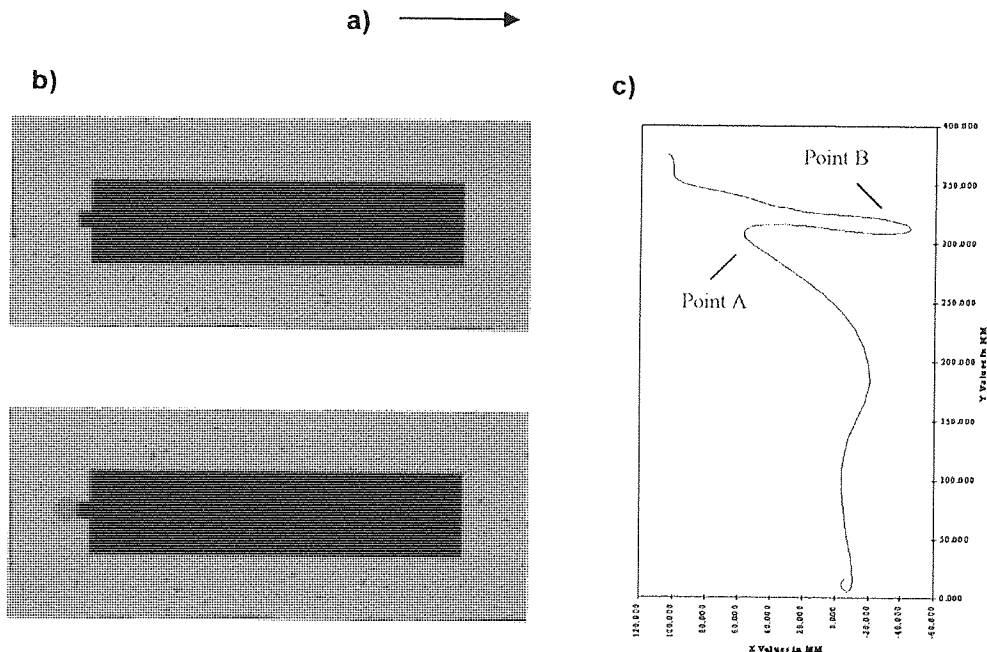
Figure 8.15: (a) Direction of initial arrow cue. (b) Top: The rectangular geometric stimulus that appeared after the right facing arrow cue. Bottom: The perturbation that appeared upon movement onset. (C) The path trajectory of I.W. on this trial. The turning manoeuvres between point A and Point B took approximately 250ms to complete.

8.3.2.3 Hit error data

Hit error was within the standard range for I.W, while the imposition of a return-task constraint did not affect hit accuracy for J.C. [Table **8.4**]. Figure **8.16** shows mean hit error towards perturbation targets for I.W. As with all control participants [see Figure 7.7], when perturbation targets appeared at the edge with the conspicuous feature, I.W. demonstrated more positive hit error scores. However, unlike these participants, I.W. also demonstrated a pattern of striking an object's handle on incoherent object stimuli trials.

8.3.2.4 Additional Findings

Whilst the majority of participants demonstrated either a speed-accuracy trade-off or both increased hit accuracy and movement time efficiency [Figure **8.17**]. I.W.

Table 8.4: Mean Hit Accuracy on Incompatible Perturbation Trials

	I.W.	J.C.	J.C. Task	L.C.	Control Participants
Compatible Perturbation Trials	$\underline{X}$ = 7.27 SE = 3.74	$\underline{X}$ = 6.40 SE = 3.23	$\underline{X}$ = 3.89 SE = 2.36	$\underline{X}$ = 5.58 SE = 2.82	$\underline{X}$ = 6.10 σ = 2.08
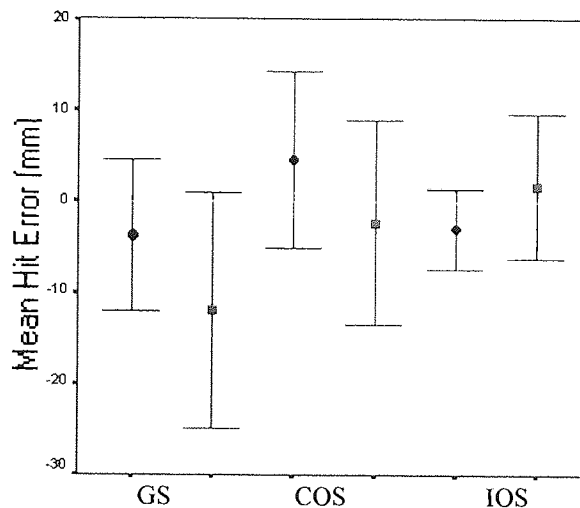
Figure 8.16: Mean hit error for I.W. when pointing towards geometric stimuli [GS], coherent object stimuli [COS] and incoherent object stimuli [IOS]. The diamond represents movement times toward the perturbation target when it appeared at the edge with the conspicuous feature. The vertical lines represent 95% confidence limits.

performed poorly on these measures (positive z-scores). Therefore, although his movement times and hit accuracy performance were within the standard range, movement efficiency differences on hit accuracy and movement time measures were evident.

8.3.2.5. Discussion: incompatible perturbation trial findings

In agreement with the micro-affordance theory of Ellis & Tucker (2000; Tucker & Ellis, 2004), I.W. demonstrated positive hit error when a movement corresponded with the direction of an object's graspable handle. Given both I.W.'s movement limitations and the fact that he was required to produce corrective movements towards a clearly defined perturbation target, this finding provides support for the notion that subconscious 'affordance' motor plan repertoires exist.
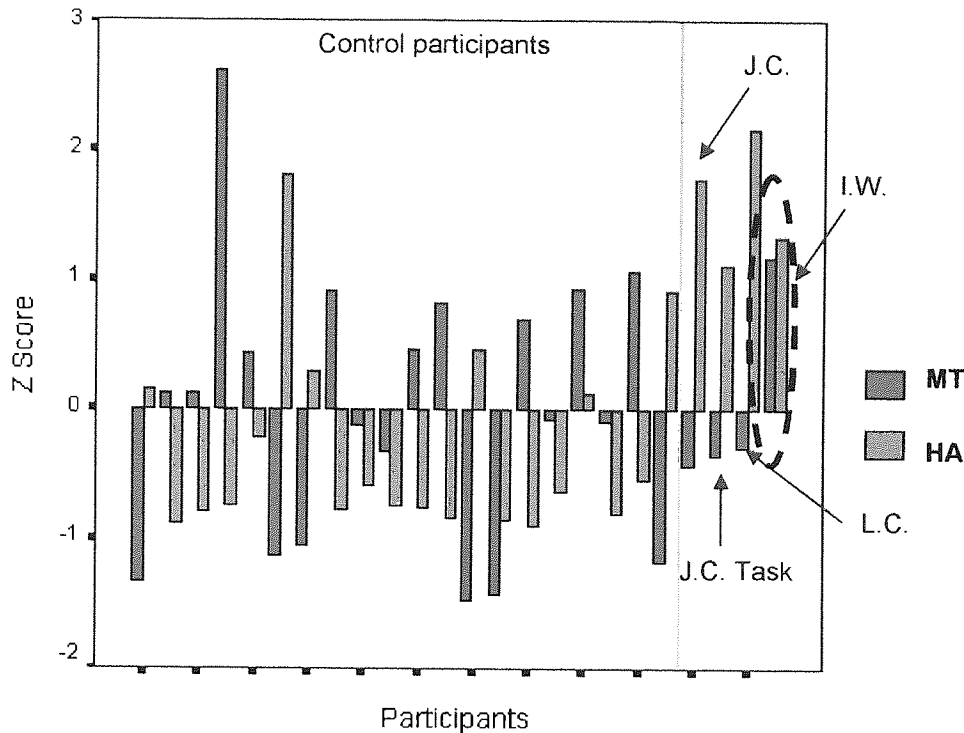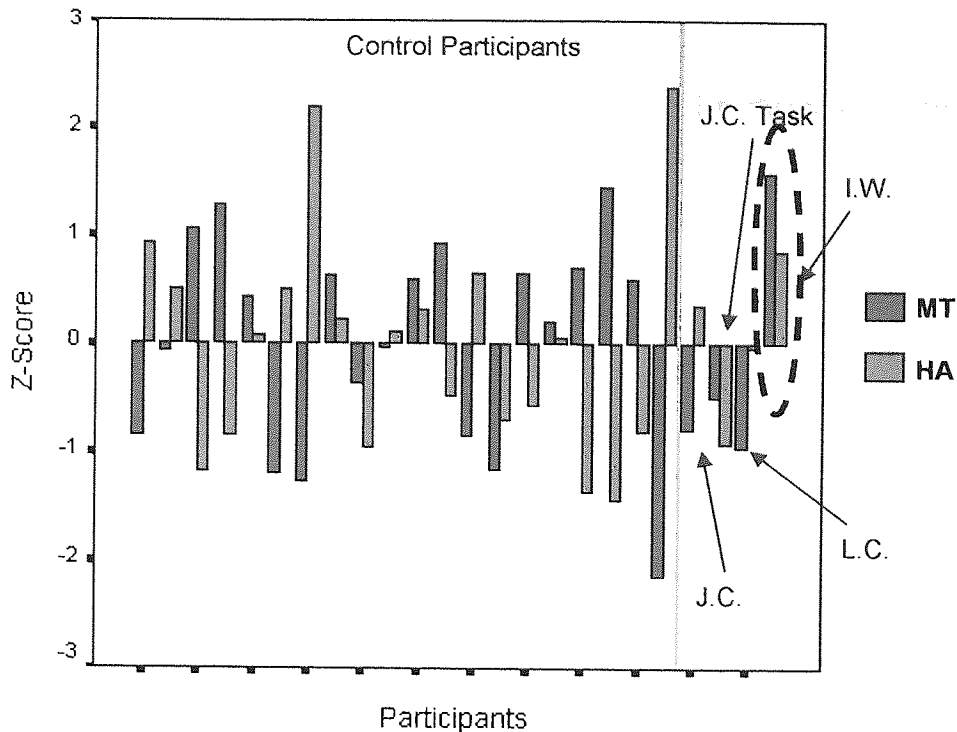
Figure 8.17: Distribution of participant's mean Z-scores for movement time (MT) and hit accuracy (HA) on incompatible perturbation trials. For I.W. no speed-accuracy trade-off is demonstrated. The positive z-scores reveal his performance on both measures was below average

Inconsistent with both theories of attention (e.g. Anderson *et al.*, 2002) and the performance of control participants, I.W. did not demonstrate decreased movement times when a movement correction corresponded with, rather than opposed, the direction of a single attentional bias. This was despite the observation of more efficient path trajectories on such trials. Additionally, a response disadvantage was observed when movement corrections were towards the direction of attentional bias *per se*. This latter finding contrasted I.W.'s performance on standard trials, where movement towards an attentional bias resulted in increased movement efficiency. Possible explanations for these paradoxical findings are discussed in detail in Section **8.4.2**.

8.3.3 Compatible Perturbation Trial Findings

With the exception of hit error, findings of stimulus properties for the age-matched control participants [see Appendix VII] replicated those of the 20 unselected control participants [see Chapters 6 & 7]. Thus, where applicable, only data pertaining to I.W. is presented.

8.3.3.1 Movement time data

Table **8.5** shows general movement time performances for all participants. Whilst the movement times of I.W. were within the normal range, it is evident that the imposition of a return-task constraint for participant J.C. increased movement times. Thus, it is possible that this return-task confound increased the time it took I.W. to complete a pointing manoeuvre on these trials.

Table 8.5: Mean Movement Times on Compatible Perturbation Trials

	I.W.	J.C.	J.C. Task	L.C.	Control Participants
Compatible Perturbation Trials	$\underline{X} = 687$ SE = 12.74	$\underline{X} = 494$ SE = 12.48	$\underline{X} = 519$ SE = 7.26	$\underline{X} = 512$ SE = 14.44	$\underline{X} = 558$ $\sigma = 108$

Figure **8.18** shows movement times towards perturbation targets dependent upon the stimulus type at which they appeared for I.W. For coherent object stimuli, in agreement with the data of all control participants, when a perturbation target appeared at the edge with the conspicuous feature, I.W. displayed increased movement efficiency. However, unlike the data of control participants [see Figure **7.8**], for geometric stimuli I.W. did not show a movement time advantage when a perturbation target appeared at the edge with the conspicuous feature. Moreover, whilst increased movement efficiency was noted for control participants when the perturbation target coincided with the conspicuous feature edge *per se*, this effect was not replicated in the data of I.W.

8.3.3.2 Path trace data

On compatible perturbation trials I.W. demonstrated movement trajectories that were comparable to those he produced on standard trials. These path traces were composed of separate mediolateral plane and anterior-posterior plane movements and often displayed end-point readjustments [refer to Figure's **8.2** & **8.4**]. However, as with control participants, I.W. displayed no path deviations towards the non-target edge. Thus no further analyses were undertaken.
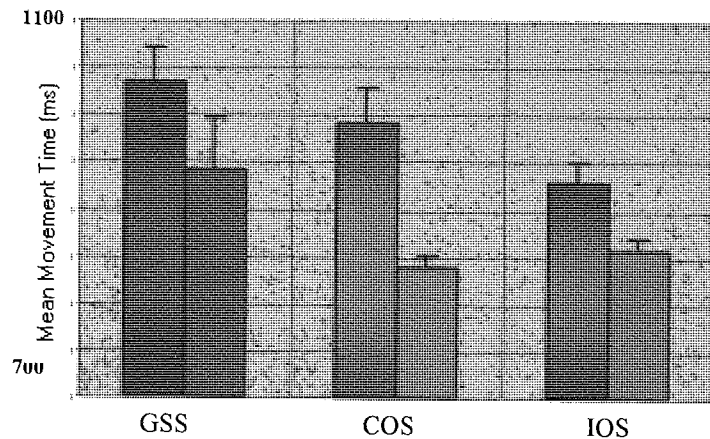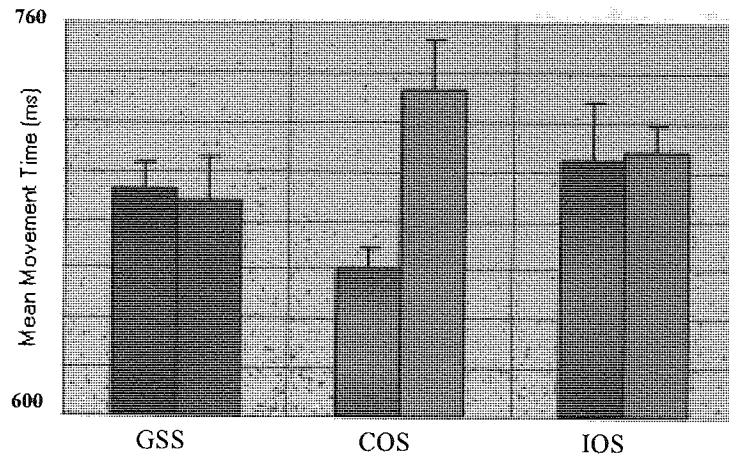
Figure 8.18: Mean movement times for I.W when perturbation targets appeared on geometric stimuli [GS], coherent object stimuli [COS] and incoherent object stimuli [IOS]. The shaded bars represent movement times towards the perturbation target when it appeared at the edge with the conspicuous feature. The vertical bars show one standard deviation of the mean [SEM].

8.3.3.3 Hit error data

For I.W. hit error was again within the standard range [see Table **8.4**]. Additionally, for participant J.C. the imposition of a return-task constraint did not affect hit accuracy. Figure **8.20** shows mean hit error rates towards perturbation targets for I.W. and the two age-matched control participants J.C. and L.C. For I.W. and these control participants no hit error differences are apparent. These finding did not accord with the unselected control participant data [see Figure **7.10**], where increased positive hit error was displayed for incoherent object stimuli when perturbation targets appeared at the edge without the conspicuous feature.

8.3.3.4 Additional Findings

Figure **8.21** shows the z-score measures for mean hit error and mean movement time for all participants. Whilst the age-matched control participants (including J.C. task) and 18 of the 20 unselected participants demonstrated either a speed-accuracy trade-off or increased efficiency (negative z-score) in both measures, I.W. performed poorly on these measures (positive z-scores). Thus, whereas I.W.'s movement times and hit accuracy performances were within the normal range, movement efficiency differences on these measures were apparent.

8.3.3.5 Discussion: compatible perturbation trials findings

Contrary to predictions, I.W. did not show a movement time advantage for perturbation

Table 8.6: Mean Hit Accuracy on Compatible Perturbation Trials

	I.W.	J.C.	J.C. Task	L.C.	Control Participants
Compatible Perturbation Trials	X = 6.80 SE = 3.46	X = 7.47 SE = 4.26	X = 5.55 SE = 3.24	X = 4.59 SE = 2.56	X = 5.05 σ = 1.61
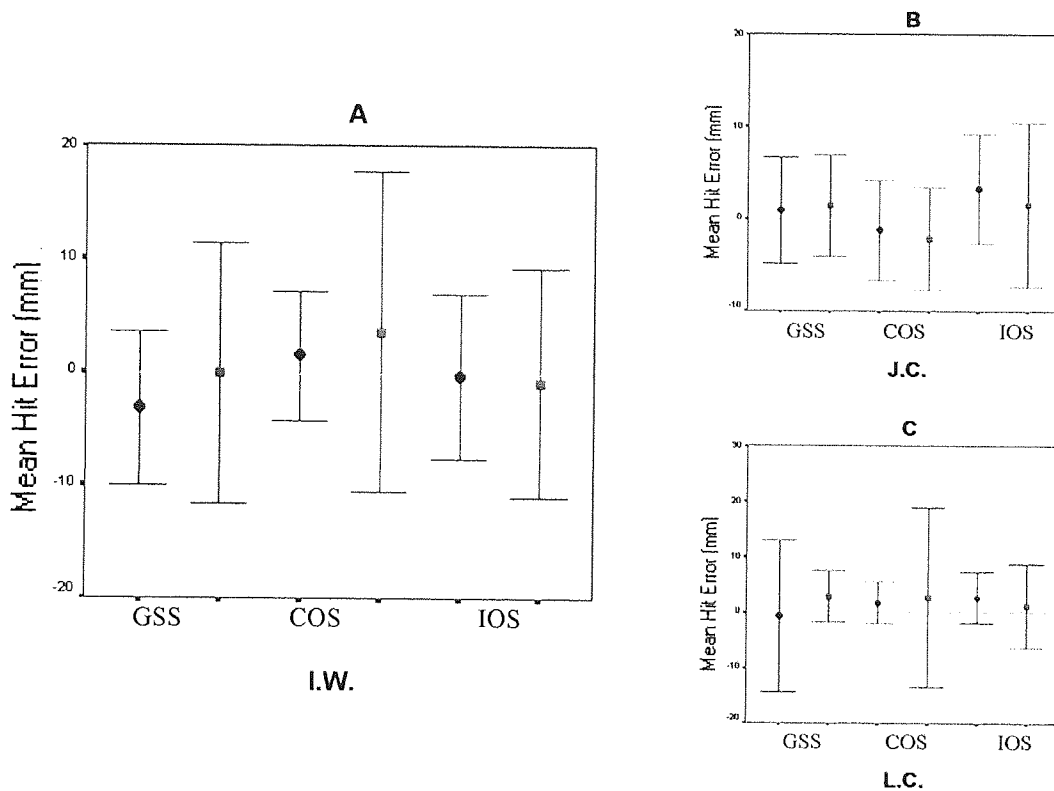
Figure 8.19: Mean hit error for I.W., J.C. and L.C. when perturbation targets appeared on the geometric stimuli [GS], coherent object stimuli [COS] and incoherent object stimuli [IOS]. The diamond represents movement times towards perturbation targets when they appeared at the edge with the conspicuous feature. The vertical lines represent 95% confidence limits.

targets when they corresponded with the direction of attentional bias. Nor did he show a pattern of positive hit error when movements were towards the direction of affordance bias. On compatible perturbation trials, however, the path trajectory adjustments required involved those associated with fine motor control (see McCombe-Waller & Whitall, 2004). This was because, to strike the perturbation target rather than the stimulus edge, a fine realignment of the stylus tip of approximately 4mm was required.
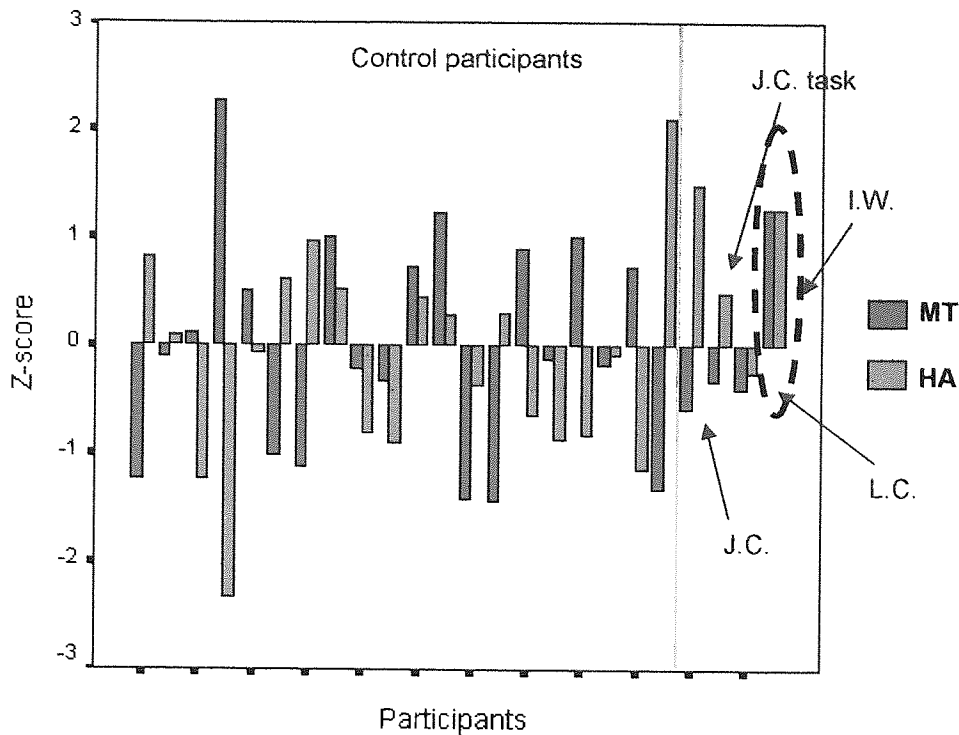
Figure 8.20: Distribution of participant's mean Z-scores for movement time (MT) and hit accuracy (HA) on compatible perturbation trials. For I.W. no speed-accuracy trade-off is demonstrated. The positive z-scores reveal his performance on both measures was below average

This is the type of movement deafferented individuals have most difficulty producing (e.g. Hermsdörfer, Hagl & Nowak, 2004). Thus, it is possible that on compatible perturbation trials, I.W. orientated attention solely towards his moving limb and the perturbation target he was required to strike to compensate for his movement difficulties. This would ensure a similar degree of movement accuracy compared with that demonstrated on standard and incompatible perturbation trials, but would limit or even negate any effects of the stimulus attributes.

For the age-matched control participants the null hit error results could reflect the confound of striking a clearly defined perturbation target. Consistent with this theory, average hit error on standard trials was almost double that on compatible perturbation trials for participant L.C. [see Table's **8.2** & **8.6**].

8.4 General Discussion

8.4.1 Deafferentation and planned movement

It has been demonstrated that the attentional and affordant properties of stimuli have a comparable effect on the production of planned movements in a deafferented individual, as they do in neurologically normal individuals. Namely, whereas the attentional attributes of stimuli are crucial for ensuring correct, speeded responses are produced, affordance attributes of stimuli are critical in determining action properties that enable an object's functional use.

Given the similarity of findings for I.W. and the control participants, one might question the severity of I.W.'s deafferentation. However, in considering I.W.'s difficulty in returning the stylus to the start position, the high number of end-point readjustments observed and the unusual path trajectories displayed, it is clear that I.W. could not make use of proprioceptive information, consistent with literature on deafferented individuals (e.g Cole, 1991; Gentilucci, Toni, Chieffi & Pavesi, 1994; see Jackson, Jackson, Hussain, Harvey, Kramer & Dow, 2000; Jackson *et al.*, 2002). Additionally, whilst I.W.'s movement time and hit error scores were within standard limits, he did not display the stereotypical speed-accuracy trade-off. Thus, the standard trial findings reveal that response saliencies associated with attentional and affordance biases can influence movement efficiency even in an individual who has to consciously plan and monitor every movement. These results are quite remarkable given the considerable mental concentration I.W. requires to produce movements.

8.4.2. Deafferentation and on-line movement control

Attentional and affordance attributes of stimuli also affected the efficiency with which I.W. produced 'on-line' movements. Similar to neurologically normal participants, the affordance properties of stimuli again affected the end-point accuracy of movements. These findings reaffirm the idea that object affordances are of critical importance in determining action-relevant responses to stimuli (e.g. Chao & Martin, 2000; Ellis & Tucker, 2000; Grezes & Decety, 2002; Tucker & Ellis, 2004). However, whilst the attentional bias of stimuli affected movement times for I.W., movement times were least efficient when a corrective movement corresponded with the direction of attentional

bias. This finding was in contrast to the data of control participants and the data of I.W. on standard trials.

A possible explanation for this discrepant movement time result is that the saliency of an attentional bias was actively inhibited when a movement opposed it (see also Fox, 1995; Castiello 1996; 1999; Doyle & Walker, 2001; 2002; Tipper *et al.*,1997; 2002; McSorley *et al.*, 2004). In consequence, when a movement correction was required towards this bias, a response would have been impeded. Nevertheless, a limitation of this argument is that affordance biases are also known to elicit response saliencies (e.g. Chao & Martin, 2000; Grezes & Decety, 2002; Grezes *et al*, 2003a; 2003b; see Creem-Regehr & Lee, 2004 for a review). Thus, for I.W., movement corrections towards an affordance bias should have been actively inhibited too, as was found for control participants when corrective movements were required for stimuli with competing attentional and affordance biases [see Chapter **7** Section *7.3.1.2*].

Resolution of this issue, however, is not problematic if one accepts that deafferented individuals do possess a superior control of attentional resources (see Nougier *et al*, 1994). Namely, given that for I.W. the attentional bias of a stimulus was the primary prerequisite for the potentiation of motor codes [Section *8.3.1.1*], a superior control of attentional resources may have resulted in a more effective inhibition of this bias (i.e. the conspicuous feature) when it opposed the direction of a planned response. Subsequently, slower movement corrections would be displayed on trials where a perturbation target suddenly appeared at a non-target edge with a conspicuous feature, which is consistent with findings.

This explanation can also accommodate the paradoxical performances of control participants. That is, for control participants, an 'inferior' control of attentional resources would lead to increased difficulty in inhibiting the response saliency of an attentional (or affordance) bias (see also Castiello, 1996; 1999; Tipper *et al.*, 1997; 1998; 2002; Tresillian, 1999; Meegan & Tipper, 1999; McSorley *et al.*, 2004). In consequence, speeded responses would be observed when a corrective movement was required towards a conspicuous feature. This is again consistent with findings.

Nonetheless, it should be noted that for I.W., measures of path trajectory efficiency were inconsistent with the measure of movement time. For path trajectory measures I.W. demonstrated increased movement efficiency when a corrective manoeuvre corresponded with the direction of a single attentional bias. These inconsistent findings could reflect limitations of using path trajectory measures with deafferented individuals. For example, I.W. displayed relatively few smooth movement transitions, questioning the reliability of this measure. Additionally, whilst he made more early transitions towards stimuli with a single attentional bias when the corrective manoeuvre corresponded with this bias, for stimuli with a shared affordance and attentional bias, he made more early transitions when the corrective manoeuvre opposed the direction of this shared bias. Thus, this result questions the validity of this measure for I.W.

In sum, from the study of on-line movement control in I.W. it is apparent that deafferented individuals may develop superior control of attentional resources to compensate for their movement difficulties. Nevertheless, whilst it is possible that I.W. does have superior control over attentional resources, from the observation that he still made path deviations and trial errors corresponding with the direction of attentional bias on standard trials [see Figure's **8.5**, **8.6** and **8.8**], it is evident that the saliency of this bias can disrupt movement efficiency when planned (or corrective) movements oppose it. This finding is in agreement with the theory that attentional biases are the critical prerequisite for the potentiation of motor codes (Anderson *et al.*, 2002).

8.4.3 Additional results

It was observed that, for planned movements, I.W. and the age-matched control L.C. demonstrated similar pointing manoeuvres towards the left-side of space. These manoeuvres did not conform to the linear traces the control participants demonstrated. However, as I.W. and L.C. were both left-handed, one explanation for the unusual left-sided trajectories these participants displayed could be that the stereotypical traces of left-handed individuals differ from those of right-handed individuals. Certainly, normative data has been based on analyses of pointing manoeuvres in right-handed participants (e.g. Palluel-Germain, Boy, Orliaguet & Coello, 2004). Alternatively, the path trajectories could reflect an experimental confound. Although, given that stereotypical diagonal path trajectory traces to the left-side of space were demonstrated in the data of a third left-handed individual who partook in a pilot study, this

explanation is unlikely. The cause for the unusual left-sided pointing manoeuvres these participants displayed therefore remains unclear.

It was also found that, comparative to I.W., three control individuals displayed a high number of non-smooth path trajectory corrections. Thus, it is possible that the complexity of stimuli, rather than I.W.'s lack of proprioceptive abilities, influenced path trajectory efficiency on incompatible perturbation trials. Indeed, Bard *et al.* (1999) have demonstrated that a deafferented individual could make smooth corrections to an unconscious perturbation of target location when simple stimuli were utilised.

Finally, the one path deviation I.W. produced when making a corrective manoeuvre [see Section *8.3.2.2*] demonstrates a remarkable degree of movement fluidity not before observed in a deafferented individual. Devoid of proprioceptive abilities, the rapid path deviation and corrective manoeuvres (i.e. the initiation of two opposing turning manoeuvres in under 250ms) must have been a consequence of fast visual feedback mechanisms, whether conscious or otherwise. This finding provides insight into the speed at which visual feedback can be utilised and could not have been inferred from neurologically normal participant data.

Chapter 9

General Conclusions

9.1 Review of Neuroimaging and Behavioural Investigations

9.1.1 The passive perception of object and abstract/geometric patterns

The neuroimaging analyses revealed activity within a range of brain areas when individuals passively viewed stimuli varying in their cognitive associations with a grasping action. For stimuli with no cognitive associations with a grasping action (i.e. abstract/geometric patterns), areas of activation included the sensori-motor cortex, the occipito-temporal cortex and the cerebellum. Activity in such regions, manifest as power decreases in alpha and beta frequency ranges, was of comparable timing and duration to alpha and beta ERD observed when individuals perform a number of movement or action-related tasks (e.g. see Pfurtscheller & colleagues, 1997, 1999; 2000; 2003; Endo et al., 1999; Guie et al., 1999; Szurhaj et al., 2003; Bastiaansen et al., 1999; Leocani et al., 1999; Pfurtscheller & Neuper, 1997). Thus, it was postulated that activity in these areas could underlie the production of fast, co-ordinated responses if a situated necessitated, consistent with research implicating regions of sensori-motor cortex and cerebellum in both the planning and production of action (e.g. Vercher & Gauthier, 1988; Kawato & Gomi, 1992; Doyon, 1994; Horne & Butler, 1995; Pfurtscheller & colleagues, 1997, 1999; 2000; 2003; Miall & Reckess, 2002; Jueptner & Weiller, 1998; Laforce & Doyon, 2001; Saab & Willis, 2003; Ohyama et al., 2003).

For standard object and graspable object patterns, power decreases in sensori-motor, occipito-temporal and cerebellar regions encompassed more neurons. Additionally, for these stimuli, power decreases in regions of superior parietal cortex were observed. This ERD activity was both similar in temporal duration and frequency to that observed in the sensori-motor, occipito-temporal and cerebella regions. A comparative analysis of activation across stimulus types further revealed that the perception of object patterns, compared with abstract/geometric patterns, was associated with power decreases in ventral premotor cortex. These power decreases again spanned alpha and beta frequency

ranges. Parietal and premotor regions are known to be active when individuals manipulate object stimuli, imagine manipulating object stimuli or simply observe object stimuli associated with action (e.g. Grafton *et al.*, 1997; Binkoski *et al.*, 1998; 1999; Inoue *et al.*, 2001; Handy *et al.*, 2003; Kellenbach *et al.*, 2003; Creem-Regehr & Lee, 2004). In agreement with the idea that certain object stimuli afford a function-specific representation for action (Chao & Martin, 2000; Ellis & Tucker, 2000; Grezes & Decety, 2002; Grezes *et al.*, 2003a; 2003b; Tucker & Ellis, 2004), it was postulated that the additional activity associated with the perception of object stimuli could enable a 'primed' motor response, or grasping action, to be prepared.

9.1.2 Directed visual attention, affordance and planned actions

The study of planned pointing manoeuvres in neurologically normal participants revealed that the direction of attentional bias within a stimulus was important for ensuring that a fast, efficient movement was constructed. Movements towards a single attentional bias were not only of decreased duration compared with those that opposed this bias, but were also more likely to demonstrate an efficient diagonal path trajectory. These findings are consistent with the idea that directed visual attention automatically potentiates motor codes (e.g. Anderson *et al.*, 2002). However, fast, efficient movement production was not observed when a stimulus had an opposing or shared affordance bias. For stimuli with a shared attentional/affordance bias, the reason for the null result(s) is unclear. One possibility is that the edge opposing the direction of shared bias elicited an idiosyncratic attentional capture [see Chapter **6** Section **6.4**]. This is in general agreement with the notion that what is perceived to capture attention can be both unpredictable and highly idiosyncratic (see Anderson *et al.*, 2002). For objects with opposing attentional and affordance biases, the findings were taken as evidence that affordance biases can also potentiate motor codes (see Craighero *et al.*, 1996, 1998; Tucker & Ellis, 1998; 2001; 2004; Rumiati & Humphreys, 1998; Ellis & Tucker, 2000; Gentilucci, 2002; Humphreys, 2001; Hommel, 2002; Phillip & Ward, 2002). Indeed, the presence of an affordance bias was key in determining the end-point accuracy of a planned movement. When a movement corresponded with the direction of affordance, participants struck the object's graspable-handle, rather than the actual stimulus edge. This finding supports the idea of micro-affordances (Ellis & Tucker, 2000; Tucker & Ellis, 2004), affordances which enable action-construction based upon subconscious

motor plan repertoires that provide basic information on how to utilise objects. Additionally, the hit error results are consistent with theories that dorsal stream and premotor neurons link visual information about object manipulability with appropriate hand and finger movements necessary for using a given object (e.g. Sakata *et al.*, 1997; Kalaska *et al.*, 1997; Chao & Martin, 2000; Rizzolatti *et al.*, 2000; 2002; Gold & Mazurek, 2002; Handy *et al.*, 2003).

9.1.3 Directed visual attention, affordance and unplanned actions

Findings of unplanned pointing manoeuvres were similar to those of planned pointing manoeuvres. Namely, whereas the attentional bias of a stimulus was of primary importance in determining the efficiency of an unplanned corrective manoeuvre, the affordance bias was key in determining the end-point accuracy of such a movement. However, contrary to previous perturbation research (e.g. Castiello and colleagues, 1993; 1998; Brenner & Smeets, 1997; Pisella *et al.*, 1998; Desmurget *et al.*, *1999*; Fourneret & Jeannerod, 1998; Boulinguez *et al.*, 2001; Dubrowski *et al.*, 2002; Grea *et al.*, 2002; Lee & van Donkelaar, 2002; Jackson *et al.*, 2002), it was revealed that corrective movements were seldom produced with minimal disruption to movement efficiency. Indeed, corrective manoeuvres were occasionally not observed even though individuals were often aware of an incompatible perturbation target. This finding demonstrates that the on-line control of action, far from being automatic (e.g. Goodale & Milner 1992; Milner & Goodale, 1995; Pisella *et al.*, 2000; Glover 2004), is influenced by the affordant and attentional properties of a to-be-pointed at stimulus.

The results also showed that corrective movements were of increased duration for stimuli with opposing attentional and affordance biases. These results, suggestive of response competition (e.g. Castiello, 1996; 1999; Tresillian, 1999; Meegan & Tipper, 1998) and negative priming (Fox, 1995; Tipper, Meegan & Howard, 2002), are consistent with the hypothesis that both attention and affordance elicit motor response codes.

9.1.4 Deafferentation, directed visual attention and affordance

The construction of planned and unplanned pointing manoeuvres in a deafferented individual [I.W.] revealed that both the attentional and affordant properties of a stimulus

affected action production. For I.W., when both planned and corrective movements were required, the direction of affordance bias was critical in determining the end-point accuracy of a movement. These results mirrored those of the control participants and provide evidence demonstrating that I.W. has access to a (non-conscious) repertoire of motor plans that provide basic information on how to utilise objects with known affordances.

The influence of attention upon action construction was, however, more complex. Whereas for I.W. planned movements corresponding with the direction of attentional bias were facilitated, unplanned movements corresponding with this bias were impeded. This paradoxical finding was postulated to reflect I.W's superior allocation of attentional resources, in agreement with the hypothesis of Nougier *et al.* (1994). Nonetheless, as I.W. occasionally displayed path deviations and trial errors corresponding with the direction of an attentional bias, it was evident that the saliency of an attentional bias could disrupt action construction even in an individual who has visually monitor every movement.

9.2 Directed Visual Attention and Action

All three behavioural investigations revealed that the attentional bias of stimuli, and not the affordance bias, was of key importance in ensuring correct movement kinematics were formulated and that a movement was constructed efficiently. For example, when a planned movement was required, the trial errors and path deviations individuals displayed were likely to veer towards the direction of attentional bias irrespective of the direction of affordance bias. Such findings indicate that neural activity associated with attentional biases is not only automatic but, on occasion, not effectively inhibited (see also Theeuwes *et al.*, 1999; Tipper and colleagues 2001; 2002; McSorley *et al.*, 2004). This was true even for a deafferented individual who has to consciously plan and visually monitor every movement.

Consistent with the behavioural results, the neuroimaging investigation revealed that the perception of graspable object patterns was not critical for activity in areas known to be involved in both the planning and production of action. Coherent oscillatory activity in sensori-motor and cerebella regions was demonstrated when individuals viewed stimuli with no cognitive associations with a grasping action (i.e. geometric/abstract patterns).

Given both the behavioural results and the common set of brain regions activated when individuals viewed both geometric/abstract and object patterns, it is postulated that activity associated with the potentiation of motor codes, through visual attention, encompasses regions of sensori-motor cortex, occipito-temporal cortex and cerebellum.

9. 3 Object Affordances and Action

Contrary to much scientific opinion (e.g. Craighero *et al.*, 1996, 1998; Grafton *et al.*, 1997; Binkoski *et al.*, 1998; 1999; Rumiati & Humphreys, 1998; Tucker & Ellis, 1998, 2001; Humphreys, 2001; Gentilucci, 2002; Grezes and colleagues 2002; 2003a; 2003b; Hommel, 2002; Phillip & Ward, 2002; Handy *et al.*, 2003; Kellenbach *et al.*, 2003; Creem-Regehr & Lee, 2004), the neuroimaging results revealed that neuronal activity in brain regions implicated in the planning and production of action was observed for both the perception of object *and* abstract patterns. Therefore, affordance *per se* is unlikely to form the basis of the neural signals generated in these areas. Consistent with this result, behavioural findings of planned pointing manoeuvres demonstrated that the affordance bias of a stimulus was not critical for ensuring an efficient movement was constructed. Rather, the attentional bias of a stimulus was the primary prerequisite in ensuring participants produced a correct action.

However, whilst the perception of an affordance bias was not critical for movement production, the studies of movement construction in neurologically normal participants did indicate that object affordances were associated with the potentiation of some motor codes. Indeed, the key finding of all behavioural investigations was that the affordance bias of a stimulus was critical in determining the end-point accuracy of a movement. When a movement corresponded with an object's graspable handle, pointing manoeuvres typically undershot the target edge, with participants tending to strike the graspable handle of the object. This finding, observed even when the manoeuvre was directed towards a clearly defined perturbation target, is in accordance with the idea of micro-affordances (Ellis & Tucker, 2000; Tucker & Ellis, 2004). Additionally, it fits well with the finding that the perception of object patterns, unlike geometric/abstract patterns, was associated with power decreases in regions of superior parietal cortex and premotor cortex. This activity, suggested to enable a 'primed' motor response to be constructed [see Chapter 3 Section 3.4], is consistent with research demonstrating that neural activity in regions of parietal and premotor cortex is observed for the visual guidance of hand actions for object manipulations (e.g. Sakata *et al.*, 1997; Kalaska *et al.*, 1997; Chao & Martin, 2000; Rizzolatti *et al.*, 2000; 2002; Gold & Mazurek, 2002; Grezes and colleagues, 2003a; 2003b; Handy *et al.*, 2003).

215

In sum, it is evident that whilst object affordances are associated with the potentiation of motor codes, they are not necessary for visual routes to action. Namely, it is postulated that motor codes elicited upon the perception of known graspable objects represent a more refined action-based knowledge. The primary purpose of this (visuomotor) knowledge is to allow for visual features of manipulable stimuli to be matched with the appropriate hand and finger movements required for using them. In accordance with previous neuroimaging research [See Chapter 1 Section 1.3.3 and Chapter 3 Section 3.1 & 3.4], the present findings indicate that the basis of such functionally related neuronal activity involves regions of superior parietal cortex and premotor cortex, in addition to activity observed in sensori-motor, occipito-temporal and cerebella regions.

9.4. Deafferentation and Action

Through the study of an individual without proprioception, it was observed that conscious awareness of movement is not sufficient to negate the influences of visual routes to action (see also Milner & Goodale, 1995; Agliotti *et al.*, 1995; Pisella *et al.*, 2000; Glover 2004). However, it is apparent that a superior allocation of attentional resources might allow for a more effective inhibition of attentional and affordance biases when they are not deemed relevant. In consequence, this research could be of use in situations where either visual scene information is complex and warrants a number of alternative actions, or in situations where action-based retroactive interference could impede efficient action construction. For example, changes of machinery interface lay-out often lead to errors; even fatal errors (see Besnard & Cacitti, *in press*).

Additionally, from the observation that I.W. could produced fast corrections to errant path trajectories, it is also apparent that visual feedback can operate within limited time constraints (i.e. under 200ms) to allow for the fast computation of movement kinematics (see Carlton, 1981; Elliott & Allard, 1985; Jackson *et al.*, 2000; Glover, 2004).

9.5 Conclusions and Implications

Both the imaging and behavioural experiments provide evidence to suggest that attention is important for fast, correct actions, whereas affordance is important for primed motor responses which reflect object functionality and manipulability.

Consistent with the theory of Anderson *et al.* (2002), it is suggested that the construction of fast, co-ordinated responses through directed visual attention would be advantageous whenever a speeded response was required. For example, in situations where fight or flight responses would be required, directed visual attention is theorised to serve as the primary visual route to action. Therefore, the absence or presence of attentional biases may be of significant practical importance in situations where fast, co-ordinated observer responses are required, such as in the design of cockpit displays or any visual interactive display units/control panels [see Chapter **6**, Section **6.4**].

This is not to discount the role of object affordances in visual routes to action. Knowing automatically the grasp type or object manipulation needed to use specific objects or tools (i.e. action-based knowledge) enables the successful completion of a multitude of everyday tasks. The accomplishment of which may well aid the day-to-day survival of higher-order primates. Thus, it is no surprise that action-based knowledge occurs earlier on in development compared with cognitive functions of language production, memory and abstract reasoning (e.g. Goswami, 2000), and remains intact long after such cognitive-based knowledge has deteriorated in various degenerative diseases (e.g. Burns, Jacoby & Levy, 1991; Roy & Black, 1998; Helmes & Østbye, 2002; Parakh, Roy, Koo & Black, 2004).

9. 6 Future Directions

From results reported in this thesis it has been hypothesised that attentional biases may be of significant practical importance in situations where fast, co-ordinated responses are required. However, whilst similarities in responding to 2-D images compared with visual interactive display units can be assumed given the relatedness of such stimuli, this may not be the case for responses to 2-D images compared with 3-D objects (e.g. non-virtual control panels). Therefore, it is important that research be conducted using 3-dimensional object stimuli. Such work would reveal whether the saliencies of attentional and/or affordance biases upon action are influenced by the modality of stimulus presentation.

Additionally, as it has been argued that shifts of attention to visual locations (or objects) recruit brain regions involved in eye movement programming and execution (e.g. Goldberg & Segraves, 1987; Corbetta & Shulman, 1998), research could also be extended to include measures of eye-movements. For example, on trials where errors or path deviations are observed, are there positive correlations between such action-errors and eye-movement? Moreover, when participants show 'attentional' idiosyncrasies, are these correlated with eye-movements? Measures of eye-movements in conjunction with measures of actual arm/hand movement would be invaluable in answering such questions.

Reference List

Abrams, R.A. & Dobkins,R.S. (1994) Inhibtion of return:Effects of attentional cuing on eye movement latencies. Journal of Experimental Psychology: *Human Perception & Performance*, **20**, 467-477.

Achim, A. (1995) Cerebral source localization paradigms - spatiotemporal source modeling. *Brain and Cognition*, **27**, 256-287.

Adam,J.J. & Keulen,R.F. (2004) fMRI evidence for and behavioural evidence against the planning-control model. *Behavioral and Brain Sciences*, **27**, 24.

Adjamian,P., Barnes,G.R., Hillebrand,A., Holliday,I.E., Singh,K.D., Furlong,P.L., Harrington,E., Barclay,C.W. & Route,P.J.G. (2004) Co-registration of magnetoencephalography with magnetic resonance imaging using bite-bar-based fiducials and surface-matching. *Clinical Neurophysiology*, **115**, 691-698.

Adrian,A.D. & Matthews,B.H.C. (1934) The Berger Rhythm: potential changes from the occipital lobes in man. *Brain*, **4**, 355-385.

Agliotti,S., Goodale,M.A. & DeSouza,J.F.K. (1995) Size-contrast illusions deceive the eye but not the hand. *Current Biology*, **5**, 679-685.

Ahlfors,S.P., Simpson,G.V., Dale,A.M., Belliveau,J.W., Liu,A.K., Korvenoja,A., Virtanen,J., Huotilainen,M., Tootell,R.B.H., Aronen,H.J. & Ilmoniemi,R.J. (1999) Spatiotemporal activity of a cortical network for processing visual motion revealed by MEG and fMRI. *Journal of Neurophysiology*, **82**, 2545-2555.

Anderson,S.J. & Yamagishi,N. (2000) Spatial localization of colour and luminance stimuli in human peripheral vision. *Vision Research*, **40**, 759-771.

Anderson,S.J. (2002) Functional neuroimaging in Amblyopia. In Moseley.M. & Fielder,A. (eds), *Amblyopia a multidisciplinary approach*. Butterworth HeineMann, Oxford, pp. 43-68.

Anderson,S.J., Yamagishi,N. & Karavia,V. (2002) Attentional Processes Link Perception and Action. *Proceedings of the Royal Society, London: B*, **269**, 1225-1232.

Avikainen,S., Forss,N. & Hari,R. (2002) Modulated Activation of the Human SI and SII Cortices during Observation of Hand Actions. *NeuroImage*, **15**, 640-646.

Baillet,S., Mosher,J.C. & Leahy,R.M. (2001) Electromagnetic brain mapping. *Ieee Signal Processing Magazine*, **18**, 14-30.

Balint,R. (1909) Seelenlamung des 'schauens', optische Ataxie raumliche Storung der Aufmerksamkeit. *Monatsschr, Psychiatr.Neurol.*, **25**, 51-81.

Balish,M. & Muratore,R. (1990) The Inverse Problem in Electroencephalography and Magnetoencephalography. In Sato,S. (ed), *Advances in Neurology*. Raven Press, New York, pp. 79-88.

Bard,C., Fleury,M., Teasdale,N., Paillard,J. & Nougier,V. (1995) Contribution of proprioception for calibrating and updating the motor space. *Canadian Journal of Physiology and Pharmacology*, **73**, 246-254.

Bard,C., Turrell,Y., Fleury,M., Teasdale,N., Lamarre,Y. & Martin,O. (1999) Deafferentation and pointing with visual double-step perturbations. *Experimental Brain Research*, **125**, 410-416.

Barnes,G.R. & Hillebrand,A. (2003) Statistical flattening of MEG beamformer images. *Human Brain Mapping*, **18**, 1-12.

Basar,E., Schurmann,M., Basar-Eroglu,C. & Karakas,S. (1997) Alpha oscillations in brain functioning: an integrative theory. *International Journal of Psychophysiology*, **26** , 5-29.

Bastiaansen,M.C.M., Brunia,C.H.M. & Bocker,K.B.E. (1999) ERD as an index of anticipatory behavior. In Pfurtscheller,G. & Lopes da Silva,F.H. (eds), *Event_Related Desynchronisation: Handbook of Electroencephalography and Clinical Neurophysiology*. Elsevier Science, Amsterdam, pp. 203-217.

Bastiaansen,M.C.M., Bocker,K.B.E., Brunia,C.H.M., de Munck,J.C. & Spekreijse,H. (2001) Event-related desynchronization during anticipatory attention for an upcoming stimulus: a comparative EEG/MEG study. *Clinical Neurophysiology*, **112**, 393-403.

Bauer,D.W. & Miller,J. (1982) Stimulus-response compatibility and the motor system. *Quarterly Journal of Experimental Psychology Section A-Human Experimental Psychology*, **34**, 367-380.

Beauchamp,M.S., Lee,K.E., Haxby,J.V. & Martin,A. (2002) Parallel visual motion processing streams for manipulable objects and human movements. *Neuron*, **34**, 149-159.

Bedard,K.P. & Proteau,L. (2003) On the role of peripheral visual afferent information for the control of rapid video-aiming movements. *Acta Psychologica*, **113**, 99-117.

Behrmann,M. & Meegan,D.V. (1998) Visuomotor Processing in Unilateral Neglect. *Consciousness and Cognition*, **7**, 381-409.

Behrmann,M. & Tipper,S.P. (1994) Object-based attentional mechanisms: Evidence from patients with unilateral neglect. In Umilita,C. & Moscovitch,M. (Eds.), *Attention and Performance XV, Conscious and Nonconscious Information Processing*. MIT Press, Cambridge.

Berger,H. (1930) Uber das Elektrenkephalogramm des Menschen II. *Journal of Psychology and Neurology*, **40**, 160-179.

Bertrand,O. & Tallon-Baudry,C. (2000) Oscillatory gamma activity in humans: a possible role for object representation. *International Journal of Psychophysiology*, **38**, 211-223.

Besnard, D. & Cacitti, L. (*in press*) Interface changes causing accidents. An empirical study of negative transfer.. *International Journal of Human-Computer Studies*

Binkofski,F., Dohle,C., Posse,S., Stephan,K.M., Hefter,H., Seitz,R.J. & Freund,H.J. (1998) Human anterior intraparietal area subserves prehension - A combined lesion and functional MRI activation study. *Neurology*, **50**, 1253-1259.

Binkofski,F., Buccino,G., Posse,S., Seitz,R.J., Rizzolatti,G. & Freund,H.J. (1999) A fronto-parietal circuit for object manipulation in man: evidence from an fMRI-study. *European Journal of Neuroscience*, **11**, 3276-3286.

Bisiach,E. & Luzatti,C. (1978) Unilateral neglect of representational space. *Cortex*, **14**, 128-133.

Bootsma,R.J., Marteniuk,R.G., Mackenzie,C.L. & Zaal,F.T.J.M. (1994) The speed-accuracy trade-off in manual prehension - effects of movement amplitude, object size and object width on kinematic characteristics. *Experimental Brain Research*, **98**, 535-541.

Boulinguez,P. & Nougier,V. (1999) Control of goal-directed movements: the contribution of orienting of visual attention and motor preparation. *Acta Psychologica*, **103**, 21-45.

Boulinguez,P., Blouin,J. & Nougier,V. (2001) The gap effect for eye and hand movements in double-step pointing. *Experimental Brain Research*, **138**, 352-358.

Braddick,O.J., O'Brien,J.M.D., Wattam-Bell,J., Atkinson,J. & Turner,R. (2000) Form and motion coherence activate independent, but not dorsal/ventral segregated, networks in the human brain. *Current Biology*, **10**, 731-734.

Bradshaw,M.F. & Watt,S.J. (2002) A dissociation of perception and action in normal human observers: the effect of temporal-delay. *Neuropsychologia*, **40**, 1766-1778.

Brenner,E. & Smeets,J.B.J. (1997) Fast responses of the human hand to changes in target position. *Journal of Motor Behavior*, **29**, 297-310.

Breschet,R. & Lecasble,R. (1965) Societe d'electroencephalographie et de neurophysiologie clinique de langue Francaise : Joint Meeting Paris, June 2 and 3, 1964 Secretaries: Brook General Hospital, Shooters Hill Road, London S.E.18 (Great Britain) and Hospital Henri-Rousselle, 1, rue Cabanis, Paris 14 (France). *Electroencephalography and Clinical Neurophysiology*, **18**, 720-726.

Bridgeman,B. (2002) Attention and Visually Guided Behaviour in Distinct Systems. *Common Mechanisms in Perception and Action*. Oxford University Press, Oxford, pp. 120-135.

221

Bridgeman,B. (2004) Defining visuomotor dissociations and an application to the oculomotor system. *Behavioral and Brain Sciences*, **27**, 27-27

Bringuier,V., Fregnac,Y., Baranyi,A., Debanne,D. & Shulz,D.E. (1997) Synaptic origin and stimulus dependency of neuronal oscillatory activity in the primary visual cortex of the cat. *Journal of Physiology-London*, **500**, 751-774.

Brouwer,A.M., Brenner,E. & Smeets,J.B.J. (2004) Using the same information for planning and control is compatible with the dynamic illusion effect. *Behavioral and Brain Sciences*, **27**, 28-28

Brunia,C.H.M. (2001) Thalamo-cortical relations in attention and consciousness. *International Journal of Psychophysiology*, **43**, 1-4.

Bruno,N. (2001) When does action resist visual illusions? *Trends in Cognitive Sciences*, **5**, 379-382.

Bullier,J. & Nowak,L.G. (1995) Parallel versus Serial Processing: New Vistas on the Distributed Organization of the Visual System. *Current Opinion in Neurobiology*, **5**, 497-503.

Burgess,A.P. & Gruzelier,J.H. (1999) Methodological advances in the analysis of event-related desynchronization data: reliability and robust analysis. In Pfurtscheller,G. & Lopes da Silva,F.H. (eds), *Handbook of Electroencephalography and clinical neurpohysiology, Revised series*. Elsevier Science, Amsterdam, pp. 139-158.

Burns,A., Jacoby,R. & Levy,R. (1991) Progression of cognitive impairment in Alzheimers disease. *Journal of the American Geriatrics Society*, **39**, 39-45.

Caplan,J.B., Kahana,M.J., Sekuler,R., Kirschen,M. & Madsen,J.R. (2000) Task dependence of human theta: The case for multiple cognitive functions. *Neurocomputing*, **32-33**, 659-665.

Carey,D.P. (2001) Do action systems resist visual illusions? *Trends in Cognitive Sciences*, **5**, 109-113.

Carlson,N.R. (2003) *Physiology of Behaviour* Allyn and Bacon, Boston, Mass.

Carlton,L.G. (1981) Processing visual feedback information for movement control. *Journal of Experimental Psychology-Human Perception and Performance*, **7**, 1019-1030.

Carmack,P.S., Spence,J., Gunst,R.F., Schucany,W.R., Woodward,W.A. & Haley,R.W. (2004) Improved agreement between Talairach and MNI coordinate spaces in deep brain regions. *Neuroimage*, **22**, 367-371.

Castiello,U., Bennett,K.M.B. & Stelmach,G.E. (1993) Reach to grasp - the natural response to perturbation of object size. *Experimental Brain Research*, **94**, 163-178.

Castiello,U. (1996) Grasping a fruit: Selection for action. *Journal of Experimental Psychology-Human Perception and Performance*, **22**, 582-603.

Castiello,U., Bennett,K. & Chambers,H. (1998) Reach to grasp: the response to a simultaneous perturbation of object position and size. *Experimental Brain Research*, **120**, 31-40.

Castiello,U. (1999) Mechanisms of selection for the control of hand action. *Trends in Cognitive Sciences*, **3**, 264-271.

Castiello,U., Paine,M. & Wales,R. (2002) Perceiving an entire object and grasping only half of it. *Neuropsychologia*, **40**, 145-151.

Caton,R. (1875) The Electric Currents of the Brain. *British Medical Journal*, **2**, 278.

Chaminade,T., Meltzoff,A.N. & Decety,J. (2002) Does the End Justify the Means? A PET Exploration of the Mechanisms Involved in Human Imitation. *NeuroImage*, **15**, 318-328.

Chao,L.L., Haxby,J.V. & Martin,A. (1999) Attribute-based neural substrates in temporal cortex for perceiving and knowing about objects. *Nature Neuroscience*, **2**, 913-919.

Chau,W. & McIntosh,A.R. (2005) The talairach coordinate of a point in the MNI space: how to interpret it. *Neuroimage*, **25**, 408-416.

Clarke,A.R., Barry,R.J., McCarthy,R. & Selikowitz,M. (2001) Excess beta activity in children with attention-deficit/hyperactivity disorder: an atypical electrophysiological group. *Psychiatry Research*, **103**, 205-218.

Coello,Y. & Rossetti,Y. (2004) Planning and controlling action in a structured environment: Visual illusion without dorsal stream. *Behavioral and Brain Sciences*, **27**, 29.

Cole,H.W. & Ray,W.J. (1985) EEG correlates of emotional tasks related to attentional demands. *International Journal of Psychophysiology*, **3**, 33-41.

Cole,J. (1991) *Pride and a daily marathon* Duckworth, London.

Cole,J.D. & Sedgewick,E.M. (1992) The perceptions of force and of movement in a man without large myelinated sensory afferents below the neck. *Journal of Physiology-London*, **449**, 503-515.

Comi,G. (1997) Electrophysiological correlates of cognitive dysfunction in multiple sclerosis. *Electroencephalography and Clinical Neurophysiology*, **103**, 53.

Cooper,R. & Shallice,T. (2000) Contention scheduling and the control of routine activities. *Cognitive Neuropsychology*, **17**, 297-338.

Corbetta,M. & Shulman,G.L. (1998) Human cortical mechanisms of visual attention during orientation and search. *Philosophical Transactions of the Royal Society: Series B*, **353**, 1353-1362.

Coslett,H.B. & Buxbaum,L.J. (2004) The planning-control model and spatio-motor deficits following brain damage. *Behavioral and Brain Sciences*, **27**, 31-31

Courtemanche,R., Pellerin,J.P. & Lamarre,Y. (2002) Local field potential oscillations in primate cerebellar cortex: Modulation during active and passive expectancy. *Journal of Neurophysiology*, **88**, 771-782.

Craighero,L., Fadiga,L., Umilta,C.A. & Rizzolatti,G. (1996) Evidence for visuomotor priming effect. *Neuroreport*, **8**, 347-349.

Craighero,L., Fadiga,L., Rizzolatti,G. & Umilta,C. (1998) Visuomotor priming. *Visual Cognition*, **5**, 109-125.

Craighero,L., Fadiga,L., Rizzolatti,G. & Umilta,C. (1999) Action for perception: A motor-visual attentional effect. *Journal of Experimental Psychology-Human Perception and Performance*, **25**, 1673-1692.

Creem-Regehr,S.H. & Lee,J.N. Neural representations of graspable objects: are tools special? *Cognitive Brain Research*, **In Press, Corrected Proof**.

Creem-Regehr, Sarah H., Dilda, V, Gold, A. E, and Lee, James N. Grasping novel objects: functional identity influences representations for real and imagined actions. 2004. *CNS Conference Proceeding*

Creem,S.H. & Proffitt,D.R. (2001) Defining the cortical visual systems: "What", "Where", and "How". *Acta Psychologica*, **107**, 43-68.

Cremades,J.G. (2002) The effects of imagery perspective as a function of skill level on alpha activity. *International Journal of Psychophysiology*, **43**, 261-271.

Crouzeix,A., Yvert,B., Bertrand,O. & Pernier,J. (1999) An evaluation of dipole reconstruction accuracy with spherical and realistic head models in MEG. *Clinical Neurophysiology*, **110**, 2176-2188.

Cuffin,B.N. (1986) Effects of measurement errors and noise on MEG moving dipole inverse solutions. *Ieee Transactions on Biomedical Engineering*, **24**, 372-381.

Davidson,A.C. & Hinkley,D.V. (1997) *Bootstrap Methods and their Application* Cambridge University Press, Cambridge.

Decety,J., Perani,D., Jeannerod,M., Bettinardi,V., Tadary,B., Woods,R., Mazziotta,J.C. & Fazio,F. (1994) Mapping motor representation with positron emission tomography. *Nature*, **371**, 600-602.

Deco,G. & Lee,T.S. (2002) A unified model of spatial and object attention based on inter- cortical biased competition. *Neurocomputing*, **44**, 775-781.

Delage,Y. (1919) *Le reve: Etude Psychologique, Philosophie et Litteraire* Presses Universitaires de Frances, Paris.

DeLoache,J.S. (2004) Scale errors by very young children: A dissociation between action planning and control. *Behavioral and Brain Sciences*, **27**, 32-32

Desimone,R. & Ungerleider,L.G. (1989) Neural Mechanisms of Visual Processing in Monkeys. In Boller,F. & Grafman,J. (eds), *Handbook of Neuropsychology*. Elsevier, Amsterdam.

Desmurget,M., Pelisson,D., Rossetti,Y. & Prablanc,C. (1998) From eye to hand: Planning goal-directed movements. *Neuroscience and Biobehavioral Reviews*, **22**, 761-788.

Desmurget,M., Epstein,C.M., Turner,R.S., Prablanc,C., Alexander,G.E. & Grafton,S.T. (1999) Role of the posterior parietal cortex in updating reaching movements to a visual target. *Nature Neuroscience*, **2**, 563-567.

Desmurget,M. & Grafton,S. (2000) Forward modeling allows feedback control for fast reaching movements. *Trends in Cognitive Sciences*, **4**, 423-431.

DeYoe,E.A. & Van Essen,D.C. (1988) Concurrent processing streams in monkey visual cortex. *Trends in Neurosciences* , **11**, 219-226.

Doyle,D. & Walker,R. (2001) Curved saccade trajectories: Voluntary and reflexive saccades curve away from irrelevant distractors. *Experimental Brain Research*, **139**, 333-344.

Doyle,M.C. & Walker,R. (2002) Multisensory interactions in saccade target selection: Curved saccade trajectories. *Experimental Brain Research*, **142**, 116-130.

Doyon,J. (1994) Contribution of the striatum, cerebellum and frontal lobes to skill learning. *Canadian Psychology-Psychologie Canadienne*, **35**, 36-36.

Driver,J. & Frith,C. (2000) Shifting baselines in attention research. *Nature Reviews Neuroscience*, **1**, 147-148.

Dubner,r. & Zeki,S. (1971) Response properties and receptive fields of cells in an anatomically defined region of the superior temporal sulcus in the monkey. *Brain Research*, **35**, 528-532.

Dubrowski,A., Bock,O., Carnahan,H. & Jungling,S. (2002) The coordination of hand transport and grasp formation during single- and double-perturbed human prehension movements. *Experimental Brain Research*, **145**, 365-371.

Duncan,J. (1984) Selective attention and the organisation of visual information. *Journal of Experimental Psychology: General*, **113**, 501-517.

Dujardin,K., Bourriez,J.L. & Guieu,J.D. (1994) Event-related desynchronisation (ERD) patterns during verbal memory tasks – effects of age. *International Journal of Psychophysiology*, **16**, 17-27.

Elliott,D. & Allard,F. (1985) The utilization of visual feedback information during rapid pointing movements. *Quarterly Journal of Experimental Psychology Section A-Human Experimental Psychology*, **37**, 407-425.

Elliott,D. & Meegan,D.V. (2004) Visual context can influence on-line control. *Behavioral and Brain Sciences*, **27**, 33.

Ellis,R. & Tucker,M. (2000) Micro-affordance: The potentiation of components of action by seen objects. *British Journal of Psychology*, **91**, 451-471.

Endo,H., Kizuka,T., Masuda,T. & Takeda,T. (1999) Automatic activation in the human primary motor cortex synchronized with movement preparation. *Cognitive Brain Research*, **8**, 229-239.

Engel,A.K., Fries,P. & Singer,W. (2001) Dynamic predictions: Oscillations and synchrony in top-down processing. *Nature Reviews Neuroscience*, **2**, 704-716.

Eriksen,C.W. & Murphy,T.D. (1987) Movement of attentional focus across the visual field: A critical look at the evidence. *Perception & Psychophysics*, **42**, 299-305.

Fagaly,R.L. (1990) Neuromagnetic Instrumentation. In Sato,S. (ed), *Advances in Neurology*. Raven Press, New York, pp. 11-32.

Faillenot,I., Decety,J. & Jeannerod,M. (1999) Human brain activity related to the perception of spatial features of objects. *NeuroImage*, **10**, 114-124.

Farrer,C., Franck,N., Paillard,J. & Jeannerod,M. (2003) The role of proprioception in action recognition. *Consciousness and Cognition*, **12**, 609-619.

Fearon,P. (2003) Big problems with small samples. *Psychologist*, **16**, 632-635.

Fecteau,J.H., Chua,R., Franks,I. & Enns,J.T. (2001) Visual awareness and the on-line modification of action. *Canadian Journal of Experimental Psychology-Revue Canadienne de Psychologie Experimentale*, **55**, 104-110.

Felleman,D.J. & Van Essen,D.C. (1990) Distributed hierarchical processing in primate cerebral cortex. *Cerebral Cortex*, **1**, 1-47.

Ferro,J.M. (1984) Transient inaccuracy in reaching caused by a posterior parietal lobe lesion. *Journal of Neurology, Neurosurgery, and Psychiatry*, **47**, 1016-1019.

Fingelkurts,A., Fingelkurts,A., Krause,C., Kaplan,A., Borisov,S. & Sams,M. (2003) Structural (operational) synchrony of EEG alpha activity during an auditory memory task. *NeuroImage*, **20**, 529-542.

Fitts,P.M. & Seeger,C.M. (1953) S-R compatibility: Spatial characteristics of stimulus and response codes. *Journal of Experimental Psychology*, **46**, 199-210.

FitzGerald,M.J.T. & Folan-Curran,J. (2002) *Clinical Neuroanatomy* W.B. Saunders, New York.

Flanagan,J.R. & Rao,A.K. (1995) Trajectory adaption to a nonlinear visuomotor transformation - evidence of motion planning in visually perceived space. *Journal of Neurophysiology*, **74**, 2174-2178.

Fleming,J., Klatzky,R.L. & Behrmann,M. (2002) Time course of planning for object and action parameters in visually guided manipulation. *Visual Cognition*, **9**, 502-527.

Fleury,M., Bard,C., Teasdale,N., Michaud,D. & Lamarre,Y. (1999) How efficient are central mechanisms for the learning and retention of coincident timing actions? *Neuropsychologia*, **37**, 723-730.

Forde,E.M.E. & Humphreys,G.W. (2002) The cognitive processes underpinning everyday actions. *NeuroCase*, **8**, 59-60.

Fourneret,P. & Jeannerod,M. (1998) Limited conscious monitoring of motor performance in normal subjects. *Neuropsychologia*, **36**, 1133-1140.

Fox,E. (1995) Negative priming from ignored distractors in visual selection - a review. *Psychonomic Bulletin & Review*, **2**, 145-173.

Fox,P.T. & Raichle,M.E. (1986) Focal physiological uncoupling of cerebral bloodflow and oxidative metabolism during somatosensory stimulation in human subjects. *Proceedings of the National Academy of Sciences of the United States of America*, **83**, 1140-1144.

Foxe,J.J., Simpson,G.V. & Ahlfors,S.P. (1998) Parieto-occipital similar to 10 Hz activity reflects anticipatory state of visual attention mechanisms. *Neuroreport*, **9**, 3929-3933.

Franz,V.H. (2001) Action does not resist visual illusions. *Trends in Cognitive Sciences*, **5**, 457-459.

Freeman,W.J. (1994) Neural networks and chaos. *Journal of Theoretical Biology*, **171**, 13-18.

Freeman,W.J. (2000) Brain Dynamics: Brain Chaos and Intentionality. In Evian,G. (ed), *Integrative Neuroscience. Bringing Together Biological, Psychological and Clinical Models of the Human Brain*. Harwood Academic Publishers, Sydney, pp. 1-6.

Friston,K.J., Holmes,A.P., Worsley,K.J., Poline,J.B., Frith,C.D. & Frackowiak,R.S.J. (1995) Statistical Parametric Maps in Functional Imaging: A General Linear Approach. *Human Brain Mapping*, **2**, 189-210.

Gabor,D. (1946) Theory of communication. *The journal of the institute of Electrical Engineers*, **93**, 429-457.

Gazzaniga,M.S., Ivry,R.B. & Mangun,R.M. (1998) *Cognitive Neuroscience* W.W.Norton & Company, New York.

Gentilucci,M., Toni,I., Chieffi,S. & Pavesi,G. (1994) The role of proprioception in the control of prehension movements – a kinematic study in a peripherally deafferented patient and in normal subjects. *Experimental Brain Research*, **99**, 483-500.

Gentilucci,M. & Gangitano,M. (1998) Influence of automatic word reading on motor control. *European Journal of Neuroscience*, **10**, 752-756.

Gentilucci,M., Benuzzi,F., Bertolani,L., Daprati,E. & Gangitano,M. (2000) Language and motor control. *Experimental Brain Research*, **133**, 468-490.

Gentilucci,M. (2002) Object motor representation and reaching-grasping control. *Neuropsychologia*, **40**, 1139-1153.

Gerardin,E., Sirigu,A., Lehericy,S., Poline,J.B., Gaymard,B., Marsault,C., Agid,Y. & Le Bihan,D. (2000) Partially overlapping neural networks for real and imagined hand movements. *Cerebral Cortex*, **10**, 1093-1104.

Ghez,C., Gordon,J. & Ghilardi,M.F. (1995) Impairments of reaching movements in patients without proprioception .2. Effects of visual information on accuracy. *Journal of Neurophysiology*, **73**, 361-372.

Gibson,J.J. (1979) *The ecological approach to visual perception* Houghton-Mifflin Company, Boston.

Gibson,B. & Egeth,H. (1994) Inhibition of return to object-based and environment-based locations. *Perception & Psychophysics*, **55**, 323-339.

Glickstein,M. (2000) How are visual areas of the brain connected to motor areas for the sensory guidance of movement? *Trends in Neurosciences*, **23**, 613-617.

Glickstein,M. & May,J. (1982) Visual control of movement: the circuits which link visual to motor areas of the brain with special reference to the visual inputto the pons and cerebellum. In Neff,D. (ed), *Contributions to Sensory Physiology.* pp. 103-135.

Glover,S. (2002) Visual illusions affect planning but not control. *Trends in Cognitive Sciences*, **6**, 288-292.

Glover,S. & Dixon,P. (2002) Dynamic effects of the Ebbinghaus illusion in grasping: Support for a planning/control model of action. *Perception & Psychophysics*, **64**, 266-278.

Glover,S. (2004) Separate visual representations in the planning and control of action. *Behavioral and Brain Sciences*, **27**, 3-24

Glover,S.R. & Dixon,P. (2001) Dynamic illusion effects in a reaching task: Evidence for separate visual representations in the planning and control of reaching. *Journal of Experimental Psychology-Human Perception and Performance*, **27**, 560-572.

Goebel,R., Khorram-Sefat,D., Muckli,L., Hacker,H. & Singer,W. (1998) The constructive nature of vision: direct evidence from functional magnetic resonance imaging studies of apparent motion and motion imagery. *The European Journal of Neuroscience*, **10**, 1563-1573.

Gold,J.I. & Mazurek,M.E. (2002) Posterior parietal cortex: not just where, but how. *Nature Neuroscience*, **5**, 506-508.

Goldberg,M.E. & Seagraves,M.A. (1987) Visuospatial and motor attention in the monkey. *Neuropsychologia* **25**, 107-118.

Goodale,M.A., Milner,A.D., Jakobson,L.S. & Carey,D.P. (1990) Kinematic analysis of limb movements in neuropsychological research – subtle deficits and recovery of function. *Canadian Journal of Psychology-Revue Canadienne de Psychologie*, **44**, 180-195.

Goodale,M.A. & Milner,A.D. (1992) Separate visual pathways for perception and action. *Trends in Neurosciences*, **15**, 20-25.

Goodale,M.A. & Haffenden,A. (1998) Frames of reference for perception and action in the human visual system. *Neuroscience and Biobehavioral Reviews*, **22**, 161-172.

Goodale,M.A. & Westwood,D.A. (2004) An evolving view of duplex vision: separate but interacting cortical pathways for perception and action 2. *Current Opinion in Neurobiology*, **14**, 203-211.

Goodale,M.A. & Milner,A.D. (2004) Plans for action. *Behavioral and Brain Sciences*, **27**, 37.

Gordon,A.M., Forssberg,H., Johansson,R.S. & Westling,G. (1991) Visual sizes cues in the programming of manipulative forces during precision grip. *Experimental Brain Research*, **83**, 477-482.

Goswami,U. (2000) *Cognition in children*. Psychology Press, Hove

Grafton,S.T., Arbib,M.A., Fadiga,L. & Rizzolatti,G. (1996) Localization of grasp representations in humans by positron emission tomography .2. Observation compared with imagination. *Experimental Brain Research*, **112**, 103-111.

Grafton,S.T., Fagg,A.H. & Arbib,M.A. (1998) Dorsal premotor cortex and conditional movement selection: A PET functional mapping study. *Journal of Neurophysiology*, **79**, 1092-1097.

Graimann,B., Huggins,J.E., Levine,S.P. & Pfurtscheller,G. (2002) Visualization of significant ERD/ERS patterns in multichannel EEG and ECoG data. *Clinical Neurophysiology*, **113**, 43-47.

Grea,H., Pisella,L., Rossetti,Y., Desmurget,M., Tilikete,C., Grafton,S., Prablanc,C. & Vighetto,A. (2002) A lesion of the posterior parietal cortex disrupts on-line adjustments during aiming movements. *Neuropsychologia*, **40**, 2471-2480.

Grezes,J. & Decety,J. (2002) Does visual perception of object afford action? Evidence from a neuroimaging study. *Neuropsychologia*, **40**, 212-222.

Grezes,J., Armony,J.L., Rowe,J. & Passingham,R.E. (2003a) Activations related to "mirror" and "canonical" neurones in the human brain: an fMRI study. *NeuroImage*, **18**, 928-937.

Grezes,J., Tucker,M., Armony,J., Ellis,R. & Passingham,R.E. (2003b) Objects automatically potentiate action: an fMRI study of implicit processing. *European Journal of Neuroscience*, **17**, 2735-2740.

Grill-Spector,K., Kourtzi,Z. & Kanwisher,N. (2001) The lateral occipital complex and its role in object recognition. *Vision Research*, **41**, 1409-1422.

Gross,J., Kujala,J., Hamalainen,M., Timmermann,L., Schnitzler,A. & Salmelin,R. (2001) Dynamic imaging of coherent sources: Studying neural interactions in the human brain. *Proceedings of the National Academy of Sciences of the United States of America*, **98**, 694-699.

Grossberg,S. (2001) Linking the laminar circuits of visual cortex to visual perception: Development, grouping, and attention. *Neuroscience and Biobehavioral Reviews*, **25**, 513-526.

Grossman,A. & Morlet,J. (1984) Decompositions of hardy functions into square intergrable wavelets. *Siam Journal of Mathematics*, **15**, 723-726.

Guieu,J.D., Bourriez,J.L., Derambure,P., Defebvre,L. & Cassim,F. (1999) Temporal and Spatial Aspects of Event-related Desynchronization and Movement-related Cortical Potentials. In Pfurtscheller,G. & Lopes da Silva,F.H. (eds), *Handbook of Electroencephalography and Clinical Neurophysiology*. Elsevier Science, Amsterdam, pp. 279-290.

Gulyas,B., Ottoson,D. & Roland,P.E. (1993) *Functional Organisation of the Human Visual Cortex* Pergamon Press, Oxford.

Haffenden,A.M. & Goodale,M.A. (1998) The effect of pictorial illusion on prehension and perception. *Journal of Cognitive Neuroscience*, **10**, 122-136.

Haig,A.R., Gordon,E., Wright,J.J., Meares,R.A. & Bahramali,H. (2000) Synchronous cortical gamma-band activity in task-relevant cognition. *Neuroreport*, **11**, 669-675.

Hamalainenen,M., Hari,R., Ilmoniemi,R.J., Knuutila,J. & Lounasmaa,O., V (1993) Magnetoencephalography - theory, instrumentation, and applications to noninvasive studies of the working human brain. *Reviews of Modern Physics*, **65**, 413-497.

Hammers,A., Koepp,M., Free,S., Brett,M., Richardson,M., Labbe,C., Cunningham,V., Brooks,D. & Duncan,J. (2002) Implementation and application of a brain template for multiple volumes of interest. *Human Brain Mapping*, **15**, 165-174.

Handlovsky,I., Hansen,S., Lee,T.D. & Elliott,D. (2004) The Ebbinghaus illusion affects on-line movement control. *Neuroscience Letters*, **366**, 308-311.

Handy,T.C., Grafton,S.T., Shroff,N.M., Ketay,S. & Gazzaniga,M.S. (2003) Graspable objects grab attention when the potential for action is recognized. *Nature Neuroscience*, **6**, 421-427.

Hari,R., Joutsiniemi,S.L. & Sarvas,J. (1988) Spatial-resolution of neuromagnetic records - theoretical calculations in a sherical model. *Electroencephalography and Clinical Neurophysiology*, **71**, 64-72.

Hari,R., Forss,N., Avikainen,S., Kirveskari,E., Salenius,S. & Rizzolatti,G. (1998) Activation of human primary motor cortex during action observation: A neuromagnetic study. *Proceedings of the National Academy of Sciences of the United States of America*, **95**, 15061-15065.

Hari,R., Levanen,S. & Raij,T. (2000) Timing of human cortical functions during cognition: role of MEG. *Trends in Cognitive Sciences*, **4**, 455-462.

Harmony,T., Fernandez,T., Reyes,A., Silva,J., Rodriguez,M., Marosi,E. & Bernal,J. (1994) Delta-activity – a sign of internal concentration during the performance of mental tasks. *International Journal of Psychophysiology*, **18**, 113.

Harmony,T., Fernandez,T., Reyes,A., Silva,J., Bernal,J., DiazComas,L., Reyes,A., Marosi,E., Rodriguez,M. & Rodriguez,M. (1996) EEG delta activity: An indicator of attention to internal processing during performance of mental tasks. *International Journal of Psychophysiology*, **24**, 161-171.

Harvey,M., Milner,A.D. & Roberts,R.C. (1994) Spatial bias in visually-guided reaching and bisection following right cerebral stroke. *Cortex*, **30**, 343-350.

Haxby,J.V., Horwitz,B., Ungerleider,L.G., Maaisog,J.M., Peitrini,P. & Grady,C.L. (1994) The functional organisation of human exstrastriate cortex: A PET-rCBF study of selective attention to faces and locations. *Journal of Neuroscience*, **14**, 6336-6353.

Hedge,A. & Marsh,N.W.A. (1975) The effect of irrelevant spatial correspondences on two-choice response-time. *Acta Psychologica*, **39**, 427-439.

Helmes,E. & Ostbye,T. (2002) Beyond memory impairment - Cognitive changes in Alzheimer's disease. *Archives of Clinical Neuropsychology*, **17**, 179-193.

Hermsdorfer,J., Hagl,E. & Nowak,D.A. (2004) Deficits of anticipatory grip force control after damage to peripheral and central sensorimotor systems. *Human Movement Science*, **23**, 643-662.

Hillebrand,A. & Barnes,G.R. (2002) A quantitative assessment of the sensitivity of whole-head MEG to activity in the adult human cortex. *NeuroImage*, **16**, 638-650.

Hillebrand,A. & Barnes,G.R. (2003) The use of anatomical constraints with MEG beamformers. *NeuroImage*, **20**, 2302-2313.

Hillebrand, A., Singh, K. D., Holliday, I. E., Furlong, P. L., and Barnes, G. R. (2005) A new approach to neuroimaging with magnetoencephalography. *NeuroImage*. **25**, 199-211.

Holliday,I.E., Anderson,S.J. & Harding,G.F.A. (1997) Magnetoencephalographic evidence for non-geniculostriate visual input to human cortical area V5. *Neuropsychologia*, **35**, 1139-1146.

Holmes, A. P. and Friston, K. J. (1998) Generalisability, Random Effects and Poulation Inference. NeuroImage 7, S754. 1998.

Holmes,B. (1998) Irresistible illusions. *New Scientist*, **159**, 32-37.

Hommel,B. (2002) Responding to object files: Automatic integration of spatial information revealed by stimulus-response compatibility effects. *Quarterly Journal of Experimental Psychology Section A-Human Experimental Psychology*, **55**, 567-580.

Horne,M.K. & Butler,E.G. (1995) The role of the Cerebello-thalamo-cortical pathway in Skilled Movement. *Progress in Neurobiology*, **46**, 199-213.

Huang,M., Aine,C.J., Supek,S., Best,E., Ranken,D. & Flynn,E.R. (1998) Multi-start downhill simplex method for spatio-temporal source localization in magnetoencephalography. *Electroencephalography and Clinical Neurophysiology/Evoked Potentials Section*, **108**, 32-44.

Hubel,D. & Wiesel,T.N. (1962) Receptive fields, binocular interaction and functional architecture in the cat's visual cortex. *Journal of Physiology-London*, **160**, 106-154.

Humphreys,G. (2001) Objects, affordances ... action! *Psychologist*, **14**, 408-412.

Humphreys,G.W. & Forde,E.M.E. (1998) Disordered action schema and action disorganisation syndrome. *Cognitive Neuropsychology*, **15**, 771-811.

Humphreys,G.W., Forde,E.M.E. & Francis,D. (2000) The organisation of Sequential Actions. In Monsell,S. & Driver,J. (eds), *Attention & Performance XVIII*. MIT Press, Cambridge.

Ingram,H.A., van Donkelaar,P., Cole,J., Vercher,J.L., Gauthier,G.M. & Miall,R.C. (2000) The role of proprioception and attention in a visuomotor adaptation task. *Experimental Brain Research*, **132**, 114-126.

Inoue,K., Kawashima,R., Sugiura,M., Ogawa,A., Schormann,T., Zilles,K. & Fukuda,H. (2001) Activation in the ipsilateral posterior parietal cortex during tool use: A PET study. *NeuroImage*, **14**, 1469-1475.

Jackson,G.M., Jackson,S.R., Husain,M., Harvey,M., Kramer,T. & Dow,L. (2000) The coordination of bimanual prehension movements in a centrally deafferented patient. *Brain*, **123**, 380-393.

Jackson,G.M., Jackson,S.R., Newport,R. & Harvey,M. (2002) Co-ordination of bimanual movements in a centrally deafferented patient executing open loop reach-to-grasp movements. *Acta Psychologica*, **110**, 231-246.

Jackson,S.R., Newport,R. & Shaw,A. (2002) Monocular vision leads to a dissociation between grip force and grip aperture scaling during reach-to-grasp movements. *Current Biology*, **12**, 237-240.

Jakobson,L.S., Archibald,Y.M., Carey,D.P. & Goodale,M.A. (1991) A kinematic analysis of reaching and grasping movements in a patient recovering from optic ataxia. *Neuropsychologia*, **29**, 803-809.

Jakobson,L.S. & Goodale,M.A. (1991) Factors affecting higher-order movement planning - a kinematic analysis of human prehension. *Experimental Brain Research*, **86**, 199-208.

James,W. (1890) *The Principles of Psychology*. Holt: New York

Jeannerod,M. (1986) Models for the programming of goal-directed movements (or how to get things less complex). *Archives Internationales de Physiologie de Biochimie et de Biophysique*, **94**, C63-C76.

Jeannerod,M. (1988) *The neural and behavioural organization of goal-directed movements* Clarendon, Oxford.

Jeannerod,M., Arbib,M.A., Rizzolatti,G. & Sakata,H. (1995) Grasping objects - the cortical mechanisms of visuomotor transformation. *Trends in Neurosciences*, **18**, 314-320.

Jeannerod,M., Decety,J. & Michael,F. (1994) Impairment of grasping movements following bilateral posterior parietal lesion. *Neuropsychologia*, 369-380.

Jensen,O., Gelfand,J., Kounios,J. & Lisman,J.E. (2002) Oscillations in the alpha band (9-12 Hz) increase with memory load during retention in a short-term memory task. *Cerebral Cortex*, **12**, 877-882.

Johnson-Frey,S.H. (2004) The organization of action representations in posterior parietal cortex. *Behavioral and Brain Sciences*, **27**, 40.

Johnson,H., van Beers,R.J. & Haggard,P. (2002) Action and awareness in pointing tasks. *Experimental Brain Research*, **146**, 451-459.

Joseph,J.E. (2001) Functional neuroimaging stuides of category specificity in object recognition: a critical review and meta-analysis. *Cognitive Behavioural Neuroscience*, **1**, 119-136.

Josephson,B. (1962) Possible New Effects in Superconducting Tunneling. *Physica C-Superconductivity and Its Applications*, **1**, 251-253.

Jueptner,M. & Weiller,C. (1998) A review of differences between basal ganglia and cerebellar control of movements as revealed by functional imaging studies. *Brain*, **121**, 1437-1449.

Kable,J.W., Lease-Spellmeyer,J. & Chatterjee,A. (2002) Neural substrates of action event knowledge. *Journal of Cognitive Neuroscience*, **14**, 795-805.

Kalaska,J.F., Scott,S.H., Cisek,P. & Sergio,L.E. (1997) Cortical control of reaching movements. *Current Opinion in Neurobiology*, **7**, 849-859.

Kanwisher,N. & Wojciulik,E. (2000) Visual attention: Insights from brain imaging. *Nature Reviews Neuroscience*, **1**, 91-100.

Kawato,M. & Gomi,H. (1992) A Computation Model of 4 regions of the cerebellum based on feedback-error learning. *Biological Cybernetics*, **68**, 95-103.

Kawato,M. & Gomi,H. (1992) The cerebellum and/or learning-models. *Trends in Neurosciences*, **15**, 445-453.

Kellenbach,M.L., Brett,M. & Patterson,K. (2003) Actions speak louder than functions: The importance of manipulability and action in tool representation. *Journal of Cognitive Neuroscience*, **15**, 30-46.

Kerzel,D., Hommel,B. & Bekkering,H. (2001) A Simon effect induced by induced motion and location: Evidence for a direct linkage of cognitive and motor maps. *Perception & Psychophysics*, **63**, 862-874.

Klatzky,R.L., Fikes,T.G. & Pellegrino,J.W. (1995) Planning for hand shape and arm transport when reaching for objects. *Acta Psychologica*, **88**, 209-232.

Klimesch,W., Schimke,H. & Schwaiger,J. (1994) Episodic and semantic memory: an analysis in the EEG theta and alpha band. *Electroencephalography and Clinical Neurophysiology*, **91**, 428-441.

Klimesch,W. (1996) Memory processes, brain oscillations and EEG synchronization. *International Journal of Psychophysiology*, **24**, 61-100.

Kolb,B. (1995) *Fundamentals of human neuropsychology* W.H.Freeman, London.

Kornblum,S., Hasbroucq,T. & Osman,A. (1990) Dimensional Overlap: Cognitive Basis for Stimulus-Response Compatibility--A Model and Taxonomy*1, *2. *Psychological Review*, **97**, 253-270.

Koshino,Y. & Niedermeyer,E. (1975) Enhancement of Rolandic mu-rhythm by pattern vision. *Electroencephalography and Clinical Neurophysiology*, **38**, 535-538.

Kozinska,D., Tretiak,O.J., Nissanov,J. & Ozturk,C. (1997) Multidimensional Alignment Using the Euclidean Distance Transform*1. *Graphical Models and Image Processing*, **59**, 373-387.

Krause,C.M., Lang,A.H., Laine,M., Kuusisto,M. & Porn,B. (1996) Event-related EEG desynchronization and synchronization during an auditory memory task. *Electroencephalography and Clinical Neurophysiology*, **98**, 319-326.

Kunde,W., Hoffmann,J. & Zellmann,P. (2002) The impact of anticipated action effects on action planning. *Acta Psychologica*, **109**, 137-155.

Laforce,R. & Doyon,J. (2001) Distinct contribution of the striatum and cerebellum to motor learning. *Brain and Cognition*, **45**, 189-211.

Lal,S.K.L. & Craig,A. (2001) Electroencephalography activity associated with driver fatigue: Implications for a fatigue countermeasure device. *Journal of Psychophysiology*, **15**, 183-189.

Lancaster,J., Kochunov,P., Woldorff,M., Liotti,M., Parsons,L., Rainey,L., Nickerson,D. & Fox,P. (2000) Automatic talairach labels for functional activation sites. *NeuroImage*, **11**, S483.

Lavie,N. (1995) Perceptual load as a necessary condition for selective attention. *Journal of Experimental Psychology: Human Perception & Performance*, **21**, 451-468.

Lee,J.H. & van Donkelaar,P. (2002) Dorsal and ventral visual stream contributions to perception- action interactions during pointing. *Experimental Brain Research*, **143**, 440-446.

Lee,T.S. (2003) Computations in the early visual cortex. *Journal of Physiology-Paris*, **97**, 121-139.

Lehtela,L., Salmelin,R. & Hari,R. (1997) Evidence for reactive magnetic 10-Hz rhythm in the human auditory cortex. *Neuroscience Letters*, **222**, 111-114.

Leocani,L., Magnani,G. & Comi,G. (1999) Event-related desynchronization during execution, imagination and witholding of movement. In Pfurtscheller,G. & Lopes da Silva,F.H. (eds), *Handbook of electroencephalography and Clinical Neurophysiology.* Elsevier Science, Amsterdam, pp. 291-301.

Leslie,A.M., Xu,F., Tremoulet,P.D. & Scholl,B. (1998) Indexing and the object concept: developing 'what' and 'where' systems. *Trends in Cognitive Sciences*, **2**, 10-18.

Lewine,J.D. & Orrison,W.W. (1995) Magnetoencephalography and Magnetic Source Imaging. In Orrison,W.W., Lewine,J.D., Sanders,J.A. & Hartshorne,M.F. (eds), *Functional brain imaging*. Mosby, St Louis, USA, pp. 369-418.

Lhermite,F. (1983) Utilisation behaviour and its relationship to lesions of the frontal lobe. *Brain*, **106**, 237-255.

Linnell,K.J., Humphreys,G.W., McIntyre., Laitinene,S. & Wing,A. (2005) Action modulates object-based selection. *Visual Research*, **17**, 2268-2286

Livinstone,M. & Hubel,D. (1988) Segregation of form, color, movement and depth - anatomy, physiology and perception. *Science*, **240**, 740-749.

Livinstone,M.S. & Hubel,D.H. (1987) Psychophysical evidence for separate channels for the perception of form, colour, movement and depth. *Journal of Neuroscience*, **7**, 3416-3468.

Lopes da Silva,F. (1991) Neural mechanisms underlying brain waves: from neural membranes to networks. *Electroencephalography and Clinical Neurophysiology*, **79**, 81-93.

Lutkenhoner,B. (1996) Current Dipoloe Localisation with an Ideal Magnetometer. *IEEE T.Biomed.Eng.*, 1049-1061.

Lutkenhoner,B. (1998) Dipole source localization by means of maximum likelihood estimation I. Theory and simulations. *Electroencephalography and Clinical Neurophysiology*, **106**, 314-321.

Lutkenhoner,B. (1998) Dipole source localization by means of maximum likelihood estimation. II. Experimental evaluation. *Electroencephalography and Clinical Neurophysiology*, **106**, 322-329.

MacKay,W.A. & Mendonca,A.J. (1995) Field potential oscillatory bursts in parietal cortex before and during reach. *Brain Research*, **704**, 167-174.

Makieg,S., Debener,S., Onton,J. & Delorme,A (2004) Mining event-related brain dynamics. *Trends in Cognitive Sciences*, **8**, 204-210

Malach,R., Reppas,J.B., Benson,R.R., Kwong,K.K., Jiang,H., Kennedy,W.A., Ledden,P.J., Brady,T.J., Rosen,B.R. & Tootell,R.B.H. (1995) Object-related activity revealed by functional magnetic resonance imaging in human occipital cortex. *Proceedings of the National Academy of Sciences of the United States of America*, **92**, 8135-8139.

Maratos,F.A., Anderson,S.J. & Barnes,G.R. (2002) Activation of the human motor cortex by visual stimuli: a magnetoencephalographic (MEG) study. *EBBS Conference Proceeding*

Maratos,F.A., Anderson,S.J. & Barnes,G.R. (2003) Do visual images elicit sensori-motor responses? - A magneto-encephalographic (MEG) investigation. *Journal of Psychophysiology*, **17**, 108.

Maratos,F.A. & Anderson,S.J. (2004) The effects of visual attention and object affordance on the on-line control of arm movements. *Journal of Vision*, **4**, 445a

Maratos,F.A., Anderson,S.J., Hillebrand,A.H., Singh,K. & Barnes,G. (2004) Magnetoencephalographic (MEG) investigation on the relationship between visual attention, affordance and action *CNS Conference Proceeding*

Marotta,J.J., McKeeff,T.J. & Behrmann,M. (2003) Hemispatial neglect: its effects on visual perception and visually guided grasping. *Neuropsychologia*, **41**, 1262-1271.

Martin,A., Wiggs,C.L., Ungerleider,L.G. & Haxby,J.V. (1996) Neural correlates of category-specific knowledge. *Nature*, **379**, 649-652.

Martinez,A., DiRusso,F., Anllo-Vento,L., Sereno,M.I., Buxton,R.B. & Hillyard,S.A. (2001) Putting spatial attention on the map: timing and localization of stimulus selection processes in striate and extrastriate visual areas. *Vision Research*, **41**, 1437-1457.

Mattingly,J. & Driver,J. (1997) Distinguishing sensory and motor deficits after parietal damage; an evaluation of response selection biases in unilateral neglect. In Karnath & T.P (eds), *Parietal Contributions to Orientation in £D Space*. Springer, Heidelberg, pp. 309-338.

Maunsell,J.H.R., Nealey,T.A. & Depriest,D.D. (1990) Magnocellular and parvocellular contributions to responses in the middle temporal visual area (MT) of the macaque monkey. *Journal of Neuroscience*, **10**, 3323-3334.

McCombe Waller,S. & Whitall,J. (2004) Fine motor control in adults with and without chronic hemiparesis: baseline comparison to nondisabled adults and effects of bilateral arm training 1 , *1. *Archives of Physical Medicine and Rehabilitation*, **85**, 1076-1083.

McSorley,E., Haggard,P. & Walker,R. (2004) Distractor modulation of saccade trajectories: spatial separation and symmetry effects. *Experimental Brain Research*, **155**, 320-333.

Messier,J., Adamovich,S., Berkinblit,M., Tunik,E. & Poizner,H. (2003) Influence of movement speed on accuracy and coordination of reaching movements to memorized targets in three-dimensional space in a deafferented subject. *Experimental Brain Research*, **150**, 399-416.

Miall,R.C., Weir,D.J. & Stein,J.F. (1987) Visuo-motor tracking during reversible inactivation of the cerebellum. *Experimental Brain Research*, **65**, 455-464.

Miall,R.C. & Reckess,G.Z. (2002) The cerebellum and the timing of coordinated eye and hand tracking. *Brain and Cognition*, **48**, 212-226.

Michaels,C.F. & Carrelo,C. (1981) *Direct Perception* Prentice-Hall, New Jersey.

Michaels,C.F. (1988) S-R Compatibility Between Response Position and Destination of Apparent Motion: Evidence of the Detection of Affordances. *Journal of Experimental Psychology: Human Perception and Performance*, **14**, 231-240.

Milner,D.A., Perrett,D.I., Johnston,R.S., Benson,P.J., Jordan,T.R. & Heeley,D.W. (1991) Perception and Action in 'Visual Form Agnosia'. *Brain*, **114**, 405-428.

Milner,D.A. & Goodale,M.A. (1995) *The Visual Brain in Action* Oxford University Press, Oxford.

Milner,D.A. (1998) Neuropsychological studies of perception and visuomotor control. *Philosophical Transactions of the Royal Society of London Series B-Biological Sciences*, **353**, 1375-1384.

Mishkin,M., Ungerleider,L.G. & Macko,K.A. (1983) Object vision and spatial vision: two cortical pathways. *Trends in Neurosciences*, **6**, 414-417.

Mountcastle,V.B. (1998) *Perceptual Neuroscience: The Cerebral Cortex* Harvard University Press, London.

Muller,H.J. & Rabbitt,P.M.A. (1989) Reflexive and Voluntary Orienting of Visual Attention: Time Course of Activation and Resistance to Interruption (1). *Journal of Experimental Psychology: Human Perception and Performance*, **15**, 315-330.

Muller,V., Lutzenberger,W., Preissl,H., Pulvermuller,F. & Birbaumer,N. (2003) Complexity of visual stimuli and non-linear EEG dynamics in humans. *Cognitive Brain Research*, **16**, 104-110.

Muthukumaraswamy,S.D., Johnson,B.W. & McNair,N.A. (2004) Mu rhythm modulation during observation of an object-directed grasp. *Cognitive Brain Research*, **19**, 195-201.

Muzur,A. (2005) Toward an integrative theory of sleep and dreaming. *Journal of Theoretical Biology*, **233**, 103-118.

Nair,D.G., Purcott,K.L., Fuchs,A., Steinberg,F. & Kelso,J.A.S. (2003) Cortical and cerebellar activity of the human brain during imagined and executed unimanual and bimanual action sequences: a functional MRI study. *Cognitive Brain Research*, **15**, 250-260.

Nealey,T.A. & Maunsell,J.H.R. (1994) Magnocellular and parvocellular contributions to responses of neurons in macaque striate cortex. *Journal of Neuroscience*, 14, 2069-2079.

Neuper,C. & Pfurtscheller,G. (1999) Motor Imagery and ERD. In Pfurtscheller,G. & Lopes da Silva,F.H. (eds), *Handbook of Electroencephalography and Clinical Neurophysiology*. Elsevier Science, Amsterdam, pp. 303-325.

Nichols,T.E. & Holmes,A.P. (2002) Nonparametric permutation tests for functional neuroimaging: A primer with examples. *Human Brain Mapping*, **15**, 1-25.

232

Nicoletti,R., Anzola,G.P., Luppino,G., Rizzolatti,G. & Umilta,C. (1982) Spatial compatibility effects on the same side of the body midline. *Journal of Experimental Psychology-Human Perception and Performance*, **8**, 664-673.

Niebur,E., Hsiao,S.S. & Johnson,K. (2002) Synchrony: a neuronal mechanism for attentional selection? *Current Opinion in Neurobiology*, **12**, 190-194.

Niedermeyer,E. (1993) *Electroencephalography, basic principles, clinical applications and related fields* Williams & Williams, London.

Nijhof,E.J. (2003) On-line trajectory modifications of planar, goal-directed arm movements. *Human Movement Science*, **22**, 13-36.

Nobili,L., Baglietto,M.G., Beelke,M., De Carli,F., De Negri,E., Gaggero,R., Rosadini,G., Veneselli,E. & Ferrillo,F. (2001) Distribution of epileptiform discharges during nREM sleep in the CSWSS syndrome: relationship with sigma and delta activities. *Epilepsy Research*, **44**, 119-128.

Noe,A. (2002) Special issue: 'Is the visual world a grand illusion?' - Editor's preface. *Journal of Consciousness Studies*, **9**, 1-12.

Nougier,V., Rossi,B., Bard,C., Fleury,M., Teasdale,N., Cole,J. & Lamarre,Y. (1994) Orienting attention in deafferented patients. *Neuropsychologia*, **32**, 1079-1088.

Nunez,P.L. (1995) *Neocortical Dynamics and Human EEG Rhythms* Oxford University Press, Oxford.

Ohyama,T., Nores,W.L., Murphy,M. & Mauk,M.D. (2003) What the cerebellum computes. *Trends in Neurosciences*, **26**, 222-227.

Okada,Y. (1982) Neurogenisis of Evoked Magnetic Fields. In Williamson,S.J., Romani,G.L., Kaufman,L. & Modena,I. (eds), *Biomagnetism: An Interdisciplinary Approach*. Planum Press, New York, pp. 399-408.

Orrison,W.W., Lewine,J.D., Sanders,J.A. & Hartshorne,M.F. (1995) *Functional Brain Imaging* Mosby, New York.

Palluel-Germain,R., Boy,F., Orliaguet,J.P. & Coello,Y. (2004) Visual and motor constraints on trajectory planning in pointing movements. *Neuroscience Letters*, **372**, 235-239.

Papanicolaou,A.C. (1995) An introduction to magnetoencephalography with some applications. *Brain and Cognition*, **27**, 331-352.

Parakh,R., Roy,E., Koo,E. & Black,S. (2004) Pantomime and imitation of limb gestures in relation to the severity of Alzheimer's disease. *Brain and Cognition*, **55**, 272-274.

Pavani,F., Boscagli,I., Benvenuti,F., Rabuffetti,M. & Farne,A. (1999) Are perception and action affected differently by the Titchener circles illusion? *Experimental Brain Research*, **127**, 95-101.

Pavese,A. & Buxbaum,L.J. (2002) Action matters: The role of action plans and object affordances in selection for action. *Visual Cognition*, **9**, 559-590.

Perenin,M.T. & Vighetto,A. (1988) Optic ataxia: a specific disruption in visuomotor mechanisms. I. Different aspects of the deficit in reaching for objects. *Brain*, **111**, 643-674.

Perrett,D.I., Mistlin,A.J. & Chitty,A.J. (1987) Visual neurones responsive to faces. *Trends in Neurosciences*, **10**, 358-364.

Pfurtscheller,G. & Neuper,C. (1992) Simultaneous EEG 10-Hz desynchronization and 40-Hz synchronization during finger movement. *Neuroreport*, **3**, 1057-1060.

Pfurtscheller,G. & Neuper,C. (1997) Motor imagery activates primary sensorimotor area in humans. *Neuroscience Letters*, **239**, 65-68.

Pfurtscheller,G. & Lopes da Silva,F.H. (1999a) Event-related EEG/MEG synchronization and desynchronization: basic principles. *Clinical Neurophysiology*, **110**, 1842-1857.

Pfurtscheller,G. & Lopes da Silva,F.H. (1999b) Functional meaning of event-related desynchronization (ERD) and synchronization (ERS). In Pfurtscheller,G. & Lopes da Silva,F.H. (eds), *Event_Related*

Desynchronisation: Handbook of Electroencephalography and Clinical Neurophysiology. Elsevier Science, Amsterdam, pp. 51-65.

Pfurtscheller,G., Pichler-Zalaudek,K. & Neuper,C. (1999) ERD and ERS in voluntary movement of different limbs. In Pfurtscheller,G. & Lopes da Silva,F.H. (eds), *Event_Related Desynchronisation: Handbook of Electroencephalography and Clinical Neurophysiology.* Elsevier Science, Amsterdam, pp. 245-267.

Pfurtscheller,G., Neuper,C. & Krausz,G. (2000) Functional dissociation of lower and-upper frequency mu rhythms in relation to voluntary limb movement. *Clinical Neurophysiology,* **111,** 1873-1879.

Pfurtscheller,G. (2001) Functional brain imaging based on ERD/ERS. *Vision Research,* **41,** 1257-1260.

Pfurtscheller,G., Graimann,B., Huggins,J.E., Levine,S.P. & Schuh,L.A. (2003) Spatiotemporal patterns of beta desynchronization and gamma synchronization in corticographic data during self-paced movement. *Clinical Neurophysiology,* **114,** 1226-1236.

Phillips,J.C. & Ward,R. (2002) S-R correspondence effects of irrelevant visual affordance: Time course and specificity of response activation. *Visual Cognition,* **9,** 540-558.

Phillips,J.G., Triggs,T.J. & Meehan,J.W. (2004) Planning and control of action as solutions to an independence of visual mechanisms. *Behavioral and Brain Sciences,* **27,** 46.
Pins,D., Meyer,M.E., Foucher,J., Humphreys,G. & Boucart,M. (2004) Neural correlates of implicit object identification. *Neuropsychologia,* **42,** 1247-1259.

Pisella,L., Arzi,M. & Rossetti,Y. (1998) The timing of color and location processing in the motor context. *Experimental Brain Research,* **121,** 270-276.

Pisella,L., Grea,H., Tilikete,C., Vighetto,A., Desmurget,M., Rode,G., Boisson,D. & Rossetti,Y. (2000) An 'automatic pilot' for the hand in human posterior parietal cortex: toward reinterpreting optic ataxia. *Nature Neuroscience,* **3,** 729-736.

Pizzella,V. & Romani,G.L. (1990) Principles of Magnetoencephalography. In Sato,S. (ed), *Advances in Neurology.* Raven Press, New York, pp. 1-10.

Plamondon,R. & Alimi,A.M. (1997) Speed/accuracy trade-offs in target-directed movements. *Behavioral and Brain Sciences,* **20,** 279-302.

Pohl,W. (1973) Dissociation of spatial discrimination deficits following frontal and parietal lesions in monkeys. *Journal of Computational Physiological Psychology,* **82,** 227-239.

Polikar, R. (2001) The engineer's ultimate guide to wavelet analysis: The Wavelet Tutorial. http://users.rowan.edu/~polikar/WAVELETS/WTtutorial.html . Accessed June-December 2004.

Pollok,B., Gross,J., Muller,K., Aschersleben,G. & Schnitzler,A. (*In Press, Corrected Proof*) The cerebral oscillatory network associated with auditorily paced finger movements. *NeuroImage*

Posner,M.I. (1980) Orienting of Attention. *Quarterly Journal of Experimental Psychology.* **32,** 3-25.

Proteau,L. & Masson,G. (1997) Visual perception modifies goal-directed movement control: Supporting evidence from a visual perturbation paradigm. *Quarterly Journal of Experimental Psychology Section A-Human Experimental Psychology,* **50,** 726-741.

Quintana,J. & Fuster,J.M. (1999) From perception to action: Temporal integrative functions of prefrontal and parietal neurons. *Cerebral Cortex,* **9,** 213-221.

Ray,W.J. & Cole,H.W. (1985) EEG activity during cognitive processing: Influence of attentional factors. *International Journal of Psychophysiology,* **3,** 43-48.

Remington,R.W., Folk,C.L. & McLean,J.P. (2001) Contingent attentional capture or delayed allocation of attention? *Perception & Psychophysics,* **63,** 298-307.

Riddoch,M.J., Edwards,M.G., Humphreys,G.W., West,R. & Heafield,T. (1998) Visual affordances direct action: Neuropsychological evidence from manual interference. *Cognitive Neuropsychology,* **15,** 645-683.

Rozzolatti,G., Riggio,L., & Sheliga,B.M. (1994) Space and selective attention. In Umilta,C. & Moscovitch,M. (eds), *Attention and Performance, vol. XV*. MIT Press, Cambridge, pp. 231-265.

Rizzolatti,G., Fogassi,L. & Gallese,V. (2000) Cortical Mechanisms Subserving Object Grasping and Action Recognition: A new View on the Cortical Motor Functions. In Gazzaniga,M.S. (ed), *The new Cognitive Neurosciences*. MIT Press, Cambridge, pp. 539-552.

Rizzolatti,G., Fogassi,L. & Gallese,V. (2002) Motor and cognitive functions of the ventral premotor cortex. *Current Opinion in Neurobiology*, 12, 149-154.

Rodriguez,E., George,N., Lachaux,J., Martinerie,J., Renault,B. & Varel,F.J. (1999) Perception's shadow: long-distance synchronization of human brain activity. *Nature*, 397, 430-433

Romani,G.L. & Pizzella,V. (1993) Localization of Brain Activity with Magnetoencephalography. In Sato,S. (ed), *Advances in Neurology*. Raven Press, New York, pp. 67-78.

Rose,D.F. & Ducla-Soares,E. (1990) Comparison of Electroencephalography and Magnetoencephalography. In Sato,S. (ed), *Magnetoencephalography*. Raven Press, New York, pp. 33-37.

Rossetti,Y. (1998) Implicit Short-Lived Motor Representations of Space in Brain Damaged and Healthy Subjects. *Consciousness and Cognition*, 7, 520-558.

Roy,E.A., Black,S.E., Blair,N. & Dimeck,P.T. (1998) Analyses of deficits in gestural pantomime. *Journal of Clinical and Experimental Neuropsychology*, 20, 628-643.

Rumelhart,D.E. & McClelland,J.L. (1986) *Parallel Distributed Processing* MIT Press, Cambridge, Massachusetts.

Rumiati,R.I. & Humphreys,G.W. (1998) Recognition by action: Dissociating visual and semantic routes to action in normal observers. *Journal of Experimental Psychology-Human Perception and Performance*, 24, 631-647.

Rushworth,M.F.S., Krams,M. & Passingham,R.E. (2001) The attentional role of the left parietal cortex: The distinct lateralization and localization of motor attention in the human brain. *Journal of Cognitive Neuroscience*, 13, 698-710.

Saab,C.Y. & Willis,W.D. (2003) The cerebellum: organization, functions and its role in nociception. *Brain Research Reviews*, 42, 85-95.

Sabes,P.N. (2000) The planning and control of reaching movements. *Current Opinion in Neurobiology*, 10, 740-746.

Sakata,H., Taira,M., Kusunoki,M., Murata,A. & Tanaka,Y. (1997) The TINS lecture - The parietal association cortex in depth perception and visual control of hand action. *Trends in Neurosciences*, 20, 350-357.

Sakata,H., Taira,M., Kusunoki,M., Murata,A., Tanaka,Y. & Tsutsui,K. (1998) Neural coding of 3D features of objects for hand action in the parietal cortex of the monkey. *Philosophical Transactions of the Royal Society of London Series B-Biological Sciences*, 353, 1363-1373.

Salenius,S., Kajola,M., Thompson,W.L., Kosslyn,S. & Hari,R. (1995) Reactivity of magnetic parieto-occipital alpha rhythm during visual imagery (1). *Electroencephalography and Clinical Neurophysiology*, 95, 453-462.

Salenius,S. & Hari,R. (2003) Synchronous cortical oscillatory activity during motor action. *Current Opinion in Neurobiology*, 13, 678-684.

Sarvas,J. (1987) Basic mathematical and electromagnetic concepts of the biomagnetic inverse problem. *Physics in Medicine and Biology*, 32, 11-22.

Savoy,R.L. (2001) History and future directions of human brain mapping and functional neuroimaging. *Acta Psychologica*, 107, 9-42.

Scarchilli,K., Vercher,J.L., Gauthier,G.M. & Cole,J. (1999) Does the oculo-manual co-ordination control system use an internal model of the arm dynamics? *Neuroscience Letters*, 265, 139-142.

Schiller,P.H. (1993) Parallel Pathways in the Visual System. In Gulyas,B., Ottoson,D. & Roland,P.E. (eds), *Functional Organisation of the Human Visual Cortex*. Pergamon Press, Oxford, pp. 43-58.

Schneider,G.E. (1969) Two Visual Systems. *Science*, 895-902.

Schubotz,R.I. & von Cramon,D.Y. (2002) Predicting perceptual events activates corresponding motor schemes in lateral premotor cortex: an fMRI study. *NeuroImage*, **15**, 787-796.

Seidler,R.D., Noll,D.C. & Thiers,G. (2004) Feedforward and feedback processes in motor control. *NeuroImage*, **22**, 1775-1783.

Shaw,B. (2002) Source Localization and Beamforming. *Ieee Signal Processing Magazine*, 30-38.

Sheliga,B.M., Craighero,L., Riggio,L. & Rizzolatti,G. (1997) Effects of spatial attention on directional manual and ocular responses. Experimental Brain Research, **114**, 339-351.

Sheth,B.R. & Shimojo,S. (2002) How the lack of visuomotor feedback affects even the early stages of goal-directed pointing movements. *Experimental Brain Research*, **143**, 181-190.

Silva,L.R., Amitai,Y. & Connors,B.W. (1991) Intrinsic oscillations of neocortex generated by layer-5 pyramidal neurons. *Science*, **251**, 432-435.

Simon,J.R. & Rudell,A.P. (1967) Auditory S-R compatibility: The effect of an irrelevant cue on information processing. *Journal of Applied Psychology*, **51**, 300-304.

Simon,J.R. (1969) Reactions towards the source of stimulation. *Journal of Experimental Psychology*, **81**, 174-176.

Simon,J.R., Sly,P.E. & Vilapakkams,S. (1981) Effect of compatibility of s-r mapping of reactions toward the stimulus source. *Acta Psychologica*, **47**, 63-81.

Singer,W. (1993) Synchronization of cortical activity and its putative role in information-processing and learning. *Annual Review of Physiology*, **55**, 349-374.

Singer,W. (1999) Neuronal synchrony: A versatile code for the definition of relations? *Neuron*, **24**, 49-65.

Singh,K.D., Barnes,G.R., Hillebrand,A., Forde,E.M.E. & Williams,A.L. (2002) Task-related changes in cortical synchronization are spatially coincident with the hemodynamic response. *NeuroImage*, **16**, 103-114.

Singh,K.D., Barnes,G.R. & Hillebrand,A. (2003) Group imaging of task-related changes in cortical synchronisation using nonparametric permutation testing. *NeuroImage*, **19** , 1589-1601.

Sinkkonen,J., Tiitinen,H. & Naatanen,R. (1995) Gabor filters - an informative way for analyzing event-related brain activity. *Journal of Neuroscience Methods*, **56**, 99-104.

Smeets,J.B.J. & Brenner,E. (1995) Perception and action are based on the same visual information - Distinction between position and velocity. *Journal of Experimental Psychology-Human Perception and Performance*, **21**, 19-31.

Sokolov,A., Pavlova,M., Lutzenberger,W. & Birbaumer,N. (2004) Reciprocal modulation of neuromagnetic induced gamma activity by attention in the human visual and auditory cortex. *NeuroImage*, **22**, 521-529.

Stein,J.F. & Glickstein,M. (1992) Role of the cerebellum in visual guidance of movement. *Physiological Reviews*, **72**, 967-1017.

Steinmetz,H., Furst,G. & Freund,H.J. (1990) Variation of Perisylvian and Calcarine Anatomic Landmarks within Sterotaxic Proportional Coordinates. *American Journal of Neuroradiology*, **11**, 1123-1130.

Steriade,M., Domich,L. & Oakson,G. (1986) Reticularis thalami neurons revisited - activity during shifts in states of vigilance. *Journal of Neuroscience*, **6**, 68-81.

Steriade,M., Gloor,P., Llinas,R.R., DaSilva,F.H.L. & Mesulam,M.M. (1990) Basic mechanisms of cerebral rhythmic activities. *Electroencephalography and Clinical Neurophysiology*, **76**, 481-508.

Sterman,M.B., Kaiser,D.A. & Veigel,B. (1996) Spectral analysis of event-related EEG responses during short- term memory performance. *Biofeedback and Self-Regulation*, **21**, 367-367.

Stewart,L., Meyer,B.U., Frith,U. & Rothwell,J. (2001) Left posterior BA37 is involved in object recognition: a TMS study. *Neuropsychologia*, **39**, 1-6.

Stippich,C., Ochmann,H. & Sartor,K. (2002) Somatotopic mapping of the human primary sensorimotor cortex during motor imagery and motor execution by functional magnetic resonance imaging. *Neuroscience Letters*, **331**, 50-54.

Stoffer TH. (1991) Attentional focussing and spatial stimulus-response compatibility. *Psychological Research*, **53**, 127-135.

Summerfield,C., Jack,A.I. & Burgess,A.P. (2002) Induced gamma activity is associated with conscious awareness of pattern masked nouns. *International Journal of Psychophysiology*, **44**, 93-100.

Supek,S. & Aine,C.J. (1993) Simulation studies of multiple dipole neuromagnetic source localisation - model order and limits of source resolution. *Ieee Transactions on Biomedical Engineering*, **40**, 529-540.

Svoboda,J., Sovka,P. & Stancak,A. (2002) Intra- and inter-hemispheric coupling of electroencephalographic 8-13 Hz rhythm in humans and force of static finger extension. *Neuroscience Letters*, **334**, 191-195.

Szurhaj,W., Derambure,P., Labyt,E., Cassim,F., Bourriez,J.L., Isnard,J., Guieu,J.D. & Mauguiere,F. (2003) Basic mechanisms of central rhythms reactivity to preparation and execution of a voluntary movement: a stereoelectroencephalographic study. *Clinical Neurophysiology*, **114**, 107-119.

Taira,M., Mine,S., Georgopoulos,A.P., Murata,A. & Sakata,H. (1990) Parietal cortex neurons of the monkey related to the visual guidance of hand movement. *Experimental Brain Research*, **83**, 29-36.

Talariach,J. & Tournoux,P. (1988) *Co-planar stereotaxic atlas of the human brain: an approach to medical cerebral imaging* Thieme Medical Publishers, Stuttgart.

Tallon-Baudry,C., Bertrand,O. & Pernier,J. (1999) A ring-shaped distribution of dipoles as a source model of induced gamma-band activity. *Clinical Neurophysiology*, **110**, 660-665.

Tallon-Baudry,C. & Bertrand,O. (1999) Oscillatory gamma activity in humans and its role in object representation. *Trends in Cognitive Sciences*, **3**, 151-162.

TallonBaudry,C., Bertrand,O., Delpuech,C. & Pernier,J. (1996) Stimulus specificity of phase-locked and non-phase-locked 40 Hz visual responses in human. *Journal of Neuroscience*, **16**, 4240-4249.

TallonBaudry,C., Bertrand,O., Delpuech,C. & Pernier,J. (1997) Oscillatory gamma-band (30-70 Hz) activity induced by a visual search task in humans. *Journal of Neuroscience*, **17**, 722-734.

Taniguchi,M., Kato,A., Fujita,N., Hirata,M., Tanaka,H., Kihara,T., Ninomiya,H., Hirabuki,N., Nakamura,H., Robinson,S.E., Cheyne,D. & Yoshimine,T. (2000) Movement-related desynchronization of the cerebral cortex studied with spatially filtered magnetoencephalography. *NeuroImage*, **12**, 298-306.

Theewues,J., Kramer,A.F., Hahn,S., Irwin,D.E. & Zelinsky,G.j. (1999) Influence of attention capture on oculomotor control. *Journal of Experimental Psychology-Human Perception and Performance*, **25**, 1595-1608.

Tipper,S.P., Lortie,C. & Baylis,G.C. (1992) Selective reaching - evidence for action-centered attention. *Journal of Experimental Psychology-Human Perception and Performance*, **18**, 891-905.

Tipper,S.P., Howard,L.A. & Jackson,S.R. (1997) Selective reaching to grasp: Evidence for distractor interference effects. *Visual Cognition*, **4**, 1-38.

Tipper,S.P., Howard,L.A. & Houghton,G. (1998) Action-based mechanisms of attention. *Philosophical Transactions of the Royal Society of London Series B-Biological Sciences*, **353**, 1385-1393.

Tipper,S.P., Jordan,H. & Weaver,B. (1999) Scene-based and object-centered inhibition of return: Evidence for dual orienting mechanisms. *Perception & Psychophysics*, **61**, 50-60.

Tipper,S.P., Meegan,D. & Howard,L.A. (2002) Action-centred negative priming: Evidence for reactive inhibition. *Visual Cognition*, **9**, 591-614.

Treisman,A. (1996) The binding problem. *Current Opinion in Neurobiology*, **6**, 171-178.

Tresilian,J.R. & Stelmach,G.E. (1997) Common organization for unimanual and bimanual reach-to-grasp tasks. *Experimental Brain Research*, **115**, 283-299.

Tresilian,J.R. (1999) Selective attention in reaching: when is an object not a distractor? *Trends in Cognitive Sciences*, **3**, 407-408.

Tucker,M. & Ellis,R. (1998) On the relations between seen objects and components of potential actions. *Journal of Experimental Psychology-Human Perception and Performance*, **24**, 830-846.

Tucker,M. & Ellis,R. (2004) Action priming by briefly presented objects. *Acta Psychologica*, **116**, 185-203.

Tucker,M. & Ellis,R. (2001) The potentiation of grasp types during visual object catergorisation. *Visual Cognition*, **8**, 769-800.

Ungerleider,L.G. & Mishkin,M. (1982) Two Cortical Visual Systems. In Ingle,D.J., Goodale,M.A. & Milner,D.A. (eds), *Analysis of behaviour*. MIT Press, Cambridge, MA.

Ungerleider,L.G. & Haxby,J.V. (1994) 'What' and 'where' in the human brain. *Current Opinion in Neurobiology*, **4**, 157-165.

Uutela,K., Hamalainen,M. & Somersalo,E. (1999) Visualization of magnetoencephalographic data using minimum current estimates. *NeuroImage*, **10**, 173-180.

van den Broek,S.P., Reinders,F., Donderwinkel,M. & Peters,M.J. (1998) Volume conduction effects in EEG and MEG. *Electroencephalography and Clinical Neurophysiology*, **106**, 522-534.

Van Essen,D.C., Felleman,D.J., DeYoe,E.A. & Knuutila,J. (1993) Probing the Primate Visual Cortex: Pathways and Perspectives. In Gulyas,B., Ottoson,D. & Roland,P.E. (eds), *Functional Organisation of the Human Visual Cortex*. Pergamon Press, Oxford, pp. 29-42.

Van Essen,D.C. & Drury,H.A. (1997) Structural and functional analyses of human cerebral cortex using a surface-based atlas. *Journal of Neuroscience*, **17**, 7079-7102.

Vandonkelaar,P. & Lee,R.G. (1994) Interactions between the eye and the hand motor systems-disruptions due to cerebellar dysfunction. *Journal of Neurophysiology*, **72**, 1674-1685.

Vanni,S., Revonsuo,A. & Hari,R. (1997) Modulation of the parieto-occipital alpha rhythm during object detection. *Journal of Neuroscience*, **17**, 7141-7147.

Vanni,S., Warnking,J., Dojat,M., Delon-Martin,C., Bullier,J. & Segebarth,C. (2004) Sequence of pattern onset responses in the human visual areas: an fMRI constrained VEP source analysis. *NeuroImage*, **21**, 801-817.

VanVeen,B.D., vanDrongelen,W., Yuchtman,M. & Suzuki,A. (1997) Localization of brain electrical activity via linearly constrained minimum variance spatial filtering. *Ieee Transactions on Biomedical Engineering*, **44**, 867-880.

Varela,F., Lachaux,J., Rodriguez,M. & Martinerie,J. (2001) The brainweb: phase synchronisation and large-scale intergration. *Nature Reviews Neuroscience*, **2**, 229-239.

Vecera,S.P., Behrmann,M. & Fliapek,J.C. (2001) Attending to the parts of a single object: Part-based selection limitations. *Perception & Psychophysics*, **63**, 308-321.

Vecera,S.P. (2002) Dissociating 'what' and 'how' in visual form agnosia: a computational investigation. *Neuropsychologia*, **40**, 187-204.

Vercher,J.L. & Gauthier,G.M. (1988) Cerebellar involvement in the coordination control of the oculo-manual tracking system – effects of cerebellar dentate nucleus lesion. *Experimental Brain Research*, **73**, 155-166.

von Stein,A., Chiang,C. & Konig,P. (2000) Top-down processing mediated by interareal synchronization. *Proceedings of the National Academy of Sciences of the United States of America*, **97**, 14748-14753.

Vrba,J. & Robinson,S.E. (2001) Signal processing in magnetoencephalography. *Methods*, **25**, 249-271.

Vrba,J. (2002) Magnetoencephalography: the art of finding a needle in a haystack. *Physica C-Superconductivity and Its Applications*, **368**, 1-9.

Walker,R. (1995) Spatial and object-based neglect. *NeuroCase*, **1**, 371-383.

Wallace,R.J. (1971) Stimulus-response compatibility and the idea of a response code. *Journal of Experimental Psychology*, **88**, 354-360.

Wascher,E., Schatz,U., Kuder,T. & Verleger,R. (2001) Validity and boundary conditions of automatic response activation in the Simon task. *Journal of Experimental Psychology-Human Perception and Performance*, **27**, 731-751.

Weiskrantz,L., Cowey,A. & Hodinott-Hill,I. (1986) Prime-sight in a blindsight subject. *Nature Neuroscience*, **5**, 101-102.

Westwood,D.A. & Goodale,M.A. (2003) Perceptual illusion and the real-time control of action. *Spatial Vision*, **16**, 243-254.

Wikswo,J.P. (1989) *Advances in Biomagnetism* Plenum, New York.

Williamson,S.J. & Kaufman,L. (1981) Biomagnetism. *Journal of Magnetism and Magnetic Materials*, **22**, 129-201.

Wise,S.P., Boussaoud,D., Johnson,P.B. & Caminiti,R. (1997) Premotor and parietal cortex: Corticocortical connectivity and combinatorial computations. *Annual Review of Neuroscience*, **20**, 25-42.

Wolpert,D.M., Ghahramani,Z. & Jordan,M.I. (1994) Perceptual-distortion contributes to the curvature of human reaching movements. *Experimental Brain Research*, **98**, 153-156.

Woods,R.P. (1996) Modeling for Intergroup Comparisons of Imaging Data. *NeuroImage*, **4**, S84-S94.

Wright,C.E. & Chubb,C. (2004) Planning differences for chromaticity- and luminance-defined stimuli: A possible problem for Glover's planning-control model. *Behavioral and Brain Sciences*, **27**, 55

Yamagishi,N., Anderson,S.J. & Ashida,H. (2001) Evidence for dissociation between the perceptual and visuomotor systems in humans. *Proceedings of the Royal Society of London Series B-Biological Sciences*, **268**, 973-977.

Zeki,S. (1973) Colour Coding in Rhesus Monkey Prestriate Cortex. *Brain Research*, **53**, 422-427.

Zeki,S. (1993) *A Vision of the Brain* Blackwell Scientific Publications, London.

Zeki,S. & Bartels,A. (1999) Toward a theory of visual consciousness. *Consciousness and Cognition*, **8**, 225-259.

Zelaznik,H.N., Hawkins,B. & Kisselburgh,L. (1987) The effects of movement distance and movement time on visual feedback processing in aimed hand movements. *Acta Psychologica*, **65**, 181-191.

Appendix I

Mathematical formulae for obtaining significant ERD/ERS through the t percentile bootstrap

Standard ERD/ERS calculation is achieved by bandpass filtering of each trial, squaring of samples and subsequent averaging over trials and sample points. The ERD/ERS is then defined as the proportional power decrease (ERD) or power increase (ERS) in relation to a specific reference interval which is usually placed several seconds before trigger onset. However, to improve the clarity of such maps, only significant patterns should be displayed. The following procedure shows how the bootstrap, specifically the t percentile bootstrap (Davidson and Hinkley, 1997), may be applied to calculate confidence intervals for the ERD/ERS estimates.

Let N be the number of trials, Y_j denotes the set of all y_{ij} of the jth sample and of all tri<als (see Eq. (1) and B is the number of bootstrap resamples. The sample mean and the sample variance of Y_j are denoted by $\bar{y}_j$ and s_j^2, respectively.

For each sample j:

1. Draw N Values from Y_j, where each value is selected at random, with replacement. The N drawn values are the bootstrap resample $\hat{Y}_j$

2. Calculate the mean $\hat{\mu}_j \hat{y}_j$ and the standard deviation of $\hat{\sigma}\hat{y}_j$ all N values in $\hat{Y}_j$.

3. Calculate $\hat{\mu}_j = (\hat{\mu}\hat{y}_j - \mu_j \bar{y}_j)/\hat{\sigma}\hat{y}_j$.

4. Repeat the first three steps to obtain B bootstrap estimates $\hat{\mu}_{j1} ... \hat{\mu}_{jB}$. B should be larger than 500.

5. To approximate the distribution of $\hat{\mu}_j$, sort all estimates so that $\hat{\mu}_{j(1)} \leq ... \leq \hat{\mu}_{j(B)}$.

6. The 100 (1 - α)% confidence interval is determined by $[\bar{y}_j - s_j \hat{\mu}_{j(k2)}, \bar{y}_j - s_j \hat{\mu}_{j(k1)}]$, where $k_1 = B\alpha/2$ and $k_2 = B - k_1 + 1$.

Finally the Values of the confidence intervals have to be considered within the context of the power of the reference interval using Eq. (3). An ERD/ERS value may be considered as significant with 100(1 - α) % confidence when both confidence values of this sample show the same sign.

Appendix II

Experimental instructions & consent form

Overview: In the following experiment you will be required to point to either 1) the far edge of a stimulus, or 2) a circle which may appear coincident with movement onset. Stimulus displayed will be recognisable objects and geometric shapes.

Experimental Procedure: To begin a new trial you will need to use the 'pointer' to press down Button A (situated on the desk). This will trigger an arrow to appear on the monitor in front of you. Please keep the pointer pressed down on this button until a stimulus appears on the monitor. If pre-stimulus, the arrow displayed was pointing in the left direction, then you are required to use the pointer to touch the far left edge of the stimulus, if the arrow was pointing in the right direction, then you are required to touch the far right edge of the stimulus. The aim is to respond quickly but accurately as soon as the stimulus appears on the screen.

On a certain amount of trials however, movement onset toward the stimulus will cause a red circle to appear. On these trials please ignore the above instructions, and quickly and accurately use the pointer to touch the red circle.

Once you have gained experience, and feel confident in performing the task above, you will be required to complete eight blocks of 40 trials. Per block you will be allotted 2.5 minutes to complete the task. If you finish a block of trials before the allotted time, return the 'pointer' to the starting position and await further instructions. Please note that the experiment is designed in such a way that you may find you make errors in your responses, do not worry if you find such errors occur! . [NB: during practice trials, the sudden appearance of a red circle is far greater than in the actual experimental blocks, this is to enable extra practice on such trials!].

Please note that if data collected is used in future work it will be rendered anonymous; and secondly, that if at anytime you feel uncomfortable, you have the right to withdraw both data collected and further participation in the experiment. Thank you

Consent: I the undersigned, have read and understood the above instructions and consent form, and agree fully to participate in the study.

Appendix III

Standard Trial Data

Movement Time

Participant	Standard Movement Time Data					
	(A) Towards Attention	(A) Against Attention	(B) Towards Att / Aff	(B) Against Att / Aff	(C) Towards Attention	(C) Towards Affordance
JL	641.59	683.93	658.63	653.09	680.31	635.75
JC	608.30	602.46	613.03	597.29	587.11	613.94
SfH	672.60	702.82	639.28	685.68	657.70	680.28
PF	661.20	649.47	667.13	617.69	684.51	654
FM	589.57	596.97	592.82	619.44	610.45	591.56
IF	427.35	420.31	431.05	423.70	407.37	424.01
AvH	560.51	551.72	582.38	567.49	579.08	554.50
JW	512.61	532.42	510.95	512.81	518.67	494.39
BW	827.31	882.51	871.98	864.48	830.23	817.18
SJA	502.03	600.53	518.88	553.06	524.48	546.10
AZ	588.42	568.18	551.75	557.03	553.67	577.57
AH	397.44	404.65	398.72	403.98	400.43	391.97
KR	646.30	643.55	653.90	637.30	641.08	640.70
SH	410.85	422.89	416.58	421.33	420.64	408.44
NM	537.34	545.62	536.95	542.13	544.76	545.41
MB	387.21	385.23	395.44	392.50	389.65	384.31
IH	432.89	428.66	430.75	426.61	440.10	429.01
MS	638.57	641.56	625.80	635.30	628.33	619.04
LM	384.15	383.45	379.16	378.64	392.53	385.22
JS	533.04	533.62	535.53	534.43	548.83	536.57

Path Deviations

Participant	Geometric Stimuli (A)		Coherent Object (B)		Incoherent Object (C)	
	Towards Attention	Against Attention	Towards Att / Aff	Against Att / Aff	Towards Attention	Towards Affordance
JL	9	1	2	2	4	2
JC	2	0	2	0	1	2
SfH	0	0	1	3	1	0
PF	4	0	1	0	0	0
FM	0	0	2	1	0	1
IF	11	0	6	1	7	3
AvH	0	2	0	2	0	2
JW	8	1	3	1	0	0
BW	4	1	3	2	3	7
SJA	15	0	4	1	2	2
AZ	2	1	0	1	0	0
AH	1	0	0	0	0	0
KR	6	1	2	1	1	0
SH	5	1	7	1	5	3
NM	8	0	0	4	2	1
MB	9	2	2	4	0	5
IH	3	0	3	4	1	2
MS	2	1	3	1	0	0
LM	6	1	4	5	6	5
JS	6	1	1	3	1	1

Hit Error

Participant	Standard Hit Error Data					
	(A) Towards Attention	(A) Against Attention	(B) Towards Att / Aff	(B) Against Att / Aff	(C) Towards Attention	(C) Towards Affordance
JL	0.271	0.396	2.292	0.278	2.016	2.489
JC	-0.208	-1.473	3.031	0.506	-0.347	2.339
SfH	2.364	0.586	2.607	-0.123	1.913	3.520
PF	3.717	3.797	3.800	2.784	3.080	3.930
FM	1.901	1.415	4.091	1.254	2.104	5.166
IF	5.553	5.835	8.338	7.905	7.093	11.614
AvH	0.057	-0.431	-2.292	-1.861	-1.125	0.276
JW	1.076	0.525	0.583	0.706	2.316	2.904
BW	-1.009	0.586	-2.389	-0.406	-0.595	3.324
SJA	0.300	-0.848	1.297	1.859	0.7323	2.233
AZ	-1.952	-0.846	-2.119	-1.165	-0.563	0.740
AH	1.328	4.358	4.172	1.386	3.493	6.717
KR	0.522	-0.575	-0.1534	0.597	0.153	4.694
SH	1.717	4.1	4.95	5.43	6.69	9.98
NM	0.639	0.401	2.247	-0.054	-0.099	6.429
MB	-0.879	1.404	-0.065	-0.756	0.798	2.681
IH	2.145	2.846	3.717	5.079	4.460	5.511
MS	0.291	-0.631	0.644	0.755	0.306	3.159
LM	3.922	0.552	7.017	3.128	4.857	6.717
JS	-1.944	-0.927	2.364	-1.389	-1.669	2.106

Trial Errors

Participant	Standard Trial Errors					
	(A) Towards Attention	(A) Against Attention	(B) Towards Att / Aff	(B) Against Att / Aff	(C) Towards Attention	(C) Towards Affordance
JL	1	0	0	0	0	0
JC	0	0	0	0	0	0
SfH	1	0	0	0	0	0
PF	0	0	0	0	2	0
FM	0	0	0	0	1	0
IF	4	0	1	1	1	0
AvH	0	1	2	1	0	0
JW	2	0	0	0	0	0
BW	0	0	0	0	0	1
SJA	0	0	0	0	0	0
AZ	0	2	0	0	1	0
AH	1	0	0	0	0	0
KR	0	0	1	0	0	0
SH	9	1	5	2	6	1
NM	0	0	0	0	0	0
MB	3	0	0	0	0	0
IH	0	0	0	0	0	0
MS	0	0	1	0	0	0
LM	0	1	1	0	0	2
JS	0	0	0	1	0	0

Appendix IV

Perturbation Trial Data

• **Incompatible perturbation Trials**

Movement time

Participant	Incompatible Perturbation Movement Data					
	(A) Towards Attention	(A) Against Attention	(B) Towards Att / Aff	(B) Against Att / Aff	(C) Towards Attention	(C) Towards Affordance
JL	877.25	836.80	852.67	737.17	796.00	799.90
JC	849.20	774.00	789.40	782.75	874.17	742.00
SfH	788.40	1003.40	826.20	753.43	851.00	830.50
PF	816.57	861.50	820.57	788.50	822.40	832.67
FM	806.33	744.83	672.00	829.78	862.75	776.75
IF	510.25	554.33	640.75	519.17	668.50	630.20
AvH	708.75	684.67	641.67	758.44	0.00	755.33
JW	724.86	772.50	0.00	798.50	758.00	631.67
BW	858.75	779.40	852.50	915.33	905.83	952.00
SJA	850.00	1012.00	918.83	909.00	999.33	945.25
AZ	734.00	930.00	816.80	817.60	857.40	938.00
AH	642.00	634.00	603.25	681.40	629.00	594.57
KR	764.67	806.00	1070.00	818.29	877.50	844.50
SH	460.22	0.00	481.86	493.00	404.00	445.00
NM	712.00	750.00	766.50	764.20	816.67	761.00
MB	546.17	602.86	587.60	627.75	531.50	585.80
IH	599.33	579.20	600.80	527.33	566.80	714.00
MS	828.00	827.50	833.29	763.20	792.57	834.50
LM	558.00	612.00	509.00	764.00	663.40	622.17
JS	662.00	586.40	811.00	672.18	720.22	707.00

Occurrence of Corrective Manoeuvres

Participant	Pertubation Correction Occurrence	Geometric Stimuli (A)		Coherent Object (B)		Incoherent Object (C)	
		Towards Attention	Against Attention	Towards Att / Aff	Against Att / Aff	Towards Attention	Towards Affordance
JL	Late > 200ms	3	10	2	3	3	9
	Early < 200ms	1	1	1	2	2	1
JC	Late > 200ms	4	3	5	8	6	3
	Early < 200ms	1	0	0	0	0	1
SfH	Late > 200ms	1	3	4	6	5	2
	Early < 200ms	6	3	3	1	1	0
PF	Late > 200ms	5	1	6	2	5	7
	Early < 200ms	3	1	1	2	0	2
FM	Late > 200ms	5	4	2	8	3	7
	Early < 200ms	1	2	2	1	1	1
IF	Late > 200ms	3	3	4	6	4	5
	Early < 200ms	1	0	0	0	0	0
AvH	Late > 200ms	4	3	3	7	0	6
	Early < 200ms	0	0	0	2	0	0
JW	Late > 200ms	6	2	0	2	3	3
	Early < 200ms	1	0	0	0	0	0
BW	Late > 200ms	2	3	2	6	5	2
	Early < 200ms	2	2	2	1	0	1
SJA	Late > 200ms	4	3	6	3	3	4
	Early < 200ms	2	0	0	0	0	0
AZ	Late > 200ms	1	10	6	5	4	2
	Early < 200ms	1	0	0	0	1	0
AH	Late > 200ms	5	3	4	5	4	7
	Early < 200ms	0	0	0	0	0	0
KR	Late > 200ms	3	4	3	5	7	4
	Early < 200ms	1	0	0	2	1	0
SH	Late > 200ms	3	0	5	2	0	0
	Early < 200ms	6	0	2	2	2	1
NM	Late > 200ms	3	6	1	4	3	5
	Early < 200ms	0	0	1	1	0	0
MB	Late > 200ms	6	7	10	8	2	5
	Early < 200ms	0	0	0	0	0	0
IH	Late > 200ms	3	5	5	9	5	2
	Early < 200ms	0	0	0	0	0	0
MS	Late > 200ms	3	2	6	3	6	7
	Early < 200ms	2	0	1	2	1	3
LM	Late > 200ms	2	1	1	1	5	5
	Early < 200ms	0	0	0	0	0	1
JS	Late > 200ms	5	5	4	11	9	3
	Early < 200ms	0	0	0	0	0	0

Hit Error

Participant	Incompatible Perturbation Measurement Data					
	(A) Towards Attention	(A) Against Attention	(B) Towards Att / Aff	(B) Against Att / Aff	(C) Towards Attention	(C) Towards Affordance
JL	3.88	-0.15	3.00	-3.00	-3.70	-2.60
JC	-4.90	-9.67	4.20	-1.50	-1.25	3.76
SfH	-1.69	-0.50	0.50	-1.38	-0.20	0.44
PF	2.00	-0.42	1.00	-1.93	-2.75	-1.75
FM	-2.84	-3.25	-6.63	-1.28	-7.88	0.00
IF	2.00	-0.83	12.75	0.58	4.88	-1.90
AvH	4.50	-2.67	-1.00	-1.69	0.00	-0.17
JW	-1.63	1.20	0.63	-1.25	-3.25	3.83
BW	-1.71	-3.25	0.00	-4.00	-6.50	9.00
SJA	-0.25	-3.33	0.67	0.00	3.00	3.50
AZ	-2.00	-1.40	-2.90	-0.90	-1.80	-6.75
AH	-1.80	-6.83	2.13	-1.20	-8.50	-3.71
KR	-2.38	-2.00	0.17	-3.43	-2.69	0.25
SH	6.61	0.00	8.93	4.88	4.00	9.50
NM	-1.33	-4.67	-8.25	-2.30	-4.17	-2.50
MB	-10.17	4.20	4.20	6.67	-3.00	-14.00
IH	-3.08	-0.64	-2.15	-2.38	-0.75	5.20
MS	-3.80	2.25	-0.57	-0.70	-3.14	2.25
LM	-5.25	-6.00	12.00	5.00	1.20	-2.25
JS	-2.10	0.00	1.90	-0.95	3.11	0.00

Incompatible Trial Errors

Participant	Incompatible Trial Errors					
	(A) Towards Attention	(A) Against Attention	(B) Towards Att / Aff	(B) Against Att / Aff	(C) Towards Attention	(C) Towards Affordance
JL	0	0	0	0	0	0
JC	0	0	0	0	0	0
SfH	1	0	0	1	0	0
PF	0	0	0	1	0	0
FM	0	1	0	0	0	0
IF	0	1	2	1	0	0
AvH	2	0	3	3	1	2
JW	2	0	0	0	1	0
BW	0	0	0	0	0	0
SJA	1	0	2	1	0	1
AZ	1	0	0	1	1	0
AH	2	0	0	0	2	0
KR	0	0	1	0	0	0
SH	0	7	1	2	4	2
NM	0	1	2	0	0	0
MB	0	0	0	0	0	0
IH	1	1	1	0	0	1
MS	0	0	0	0	0	0
LM	2	0	2	1	1	0
JS	0	0	1	1	0	0

- ## Compatible perturbation trials

Movement time

Participant	Compatible Perturbation Movement Data					
	(A) Towards Attention	(A) Against Attention	(B) Towards Att / Aff	(B) Against Att / Aff	(C) Towards Attention	(C) Towards Affordance
JL	620.00	701.67	682.67	659.20	665.00	662.83
JC	623.40	644.50	615.00	630.40	697.40	634.17
SfH	692.75	691.86	675.13	677.67	643.88	683.80
PF	627.33	667.33	692.75	671.50	665.75	661.00
FM	620.89	621.00	583.71	621.60	611.00	633.00
IF	443.80	492.00	432.75	410.75	447.86	508.33
AvH	504.67	560.40	525.67	605.20	540.00	536.50
JW	491.25	540.38	491.00	546.75	512.83	522.20
BW	752.00	778.64	822.00	819.15	827.71	790.71
SJA	580.67	576.00	512.63	516.00	528.63	564.25
AZ	546.00	557.20	547.50	593.14	603.00	555.50
AH	458.00	423.00	416.80	418.67	434.75	417.00
KR	698.44	683.25	686.33	683.75	664.67	793.00
SH	380.50	389.80	400.00	444.67	433.57	372.00
NM	538.25	584.00	514.67	547.80	528.50	538.13
MB	389.50	379.00	424.83	411.67	418.88	389.18
IH	412.67	411.00	460.91	454.00	457.50	415.88
MS	626.14	688.33	640.33	649.00	627.50	725.50
LM	413.14	479.33	388.80	390.00	386.67	396.25
JS	620.00	701.67	682.67	659.20	665.00	662.83

Hit Error

Participant	Compatible Perturbation Measurement Data					
	(A) Towards Attention	(A) Against Attention	(B) Towards Att / Aff	(B) Against Att / Aff	(C) Towards Attention	(C) Towards Affordance
JL	-2.17	-1.83	0.33	0.70	-0.93	5.58
JC	0.25	0.83	6.13	2.70	-3.60	-0.33
SfH	-0.83	-1.67	0.13	-3.08	1.13	5.70
PF	-1.25	-0.50	0.50	-0.75	0.50	1.10
FM	-1.72	-2.00	1.14	-3.50	0.40	1.75
IF	0.30	8.33	0.81	3.06	0.36	1.83
AvH	-2.63	1.80	-3.33	-1.00	-2.00	3.38
JW	0.33	-0.18	1.83	0.77	2.07	5.50
BW	-0.13	-0.42	1.33	0.25	-1.08	-1.40
SJA	3.33	1.83	0.75	4.75	1.00	3.19
AZ	-1.17	-0.92	0.33	-0.38	-1.50	3.75
AH	-7.33	-6.10	-0.20	3.25	-3.25	0.10
KR	-3.33	-3.40	-1.67	-3.38	-6.83	-9.50
SH	2.21	-3.90	0.75	6.89	2.21	1.25
NM	-3.63	0.63	0.00	-0.10	0.75	0.81
MB	-4.57	-2.00	-5.23	-5.50	-4.00	7.56
IH	0.50	3.88	-0.75	-0.50	3.81	-0.36
MS	-2.14	-0.50	1.08	1.50	1.63	2.88
LM	2.00	-2.00	0.90	0.19	-0.33	0.38
JS	-3.75	-0.25	-2.13	-2.55	0.50	4.50

Appendix V

Movement time

Participant	Standard Movement Time Data					
	(A) Towards Attention	(A) Against Attention	(B) Towards Att / Aff	(B) Against Att / Aff	(C) Towards Attention	(C) Towards Affordance
JC	505.19	507.07	501.64	498.13	492.92	49665
JC Task	495.29	513.29	514.63	521.83	525.18	498.62
LC	507.63	545.70	511.78	517.91	497.70	533.47

Path Deviations

Participant	Geometric Stimuli		Coherent Object		Incoherent Object	
	Towards Attention	Against Attention	Towards Att / Aff	Against Att / Aff	Towards Attention	Towards Affordance
JC	3	-	-	1	1	1
LC	6	-	-	-	-	-

Hit Error

Participant	Standard Hit Error Data					
	(A) Towards Attention	(A) Against Attention	(B) Towards Att / Aff	(B) Against Att / Aff	(C) Towards Attention	(C) Towards Affordance
JC	6.046	4.448	4.846	1.094	8.292	5.100
JC Task	3.143	4.543	6.630	3.440	6.636	3.500
LC	4.975	5.477	7.730	6.889	10.174	8.813

Trial Errors

Participant	Standard Trial Errors					
	(A) Towards Attention	(A) Against Attention	(B) Towards Att / Aff	(B) Against Att / Aff	(C) Towards Attention	(C) Towards Affordance
IW	4	-	1	-	-	-
JC	-	-	-	-	-	-
IC	-	-	-	-	-	-

Appendix VI

Movement time

Participant	Incompatible Perturbation Movement Data					
	(A) Towards Attention	(A) Against Attention	(B) Towards Att / Aff	(B) Against Att / Aff	(C) Towards Attention	(C) Towards Affordance
JC	674.08	601.6	656.00	621.83	608.33	687.33
LC	620.30	626.50	550.00	625.75	668.17	609.00

Occurrence of Corrective Manoeuvre

Participant	Pertubation Correction Occurrence	Geometric Stimuli		Coherent Object		Incoherent Object	
		Towards Attention	Against Attention	Towards Att / Aff	Against Att / Aff	Towards Attention	Towards Affordance
JC	Late > 200ms	2	4	6	3	4	4
	Early < 200ms	2	1	2	0	1	1
JC Task	Late > 200ms	7	0	1	4	2	2
	Early < 200ms	0	0	1	0	0	2
LC	Late > 200ms	2	2	1	3	5	3
	Early < 200ms	7	4	1	1	1	2

Hit Error

Participant	Incompatible Perturbation Measurement Data					
	(A) Towards Attention	(A) Against Attention	(B) Towards Att / Aff	(B) Against Att / Aff	(C) Towards Attention	(C) Towards Affordance
JC	1.903	2.134	-2.110	-3.732	4.576	2.105
LC	-1.000	-0.143	7.333	3.000	2.167	3.750

Appendix VII

Movement time

Participant	Compatible Perturbation Movement Data					
	(A) Towards Attention	(A) Against Attention	(B) Towards Att / Aff	(B) Against Att / Aff	(C) Towards Attention	(C) Towards Affordance
JC	505.18	525.14	507.00	518.60	534.20	481.50
LC	483.80	544.00	586.00	448.00	531.00	471.50

Hit Error

Participant	Compatible Perturbation Measurement Data					
	(A) Towards Attention	(A) Against Attention	(B) Towards Att / Aff	(B) Against Att / Aff	(C) Towards Attention	(C) Towards Affordance
JC	2.213	2.734	-1.934	3.234	5.015	1.987
LC	-0.052	-4.122	1.975	3.864	3.982	2.133